



## UvA-DARE (Digital Academic Repository)

### Regulation of human B cell differentiation

Marsman, C.

**Publication date**

2023

**Document Version**

Final published version

[Link to publication](#)

**Citation for published version (APA):**

Marsman, C. (2023). *Regulation of human B cell differentiation*. [Thesis, fully internal, Universiteit van Amsterdam].

**General rights**

It is not permitted to download or to forward/distribute the text or part of it without the consent of the author(s) and/or copyright holder(s), other than for strictly personal, individual use, unless the work is under an open content license (like Creative Commons).

**Disclaimer/Complaints regulations**

If you believe that digital publication of certain material infringes any of your rights or (privacy) interests, please let the Library know, stating your reasons. In case of a legitimate complaint, the Library will make the material inaccessible and/or remove it from the website. Please Ask the Library: <https://uba.uva.nl/en/contact>, or a letter to: Library of the University of Amsterdam, Secretariat, Singel 425, 1012 WP Amsterdam, The Netherlands. You will be contacted as soon as possible.



# REGULATION OF HUMAN B CELL DIFFERENTIATION

REGULATION OF HUMAN B CELL DIFFERENTIATION

CASPER MARSMAN | 2023

CASPER MARSMAN

# Regulation of human B cell differentiation

**Casper Marsman**



The Research described in this thesis was performed at the Department of Immunopathology of Sanquin Research (Amsterdam, The Netherlands)

The studies in this thesis were financially supported by Landsteiner Foundation for Blood Transfusion Grant 1609 and Sanquin Product and Process Development Call 2020.

Copyright © Casper Marsman, 2023

The Netherlands. All rights reserved. No parts of this thesis may be reproduced, stored in a retrieval system or transmitted in any form or by any means without permission of the author.

ISBN: 978-94-6458-721-0

Provided by thesis specialist Ridderprint, [ridderprint.nl](http://ridderprint.nl)

Printing: Ridderprint

Cover design: Casper Marsman

Layout and design: Eduard Boxem, [persoonlijkproefschrift.nl](http://persoonlijkproefschrift.nl)

Regulation of human B cell differentiation

## ACADEMISCH PROEFSCHRIFT

ter verkrijging van de graad van doctor  
aan de Universiteit van Amsterdam op  
gezag van de Rector Magnificus  
prof. dr. ir. P.P.C.C. Verbeek  
ten overstaan van een door het College voor Promoties ingestelde commissie,  
in het openbaar te verdedigen in de Agnietenkapel  
op donderdag 9 februari 2023, te 16.00 uur

door Casper Marsman  
geboren te Hoorn

## **Promotiecommissie**

<i>Promotor:</i>	prof. dr. S.M. van Ham	Universiteit van Amsterdam
<i>Copromotor:</i>	dr. J.A. ten Brinke	Sanquin Research
<i>Overige leden:</i>	prof. dr. T.W. Kuijpers	Universiteit van Amsterdam
	prof. dr. C.E. van der Schoot	Universiteit van Amsterdam
	prof. dr. ing. A.H.C. van Kampen	Universiteit van Amsterdam
	prof. dr. M.A. Haring	Universiteit van Amsterdam
	prof. dr. A. Radbruch	Charité - Universitätsmedizin
	dr. O.B.J. Corneth	Erasmus Medisch Centrum

Faculteit der Natuurwetenschappen, Wiskunde en Informatica

## TABLE OF CONTENTS

<b>Chapter 1</b>	General Introduction	8
<b>Chapter 2</b>	Optimized Protocols for <i>In-Vitro</i> T cell-Dependent And T cell-Independent Activation for B-Cell Differentiation Studies Using Limited Cells	24
<b>Chapter 3</b>	Flow Cytometric Methods for the Detection of Intracellular Signaling Proteins and Transcription Factors Reveal Heterogeneity in Differentiating Human B Cell Subsets	72
<b>Chapter 4</b>	Soluble FAS ligand enhances suboptimal CD40L/IL-21-mediated human memory B cell differentiation into antibody-secreting cells	106
<b>Chapter 5</b>	Termination of CD40L co-stimulation promotes human B cell differentiation into antibody-secreting cells	134
<b>Chapter 6</b>	Oxygen level is a critical driver of human B cell differentiation and IgG class switch recombination	162
<b>Chapter 7</b>	Summarizing discussion	194
<b>Appendix</b>	English Summary	212
	Nederlandse Samenvatting	216
	List of publications	220
	Contributing authors	222
	PhD portfolio	225
	Curriculum Vitae	227
	Acknowledgements	228





# **CHAPTER 1**

General introduction

## THE HUMAN IMMUNE SYSTEM

The human immune system is divided into two, tightly interwoven parts, innate and adaptive immunity. The innate immune system provides the first line of defense against pathogens through the complement system<sup>1</sup> and innate immune cells recognizing pathogen-associated molecular patterns<sup>2,3</sup>. The second arm of immunity, the adaptive response, consists of T and B cells that express specific receptors recognizing antigen present on pathogens. After a first immune response upon encounter with a specific pathogen, T and B cells can generate immunological memory and due to this memory, the adaptive immune system can react and clear pathogens faster upon reinfection. B cells can bind and get activated by antigens. During the B cell response the cells can differentiate into two lineages; memory B cells which can recognize and quickly react to antigens upon reinfection and antibody-secreting cells (ASCs) which produce specific antibody targeted against the antigen. These antibodies bind antigens and, in cooperation with the innate immune system, antibody-coated pathogens are rapidly cleared.

An efficient immune response will result in an immune memory compartment consisting of both cellular and humoral components that provides a long lasting or lifetime protection against pathogens.

### T-dependent B cell responses

In order to effectively respond to antigens, B cells require the help of a specific subset of T cells, the CD4 T-helper cell ( $T_H$ ). In short (figure 1), in secondary lymphoid organs (SLOs), after a naïve B cell has specifically recognized and internalized antigen via the B cell receptor (BCR) they will degrade the antigen and present antigenic peptides on Major Histocompatibility Complex class II (MHCII) on the B cell surface. At the same time, naïve  $T_H$  cells can encounter and recognize antigenic peptides presented by MHCII<sup>+</sup> dendritic cells (DCs)<sup>4</sup>. The DCs provide co-stimulatory molecules and cytokines to the naïve  $T_H$  cell to induce proliferation and differentiation into effector  $T_H$  cells. For the T-dependent (TD) B cell response it is crucial that the DC- $T_H$  interaction results in the generation of T-follicular helper cells ( $T_{FH}$ ), as these migrate to the B cell zone in SLOs and provide help to and maintain germinal center (GC) B cells. Activated  $T_H$  cells can specifically recognize the peptide presented by the B cell on MHCII through the T cell receptor (TCR) and through this recognition, B and T cells form cognate interactions. During these interactions, the  $T_H$  can provide stimulation to the B cell through both co-stimulatory surface molecules (e.g. CD40L – CD40 binding) and secreted cytokines (e.g. IL-21 and IL-4) resulting in the formation of a GC reaction.

After receiving co-stimulatory and cytokine signals from  $T_H$  cells and before formation of the GC, activated B cells can undergo class-switch recombination (CSR)<sup>5</sup>. During this process the B cells class-switch the constant region of their BCR from the native IgM isotype to others like IgG, IgE or IgA. This to tailor the response to certain pathogens<sup>6</sup>

as the constant region of the BCR (and later on secreted antibody) determines the effector function of the molecule<sup>6,7</sup>. IgM antibodies are produced early during the immune response and usually of lower affinity towards the antigenic peptide than their class-switched counterparts. To compensate for the lower affinity, IgM is produced as a penta- or hexameric structure to increase avidity. IgG can be further divided into 4 subclasses: IgG1, IgG2, IgG3 and IgG4. IgG antibodies are the most abundant isotype found in blood and these subclasses have a high affinity for their antigen. IgM, IgG1 and IgG3 are potent complement activators and binding of these isotypes to antigen will result in phagocytosis or direct killing of pathogens<sup>8</sup>. Secondly, IgG can be recognized by specific Fcγ receptors expressed by phagocytes, enabling efficient phagocytosis of IgG-coated pathogens<sup>7</sup>. IgG2 is capable of both complement and Fcγ receptor binding but is markedly less efficient than IgG1 or IgG3. The IgG4 subclass is an exceptional IgG as it shows reduced binding to Fcγ receptors, an inability to activate the complement system and the ability to exchange half-molecules of the antibody structure and form a bivalent antibody specific for two different antigens. IgA is mainly produced against pathogens present in mucosal tissues. The IgE isotype can be recognized by Fcε receptors expressed by granulocytes, resulting in the release of anti-parasitic inflammatory molecules<sup>9</sup>. IgE also plays a major role in allergic responses, where instead of recognizing parasites, IgE antibodies recognize normally harmless molecules derived from food or pollen<sup>10</sup>. Finally, the IgA isotype is mainly produced at mucosal surfaces where it not only protects these areas by binding and preventing epithelium transmigration of toxins, bacteria and viruses but also by maintaining a healthy gut ecosystem<sup>11,12</sup>.

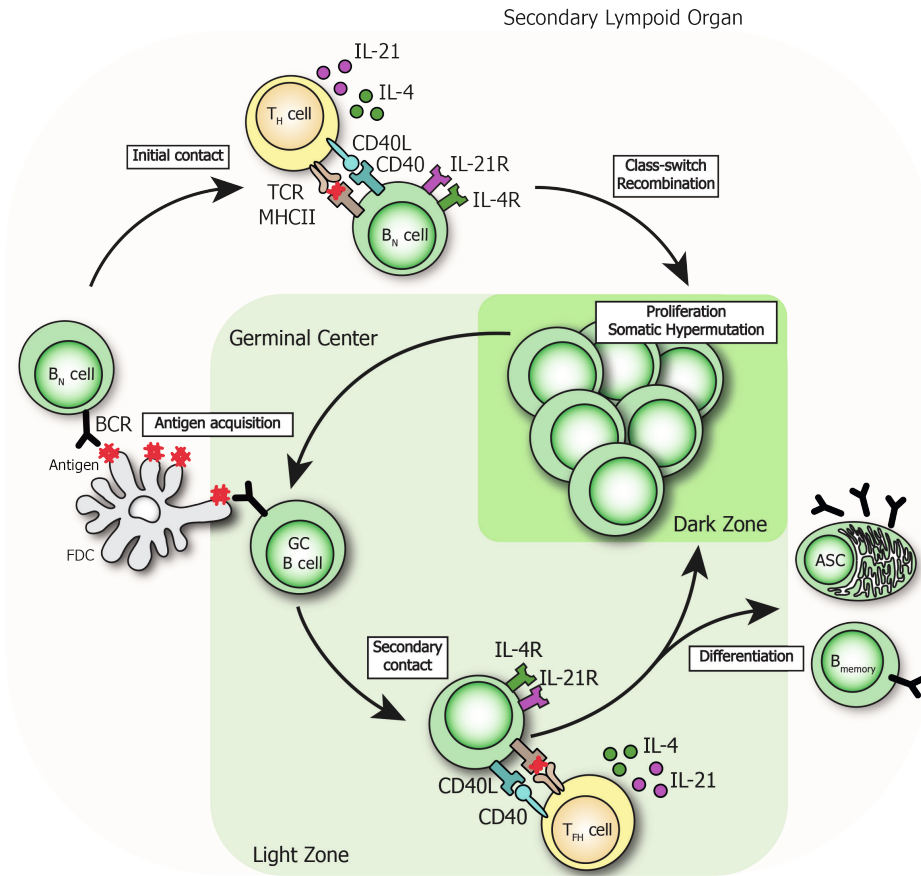


**Figure 1. The T cell dependent germinal center response.** Naïve B cells are activated by specifically recognizing presented antigen in SLOs and subsequently degrading the antigen and presenting antigenic peptides to activated T<sub>H</sub>-cells. After receiving cognate stimulation (CD40L, IL-21 and/or IL-4) from the T<sub>H</sub>-cell, B cells can undergo CSR and form the GC reaction. The B cells form the GC dark zone by proliferating and undergoing SHM. After some rounds of proliferation, GC B cells can move out of the dark zone and into the GC light zone. Here BCR affinity selection takes place as B cells re-acquire antigen and stimulation from T<sub>H</sub>-cells. GC B cells can continue cycling between GC dark and light zones and during cycling GC B cells can differentiate into memory B cells and ASCs that provide immune protection against re-infection with the antigen

### The germinal center reaction

Upon receiving T cell help and potentially undergoing CSR, B cells migrate away from the T cell zone and back into the B cell follicles<sup>13,14</sup>. Here the B cells start to divide rapidly, forming the GC dark zone while pushing aside other cells. It is during this massive burst of proliferation that B cells can undergo somatic hypermutation (SHM), a process during which the gene encoding for antibody is mutated generating B cells with a variety of affinities towards the specific antigen. After some rounds of proliferation, B cells can migrate out of the GC dark zone into what is now called the GC light zone<sup>15</sup>. It is here that B cells need to re-acquire antigen from follicular dendritic cells (FDCs) and subsequently

present it to follicular T-helper cells ( $T_{FH}$ ) for an additional round of stimulation. Acquisition of antigen in the GC light zone and the subsequent  $T_{FH}$  stimulation are a crucial part of selection for high affinity, class-switched antibodies. B cells that, through SHM, have an increased affinity against antigen have a competitive advantage over other B cells without mutation or with adverse mutations. The higher affinity B cells can acquire more antigen from FDCs and will subsequently present more surface MHCII-peptide, making them better at binding  $T_{FH}$  cells for stimulation than their lower affinity siblings<sup>13,15,16</sup>. More stimulation will lead to more divisions in the dark zone<sup>17,18</sup> and thus propagate the favorable mutations. B cells that have acquired unfavorable mutations are either not allowed to leave the dark zone at all if these don't express a functional BCR<sup>19</sup> or, they will go into apoptosis due to competition and lack of acquiring  $T_{FH}$  stimulation<sup>20</sup>. This process of antigen-driven selection of B cells expressing higher affinity BCRs over lower affinity ones is also known as affinity maturation and is crucial for an effective immune response. After acquiring  $T_{FH}$  stimulation, B cells migrate back into the GC dark zone for additional rounds of proliferation. This dark zone – light zone cyclic migration is associated with continuous affinity maturation. B cells can go through multiple cycles and eventually exit the GC and differentiate into memory B or ASCs. Memory B cells are classically described to express CD27 on the B cell surface. Recently, expression of glycosylated CD45RB (glyCD45RB), without expression of CD27, has been shown to mark antigen-experienced, early memory-like B cells whereas glyCD45RB+CD27+ cells represent the mature memory B cell population<sup>21,22</sup>. Next to memory B cells, GC reactions can give rise to two sets of ASCs; plasmablast (PBs) and plasma cells (PCs)<sup>23</sup>. Both these subsets express CD27 and CD38 on the surface. In general however, PBs are distinguished from PCs based on their ability to proliferate and by their lower affinity and quantity of antibody they are able to produce<sup>24–26</sup>. PCs on the other hand often also express CD138 on the surface and are non-dividing, terminally differentiated cells. Some of the PCs migrate to the bone marrow (BM)<sup>27,28</sup>. Here, PCs localize to survival niches supported by both direct contact with stromal cells and stromal-cell derived secreted factors such as APRIL, BAFF and IL-6<sup>29–31</sup>. Settled in the BM survival niche, PCs can survive and secrete antibody for decades. It is still a matter of debate whether short-lived PBs can give rise to long-lived PCs if they reach a BM survival niche or that this longevity is imprinted upon ASC generation at the GC or possibly during migration in the blood<sup>25,32–34</sup>.

To this day, little is known about what exact combination of stimuli or circumstances determines whether a B cell, during the GC response, either re-cycles through the GC or undergoes differentiation into either a memory or an ASC. Factors controlling the fate choices are highly sought after. In recent years it has been shown that memory B cells are mainly produced early during the GC response while ASCs come late<sup>35</sup>. Next to this,  $T_{FH}$  cells have also been shown to progressively differentiate from producing mainly IL-21 in the early GC response to IL-4 production in the late GC response<sup>36</sup>. These mice studies have improved our understanding of GC responses but many questions remain. Next to that, research in the last years have been focused on applying single or multiple stimuli

*in vitro* and analyzing the effects directly on signaling pathways, up or downregulation of transcription factors (TFs) and the cellular differentiation markers CD27, CD38 and CD138. This thesis will focus on what the requirements are for human B cells to differentiate and how signaling timing and physiological relevant environments *in vitro* can contribute to this.

### **Regulators of B cell differentiation**

The T cell derived CD40L, IL-21 and IL-4 regulate B cell proliferation and differentiation through activation of NF- $\kappa$ B, STAT3 and STAT6 pathways respectively. These pathways in turn regulate a complex network of TFs (Fig 2). First, the T<sub>FH</sub> cell expresses surface CD40L which triggers CD40 on the B cell surface. This stimulation is absolutely required for the B cell response to occur, as patients with a genetic mutation in CD40, CD40L or the downstream signaling protein NF- $\kappa$ B suffer from hyper-IgM syndrome and are unable to form germinal centers, preventing the production of high affinity IgG antibodies<sup>37,38</sup>. Activation and nuclear translocation of NF- $\kappa$ B, induces expression of C-MYC. This transcription factor has been studied intensively and is known to mainly regulate proliferation and cycling of GC B cells<sup>18,39</sup>. Of note, recently it was shown that induction of MYC is a direct result of the amount of T cell help and that subsequently, the amount of MYC directly dictated the cell size and division capacity of GC B cells<sup>40</sup>. Secondly, activation of the NF- $\kappa$ B pathway induces the expression of IRF4<sup>41</sup>. This TF plays a crucial role in B cell fate decision as at low levels it promotes GC B cell development and expression of B cell identity TF PAX5 while at high levels, IRF4 promotes expression of ASC differentiation TF BLIMP1<sup>42,43</sup>. Differentiation of B cells into ASCs requires the inhibition of both PAX5 and C-MYC together with the upregulation of BLIMP1. Secondly, the T<sub>FH</sub> cell secretes cytokines, often into the synapse formed between the B and T cell. Critical to the B cell response is T<sub>FH</sub> cell derived IL-21 that triggers the IL-21R on the B cell surface, resulting intracellularly in the phosphorylation of STAT3 (pSTAT3). This IL-21 – pSTAT3 pathway is crucial as patients with mutated STAT3 show reduced affinity maturation and IgM and IgG production while patient can also exhibit hyper IgE syndrome<sup>44–46</sup>. Master regulator of ASC differentiation, BLIMP1, is mainly induced by the IL-21 - pSTAT3 pathway and while CD40L co-stimulation has been shown to inhibit BLIMP1 expression<sup>47</sup>, both CD40L and IL-21 are required for ASC differentiation to occur<sup>48</sup>. T<sub>FH</sub> cells can also secrete IL-4 which triggers the IL-4R on the B cell surface. IL-4 stimulation leads to phosphorylation of STAT6 (pSTAT6) and this pathway majorly contributes to the GC and the process of class-switch recombination (CSR) as mice deficient in this pathway show reduced numbers of GC B cells and class-switch to IgG1 and IgE<sup>49,50</sup>. Together with CD40L stimulation, IL-4 induces higher levels of AID<sup>51,52</sup>. This particular TF regulates CSR of activated B cells. Next to CSR, AID is crucial for SHM to occur as this TF can actively deaminate cytosine bases in the DNA encoding for the BCR or antibody. Deamination of cytosine converts it to an uracil base, the error-prone DNA repair machinery active in GC B cells then recognizes and repairs this uracil resulting in mutations<sup>53</sup>. Next to this, IL-4 has been shown, together with IL-21 stimulation, to stabilize BCL6 expression<sup>54</sup>. This TF is responsible for maintaining the

GC B cell state<sup>55</sup>. Finally, activation of the IL-4 - pSTAT6 pathway stimulates expression of XBP-1s, a crucial TF that regulates the unfolded protein response (UPR) allowing ASC to handle the cellular stress that accompanies the production of massive amounts of antibodies. Recently however it was shown that the IL-4 – pSTAT6 pathway is extinguished during early ASC differentiation<sup>56</sup>, indicating that IL-4 stimulation is only beneficial before ASC differentiation occurs. T<sub>FH</sub> derived CD40L, IL-21 and IL-4 initiate different signaling cascades which in turn regulate different transcription factors and, through each pathway, each separate stimulating factor has their own unique contribution to the formation and maintenance of the GC and the eventual differentiation of B cells into memory B or ASCs.

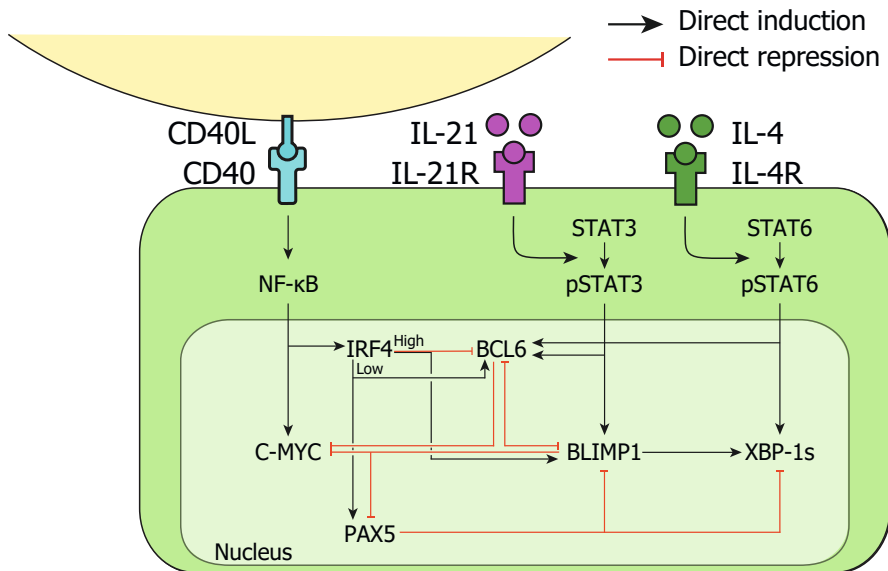


**Figure 2. Schematic overview of intracellular (phospho)signaling pathways and the transcription factor network that regulate B cell differentiation.** T cell derived CD40L triggers the NF- $\kappa$ B pathway which in turn promotes expression of C-MYC and IRF4 transcription factors. IL-21 triggers the IL-21R on the B cell surface and mainly induces phosphorylation of STAT3 which, in turn, promotes BCL6 and BLIMP1 expression. IL-4 triggers the IL-4R on the B cell surface and induces phosphorylation of STAT6 which, in turn, promotes BCL6 and XBP-1s. Some transcription factors also promote or inhibit expression of other transcription factors. Adapted from: Chapter 6, *Oxygen level is a critical driver of human B cell differentiation and IgG class switch recombination in vitro*

### Other anatomical factors controlling B cell responses

One key aspect of B cell responses is the ability and requirement of B cells to migrate to specific anatomical sites. First, after acquiring antigen from antigen-presenting cells, activated B cells upregulate the expression of chemokine receptor CCR7<sup>57</sup>. This facilitates the migration towards CCR7 ligands CCL19 and CCL21 that are expressed in SLO T cell zones, enabling B cells to find and acquire T cell help. Next, downregulation of both CCR7 and EBI2 allows the B cell to move back to the center of the B cell follicle where it will form the GC dark zone<sup>58</sup>. Within the germinal center, stromal cells in the dark zone

produce CXCL12 (ligand for CXCR4) and FDCs produce CXCL13 (ligand for CXCR5)<sup>59</sup>. While undergoing massive proliferation in the dark zone, GC B cells express CXCR4 to maintain their localization. Once these cells are done proliferating, CXCR4 is downregulated while expression of CXCR5 enables migration out of the dark zone and towards FDCs and subsequently T<sub>FH</sub> cells in the light zone<sup>60-62</sup>. The up- and downregulation of CXCR4 enables the cyclic movement of GC B cells between dark and light zones and is key in the spatio-dynamic organization. Unfortunately, this cycling of GC B cell between zones of stimulation and zones of proliferation is an aspect in GC biology that is overlooked in *in vitro* B cell studies.

Next to timed stimulation, another underappreciated aspect in B cell biology is the role of partial oxygen pressure (pO<sub>2</sub>). While healthy human tissues show pO<sub>2</sub> levels of around 3-6%<sup>63,64</sup> there are also distinct hypoxic regions specifically observed in GC light zones where pO<sub>2</sub> is only around 1%<sup>65-67</sup>. Variations in pO<sub>2</sub> have not only been shown to affect cellular metabolism but also directly regulate transcription factor expression through induction of hypoxia-inducible factors<sup>66,68,69</sup> which in turn could affect signaling and transcriptional profiles important in B differentiation.

### **T cell independent B cell responses**

Some B cell responses can occur without T cell help, also known as T cell independent (TI) B cell responses<sup>70</sup>. During these responses, TI antigens can stimulate B cells through binding of the BCR and triggering of specific Toll-like receptors (TLRs) such as TLR4 and TLR9<sup>71-74</sup>. Specific subsets of B cells are prone to participate in TI responses; the marginal zone (MZ) and B1 cells<sup>75,76</sup>. As the name suggest, MZ B cells reside in the marginal zone of SLO and express polyreactive BCRs, making them ideally suited to quickly respond to particulate antigen entering the marginal zone from the circulation. B1 cells are mainly found in murine peritoneal and pleural cavities and also express polyreactive BCRs. TI B cell responses are marked by a short-lived, rapid production of low-affinity IgM antibodies and form the first antibody-mediated line of defense against invading microbes. Affinity maturation does not occur as no GC response is present. However, these TI responses can nonetheless lead to immunological memory in the form of long-lived antibody production<sup>77</sup>.



### Scope of this thesis

The scope of this thesis is to address various regulatory mechanisms governing human B cell differentiation. **Chapter 2** of this thesis sought to address the need for minimalistic, one-step B cell differentiation assays that use low amounts of B cells, making these ideally suited for future clinical B cell differentiation studies where the availability of patient material is limited. This was done by comparing cell densities, various TD and TI stimuli and isolated B cells versus PBMC cultures, addressing the heterogeneity and disparity found in literature describing various TD and TI human B cell differentiation cultures. In order to further understand the regulation of B cell differentiation, we pursued to analyse (phospho)signaling and transcription factor expression together with B cell differentiation markers expressed on the plasma membrane. **Chapter 3** describes flow cytometric methods that allow for the multiparameter detection of B cell differentiation membrane markers with either intracellular signaling proteins or transcription factors. In **Chapter 4**, to identify novel soluble proteins that drive B cell differentiation into ASCs a previously generated secreted protein library is applied to a TD *in vitro* B cell system. This led to the discovery that the type I IFNs promote ASC differentiation from both naïve and memory B cells while, notably, soluble FAS ligand specifically promotes ASC differentiation from memory B cells by promoting expression of BLIMP1 and downregulating of PAX5. In **Chapter 5**, to investigate regulation of B cell differentiation by T cell help we investigated the transient and dynamic nature of *in vivo* CD40L stimulation. To determine whether transient CD40L stimulation is regulating ASC differentiation we sought to terminate CD40L stimulation *in vitro*. By utilizing and expanding on methods described in **chapter 3**, the cultures were analyzed in depth showing that temporal instead of continued T<sub>FH</sub> stimulation significantly increased ASC differentiation efficiency by inhibiting the B cell identity and proliferative TFs while promoting ASC differentiation TF BLIMP1. In **Chapter 6** we wanted to determine whether partial oxygen pressures (pO<sub>2</sub>) found in GCs play a regulating role in TD B cell responses. To address this, naïve B cells were cultured at physiologically relevant pO<sub>2</sub> showing that GC dark zone-associated normoxia (3% pO<sub>2</sub>) and GC light zone-associated hypoxia (1% pO<sub>2</sub>) and the time-dependent transitions between these pressures play a key role in regulating B cell metabolism, signaling, transcriptional regulation and differentiation profiles. Finally, in **Chapter 7** the findings and results presented in this thesis are summarized and discussed.

**REFERENCES**

1. Jr JCA, York N, Science G. The complement system and innate immunity Complement. Published online 2001:1-14.
2. Kawai T, Akira S. The role of pattern-recognition receptors in innate immunity: update on Toll-like receptors. *Nat Immunol.* 2010;11(5):373-384. doi:10.1038/ni.1863
3. Kumar H, Kawai T, Akira S. Pathogen recognition by the innate immune system. *Int Rev Immunol.* 2011;30(1):16-34. doi:10.3109/08830185.2010.529976
4. Krishnaswamy JK, Alsén S, Yrlid U, Eisenbarth SC, Williams A. Determination of T Follicular Helper Cell Fate by Dendritic Cells. *Frontiers in Immunology.* 2018;9:2169. doi:10.3389/FIMMU.2018.02169/BIBTEX
5. Roco JA, Mesin L, Binder SC, et al. Class-Switch Recombination Occurs Infrequently in Germinal Centers. *Immunity.* 2019;51(2):337-350.e7. doi:10.1016/J.IMMUNI.2019.07.001
6. Stavnezer J, Guikema JEJ, Schrader CE. Mechanism and Regulation of Class Switch Recombination. Published online 2008. doi:10.1146/annurev.immunol.26.021607.090248
7. Vidarsson G, Dekkers G, Rispens T, Klinman D. IgG subclasses and allotypes: from structure to effector functions. Published online 2014. doi:10.3389/fimmu.2014.00520
8. Daha NA, Banda NK, Roos A, et al. Complement activation by (auto-) antibodies. *Molecular Immunology.* 2011;48(14):1656-1665. doi:10.1016/J.MOLIMM.2011.04.024
9. Mukai K, Tsai M, Starkl P, #4 TM, Galli SJ. IgE and mast cells in host defense against parasites and venoms HHS Public Access. *Semin Immunopathol.* 2016;38(5):581-603. doi:10.1007/s00281-016-0565-1
10. Stone KD, Prussin C, Metcalfe DD. IgE, Mast Cells, Basophils, and Eosinophils. Published online 2009. doi:10.1016/j.jaci.2009.11.017
11. Pabst O, Slack E. IgA and the intestinal microbiota: the importance of being specific. doi:10.1038/s41385-019-0227-4
12. Cerutti A, Chen K, Chorny A. Immunoglobulin Responses at the Mucosal Interface. <http://dx.doi.org/10.1146/annurev-immunol-031210-101317>. 2011;29:273-293. doi:10.1146/ANNUREV-IMMUNOL-031210-101317
13. Gitlin AD, Shulman Z, Nussenzweig MC. Clonal selection in the germinal centre by regulated proliferation and hypermutation. *Nature.* 2014;509(7502):637-640. doi:10.1038/nature13300
14. Allen CDC, Okada T, Cyster JG. Germinal-center organization and cellular dynamics. *Immunity.* 2007;27(2):190-202. doi:10.1016/j.immuni.2007.07.009
15. Bannard O, Horton RM, Allen CDC, An J, Nagasawa T, Cyster JG. Germinal center centroblasts transition to a centrocyte phenotype according to a timed program and depend on the dark zone for effective selection. *Immunity.* 2013;39(5):912-924. doi:10.1016/j.immuni.2013.08.038
16. Shulman Z, Gitlin AD, Weinstein JS, et al. Dynamic signaling by T follicular helper cells during germinal center B cell selection. *Science (1979).* 2014;345(6200):1058-1062. doi:10.1126/science.1257861
17. Finkin S, Hartweg H, Oliveira TY, Kara EE, Nussenzweig MC. Protein Amounts of the MYC Transcription Factor Determine Germinal Center B Cell Division Capacity. *Immunity.* 2019;51(2):324-336.e5. doi:10.1016/J.IMMUNI.2019.06.013

18. Dominguez-Sola D, Victora GD, Ying CY, et al. c-MYC is required for germinal center selection and cyclic re-entry HHS Public Access. *Nat Immunol.* 2012;13(11):1083-1091. doi:10.1038/ni.2428
19. Stewart I, Radtke D, Phillips B, McGowan SJ, Bannard O. Germinal Center B Cells Replace Their Antigen Receptors in Dark Zones and Fail Light Zone Entry when Immunoglobulin Gene Mutations are Damaging. *Immunity.* 2018;49(3):477-489.e7. doi:10.1016/J.IMMUNI.2018.08.025
20. Guzman-Rojas L, Sims-Mourtada JC, Rangel R, Martinez-Valdez H. *Life and Death within Germinal Centres: A Double-Edged Sword.*
21. Glass DR, Tsai AG, Oliveria JP, et al. An Integrated Multi-omic Single-Cell Atlas of Human B Cell Identity. *Immunity.* 2020;53(1):217-232.e5. doi:10.1016/J.IMMUNI.2020.06.013
22. Koers J, Pollastro S, Tol S, et al. CD45RB Glycosylation and Ig Isotype Define Maturation of Functionally Distinct B Cell Subsets in Human Peripheral Blood. *Frontiers in Immunology.* 2022;0:1936. doi:10.3389/FIMMU.2022.891316
23. Nutt SL, Hodgkin PD, Tarlinton DM, Corcoran LM. The generation of antibody-secreting plasma cells. *Nat Rev Immunol.* 2015;15(3):160-171. doi:10.1038/nri3795
24. Caraux A, Klein B, Paiva B, et al. Circulating human b and plasma cells. age-associated changes in counts and detailed characterization of circulating normal CD138- and CD138 plasma cells. *Haematologica.* 2010;95(6):1016-1020. doi:10.3324/haematol.2009.018689
25. Jourdan M, Caraux A, de Vos J, et al. An in vitro model of differentiation of memory B cells into plasmablasts and plasma cells including detailed phenotypic and molecular characterization. *Blood.* 2009;114(25). Accessed April 10, 2017. <http://www.bloodjournal.org/content/114/25/5173.long?sso-checked=true>
26. Arumugakani G, Stephenson SJ, Newton DJ, et al. Early Emergence of CD19-Negative Human Antibody-Secreting Cells at the Plasmablast to Plasma Cell Transition. *J Immunol.* 2017;198(12):4618-4628. doi:10.4049/JIMMUNOL.1501761
27. Radbruch A, Muehlinghaus G, Luger EO, et al. Competence and competition: the challenge of becoming a long-lived plasma cell. *Nat Rev Immunol.* 2006;6(10):741-750. doi:10.1038/nri1886
28. Oracki SA, Walker JA, Hibbs ML, Corcoran LM, Tarlinton DM. Plasma cell development and survival. *Immunological Reviews.* 2010;237(1):140-159. doi:10.1111/j.1600-065X.2010.00940.x
29. Cornelis R, Hahne S, Taddeo A, et al. Stromal Cell-Contact Dependent PI3K and APRIL Induced NF- $\kappa$ B Signaling Prevent Mitochondrial- and ER Stress Induced Death of Memory Plasma Cells. *Cell Rep.* 2020;32(5). doi:10.1016/J.CELREP.2020.107982
30. Nguyen DC, Duan M, Ali M, Ley A, Sanz I, Lee FEH. Plasma cell survival: The intrinsic drivers, migratory signals, and extrinsic regulators. *Immunological Reviews.* 2021;303(1):138-153. doi:10.1111/imr.13013
31. Slamanig SA, Nolte MA. The Bone Marrow as Sanctuary for Plasma Cells and Memory T cells: Implications for Adaptive Immunity and Vaccinology. *Cells.* 2021;10(6). doi:10.3390/CELLS10061508
32. Halliley JL, Tipton CM, Liesveld J, et al. Long-Lived Plasma Cells Are Contained within the CD19(-)CD38(hi)CD138(+) Subset in Human Bone Marrow. *Immunity.* 2015;43(1):132-145. doi:10.1016/j.immuni.2015.06.016
33. Tangye SG. Staying alive: Regulation of plasma cell survival. *Trends in Immunology.* 2011;32(12):595-602. doi:10.1016/j.it.2011.09.001
34. Chu VT, Berek C. The establishment of the plasma cell survival niche in the bone marrow. *Immunological Reviews.* 2013;251(1):177-188. doi:10.1111/imr.12011

35. Weisel FJ, Zuccarino-Catania G v., Chikina M, Shlomchik MJ. A Temporal Switch in the Germinal Center Determines Differential Output of Memory B and Plasma Cells. *Immunity*. 2016;44(1):116-130. doi:10.1016/j.immuni.2015.12.004
36. Weinstein JS, Herman EI, Lainez B, et al. TFH cells progressively differentiate to regulate the germinal center response. *Nature Immunology*. 2016;17(10):1197-1205. doi:10.1038/ni.3554
37. Korthauer U, Graf D, Mages HW, et al. *Defective Expression of T cell CD40 Ligand Causes X-Linked Immunodeficiency with Hyper-IgM*; 1993.
38. Ferrari S, Giliani S, Insalaco A, et al. Mutations of CD40 gene cause an autosomal recessive form of immunodeficiency with hyper IgM. *Proc Natl Acad Sci U S A*. 2001;98(22):12614-12619. doi:10.1073/PNAS.221456898
39. Grumont RJ, Strasser A, Gerondakis S. B cell growth is controlled by phosphatidylinositol 3-kinase-dependent induction of Rel/NF-kappaB regulated c-myc transcription. *Mol Cell*. 2002;10(6):1283-1294. doi:10.1016/S1097-2765(02)00779-7
40. Finkin S, Hartweg H, Oliveira TY, Kara EE, Nussenzweig MC. Protein Amounts of the MYC Transcription Factor Determine Germinal Center B Cell Division Capacity. *Immunity*. 2019;51(2):324-336.e5. doi:10.1016/j.immuni.2019.06.013
41. Grumont RJ, Gerondakis S. Rel induces interferon regulatory factor 4 (IRF-4) expression in lymphocytes: modulation of interferon-regulated gene expression by rel/nuclear factor kappaB. *J Exp Med*. 2000;191(8):1281-1291. doi:10.1084/JEM.191.8.1281
42. Ochiai K, Maienschein-Cline M, Simonetti G, et al. Transcriptional Regulation of Germinal Center B and Plasma Cell Fates by Dynamical Control of IRF4. *Immunity*. 2013;38(5):918-929. doi:10.1016/j.immuni.2013.04.009
43. Sciammas R, Shaffer AL, Schatz JH, Zhao H, Staudt LM, Singh H. Graded Expression of Interferon Regulatory Factor-4 Coordinates Isotype Switching with Plasma Cell Differentiation. *Immunity*. 2006;25(2):225-236. doi:10.1016/j.immuni.2006.07.009
44. Kane A, Lau A, Brink R, Tangye SG, Deenick EK. B-cell specific STAT3 deficiency: Insight into the molecular basis of autosomal-dominant hyper-IgE syndrome. *Journal of Allergy and Clinical Immunology*. 2016;138(5):1455-1458.e3. doi:10.1016/j.jaci.2016.05.018
45. Moens L, Schaballie H, Bosch B, et al. AD Hyper-IgE Syndrome Due to a Novel Loss-of-Function Mutation in STAT3: a Diagnostic Pursuit Won by Clinical Acuity. *Journal of Clinical Immunology*. Published online 2016. doi:10.1007/s10875-016-0351-9
46. Avery DT, Deenick EK, Ma CS, et al. B cell-intrinsic signaling through IL-21 receptor and STAT3 is required for establishing long-lived antibody responses in humans. *The Journal of Experimental Medicine*. 2010;207(1):155-171. doi:10.1084/jem.20091706
47. Upadhyay M, Priya GK, Ramesh P, et al. CD40 signaling drives B lymphocytes into an intermediate memory-like state, poised between naïve and plasma cells. *J Cell Physiol*. 2014;229(10):1387-1396. doi:10.1002/JCP.24572
48. Ding BB, Bi E, Chen H, Yu JJ, Ye BH. IL-21 and CD40L Synergistically Promote Plasma Cell Differentiation through Upregulation of Blimp-1 in Human B Cells. *The Journal of Immunology*. 2013;190(4):1827-1836. doi:10.4049/jimmunol.1201678
49. Turqueti-Neves A, Otte M, Prazeres Da Costa O, et al. B-cell-intrinsic STAT6 signaling controls germinal center formation. *Eur J Immunol*. 2014;44:2130-2138. doi:10.1002/eji.201344203
50. King Alexandre P Meli IL, Fontés G, Leung Soo and C. Intestinal Helminth Infection Required for IgE Production during Derived IL-4 Is – T Follicular Helper Cell. *J Immunol References*. 2022;199:244-252. doi:10.4049/jimmunol.1700141

51. Muramatsu M, Kinoshita K, Fagarasan S, Yamada S, Shinkai Y, Honjo T. Class Switch Recombination and Hypermutation Require Activation-Induced Cytidine Deaminase (AID), a Potential RNA Editing Enzyme Figure 1. Induced Expression of AID in CH12F3-2 Cells. *Cell*. 2000;102:553-563. doi:10.1016/S0092-8674(00)00078-7
52. Unger PPA, Verstegen NJM, Marsman C, et al. Minimalistic In Vitro Culture to Drive Human Naive B Cell Differentiation into Antibody-Secreting Cells. *Cells*. 2021;10(5). doi:10.3390/cells10051183
53. Neuberger MS, Milstein C. Somatic hypermutation. *Curr Opin Immunol*. 1995;7(2):248-254. doi:10.1016/0952-7915(95)80010-7
54. Chevrier S, Kratina T, Emslie D, Tarlinton DM, Corcoran LM. IL4 and IL21 cooperate to induce the high Bcl6 protein level required for germinal center formation. *Immunol Cell Biol*. 2017;95(10):925-932. doi:10.1038/ICB.2017.71
55. Basso K, Dalla-Favera R. BCL6: Master Regulator of the Germinal Center Reaction and Key Oncogene in B Cell Lymphomagenesis. *Advances in Immunology*. 2010;105(C):193-210. doi:10.1016/S0065-2776(10)05007-8
56. Pignarre A, Chatonnet F, Caron G, Haas M, Desmots F, Fest T. Plasmablasts derive from CD23-activated B cells after the extinction of IL-4/STAT6 signaling and IRF4 induction. *Blood*. 2021;137(9):1166-1180. doi:10.1182/BLOOD.2020005083
57. Okada T, Miller MJ, Parker I, et al. Antigen-Engaged B Cells Undergo Chemotaxis toward the T Zone and Form Motile Conjugates with Helper T Cells. *PLoS Biology*. 2005;3(6):e150. doi:10.1371/JOURNAL.PBIO.0030150
58. Pereira JP, Kelly LM, Xu Y, Cyster JG. EB12 mediates B cell segregation between the outer and centre follicle. *Nature* 2009 460:7259. 2009;460(7259):1122-1126. doi:10.1038/nature08226
59. Stebegg M, Kumar SD, Silva-Cayetano A, Fonseca VR, Linterman MA, Graca L. Regulation of the germinal center response. *Frontiers in Immunology*. 2018;9(OCT):2469. doi:10.3389/FIMMU.2018.02469/BIBTEX
60. Allen CDC, Ansel KM, Low C, et al. Germinal center dark and light zone organization is mediated by CXCR4 and CXCR5. *Nature Immunology*. 2004;5(9):943-952. doi:10.1038/ni1100
61. Mesin L, Ersching J, Victora GD. Germinal Center B Cell Dynamics. *Immunity*. 2016;45(3):471-482. doi:10.1016/j.immuni.2016.09.001
62. Victora GD, Schwickert TA, Fooksman DR, et al. Germinal center dynamics revealed by multiphoton microscopy with a photoactivatable fluorescent reporter. *Cell*. 2010;143(4):592-605. doi:10.1016/j.cell.2010.10.032
63. Atkuri KR, Herzenberg LA, Herzenberg LA. Culturing at atmospheric oxygen levels impacts lymphocyte function. *Proc Natl Acad Sci U S A*. 2005;102(10):3756-3759. doi:10.1073/pnas.0409910102
64. Burrows N, Maxwell PH. Hypoxia and B cells. *Experimental Cell Research*. 2017;356(2):197-203. doi:10.1016/j.yexcr.2017.03.019
65. Cho SH, Raybuck AL, Stengel K, et al. Germinal centre hypoxia and regulation of antibody qualities by a hypoxia response system. *Nature*. 2016;537(7619):234-238. doi:10.1038/nature19334
66. Cho SH, Raybuck AL, Blagih J, et al. Hypoxia-inducible factors in CD4+ T cells promote metabolism, switch cytokine secretion, and T cell help in humoral immunity. *Proc Natl Acad Sci U S A*. 2019;116(18):8975-8984. doi:10.1073/pnas.1811702116

67. Abbott RK, Thayer M, Labuda J, et al. Germinal Center Hypoxia Potentiates Immunoglobulin Class Switch Recombination. *The Journal of Immunology*. 2016;197(10):4014-4020. doi:10.4049/jimmunol.1601401
68. Halligan DN, Murphy SJE, Taylor CT. The hypoxia-inducible factor (HIF) couples immunity with metabolism. *Seminars in Immunology*. 2016;28(5):469-477. doi:10.1016/j.smim.2016.09.004
69. Burrows N, Bashford-Rogers RJM, Bhute VJ, et al. Dynamic regulation of hypoxia-inducible factor-1 $\alpha$  activity is essential for normal B cell development. *Nature Immunology*. 2020;21(11):1408-1420. doi:10.1038/s41590-020-0772-8
70. Vos Q, Lees A, Wu ZQ, Snapper CM, Mond JJ. B-cell activation by T cell-independent type 2 antigens as an integral part of the humoral immune response to pathogenic microorganisms. *Immunol Rev*. 2000;176:154-170. doi:10.1034/J.1600-065X.2000.00607.X
71. Huggins J, Pellegrin T, Felgar RE, et al. CpG DNA activation and plasma-cell differentiation of CD27<sup>-</sup> naive human B cells. *Blood*. 2007;109(4):1611-1619. doi:10.1182/BLOOD-2006-03-008441
72. Pone EJ, Lou Z, Lam T, et al. B cell TLR1/2, TLR4, TLR7 and TLR9 interact in induction of class switch DNA recombination: Modulation by BCR and CD40, and relevance to T-independent antibody responses. <http://dx.doi.org/103109/089169342014993027>. 2014;48(1):1-12. doi:10.3109/08916934.2014.993027
73. Pone EJ, Zan H, Zhang J, Al-Qahtani A, Xu Z, Casali P. Toll-Like Receptors and B-Cell Receptors Synergize to Induce Immunoglobulin Class-Switch DNA Recombination: Relevance to Microbial Antibody Responses. *Critical Reviews & Trade; in Immunology*. 2010;30(1):1-29. doi:10.1615/CRITREVIIMMUNOL.V30.I1.10
74. Nothelfer K, Sansonetti PJ, Phalipon A. Pathogen manipulation of B cells: the best defence is a good offence. *Nat Rev Microbiol*. 2015;13(3):173-184. doi:10.1038/NRMICRO3415
75. Flavius Martin, Alyce M. Oliver, John F. Kearney. *Marginal Zone and B1 B Cells Unite in the Early Response against T-Independent Blood-Borne Particulate Antigens.*; 2001.
76. Allman D, Wilmore JR, Gaudette BT. The continuing story of T cell independent antibodies. *Immunological Reviews*. 2019;288(1):128-135. doi:10.1111/imr.12754
77. Bortnick A, Chernova I, Quinn WJ, Mugnier M, Cancro MP, Allman D. Long-lived bone marrow plasma cells are induced early in response to T cell-independent or T cell-dependent antigens. *J Immunol*. 2012;188(11):5389-5396. doi:10.4049/JIMMUNOL.1102808







# CHAPTER 2

## Optimized Protocols for In-Vitro T-Cell-dependent and T-Cell-Independent Activation for B-Cell Differentiation Studies Using Limited Cells

Casper Marsman\*, Dorit Verhoeven\*, Jana Koers, Theo Rispens, Anja ten Brinke, S. Marieke van Ham‡ and Taco W. Kuijpers‡

*Frontiers in Immunology (2022), 13:815449*

\*These authors have contributed equally to this work and share first authorship

‡These authors have contributed equally to this work and share senior authorship

## ABSTRACT

Background/methods: For mechanistic studies, *in vitro* human B cell differentiation and generation of plasma cells are invaluable techniques. However, the heterogeneity of both T cell-dependent (TD) and T cell-independent (TI) stimuli and the disparity of culture conditions used in existing protocols makes interpretation of results challenging. The aim of the present study was to achieve the most optimal B cell differentiation conditions using isolated CD19<sup>+</sup> B cells and PBMC cultures. We addressed multiple seeding densities, different durations of culturing and various combinations of TD stimuli and TI stimuli including B cell receptor (BCR) triggering. B cell expansion, proliferation and differentiation was analyzed after 6 and 9 days by measuring B cell proliferation and expansion, plasmablast and plasma cell formation and immunoglobulin (Ig) secretion. In addition, these conditions were extrapolated using cryopreserved cells and differentiation potential was compared.

Results: This study demonstrates improved differentiation efficiency after 9 days of culturing for both B cell and PBMC cultures using CD40L and IL-21 as TD stimuli and 6 days for CpG and IL-2 as TI stimuli. We arrived at optimized protocols requiring 2500 and 25.000 B cells per culture well for TD and TI assays, respectively. The results of the PBMC cultures were highly comparable to the B cell cultures, which allows dismissal of additional B cell isolation steps prior to culturing. In these optimized TD conditions, the addition of anti-BCR showed little effect on phenotypic B cell differentiation, however it interferes with Ig secretion measurements. Addition of IL-4 to the TD stimuli showed significantly lower Ig secretion. The addition of BAFF to optimized TI conditions showed enhanced B cell differentiation and Ig secretion in B cell but not in PBMC cultures. With this approach, efficient B cell differentiation and Ig secretion was accomplished when starting from fresh or cryopreserved samples.

Conclusion: Our methodology demonstrates optimized TD and TI stimulation protocols for more in-depth analysis of B cell differentiation in primary human B cell and PBMC cultures while requiring low amounts of B cells, making them ideally suited for future clinical and research studies on B cell differentiation of patient samples from different cohorts of B cell-mediated diseases.

## INTRODUCTION

B cells are an essential arm of the adaptive immunity as their differentiation in response to foreign antigen generates protective antibodies and immunological memory (1). The process of B cell differentiation into plasmablasts and plasma cells involves profound molecular changes in morphology, phenotype and gene expression, enabling the cells to produce and secrete large amounts of immunoglobulins (Igs). B cell differentiation is initiated by activation of B cells by exposure to antigen. Classically, B cell responses are categorized in two different B cell responses dependent on the type of antigen, known as T cell-dependent (TD) and T cell-independent (TI) responses (1, 2).

In TD B cell responses, B cells are usually activated by proteinaceous antigens in the secondary lymphoid organs through recognition of their cognate antigen by the B cell receptor (BCR). Differentiation of B cells in these circumstances requires T cell help in the form of CD40-CD40L co-stimulation with T cell-derived cytokines such as IL-4 and IL-21 (3-5). Initially, this process results in the generation of memory B cells, which can rapidly differentiate into high-affinity antibody producing plasma cells during secondary antigen exposure (6, 7). Secondly, long-lived plasma cells are generated that move to bone-marrow niches from where they secrete high affinity antibodies (8). These two compartments of humoral immunological memory are hallmarks of many vaccination strategies.

In TI B cell responses, B cells are activated without T cell help (9). TI antigens include multimeric antigens, like bacterial capsule polysaccharides (PS) and bacterial DNA, which can activate B cells through binding of the BCR and engagement of specific Toll like receptors (TLRs) such as TLR-4 and TLR-9 (10-13). In addition to this, multiple different cytokines, produced by multiple immune cells, can interact with their respective receptor expressed on B cells and could potentially modulate the response. TI B cell responses are short-lived and do not result in selection of affinity matured antibodies. However, these TI B cell responses have been shown to result in long-lived antibody production in specific cases (14). Although antibodies are of fundamental importance in the protection against pathogens, aberrant B cell differentiation may lead to autoimmune diseases when tolerance governed by immunological checkpoints is lost (15).

A major hurdle in the study of *in vitro* human B cell differentiation consists of the various methods described to generate *in vitro* plasmablasts and plasma cells, which often fail to exactly mimic *in vivo* responses. In these methods TD and TI antigens are often combined (**Table 1**). While this is an effective method to induce B cell differentiation *in vitro* and combining TD and TI antigens could be of great importance to answer specific research questions (e.g. understanding B cell responses to specific viruses, bacteria or vaccines using adjuvants) it does not allow evaluation of the separate and distinct routes of B cell activation that each are characterized by their own antibody output.

Optimal conditions are still elusive and there are many determinant factors. Thus, this study was designed to investigate the most optimal B cell differentiation conditions with regards to several essential factors, i.e. using isolated CD19<sup>+</sup> B cells or PBMC cultures, multiple seeding densities, different durations of culturing and various combinations of TD stimuli or TI stimuli. B cell expansion, proliferation and differentiation was analyzed by flow cytometry after 6 and 9 days by measuring B cell numbers, Cell Trace Yellow (CTY) dilution, CD27<sup>+</sup>CD38<sup>+</sup> plasmablast and CD27<sup>+</sup>CD38<sup>+</sup>CD138<sup>+</sup> plasma cell formation and immunoglobulin (Ig) secretion in culture supernatants by Enzyme Linked Immunosorbent Assay (ELISA). In addition, these conditions were extrapolated using cryopreserved cells and differentiation potential of cryopreserved and freshly isolated cells were compared. Resulting protocols are 1-step and minimalistic, ensuring that results from different labs are comparable.

## **MATERIALS & METHODS**

### **Literature review**

In order to identify stimuli described in previously reported B cell differentiation protocols, a literature review was carried out using the following search terms: B cell culture, B cell expansion, B cell stimulation, B cell activation, human B cell differentiation, human plasma cell differentiation using the NCBI Pubmed database (<https://www.ncbi.nlm.nih.gov/pubmed>). The results of this literature review is summarized in Table 1.

### **Cell Lines**

NIH3T3 fibroblasts expressing human CD40L (3T3-CD40L<sup>+</sup>) (16) were cultured in IMDM (Lonza, Basel 4002, Switzerland) containing 10% FCS (Serana, 14641 Pessin, Germany), 100 U/mL penicillin (Invitrogen, through Thermo Fisher, 2665 NN Bleiswijk, The Netherlands), 100 µg/mL streptomycin (Invitrogen), 2 mM l-glutamine (Invitrogen), 50 µM β-mercaptoethanol (Sigma Aldrich, 3330 AA, Zwijndrecht, The Netherlands) and 500 µg/mL G418 (Life Technologies, through Thermo Fisher).

### **Isolation of PBMCs and B Cells from Human Healthy Donors**

Buffy coats of healthy human donors were obtained from Sanquin Blood Supply. All the healthy donors provided written informed consent in accordance with the protocol of the local institutional review board, the Medical Ethics Committee of Sanquin Blood Supply, and the study conformed to the principles of the Declaration of Helsinki. The mean age of the healthy donors was 41,3 years at the time of blood withdrawal [range 27-61 years], male n=2, female n = 4. Peripheral blood mononucleated cells (PBMCs) were isolated from buffy coats using a Lymphoprep (Axis-Shield PoC AS, Dundee DD2 1XA, Scotland) density gradient. Afterwards, from half of the fraction of PBMCs, CD19<sup>+</sup> B cells were isolated using magnetic Dynabeads and DETACHaBEAD (Thermo Fisher) according to the manufacturer's instructions. The purity of B cells after isolation and the B cell compartment distribution at baseline was assessed by flow cytometry. All B cell isolations had a purity of >92%. Excess cells were resuspended to 20-50\*10<sup>6</sup> cells per

ml in culture medium and slowly cold freezing medium (80% DMSO / 20% FCS, Thermo Fisher) was added in a 1:1 ratio. The cell suspension was resuspended and divided over cryo-vials. Cells were frozen overnight to -80 °C in a Mr. Frosty and transferred to cryo-storage the next morning.

### **In Vitro PBMC and B Cell Stimulation Cultures**

3T3-CD40L<sup>+</sup> were harvested, irradiated with 30 Gy and seeded in B cell medium (RPMI 1640, Gibco through Thermo Fisher) without phenol red containing 5% FCS, 100 U/mL penicillin, 100 µg/mL streptomycin, 2 mM L-glutamine, 50 µM β-mercaptoethanol and 20 µg/mL human apo-transferrin (Sigma Aldrich; depleted for human IgG with protein G sepharose (GE Healthcare, 3871MV, Hoevelaken, The Netherlands)) on 96-well flat-bottom plates (Nunc through Thermo Fisher) to allow adherence overnight. 3T3-CD40L<sup>+</sup> were seeded by adding 100 µl of  $0.1 \times 10^6$  cells/ml (or 10,000) cells per well. In some experiments PMBCs were thawed from cryo-storage and washed with B cell medium. PBMCs or B cells were rested at 37 °C for 1h before counting. Then, 50 µl of CD19<sup>+</sup> B cells at a concentration of 0.005-, 0.05- or  $0.5 \times 10^6$  cells/ml (250, 2500 or 25000 cells resp.) were co-cultured in duplicate in the presence or absence of PBMCs with the irradiated 3T3-CD40L<sup>+</sup> fibroblasts in TD settings or in 96-well U-bottom plates for TI settings. 50 µl of stimuli were added as indicated: F(ab')<sub>2</sub> fragment Goat Anti-Human IgA/G/M (5 µg/mL; Jackson ImmunoResearch, Ely CB7 4EZ, UK), IL-4 (25 ng/mL; Cellgenix, 79107 Freiburg, Germany), IL-21 (50 ng/mL; Peprotech, London W6 8LL, UK), CpG ODN 2006 (1 µM, Invivogen), IL-2 (50 ng/ml, Miltenyi Biotec) and BAFF (100 ng/ml R&D) for up to 9 days. After adding the B cells to the wells, the plate was centrifuged for 1 min at 400x g to force all the cells onto the 3T3-CD40L<sup>+</sup> layer. Cryopreserved cells were thawed by agitating the tubes gently in a 37 °C waterbath until only a small ice clump was left. The cells were transferred to a 50 ml tube and cold B cell medium was added drop-wise while the tube was constantly agitated.

### **CellTraceYellow labeling**

CD19<sup>+</sup> B cells or PBMCs were washed with 10 ml PBS/0.1% bovine serum albumin (BSA, Sigma Aldrich) and resuspended to a concentration of  $2 \times 10^7$  cells/ml in PBS/0.1%BSA. Cells and 10 µM CellTrace Yellow (Thermo Fisher Scientific) were mixed at a 1:1 ratio and incubated 20 minutes in a 37°C waterbath in the dark, vortexing the tube every 5 minutes to ensure uniform staining. Cells were washed twice using a 10 times volume of cold culture medium to end labeling. Thereafter, B cells were cultured according to the protocol described above.

### **Flow cytometry**

Wells were resuspended and transferred to 96-well V-bottom plates (Nunc). Cells were centrifuged 2 min at 600x g, supernatant was transferred to V-bottom plates, sealed with an ELISA sticker and stored at -20°C. Samples were washed twice with 150 µl PBS/0.1%BSA. Cells were stained in a 25 µL staining mix with 1:1000 LIVE/DEAD Fixable Near-IR Dead cell stain kit (Invitrogen) and antibodies diluted in PBS/%0.1 BSA for 20

minutes at RT in the dark. The samples were wash 2x with 150  $\mu$ l PBS/%0.1BSA. Finally, the samples were resuspended in a volume of 140  $\mu$ l, of which 90  $\mu$ l was measured on a LSRII or FACSymphony flow cytometer. Samples were measured on LSRII or Symphony and analyzed using Flowjo software. The gating strategy is shown in Suppl.Fig.1.

<b>Ab</b>	<b>Conjugate</b>	<b>Manufacturer</b>	<b>Clone</b>	<b>Catalog No.</b>	<b>Dilution*</b>
CD19	BV510	BD	SJ25-C1	562947	1:100
CD20	PerCP-Cy5.5	BD	L27	332781	1:25
CD27	PE-Cy7	eBioscience	0323	25-0279-42	1:50
CD38	V450	BD	HB7	646851	1:100
CD138	FITC	BD	MI15	561703	1:50
IgG	BUV395	BD	G17-145	564229	1:100
IgM	APC	Biolegend	MHM-88	314510	1:100
CD3	PerCP	BD	SK7	345766	1:20
LIVE/DEAD	APC-Cy7	Invitrogen		L34976	1:1000

\*Optimal antibody dilutions as defined for the method and staining procedure used in this paper. As the staining conditions and flow cytometer settings may differ per lab, it is advised that these dilutions are taken as guidelines and that these are validated within each individual lab.

### **ELISA of culture supernatants**

Supernatants of eligible conditions were tested for secreted IgG, IgA and IgM with a sandwich ELISA using polyclonal rabbit anti-human IgG, IgA and IgM reagents and a serum protein calibrator (X0908, Dako, Glostrup) all from Dako (Glostrup; product numbers A0423, Q0332 and A0425 respectively). The polyclonal rabbit anti-human IgG, IgA and IgM were diluted in coating buffer to a concentration of 5  $\mu$ g/ml, then 100  $\mu$ l was used to coat Nunc MaxiSorp flat bottom 96 well plates (Thermo Fisher) overnight at 4°C. Plates were washed with PBS/0.05% Tween- 20 and blocked with 100  $\mu$ l PBS/1% bovine serum albumin (BSA) (Sigma Aldrich) for 1 hour at room temperature (RT). Plates were then washed and 100  $\mu$ l of serum protein calibrator (X0908, Dako, Glostrup) or culture supernatant diluted in HPE buffer (M1940, Sanquin reagents) (1:25 for IgG and IgA and 1:30 for IgM) was added to each well and incubated for 1.5 hour at RT. Human serum protein low control (X0939, Dako, Glostrup) was used as reference sample on each plate. Following incubation and washing, 100  $\mu$ l of detection antibody diluted in blocking buffer was added: poly rabbit anti-human IgG/HRP (1.3 g/L, 1:15,000), IgA/HRP (1.3 g/L, 1:15,000), and IgM/HRP (1.3 g/L, 1:10,000) (Dako, Glostrup; product numbers: P0214, P0215, P0216 respectively). Plates were washed and developed using TMB (00-4201-56, Invitrogen by Thermofisher), stopped using 1M H<sub>2</sub>SO<sub>4</sub> stopping solution and read using the Biotek microplate reader

(450-540nm) (Synergy HT, Biotek) and IgM, IgA and IgG concentrations were calculated relative to a titration curve of the serum protein calibrator.

### Interference ELISA

The interference ELISA assay was developed as described in the sandwich ELISA above. Serial dilutions of F(ab')<sub>2</sub> fragment Goat Anti-Human IgA/G/M (5, 2.5, 1.25 and 0.625 µg/mL; Jackson ImmunoResearch, Ely CB7 4EZ, UK) in HPE buffer (M1940, Sanquin reagents) were incubated (60 min, RT) with the standard curve dilutions of the serum protein calibrator (X0908, Dako, Glostrup). The results were plotted as titration curves.

### Graphics

Schematic overviews were created using images from Servier Medical Art, which are licensed under a Creative Commons Attribution 3.0 Unported License (<http://smart.servier.com>).

### Statistics

Statistical analysis was performed using GraphPad Prism (version 8; Graphpad Software). Data were analyzed using t tests, Repeated Measures one-way ANOVA or Repeated Measures two-way ANOVA where appropriate. Results were considered significant at  $p < 0.05$ . Significance was depicted as \* ( $p < 0.05$ ) or \*\* ( $p < 0.01$ ), \*\*\* ( $p < 0.001$ ) or \*\*\*\* ( $p < 0.0001$ ). Correlation analyses between flow cytometry and immunoglobulin ELISA data were performed with Pearson's correlation test. \* $p < 0.05$ . The statistical tests performed are indicated in the figure legends.

## RESULTS

### Frequently reported B cell differentiation stimuli for human naïve and/or memory B cells in literature

The first step in establishing optimized *in vitro* protocols for TD and TI stimulation of B cells to induce B cell differentiation was to identify frequently used and reported culture conditions by literature review (**Table 1**). Following identification of a wide range of stimuli, together with consortium partner labs, standard TD and TI combinations were chosen using concentrations reflective of the publications obtained through literature review or by previous experimental work. For TD stimuli, the combination of CD40L and IL-21 was selected, a combination frequently used to mimic CD4<sup>+</sup> T cell help (5). Although multiple methods of CD40L stimulation are reported (either soluble or using feeder cells), here a monolayer of feeder cells consisting of 3T3 mouse fibroblast expressing high levels of human CD40L was selected. For TI the combination of CpG, a well-known ligand of TLR-9, together with IL-2, a B cell survival factor, was set up (17, 18). These combinations of stimuli were either constantly or most frequently used and therefore found to be essential.

**Table 1.** Frequently reported B cell differentiation stimuli for human naïve and/or memory B cells in literature

Stimuli	Target(s)	Concentrations	Reference
Anti-IgM anti-IgG/IgM F(ab') <sub>2</sub> anti-IgG/IgA/IgM F(ab') <sub>2</sub>	BCR	2, <b>5</b> , 10 µg/ml	(5), (17), (19), (27), (36), (37), (38), (39)
BAFF	BAFF-R. BMCA. TACI	75, <b>100</b> ng/ml	(36), (40)
aCD40, CD40L	CD40	50, 500 ng/ml 1, 5 µg/ml	(5), (17), (27), (38), (39), (41), (42), (43)
CD40L expressing L cells 3T3-CD40L fibroblasts	CD40	Various ratios of B cell : feeder cell	(3), (19), (36), (37)
CpG-ODN 2006	TLR9	1.0, 2.5, 3.2, 6.0, 10 µg/ ml 0.35, <b>1.0</b> µM	(17), (27), (36), (38), (39), (40), (41), (42), (43)
IFNα	IFNAR	100, 500 U/ml	(37), (41)
IL-2	IL-2R	20, 50, 100 U/ml 25, <b>50</b> ng/ml	(3), (5), (37), (38), (39), (41), (42)
IL-4	IL-4R	10, <b>25</b> , 50, 100, 200 ng/ ml	(3), (5), (17), (19), (36), (38), (41), (43)
IL-6	IL-6R	10, 50 ng/ml	(37), (41)
IL-10	IL-10R	25, 50, 200 ng/ml	(5), (36), (38), (41), (43)
IL-15	IL-15R	10 ng/ml	(36), (41)
IL-21	IL-21R	2, 20, <b>50</b> , 100 ng/ml	(5), (19), (27), (36), (37), (39), (40), (42), (43)

Abbreviations: BAFF: B cell activating factor. BCMA: B cell maturation antigen. IFN: interferon. IL: interleukin. ODN: oligodeoxynucleotide. TACI (TNFRSF13B): transmembrane activator and CAML interactor. TLR: toll like receptor. The used concentrations in this study are depicted in **bold**.

Following the identification of CD40L and IL-21 as TD stimuli and CpG and IL-2 as TI stimuli, the effect of **(1)** culture duration and **(2)** different seeding densities (or starting B cell numbers) were determined. These experiments were performed with cells from healthy donors either using **(3)** purified CD19<sup>+</sup> B cells or **(4)** PBMC cultures corrected for B cell count, comprising of B cells and other PBMCs (mainly T cells and small fractions of monocytes and NK cells) since such cultures do not require B cell isolation and are thus more practical for routine use. For this, PBMCs from the same healthy donors were used to avoid donor variability. Additionally, the augmenting effect of **(5)** additional stimuli, i.e. anti-BCR and IL-4 for TD, anti-BCR and BAFF for TI, was investigated and **(6)** the effect of cryopreservation on B cell differentiation potential was checked. All conditions were cultured in duplicate.



### **Efficient *in vitro* B cell differentiation after 9 days using T cell-dependent stimulation with CD40L and IL-21 using 2500 starting B cells**

In the TD assay either 25,000, 2500 or 250 starting B cells were co-cultured with CD40L-feeder cells and IL-21 enabling 3 conditions, from now on referred to as condition I, II and III (**Fig.1A**). Due to these settings, different ratios of B cell to feeder cell (1:0.4, 1:4 and 1:40 respectively) were created, resulting in different availability of CD40L during culturing. For each condition, B cell expansion and proliferation was assessed by flow cytometry after 6 and 9 days as well as plasmablast (CD27<sup>+</sup>CD38<sup>+</sup>) and plasma cell (CD27<sup>+</sup>CD38<sup>+</sup>CD138<sup>+</sup>) formation (for gating strategy, see Suppl.Fig.1). Additionally, the IgG, IgA and IgM secretion was measured by ELISA in culture supernatants, which acts as a second readout for B cell differentiation as B cells differentiate from surface Ig-expressing cells to Ig-secreting cells.

To assess expansion of B cells during culturing, the number of CD19<sup>+</sup> live B cells were determined. The conditions II and III showed significant more CD19<sup>+</sup> live B cells compared to its specific starting B cell numbers at day 6 and day 9 whilst a significant decline in CD19<sup>+</sup> live B cells in condition I was observed (**Fig.1B**). Condition II showed a 4-fold amplification ( $\pm 0.6$ ; n=4) on day 6 and a -4fold amplification ( $\pm 1.3$ ; n=4) on day 9 compared to its starting B cell number (**Table 2**). Condition III showed a 7-fold amplification ( $\pm 0.9$ ; n=4) on day 6 and a -27fold amplification ( $\pm 5.2$ ; n=4) on day 9. Interestingly, in all three conditions a similar yield of CD19<sup>+</sup> live B cells was detected at day 9, but not at day 6, whilst the starting B cell numbers was different, i.e. 10-100-fold. As shown before, this suggests that the amount of available CD40L critically influences B cell survival and/or expansion during culture (19). For further FACS analysis, we set a cut-off value at a minimum of 1000 events of CD19<sup>+</sup> live B cells. To assess proliferation, B cells were labeled with Cell Trace Yellow (CTY) prior to culturing. Proliferation was observed in all conditions at day 6 (**Fig.1C**), however conditions II and III showed a significant higher dilution of CTY in accordance with the amplification in cell numbers observed. A significant increase in the percentage of CD27<sup>+</sup>CD38<sup>+</sup> cells between day 6 and day 9 in each condition was observed, suggesting that a 9-day culture period induced higher levels of differentiation (**Fig.1D**). However, we did not observe differences in plasma cell formation between day 6 and day 9 (**Fig.1E**) and there was no significant difference between the 3 culture conditions (statistics not shown). Measurement of secreted IgG, IgA and IgM showed a significant increase between day 6 and day 9, confirming a 9-day culture period induces higher levels of differentiation and Ig secretion (**Fig.1F**). Notably, although the yield of CD19<sup>+</sup> live B cells and phenotypically differentiated plasmablasts and plasma cells was comparable in each condition at day 9, different Ig secretion patterns between the 3 conditions was observed. When we compared the 3 conditions in the flow cytometry analysis, significantly higher percentages of CD27<sup>+</sup>CD38<sup>+</sup> B cells were observed in condition II and III (**Suppl.Fig.2A-B**).

**Table 2.** B cell survival and proliferation during different B cell differentiation conditions

<b>Isolated CD19<sup>+</sup> B cells (TD)</b>							
	<b>Condition I</b>		<b>Condition II</b>		<b>Condition III</b>		
Starting B cell number	25.000		2500		250		
3T3-CD40L cell	10.000		10.000		10.000		
Ratio B cell : 3T3-CD40L cell	1 : 0.4		1 : 4		1 : 40		
Cytokines	IL-21		IL-21		IL-21		
Mean CD19 <sup>+</sup> live cells							
Day 0	25.000		2500		250		
Day 6	12438	± 3120; n=4	9736	± 1566; n=4	1656	± 224; n=4	
Day 9	8012	± 2643; n=4	8899	± 3196; n=4	6769	± 1305; n=4	
Mean amplification (compared to starting B cell number)							
Day 6	0.5	± 0.1; n=4	3.9	± 0.6; n=4	6.6	± 0.9; n=4	
Day 9	0.3	± 0.1; n=4	3.6	± 1.3; n=4	27.1	± 5.2; n=4	
<b>PBMCs (TD)</b>							
	<b>Condition I.2</b>		<b>Condition II.2</b>		<b>Condition III.2</b>		
Starting B cell number	25.000		2500		250		
3T3-CD40L cell	10.000		10.000		10.000		
Ratio B cell : 3T3-CD40L cell	1 : 0.4		1 : 4		1 : 40		
Cytokines	IL-21		IL-21		IL-21		
Mean CD19 <sup>+</sup> live cells							
Day 0	25.000		2500		250		
Day 6	8601	± 1397; n=3	14487	± 4320; n=3	4139	± 311; n=3	
Day 9	6019	± 695; n=3	7819	± 2713; n=3	12826	± 3750; n=3	
Mean amplification (compared to starting B cell number)							
Day 6	0.3	± 0.1; n=3	5.8	± 1.7; n=3	16.6	-	
Day 9	0.2	± 0.1; n=3	4.2	± 1.1; n=3	51.3	-	

**Table 2.** Continued

<b>Isolated CD19<sup>+</sup> B cells (TI)</b>							
	<b>Condition IV</b>		<b>Condition V</b>		<b>Condition VI</b>		
Starting B cell number	25.000		2500		250		
TLR ligand	CpG		CpG		CpG		
Cytokines	IL-2		IL-2		IL-2		
Mean CD19 <sup>+</sup> live cells							
Day 0	25.000		2500		250		
Day 6	4751	± 1397; n=4	85	± 22.7; n=4	17	± 2.3; n=4	
Day 9	1571	± 695; n=4	29	± 13.8; n=4	2	± 0.8; n=4	
Mean amplification (compared to starting B cell number)							
Day 6	0.2	± 0.1; n=4	-	-	-	-	
Day 9	0.1	± 0.0; n=4	-	-	-	-	
<b>PBMCs (TI)</b>							
	<b>Condition IV.2</b>		<b>Condition V.2</b>		<b>Condition VI.2</b>		
Starting B cell number	25.000		2500		250		
TLR ligand	CpG		CpG		CpG		
Cytokines	IL-2		IL-2		IL-2		
Mean CD19 <sup>+</sup> live cells							
Day 0	25.000		2500		250		
Day 6	8978	± 1985; n=3	3823	± 1983; n=3	58	± 18; n=3	
Day 9	7841	± 2127; n=3	2463	± 1055; n=3	47	± 26; n=3	
Mean amplification (compared to starting B cell number)							
Day 6	0.4	± 0.1; n=3	1.5	± 0.8; n=3	-	-	
Day 9	0.3	± 0.1; n=3	1.0	± 0.4; n=3	-	-	

Purified B cells or non-purified B cells (PBMC cultures) were cultured using a 1-step culture system for 6 and 9 days with either TD (CD40L + IL-21) or TI (CpG + IL-2) stimuli. On day 6 and day 9 cell counts and viability were determined using flow cytometry with fluorochrome-conjugated Live/Dead and anti-CD19. Results are shown as the mean ± SEM of n = 4 (B cell cultures) or n = 3 (PBMC cultures) donors. – indicates no further analysis due to <1000 CD19<sup>+</sup> live events.

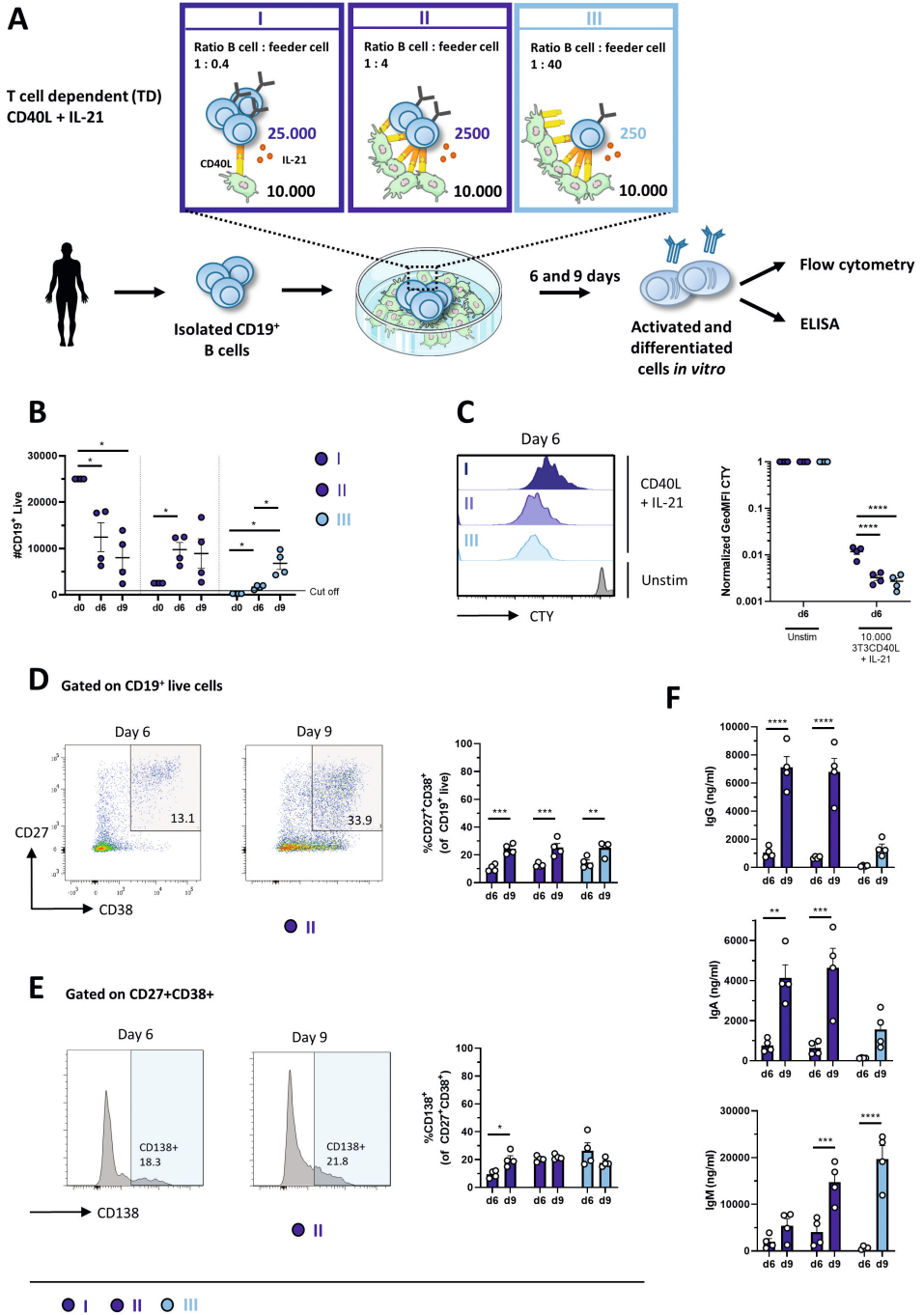


**Figure 1. Proliferation, differentiation and antibody production after T cell dependent in vitro stimulation and culturing of low numbers of primary human CD19<sup>+</sup> B cells.** (A) Schematic overview of the T cell dependent (TD) culture system to induce B cell differentiation. A total of 25000, 2500 or 250 CD19<sup>+</sup> human B cells (n = 4) were stimulated with a human-CD40L-expressing 3T3 feeder layer and recombinant IL-21 (50 ng/mL) enabling condition I (dark blue), II (cobalt blue) and III (light blue). Cells were analyzed at day 6 and day 9 by flow cytometry to evaluate (B) number of live CD19<sup>+</sup> events, (C) amount of proliferation by CTY dilution and frequency of (D) plasmablast (CD27<sup>+</sup>CD38<sup>+</sup> B cells) and (E) plasma cell (CD27<sup>+</sup>CD38<sup>+</sup>CD138<sup>+</sup> B cells). A cut off of 1000 events was used to proceed with further analysis. (F) The supernatant was collected at day 6 and day 9 to evaluate IgG, IgA and IgM production by ELISA (n = 4). Each data point represents the mean of an individual donor with duplicate culture measurements. Mean values are represented by bars and the error bars depict SEM. P values were calculated using two-way ANOVA with Sidak's multiple comparison test. \* P ≤ 0.05, \*\* P ≤ 0.01, \*\*\* P ≤ 0.001, \*\*\*\* P ≤ 0.0001.

In parallel experiments, PBMCs (corrected for 250, 2500 and 25.000 B cells) were cultured in similar conditions, which created conditions I.2, II.2 and III.2 (**Suppl.Fig.3A**). Here, we observed again significantly more B cell expansion and proliferation in condition II.2 and III.2 with higher CD40L availability (**Suppl.Fig.3B-C, Table 2**). The number of CD19<sup>+</sup> live cells and dilution of CTY showed similar results as in condition I, II and III suggesting limited effect of the presence of PBMCs with CD40L and IL-21 stimulation. Proliferation analysis of CD3<sup>+</sup> T cells did not show any increased proliferation compared to unstimulated controls, indicating that the used stimuli did not activate T cells which would influence B cell differentiation (data not shown). Again, there was no significant difference between the 3 conditions (statistics not shown) (**Suppl.Fig.3D**). No effect was observed of the presence of PBMCs on the efficacy of plasmablasts or plasma cell induction (**Fig.1D-E, Suppl.Fig.3D-E**). Ig measurements in the supernatants of the PBMC cultures showed a significant increase in IgA and IgM secretion between day 6 and 9, indicating that a 9-day culture period induces higher levels of differentiation and Ig secretion (**Suppl.Fig.3F**).

Taken together, condition I, II and III with 250, 2500, 25.000 starting B cells respectively were all suitable for generating CD27<sup>+</sup>CD38<sup>+</sup> plasmablasts and IgG secretion at day 9, two important hallmarks of B cell differentiation. The optimal differentiation conditions for TD stimulation with limited numbers of B cells was defined here as condition II and II.2, being 2500 CD19<sup>+</sup> cells per 96-well with or without other PBMCs, which were used for further experiments.

### **CD40L and IL-21 stimulation in combination with anti-BCR and/or IL-4 does not increase B cell differentiation and immunoglobulin secretion**

In an attempt to drive differentiation and expansion even further in our 1-step *in vitro* B cell differentiation assay, the effect of additional stimuli in our culture conditions was tested. For this purpose, the reference stimuli CD40L and IL-21 were combined with or without F(ab)<sub>2</sub> fragments targeting IgM, IgG and IgA to induce BCR signaling (also referred to as anti-BCR). Secondly, we tested whether the addition of IL-4, a cytokine important for naïve B cells during the GC reactions, can augment *in vitro* B cell differentiation induced by CD40L and IL-21. In these cultures, 2500 freshly isolated CD19<sup>+</sup> B cells (condition II) or PBMCs corrected for B cell number (2500 B cells; condition II.2) were used from the

same donors shown in the previous experiments. Flow cytometry was performed on day 6 and day 9 to classify CD19<sup>+</sup> cells as CD27<sup>+</sup>CD38<sup>+</sup> plasmablasts and IgG, IgA and IgM secretion was measured in culture supernatants. In condition II we observed a significant increase in plasmablasts upon adding anti-BCR both on day 6 as on day 9 compared to CD40L and IL-21 alone (**Fig.2A**). In condition II.2 no combination of stimuli was superior to CD40L and IL-21 (**Fig.2B**). Prolonged culture to 9 days allowed a significant increase in plasmablasts in all 4 combinations of stimuli both in condition II and II.2 (statistics not shown). As addition of anti-BCR and/or IL-4 stimulation to conditions I, II or III (and PBMC culture variants of these) could also affect proliferation of CD19<sup>+</sup> cells this was investigated, showing no significant differences (**Suppl.Fig.4A-B**). In the main condition with 2500 cells, significantly less cells were found when adding IL-4 to isolated CD19<sup>+</sup> cultures at day 6 but not on day 9, or in PBMC cultures (**Suppl.Fig.4C-D**). As use of the mixture of F(ab)<sub>2</sub> fragments in our cultures might interfere with the IgG, IgA and IgM ELISA assay, an interference ELISA was performed. Indeed, we observed a decrease in measured IgG, IgA and IgM when F(ab)<sub>2</sub> fragments in different concentrations were added to the standard curve (**Suppl.Fig.5A-C**). Therefore, samples containing anti-BCR stimulation were excluded for further analysis of secreted Ig. Although the percentages of plasmablasts on day 9 were similar (or higher) upon addition of IL-4, we observed significant lower secreted IgG, IgA and IgM in culture supernatants in the conditions where IL-4 was added (**Fig.2C-D**). In conclusion, an augmenting effect of anti-BCR on TD induced B cell differentiation was found but its use prevents Ig secretion analysis. Notably, although we observed no significant effect on plasmablast differentiation, IL-4 reduced Ig secretion under all conditions tested.

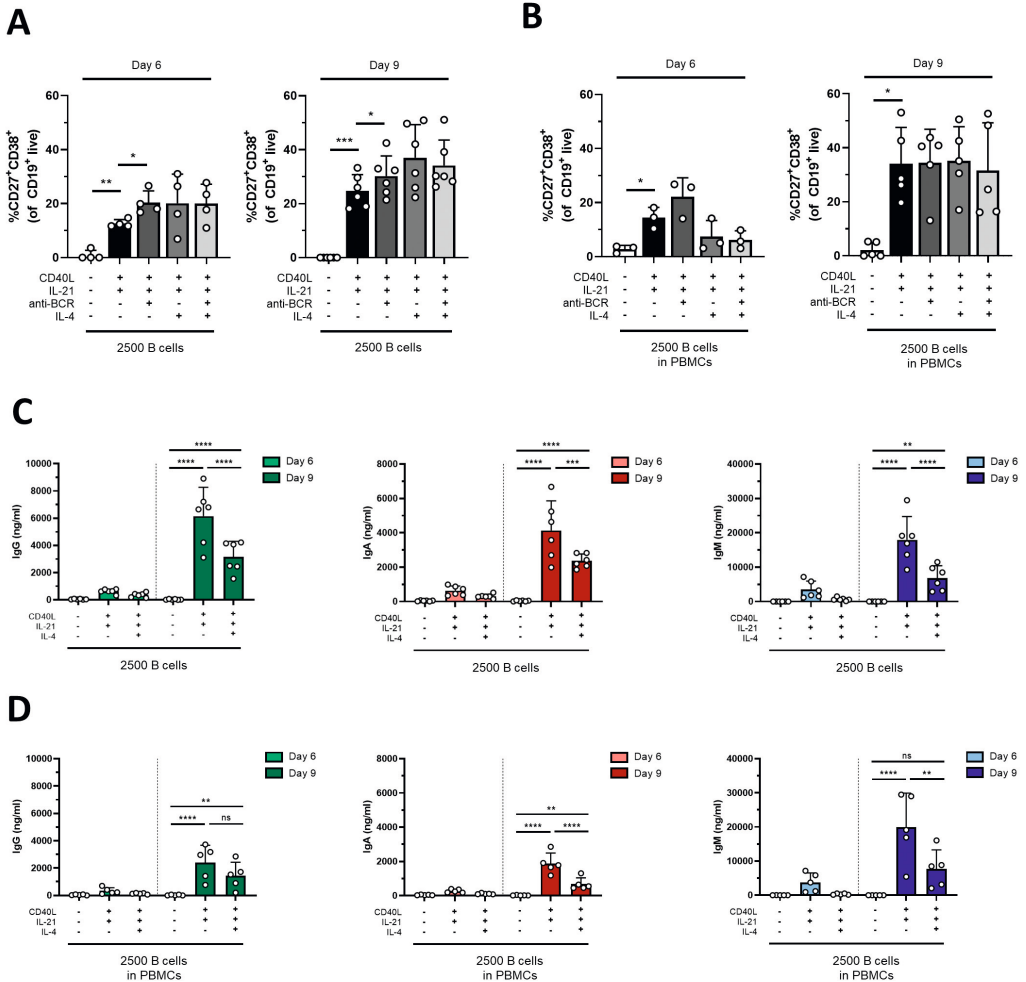


**Figure 2. Addition of anti-BCR stimuli in a T cell dependent stimulation results in increased B cell differentiation while IL-4 severely inhibits antibody production.** Human primary B cells obtained from healthy donors were stimulated under conditions described in Figure 1A (condition II) and Suppl. Fig. 2A (condition II.2, PBMC cultures) with or without anti-BCR (anti-Ig F(ab)2 mix (5 µg/mL) targeting IgM, IgG and IgA) and/or recombinant IL-4 (25 ng/mL). Frequencies of CD27<sup>+</sup>CD38<sup>+</sup> B cells on day 6 and day 9 in **(A)** condition II and **(B)** condition II.2 ( $n = 4-6$ ). **(C-D)** Total secretion of IgG, IgA and IgM measured in culture supernatants of eligible conditions after 6 and 9 days **(C)** without PBMCs (condition II) and **(D)** within PBMC cultures (condition II.2). Each data point represents the mean of an individual donor with duplicate culture measurements. Mean values are represented by bars and the error bars depict SEM. P values were calculated using one-way ANOVA with Dunnett's multiple comparison test (A-B) or two-way ANOVA with Sidak's multiple comparison test (C-D). \*  $P \leq 0.05$ , \*\*  $P \leq 0.01$ , \*\*\*  $P \leq 0.001$ , \*\*\*\*  $P \leq 0.0001$ .

**Efficient *in vitro* B cell differentiation after 6 days using T cell-independent (TI) stimulation with CpG and IL-2 with 25.000 starting B cells**

In the TI assay the effect of (1) culture duration and (2) different seeding densities (or starting B cell numbers) were also determined. Again 25.000, 2500 or 250 CD19<sup>+</sup> B cells were cultured, enabling condition IV, V and VI (**Fig.3A**). We assessed B cell differentiation by flow cytometry analysis and measurements of Ig secretion on day 6 and day 9. Culturing CD19<sup>+</sup> B cells with TI stimuli resulted in a decline in CD19<sup>+</sup> B cells (**Fig.3B, Table 2**). Flow cytometry analysis of condition V and VI showed less than 1000 events on day 6 and day 9 and these conditions were therefore excluded from further analysis. In condition IV, a significant decline in CD19<sup>+</sup> live cells was observed on day 9 compared to day 6, with two out of 4 donors not meeting the cut-off of 1000 events, thus longer culture periods under TI conditions results in lower B cell survival and/or expansion. Samples eligible for further flow cytometry analysis showed sufficient proliferation on day 6 (**Fig.3C**). There was no significant difference between day 6 and day 9 in terms of CD27<sup>+</sup>CD38<sup>+</sup> plasmablasts, but a significant increase in CD27<sup>+</sup>CD38<sup>+</sup>CD138<sup>+</sup> plasma cells on day 9 (**Fig.3D-E**). Accordingly, a small increase of secreted IgG, IgA and IgM in culture supernatants was observed on day 9 (**Fig.3F**).

Extrapolation of the TI conditions to PBMC cultures enabled conditions IV.2, V.2 and VI.2 (**Suppl.Fig.6A**). Consistent with condition IV, we observed a significant decrease in CD19<sup>+</sup> live B cells condition IV.2 (**Suppl.Fig.6B**). Interestingly, we observed a 1.0 and 1.5-fold ( $\pm 0.8$ ;  $n=3$ ,  $\pm 0.4$ ;  $n=3$ ) amplification of B cell numbers on day 6 and 9 in condition V.2, which provided sufficient B cell numbers for further analysis (in contrast to condition V) (**Suppl.Fig.6B, Table 2**). As shown before, this suggests an additional pro-survival effect of PBMCs in these culture (17). Condition VI.2 did not meet the cut off of 1000 events and was also excluded from further analysis. Proliferation analysis by CTY dilution showed a significant difference in proliferation of CD19<sup>+</sup> live B cells at day 6 between conditions IV.2 and V.2 (**Suppl.Fig.6C**). Proliferation analysis of CD3<sup>+</sup> T cells showed minimal proliferation compared to unstimulated controls in the conditions IV.2 and V.2, which suggests that the used stimuli (likely IL-2) could activate the T cells in these PBMC cultures possibly influencing B cell differentiation (**Suppl.Fig.6D**). Further analysis showed no significant difference between day 6 and day 9 in terms of plasmablasts and plasma cells (**Suppl. Fig.6E-F**). Despite the lack of increase in the percentages of CD27<sup>+</sup>CD38<sup>+</sup> plasmablasts and CD27<sup>+</sup>CD38<sup>+</sup> CD138<sup>+</sup> plasma cells between day 6 and day 9, a small increase of secreted IgG, IgA and IgM was observed in culture supernatants on day 9 in condition IV.2 and V.2 (**Suppl.Fig.6G**). These experiments identified condition IV and condition IV.2, being 25.000 CD19<sup>+</sup> cells per well, as most suitable for the assessment of B cell differentiation using TI stimulation.



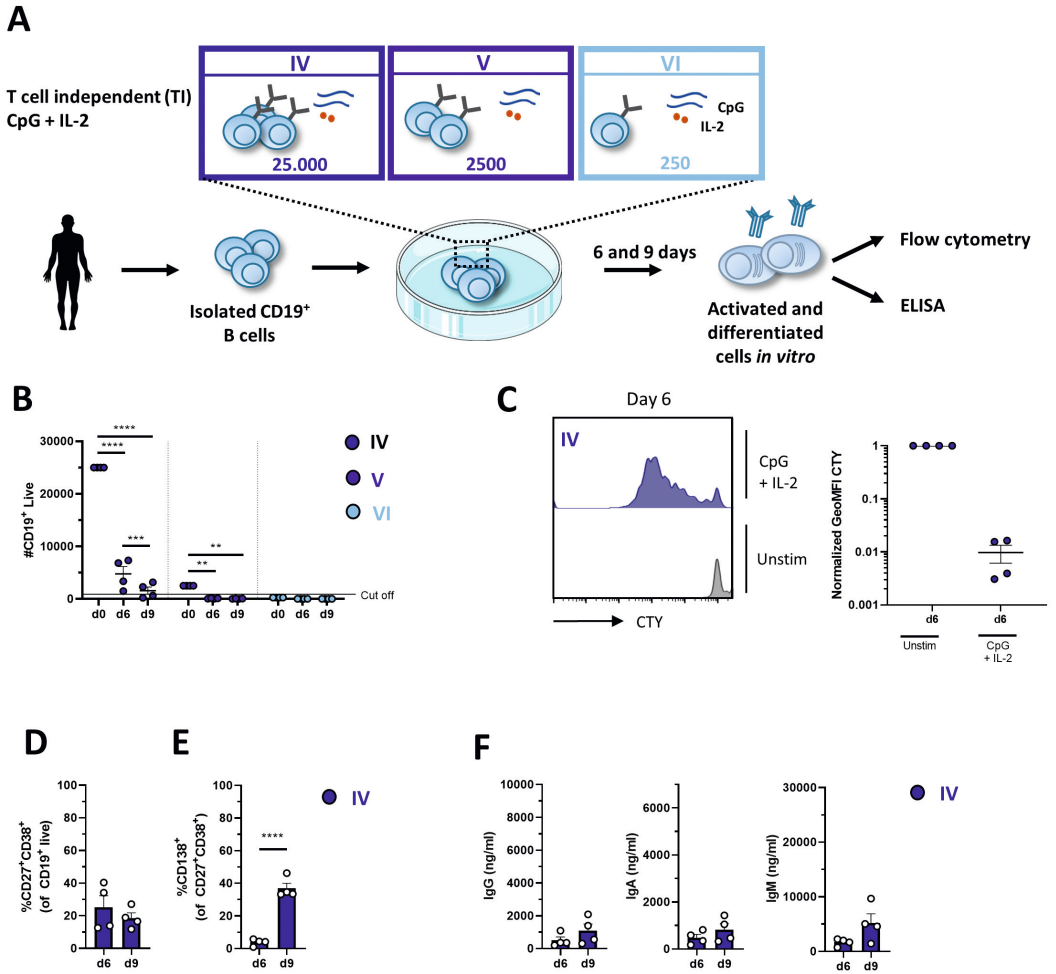


**Figure 3. Proliferation, differentiation and antibody production after T cell independent in vitro stimulation and culturing of low numbers of primary human CD19<sup>+</sup> B cells.** (A) Schematic overview of the T cell independent (TI) culture system to induce B cell differentiation. A total of 25000, 2500 or 250 CD19<sup>+</sup> human B cells ( $n = 4$ ) were stimulated with CpG (1  $\mu$ M) and IL-2 (50 ng/ml) enabling condition IV (dark blue), V (cobalt blue) and VI (light blue). Cells were analyzed at day 6 and day 9 by flow cytometry to evaluate (B) number of live CD19<sup>+</sup> events, (C) amount of proliferation by CTY dilution and frequency of (D) plasmablast (CD27<sup>+</sup>CD38<sup>+</sup>) and (E) plasma cell (CD27<sup>+</sup>CD38<sup>+</sup>CD138<sup>+</sup>) generation. A cut off of 1000 events was used to proceed with further analysis. (F) The supernatant was collected at day 6 and day 9 to evaluate IgG, IgA and IgM production by ELISA ( $n = 4$ ). Each data point represents the mean of an individual donor with duplicate culture measurements. Mean values are represented by bars and the error bars depict SEM. P values were calculated using two-way ANOVA with Sidak's multiple comparison test (B) or unpaired t test (D-F). \*  $P \leq 0.05$ , \*\*  $P \leq 0.01$ , \*\*\*  $P \leq 0.001$ , \*\*\*\*  $P \leq 0.0001$ .

### **CpG and IL-2 induced B cell differentiation can be amplified by anti-BCR and BAFF stimulation**

To assess potential further assay optimization, the effect of additional stimuli to augment TI induced differentiation was investigated. For this purpose, anti-BCR stimulation with or without B cell activating factor (BAFF), another well-known survival factor and differentiation signal for B cells, were supplemented to the reference stimuli CpG and IL-2. Studies primarily done *in vitro* have shown that BAFF can be expressed by different immune cell types (including monocytes, macrophages, follicular dendritic cells), which BAFF-producing cells contribute to specific B cell responses *in vivo* is not yet understood (20-22). In these cultures, 25,000 freshly isolated CD19<sup>+</sup> B cells (condition IV) or PBMCs corrected for B cell number (25,000 B cells; condition IV.2) were used from the same donors shown in the previous experiments. We observed a small increase in plasmablasts upon addition of anti-BCR and/or BAFF both on day 6 and day 9 in condition IV but not in IV.2 suggesting that anti-BCR, BAFF or a combination of both can amplify plasmablast formation in the cultures without the presence of other PBMCs (**Fig.4A-B**). Prolonged culture to 9 days did not result in higher percentages of plasmablasts in any 4 combinations of stimuli both in condition IV and IV.2 (statistics not shown). Analysis of samples without anti-BCR stimulation showed that in condition IV the addition of BAFF resulted in significant higher secreted IgG, IgA and IgM in culture supernatants, while this effect was not present in condition IV.2 where other PBMCs were present (**Fig.4C-D**). As addition of anti-BCR and/or BAFF stimulation to conditions IV, V or VI (and PBMC culture variants of these) could also affect proliferation of CD19<sup>+</sup> cells this was investigated, showing no significant differences (Suppl Fig 7A-B). In the main condition with 2500 cells, significantly more cells were found when anti-BCR stimulation was added to isolated CD19<sup>+</sup> cultures at day 6 but not on day 9 (Suppl Fig 7C). In PBMC cultures there is a trend towards higher CD19<sup>+</sup> counts when BAFF is present although this was not significant (**Suppl.Fig.7D**). Taken together, the addition of BAFF stimulation to CpG and IL-2 augments TI induced differentiation and Ig secretion upon culturing purified B cells, but this effect is absent in PBMC cultures.

### **Proportion of CD27-expressing and class-switched cells at start of culture correlate with *in vitro* induced differentiation and Ig-secretion**

The ratio of naive to memory cells or the proportion of IgM or Ig-switched cells at the start of culture could be a determining factor for both TD and TI culture results. Thus, we investigated if specific B cell memory- or Ig-subsets at day 0 (**Suppl.Fig.8**) correlated with culture end-points such as CD27<sup>+</sup>CD38<sup>+</sup> plasmablast differentiation and IgG, IgA and IgM secretion in culture supernatant. This analysis demonstrated that mainly the proportion of CD27<sup>+</sup> cells at the start of culture correlates with differentiation into CD27<sup>+</sup>CD38<sup>+</sup> cells at day 6 and 9 in both TD and TI stimuli (**Suppl. Table 1 and 2**). Interestingly, the CD40L, IL-21 and IL-4 stimulation shows a negative correlation between the proportion of CD27<sup>+</sup> cells and differentiation (**Suppl.Table 1**).

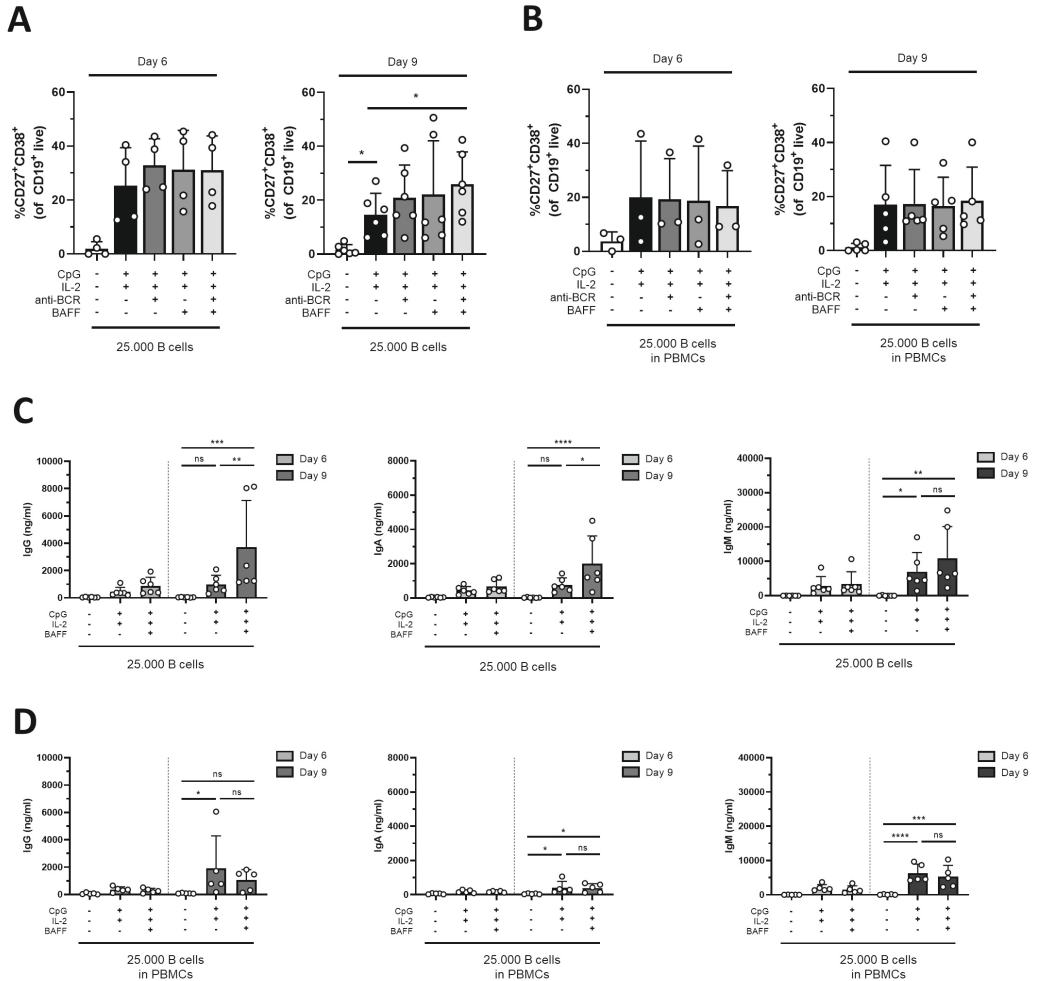


**Figure 4. Addition of BAFF in T cell independent stimulation results in increased IgG and IgA production in isolated B cell cultures.** Human primary B cells obtained from healthy donors were stimulated under conditions described in Figure 3A (condition IV) and Suppl. Fig. 4A (condition IV.2, PBMC cultures) with or without anti-BCR (anti-Ig F(ab)2 mix (5  $\mu$ g/mL) targeting IgM, IgG and IgA) and/or BAFF (100 ng/mL). Frequencies of CD27<sup>+</sup>CD38<sup>+</sup> B cells on day 6 and day 9 in **(A)** condition IV and **(B)** condition IV.2 (n = 3-5). **(C-D)** Total secretion of IgG, IgA and IgM measured in culture supernatants of eligible conditions after 6 and 9 days **(C)** without PBMCs (condition IV) and **(D)** as PBMC culture (condition IV.2). Each data point represents the mean of an individual donor with duplicate culture measurements. Mean values are represented by bars and the error bars depict SEM. P values were calculated using one-way ANOVA with Dunnett's multiple comparison test (A-B) or two-way ANOVA with Sidak's multiple comparison test (C-D). \* P  $\leq$  0.05, \*\* P  $\leq$  0.01, \*\*\* P  $\leq$  0.001, \*\*\*\* P  $\leq$  0.0001.

This negative correlation is however again reversed when anti-BCR stimulation is also added. With regards to Ig-specific secretion, the addition of IL-4 positively correlated with day 6 IgG concentrations but negatively correlated with day 9 IgG concentrations. In TI conditions, the proportion of CD27<sup>+</sup>IgG<sup>+</sup> and CD27<sup>+</sup>IgM<sup>-</sup> cells positively correlated with CD27<sup>+</sup>CD38<sup>+</sup> differentiation in all combinations of CpG, IL-2, BAFF and anti-BCR stimuli, indicating that these subsets undergo more efficient differentiation in response to these stimuli compared to other subsets. With regards to Ig-specific secretion, a higher proportion of CD27<sup>-</sup> cells at the start of culture negatively correlated with IgG and IgA secretion. Taken together, the proportion CD27<sup>+</sup> and isotype-specific subsets does significantly determine the result of TD and TI cultures.

### **Preserved *in vitro* B cell differentiation in cryopreserved PBMCs**

The decision to use fresh PBMCs or cryopreserved PBMCs for an assay or study will depend on the assay itself as well as the logistics of handling of samples. Collection of patient samples often involves freezing of samples, therefore the effect of freezing and thawing was assessed on the B cell differentiation potential in our optimized TD and TI assays. For this purpose, the B cell differentiation experiments were repeated on frozen samples of previously used healthy donors, either total PBMCs or isolated CD19<sup>+</sup> B cells from thawed PBMCs, and assessed their B cell proliferation, differentiation potential by plasmablast formation using FACS and Ig secretion. Interestingly, the CD19<sup>+</sup> counts showed an increase in TD stimulated frozen samples compared to fresh samples, although this difference was not significant (**Suppl.Fig.9A-B**). These trends were less clear in TI stimulated frozen samples (**Suppl.Fig.9C-D**). Using the culturing conditions II and II.2 described above with CD40L and IL-21 stimulation, with or without IL-4, we detected a tendency to generate less CD27<sup>+</sup>CD38<sup>+</sup> plasmablasts and subsequently lower secretion of IgG, IgA and IgM in supernatants of frozen samples after 6 and 9 days of culturing in all conditions tested, although we found no significant difference using the preferred CD40L and IL-21 stimulation (**Fig.5A-B, Suppl.Fig.10A-B**). Using the aforementioned conditions IV and IV.2 starting with 25.000 B cells and CpG and IL-2 stimulation supplemented with or without BAFF, again, we observed lower percentages of CD27<sup>+</sup>CD38<sup>+</sup> plasmablasts and IgG, IgA and IgM secretion in culture supernatants after 6 and 9 days of culturing when compared to their matched fresh sample (**Fig.5C-D, Suppl.Fig.10C-D**). Thus, B cells obtained from cryopreserved PBMCs retain their ability to differentiate after *in vitro* culturing using TD and TI stimulation though we observed a small decrease in their differentiation potential.

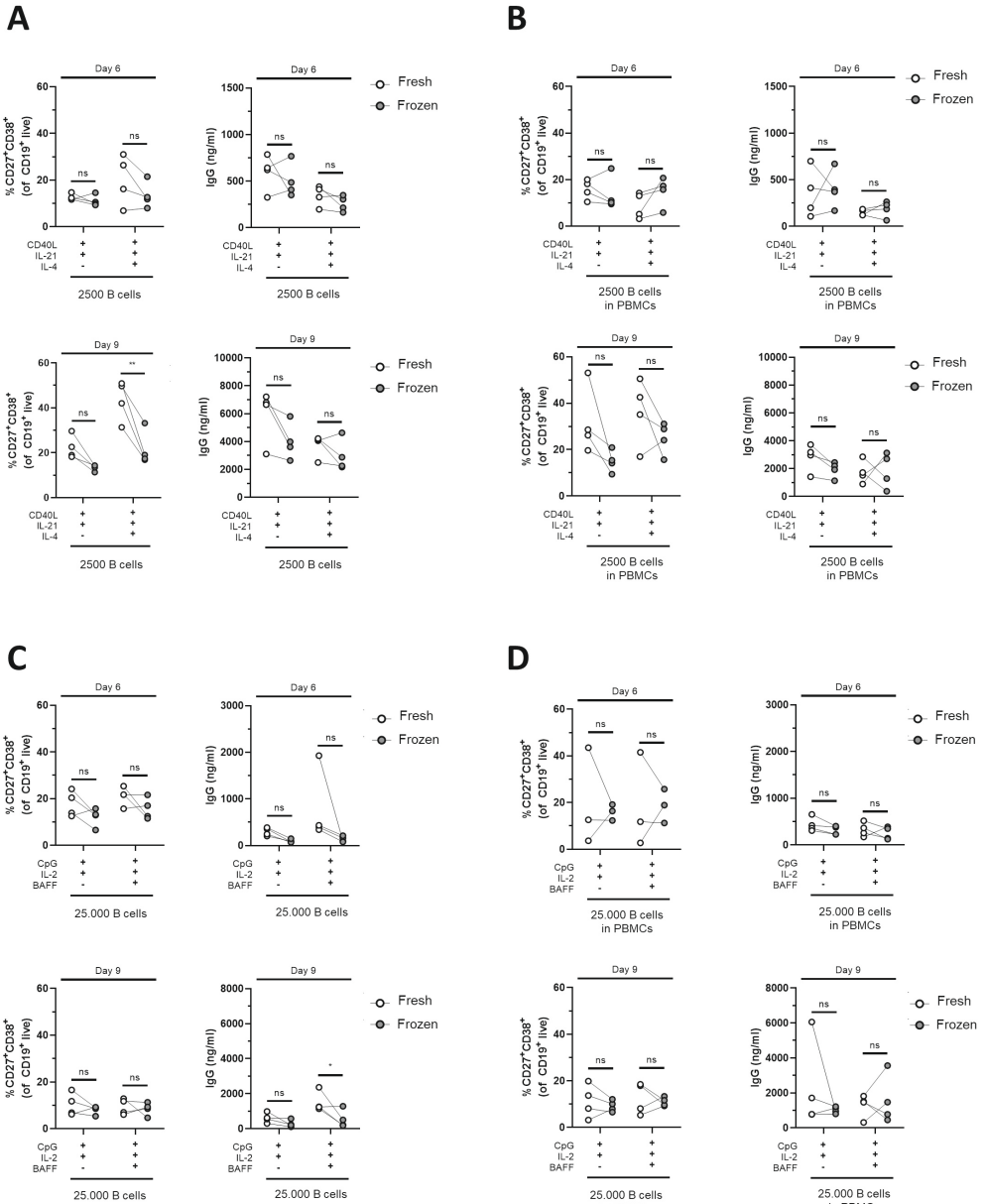


**Figure 5. Cryopreserved B cells respond similarly to freshly isolated cells in T cell dependent and independent assays.** Total human B cells were isolated from fresh PBMCs (indicated in white) or frozen PBMCs (indicated in gray) and cultured for 6 and 9 days (n=4). **(A-B)** Using T cell dependent (TD) stimuli (CD40L and IL-21 with/without IL-4) 2500 B cells (fresh and frozen) were cultured under conditions described previously **(A)** without PBMCs (condition II) and **(B)** as PBMC culture (condition II.2). Frequencies of CD27<sup>+</sup>CD38<sup>+</sup> B cells (left panel) and IgG production (right panel) on day 6 (upper graphs) and day 9 (lower graphs) are shown. **(C-D)** Using T cell independent (TI) stimuli (CpG and IL-2 with/without BAFF) 25000 B cells (fresh and frozen) were cultured under conditions described previously **(C)** without PBMCs (condition IV) and **(D)** with PBMCs (condition IV.2). Frequencies of CD27<sup>+</sup>CD38<sup>+</sup> B cells (left panel) and IgG production (right panel) on day 6 (upper graphs) and day 9 (lower graphs) are shown. Each data point represents the mean of an individual donor with duplicate culture measurements. Mean values are represented by bars and the error bars depict SEM. P values were calculated using two-way ANOVA with Sidak's multiple comparison test. \* P ≤ 0.05.

## DISCUSSION

In this study we report optimized and efficient protocols for *in vitro* B cell differentiation using both TD and TI stimulation while requiring very low numbers of B cells. This has been accomplished by comparing several factors essential for optimal expansion, proliferation and differentiation of B cells, including stimulation duration, seeding density and combinations of activating stimuli reported in various publications for *in vitro* B cell differentiation. Here, we provide a 1-step culture system starting with isolated CD19<sup>+</sup> B cells or PBMCs corrected for B cell counts. We demonstrate successful generation of plasmablasts and plasma cells by measuring different parameters, including phenotypic markers (CD27, CD38 and CD138) combined with functional characteristics (IgG, IgA and IgM secretion). Despite the small decrease in differentiation efficiency when using cryopreserved samples, there are numerous reasons why using frozen PBMCs is favored over fresh samples. The two main reasons being that patient sampling is often done in outpatient clinics that are not in close proximity to laboratory facilities where cellular assays are performed. Secondly, patient cohorts are often sampled longitudinally and to prevent assay-to-assay variation, samples are stored for prolonged periods of time and thawed simultaneously. The loss in assay sensitivity in regards to differentiation may be minimized by narrowing down the time span in which all samples are handled or by taking along a known control. However, it should be noted that controls are preferentially also frozen PBMCs and handled in a comparable manner as the patient samples. The low number of required B cells determined here is ideal as patient samples are scarce and have value for multiple immunological assays. We believe that the conclusions and recommendations from this study will provide a base for optimized protocols that can be used to study patient related differences amongst patient cohorts of B cell mediated diseases and to screen compounds that target B cell differentiation.

To date, a plethora of different conditions for inducing B cell differentiation have been published (**summarized in Table 1**). The strength of the current study is the inclusion and comparison of many variables and different stimuli. However, due to study size limitations it was not possible to include and compare all previously reported stimuli. The chosen reference stimuli for the TD assay, CD40L and IL-21, mimics the *in vivo* activation and differentiation in germinal centers (GCs), where B cells interact with CD40L and IL-21 expressing follicular T helper cells (1, 23). In our experience, CD40L-expressing fibroblasts are the strongest activators of B cells by providing sufficient CD40 binding and crosslinking (data not shown). Interestingly, in both B cell and PBMC assay different kinetics of B cell expansion, proliferation and Ig secretion were observed when the ratio of starting B cell to 3T3-CD40L feeder cell was increased. Specifically, in condition III and III.2, starting with only 250 B cells, very high levels of IgM (but limited IgG) were observed on day 9, coinciding with an increased percentage of B cells with a CD27<sup>+</sup>CD38<sup>+</sup> transitional-like phenotype. It is important to note that comparing the three conditions in terms of absolute Ig production during the 6- and 9-day culture period has its limitations as the number of B cells during these culture periods differed to great extent and this could influence the height of Ig

secretion (**Fig.1B, Suppl.Fig.2B**). In our data higher availability of CD40L resulted in increased expansion of B cells and, despite cell number differences, a higher ratio of secreted IgM compared to IgA and IgG. As many facets of B cell differentiation are linked to cell division, it is possible that the timing of isotype switching or the outgrowth of specific B cell subsets occurs differently in these culture settings. Since we studied B cell differentiation in bulk B cells and PBMCs, the specific effects of CD40L on naïve B cells, IgM<sup>+</sup>- or isotype switched-memory cells cannot be distinguished. These subsets however have been shown to have different requirements for stimulation with regard to differentiation into antibody-secreting cells (24, 25). Although we cannot make firm conclusions based on our data, it suggests and is in agreement with previous data that CD40 co-stimulation together with IL-21 regulates B cell differentiation and Ig production, and that these read-outs are driven by CD40L availability (19). However, we acknowledge that the effect of media exhaustion could also play a role in these cultures. Refreshing the culture media could lead to increased differentiation and Ig secretion, specifically in cultures with higher starting cell numbers. This was not opted for in the current study as we sought to maintain a one-step, easy and simple culture to be used in clinical studies. Concluding from our data, we choose 2500 B cells as the optimal starting number to not preferentially outgrow specific subpopulations or isotypes. In order to mimic the *in vivo* response to cognate antigen more closely, we added an anti-BCR trigger (26). However, we show that this hampers Ig detection. This has to be taken into account when these assays are applied for specific research questions where omitting an anti-BCR trigger is not desirable. The same holds true for adding IL-4 to the assays. Previously, we have shown that IL-4 addition is beneficial for B cell differentiation of naïve B cells but only in circumstances with low CD40L stimulation (19). In accordance with other studies using total CD19<sup>+</sup> B cells, we show that continuous IL-4 in our assay hampers Ig secretion compared to CD40L and IL-21 alone, indicating a lack of commitment to antibody secretion (5). Because of this we do not recommend using IL-4 when the investigating induction of plasmablast differentiation. However, as IL-4 plays a major role regarding pre-GC B cell priming and promotes class-switch to IgG4 and IgE, studies focusing on e.g. IgG4-related disease or allergy might want to use IL-4 nonetheless. IgE and IgG-subclass production were however not determined in the cultures presented here.

To mimic *in vivo* TI responses, the most commonly used stimulation is TLR-9 activation through CpG, mimicking antigen activation (**Table 1**). Activation with CpG induces proliferation of both human naïve and memory B cells (data not shown), whilst the differentiation of naïve B cells is only observed in cultures where PBMCs are present or T cell derived cytokines such as IL-2 are supplemented (17, 27). Adding to this, *in vivo* TI stimulation has been shown to result in long-lived plasma cell generation (14). This together indicates that though direct T-B interactions may not be required, a supportive microenvironment may be crucial to gain plasmablast fate and sustain plasma cell generation in TI responses *in vitro*. Condition IV with 25.000 starting B cells was identified as a minimum when stimulating isolated CD19<sup>+</sup> B cells with CpG and IL-2 due to limited

B cell survival in this culture. Considering the significant decrease of CD19<sup>+</sup> B cells between day 6 and day 9 in condition IV, we do not recommend culturing longer than 6 days, although higher amounts of immunoglobulins can be measured with a longer culture period. Re-stimulation of cells can be opted for, but this was not investigated in this study. Finally, compared to isolated B cell cultures, PBMC TI cultures showed better survival of B cells (condition IV and V versus IV.2 and V.2 (**Table 2**). Although the microenvironment provided by PBMCs may support survival there was no observation of increased differentiation.

BAFF protein is expressed by myeloid lineage cells and acts as both cell surface-associated and soluble forms (28, 29). BAFF has been shown to activate class switch recombination in human B cells, which can be enhanced by BCR crosslinking (30). Ever since, research groups have used BAFF in B cell differentiation assays but most frequently in combinatorial use with CD40 stimulation, preventing the dissection of their individual effects. In the current study, limited effects of BAFF, in addition to anti-BCR stimulation, were found on plasmablasts formation. Interestingly, a donor-dependent effect of BAFF stimulation on the Ig secretion was observed. Healthy donors, and patients, possibly differ in their expression of BAFF-responding receptors at baseline. Furthermore, because activated monocytes and T cells can also express BAFF-responding receptors, it raises the possibility that in the PBMC cultures the addition of BAFF will stimulate the rest of the PBMCs rather than the B cells. Finally, as monocytes are known to increase BAFF secretion upon TLR-9 stimulation, it is possible that these cells were already supplying sufficient BAFF to the B cells within the PBMC TI cultures (20). Altogether, although no detrimental effects of BAFF on B cell differentiation was observed in our assay, using BAFF should be complemented with appropriate analysis of its compliant receptors at baseline and throughout the assay.

The data presented here shows that for the TD condition stimulating as little as 2500 CD19<sup>+</sup> B cells with CD40L and IL-21 results in significant expansion, differentiation and secretion of IgM, IgA and IgG. For specific purposes, even lower cell numbers can be used. Interestingly, IL-4 did not affect differentiation but did significantly reduce antibody secretion. For studying TI responses, stimulating 25.000 CD19<sup>+</sup> B cells with CpG and IL-2 results in proliferation, differentiation and IgM, IgA and IgG production. We do not recommend using lower cell numbers for this condition. Interestingly, addition of BAFF resulted in significant increases of IgM, IgA and IgG production in TI CD19<sup>+</sup> B cell cultures. However, this effect is absent in PBMC cultures. Furthermore, we show that both these protocols can be performed with PBMC cultures, omitting the need for B cell isolation and thus making them highly suitable for clinical research. We do however recommend that B cell numbers are corrected using measured B cell percentages, after thawing, as these percentages are variable between donors. Furthermore, monocyte and T cell involvement in these cultures could not entirely be excluded possibly explaining mixed results when comparing this and previous studies (17, 27). In addition, we recommend determining



the B-cell subset and Ig-isotype composition in (patient) samples before culture as the proportion of CD27<sup>+</sup> and class-switched cells correlate with differentiation and Ig-secretion results. As healthy donor cells were used here, it will be interesting to monitor, for example, (longitudinal) auto-immune patient sample composition to determine if the same correlations are present and if these are affected during immunosuppressive treatment. Finally, we acknowledge that for specific research questions or patient samples it will be worthwhile to study additional B cell functions (e.g. pro- and anti-inflammatory cytokine production) (31) or to sort B cell subsets like naïve (19), memory or MZ B cells (32, 33) or IgG4-expressing cells (34). It should be taken into consideration however how much material is available, how much material will be lost upon sorting and if instead it is possible to investigate the subset of interest within PBMC cultures.

In conclusion, it is still an active area of investigation to define how autonomous factors control TD and TI responses in healthy donors or patients with B cell mediated diseases. Future research is needed to define these autonomous factors and address signaling pathways involved in both beneficial and unwanted plasma cell development. Comparing patients and healthy donors in optimized cultures and assays that detect gene expression and post-translational modifications such as phosphorylation or ubiquitination by intracellular staining methods (35) may aid in these research questions. The TD and TI assay described here in condition II (and II.2), being 2500 CD19<sup>+</sup> B cells stimulated with CD40L and IL-21, and condition IV (and IV.2), being 25.000 CD19<sup>+</sup> B cells stimulated with CpG, IL-2 and possibly BAFF, supports efficient differentiation of human primary B cells into plasma cells, with warranted B cell expansion, proliferation and quantifiable production of IgG, IgA and IgM. Due to the minimalistic nature of the protocols, results from different labs and facilities will be highly comparable. These assays will allow in-depth dissection of B cell differentiation pathways in B cells of healthy individuals and patients.

**Authorship contributions:**

J.K., C.M., D.V. designed experiments. C.M., D.V. performed experiments and analyzed data. T.R. and A.T.B. critically revised the manuscript. S.M.H. and T.W.K. devised the concept, supervised data interpretation and critically revised the manuscript. The manuscript was revised and approved by all authors.

**Acknowledgements:**

We acknowledge the support of patient partners, private partners and active colleagues of the T2B consortium; see **appendix 1** and website: [www.target-to-b.nl](http://www.target-to-b.nl). We thank Simon Tol, Erik Mul, Mark Hoogenboezem and Tom Ebbes of the Sanquin Central Facility for the maintenance and calibration of the FACS machines.

**Conflicts-of-interest disclosure:**

The authors declare that this research was conducted in the absence of commercial or financial relationships that could be construed as a potential conflict of interest.

**Funding:**

This collaboration project is financed by the PPP Allowance made available by Top Sector Life Sciences & Health to Samenwerkende Gezondheidsfondsen (SGF) under projectnumber LSHM18055-SGF to stimulate public-private partnerships and co-financing by health foundations that are part of the SGF. This project was also funded by the Landsteiner Foundation for Blood Transfusion Research—project grant number: LSBR 1609—and Sanquin Product and Process Development Call 2020.

## REFERENCES

1. Nutt SL, Hodgkin PD, Tarlinton DM, Corcoran LM. The generation of antibody-secreting plasma cells. *Nat Rev Immunol.* 2015;15(3):160-71.
2. Allman D, Wilmore JR, Gaudette BT. The continuing story of T-cell independent antibodies. *Immunol Rev.* 2019;288(1):128-35.
3. Ding BB, Bi E, Chen H, Yu JJ, Ye BH. IL-21 and CD40L synergistically promote plasma cell differentiation through upregulation of Blimp-1 in human B cells. *J Immunol.* 2013;190(4):1827-36.
4. Shulman Z, Gitlin AD, Weinstein JS, Lainez B, Esplugues E, Flavell RA, et al. Dynamic signaling by T follicular helper cells during germinal center B cell selection. *Science.* 2014;345(6200):1058-62.
5. Ettinger R, Sims GP, Fairhurst A-M, Robbins R, da Silva YS, Spolski R, et al. IL-21 Induces Differentiation of Human Naive and Memory B Cells into Antibody-Secreting Plasma Cells. *The Journal of Immunology.* 2005;175(12):7867-79.
6. Weisel FJ, Zuccarino-Catania GV, Chikina M, Shlomchik MJ. A Temporal Switch in the Germinal Center Determines Differential Output of Memory B and Plasma Cells. *Immunity.* 2016;44(1):116-30.
7. Good KL, Tangye SG. Decreased expression of Kruppel-like factors in memory B cells induces the rapid response typical of secondary antibody responses. *Proc Natl Acad Sci U S A.* 2007;104(33):13420-5.
8. Victora GD, Nussenzweig MC. Germinal centers. *Annu Rev Immunol.* 2012;30:429-57.
9. Vos Q, Lees A, Wu ZQ, Snapper CM, Mond JJ. B-cell activation by T-cell-independent type 2 antigens as an integral part of the humoral immune response to pathogenic microorganisms. *Immunol Rev.* 2000;176:154-70.
10. Huggins J, Pellegrin T, Felgar RE, Wei C, Brown M, Zheng B, et al. CpG DNA activation and plasma-cell differentiation of CD27- naive human B cells. *Blood.* 2007;109(4):1611-9.
11. Pone EJ, Lou Z, Lam T, Greenberg ML, Wang R, Xu Z, et al. B cell TLR1/2, TLR4, TLR7 and TLR9 interact in induction of class switch DNA recombination: modulation by BCR and CD40, and relevance to T-independent antibody responses. *Autoimmunity.* 2015;48(1):1-12.
12. Pone EJ, Zan H, Zhang J, Al-Qahtani A, Xu Z, Casali P. Toll-like receptors and B-cell receptors synergize to induce immunoglobulin class-switch DNA recombination: relevance to microbial antibody responses. *Crit Rev Immunol.* 2010;30(1):1-29.
13. Nothelfer K, Sansonetti PJ, Phalipon A. Pathogen manipulation of B cells: the best defence is a good offence. *Nature Reviews Microbiology.* 2015;13(3):173-84.
14. Bortnick A, Chernova I, Quinn WJ, 3rd, Mugnier M, Cancro MP, Allman D. Long-lived bone marrow plasma cells are induced early in response to T cell-independent or T cell-dependent antigens. *J Immunol.* 2012;188(11):5389-96.
15. DeFranco AL. Germinal centers and autoimmune disease in humans and mice. *Immunol Cell Biol.* 2016;94(10):918-24.
16. Urashima M, Chauhan D, Hatziyanni M, Ogata A, Hollenbaugh D, Aruffo A, et al. CD40 ligand triggers interleukin-6 mediated B cell differentiation. *Leuk Res.* 1996;20(6):507-15.
17. aan de Kerk DJ, Jansen MH, ten Berge IJ, van Leeuwen EM, Kuijpers TW. Identification of B cell defects using age-defined reference ranges for in vivo and in vitro B cell differentiation. *J Immunol.* 2013;190(10):5012-9.

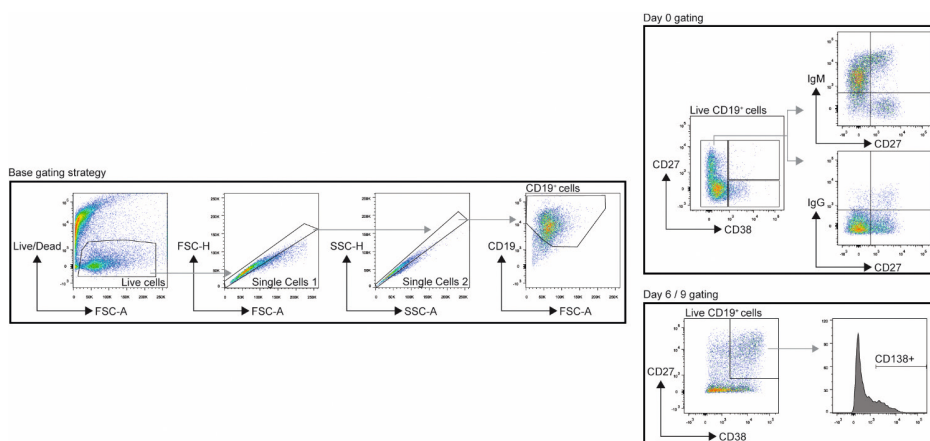
18. Bernasconi NL, Onai N, Lanzavecchia A. A role for Toll-like receptors in acquired immunity: up-regulation of TLR9 by BCR triggering in naive B cells and constitutive expression in memory B cells. *Blood*. 2003;101(11):4500-4.
19. Unger P-PA, Verstegen NJM, Marsman C, Jorritsma T, Rispens T, ten Brinke A, et al. Minimalistic In Vitro Culture to Drive Human Naive B Cell Differentiation into Antibody-Secreting Cells. *Cells*. 2021;10(5):1183.
20. Mackay F, Schneider P. Cracking the BAFF code. *Nat Rev Immunol*. 2009;9(7):491-502.
21. Smulski CR, Eibel H. BAFF and BAFF-Receptor in B Cell Selection and Survival. *Front Immunol*. 2018;9:2285.
22. Giordano D, Kuley R, Draves KE, Roe K, Holder U, Giltiay NV, et al. BAFF Produced by Neutrophils and Dendritic Cells Is Regulated Differently and Has Distinct Roles in Antibody Responses and Protective Immunity against West Nile Virus. *J Immunol*. 2020;204(6):1508-20.
23. Weinstein JS, Herman EI, Lainez B, Licona-Limón P, Esplugues E, Flavell R, et al. TFH cells progressively differentiate to regulate the germinal center response. *Nat Immunol*. 2016;17(10):1197-205.
24. Deenick EK, Avery DT, Chan A, Berglund LJ, Ives ML, Moens L, et al. Naive and memory human B cells have distinct requirements for STAT3 activation to differentiate into antibody-secreting plasma cells. *J Exp Med*. 2013;210(12):2739-53.
25. Huse K, Wogsgland CE, Polikowsky HG, Diggins KE, Smeland EB, Myklebust JH, et al. Human Germinal Center B Cells Differ from Naive and Memory B Cells in CD40 Expression and CD40L-Induced Signaling Response. *Cytometry A*. 2019;95(4):442-9.
26. Cyster JG, Allen CDC. B Cell Responses: Cell Interaction Dynamics and Decisions. *Cell*. 2019;177(3):524-40.
27. Marasco E, Farroni C, Cascioli S, Marcellini V, Scarsella M, Giorda E, et al. B-cell activation with CD40L or CpG measures the function of B-cell subsets and identifies specific defects in immunodeficient patients. *Eur J Immunol*. 2017;47(1):131-43.
28. Moore PA, Belvedere O, Orr A, Pieri K, LaFleur DW, Feng P, et al. BLYS: member of the tumor necrosis factor family and B lymphocyte stimulator. *Science*. 1999;285(5425):260-3.
29. Nardelli B, Belvedere O, Roschke V, Moore PA, Olsen HS, Migone TS, et al. Synthesis and release of B-lymphocyte stimulator from myeloid cells. *Blood*. 2001;97(1):198-204.
30. Litinskiy MB, Nardelli B, Hilbert DM, He B, Schaffer A, Casali P, et al. DCs induce CD40-independent immunoglobulin class switching through BLYS and APRIL. *Nat Immunol*. 2002;3(9):822-9.
31. Lighaam LC, Unger PA, Vredevoogd DW, Verhoeven D, Vermeulen E, Turksma AW, et al. In vitro-Induced Human IL-10(+) B Cells Do Not Show a Subset-Defining Marker Signature and Plastically Co-express IL-10 With Pro-Inflammatory Cytokines. *Front Immunol*. 2018;9:1913.
32. van Asten SD, Unger PP, Marsman C, Bliss S, Jorritsma T, Thielens NM, et al. Soluble FAS Ligand Enhances Suboptimal CD40L/IL-21-Mediated Human Memory B Cell Differentiation into Antibody-Secreting Cells. *J Immunol*. 2021;207(2):449-58.
33. Budeus B, Schweigle de Reynoso S, Przekopowicz M, Hoffmann D, Seifert M, Küppers R. Complexity of the human memory B-cell compartment is determined by the versatility of clonal diversification in germinal centers. *Proc Natl Acad Sci U S A*. 2015;112(38):E5281-9.
34. Liu C, Zhang P, Zhang W. Immunological mechanism of IgG4-related disease. *J Transl Autoimmun*. 2020;3:100047.

35. Marsman C, Jorritsma T, Ten Brinke A, van Ham SM. Flow Cytometric Methods for the Detection of Intracellular Signaling Proteins and Transcription Factors Reveal Heterogeneity in Differentiating Human B Cell Subsets. *Cells*. 2020;9(12).
36. Henn AD, Rebhahn J, Brown MA, Murphy AJ, Coca MN, Hyrien O, et al. Modulation of single-cell IgG secretion frequency and rates in human memory B cells by CpG DNA, CD40L, IL-21, and cell division. *J Immunol*. 2009;183(5):3177-87.
37. Cocco M, Stephenson S, Care MA, Newton D, Barnes NA, Davison A, et al. In vitro generation of long-lived human plasma cells. *J Immunol*. 2012;189(12):5773-85.
38. Le Gallou S, Caron G, Delaloy C, Rossille D, Tarte K, Fest T. IL-2 requirement for human plasma cell generation: coupling differentiation and proliferation by enhancing MAPK-ERK signaling. *J Immunol*. 2012;189(1):161-73.
39. Tuijnenburg P, Aan de Kerk DJ, Jansen MH, Morris B, Lieftink C, Beijersbergen RL, et al. High-throughput compound screen reveals mTOR inhibitors as potential therapeutics to reduce (auto)antibody production by human plasma cells. *Eur J Immunol*. 2020;50(1):73-85.
40. Lepse N, Land J, Rutgers A, Kallenberg CG, Stegeman CA, Abdulahad WH, et al. Toll-like receptor 9 activation enhances B cell activating factor and interleukin-21 induced anti-proteinase 3 autoantibody production in vitro. *Rheumatology (Oxford)*. 2016;55(1):162-72.
41. Jourdan M, Caraux A, De Vos J, Fiol G, Larroque M, Cognot C, et al. An in vitro model of differentiation of memory B cells into plasmablasts and plasma cells including detailed phenotypic and molecular characterization. *Blood*. 2009;114(25):5173-81.
42. Cao Y, Gordic M, Kobold S, Lajmi N, Meyer S, Bartels K, et al. An optimized assay for the enumeration of antigen-specific memory B cells in different compartments of the human body. *J Immunol Methods*. 2010;358(1-2):56-65.
43. Sundström Y, Shang MM, Panda SK, Grönwall C, Wermeling F, Gunnarsson I, et al. Identifying novel B-cell targets for chronic inflammatory autoimmune disease by screening of chemical probes in a patient-derived cell assay. *Transl Res*. 2021;229:69-82.

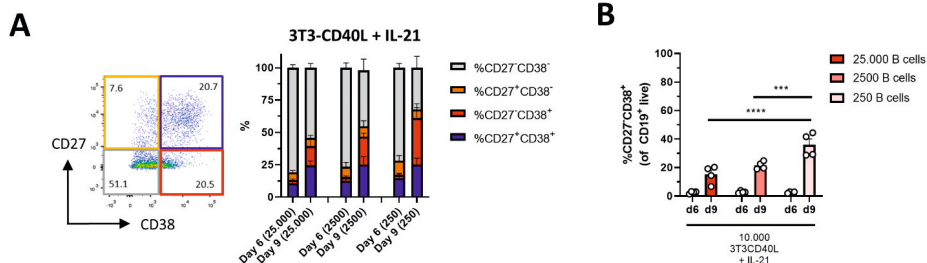
## SUPPLEMENTARY MATERIAL

### Optimized protocols for in vitro T cell-dependent and T cell-independent activation for B cell differentiation studies using limited cells

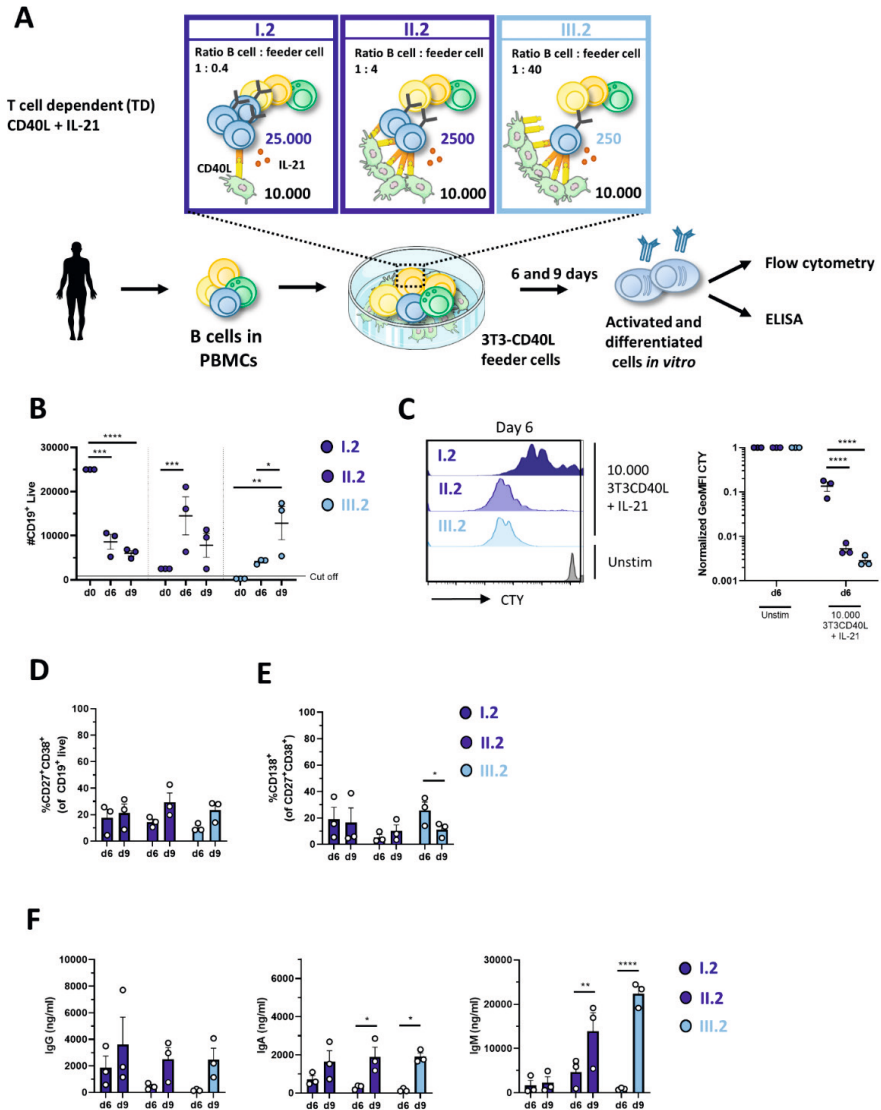
Marsman, Verhoeven et al.



**Supplemental Figure 1. Flow cytometry gating strategy.** Total lymphocytes were first gated on a forward scatter (FSC-A) versus Live/Dead plot and then gated on single cells using both FSC-H/FSC-A and SSC-H/SSC-A plots. Next, CD19<sup>+</sup> B cells were gated and subsets of interest were gated within the CD19<sup>+</sup> B cells. On day 0 the initial characterization of the B cell compartment was performed, including pre-existing CD27<sup>+</sup> CD38<sup>+</sup> plasmablasts, CD27<sup>-</sup> CD38<sup>+</sup> and CD27<sup>hi</sup> CD38<sup>-</sup> B cells. IgM and IgG expression within the CD27<sup>hi</sup> CD38<sup>-</sup> B cells was used to determine the naïve, non-switched memory and switched memory population at baseline. On day 6 and day 9 CD27<sup>-</sup> CD38<sup>+</sup> plasmablasts and CD27<sup>+</sup> CD38<sup>+</sup> CD138<sup>+</sup> plasma cells were analyzed.

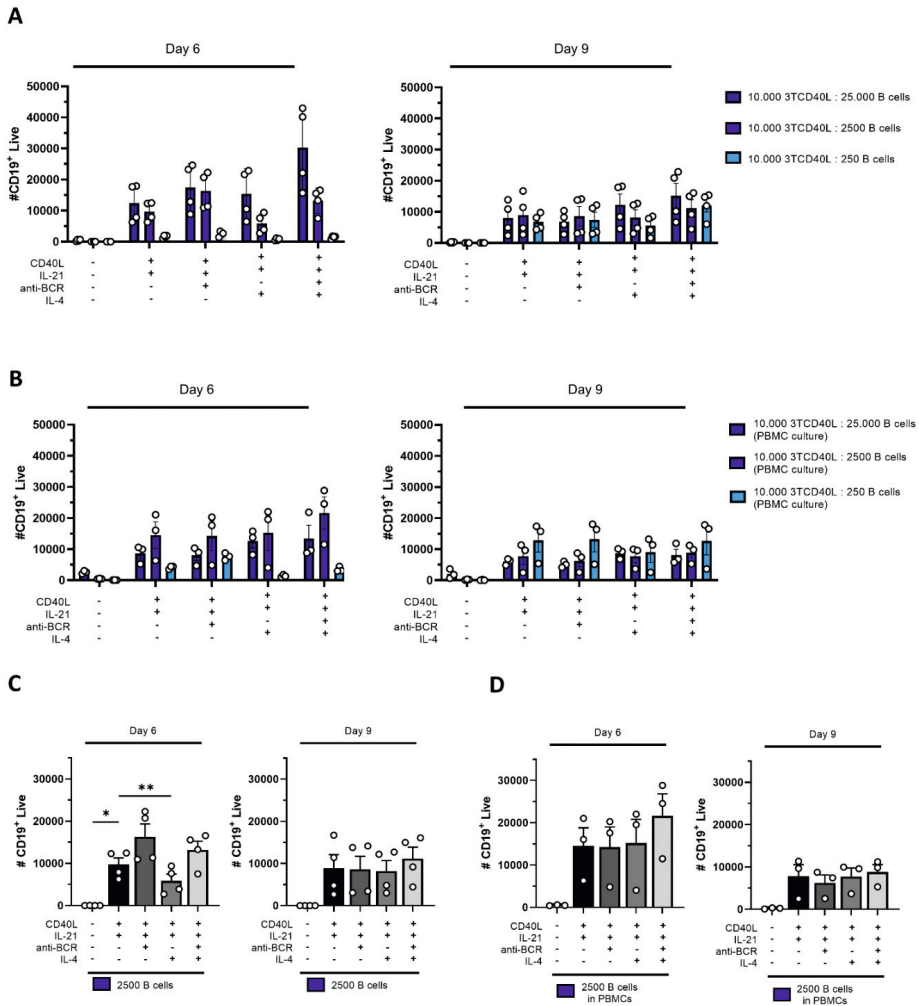


**Supplemental Figure 2. CD27 and CD38 expression of stimulated primary human B cells. (A)** Representative FACS plot (left panel) show gating strategy of CD27/CD38 subpopulations and quantification of the relative percentages of CD27 and CD38 subpopulations in the total CD19<sup>+</sup> B cell population between 6 and 9 days of culture ( $n = 4$ ). **(B)** The frequency of CD27<sup>+</sup> CD38<sup>+</sup> B cells. Each data point represents the mean of an individual donor with duplicate culture measurements. Mean values are represented by bars and the error bars depict SEM. P values were calculated using two-way ANOVA with Tukey's multiple comparison test. \*\*\*  $P \leq 0.001$ , \*\*\*\*  $P \leq 0.0001$ .



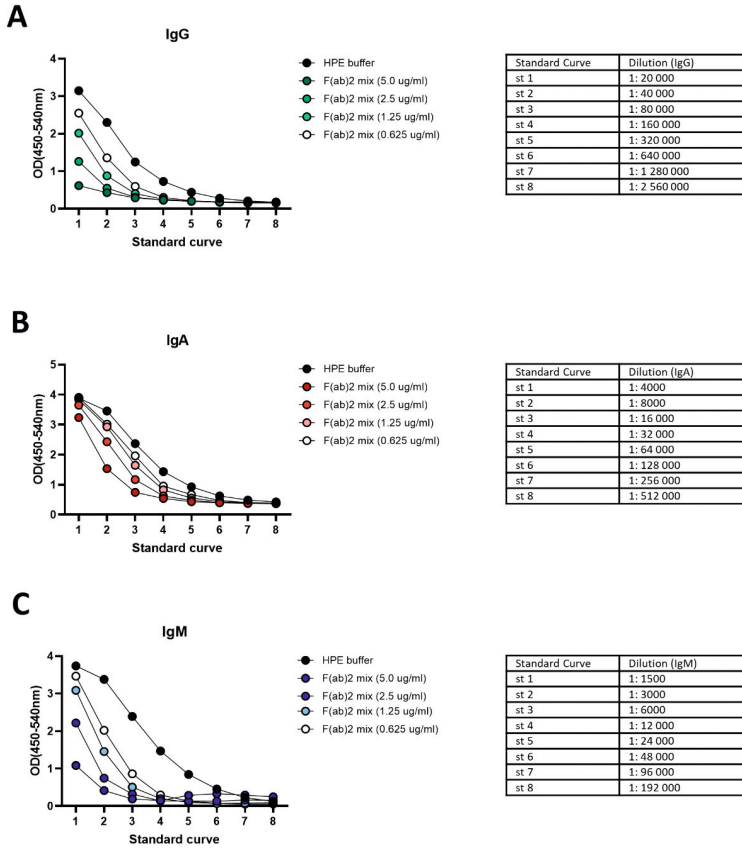
**Supplemental Figure 3. Proliferation, differentiation and antibody production of primary human CD19<sup>+</sup> B cells after T cell dependent in vitro stimulation and culturing of PBMCs. (A)** Schematic overview of the T cell dependent (TD) culture system to induce B cell differentiation. A total of 25000, 2500 or 250 CD19<sup>+</sup> human B cells in PBMCs ( $n = 3$ ) were stimulated with a human-CD40L-expressing 3T3 feeder layer and recombinant IL-21 (50 ng/mL) enabling condition I.2 (dark blue), II.2 (cobalt blue) and III.2 (light blue). Cells were analyzed at day 6 and day 9 by flow cytometry to evaluate plasmablast and plasma cell generation. The supernatant was collected at day 6 and day 9 to evaluate IgG, IgA and IgM production by ELISA. **(B)** The number of live CD19<sup>+</sup> events was analyzed using flow cytometry. A cut off of 1000 events was used to proceed with further analysis. **(C)** Representative histograms of CTY dilution (left panel) and quantification (right panel) on day 6 compared to their unstimulated condition. **(D)** The frequency of CD27<sup>+</sup>CD38<sup>+</sup> B cells and **(E)** CD27<sup>+</sup>CD38<sup>+</sup>CD138<sup>+</sup> B cells was analyzed by using flow cytometry. **(F)** IgG, IgA and IgM production in culture supernatants was evaluated by ELISA after 6 and 9 days ( $n = 3$ ). Each data point represents the mean of an individual donor with duplicate culture measurements. Mean values are represented by bars and the error bars depict SEM. P values were calculated using two-way ANOVA with Sidak's multiple comparison test. \* P

$\leq 0.05$ , \*\*  $P \leq 0.01$ , \*\*\*  $P \leq 0.001$ , \*\*\*\*  $P \leq 0.0001$ .

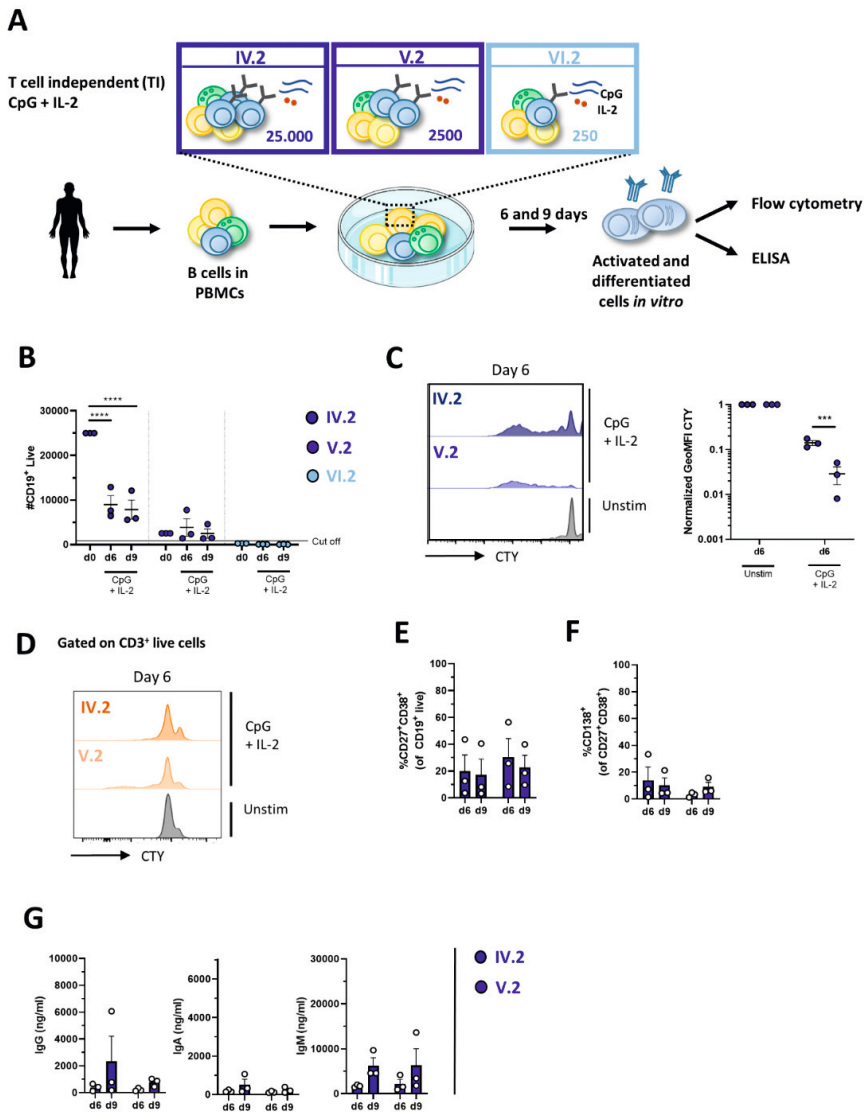


**Supplemental Figure 4. CD19<sup>+</sup> live cells in TD cultures with anti-BCR and IL-4. (A – B)** Frequencies of CD19<sup>+</sup> live cells on day 6 and day 9 in conditions described in Figure 1A (condition I, II, III) and Suppl. Fig. 3A (condition I.2, II.2, III.2) (PBMC cultures) with or without anti-BCR (anti-Ig F(ab)<sub>2</sub> mix (5 µg/mL) targeting IgM, IgG and IgA) and/or recombinant IL-4 (25 ng/mL). Frequencies of CD19<sup>+</sup> live cells on day 6 and day 9 in **(C)** condition II (n=4) and **(D)** condition II.2 (n = 3) including statistics. Each data point represents the mean of an individual donor with duplicate culture measurements. Mean values are represented by bars and the error bars depict SEM. P values were calculated using two-way ANOVA with Sidak's multiple comparison test. \*  $P \leq 0.05$ , \*\*  $P \leq 0.01$ .

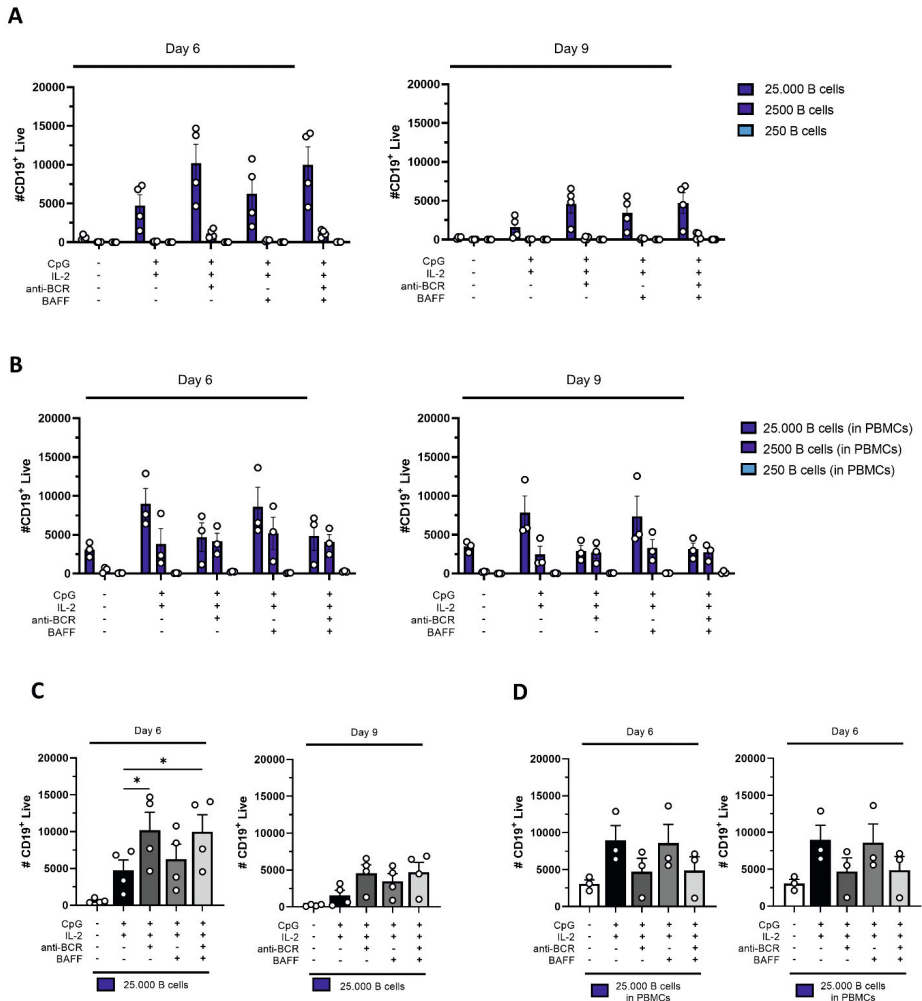




**Supplemental Figure 5. Anti-IgA/G/M F(ab')<sub>2</sub> fragments interfere with ELISA readouts.** Interference of F(ab')<sub>2</sub> fragment Goat Anti-Human IgA/G/M in **(A)** IgG, **(B)** IgA and **(C)** IgM ELISA. Serial dilutions of F(ab')<sub>2</sub> fragments (5, 2.5, 1.25 and 0.625 µg/mL) were added to the standard curve dilutions as indicated. Black lines indicate no F(ab')<sub>2</sub> fragments added.

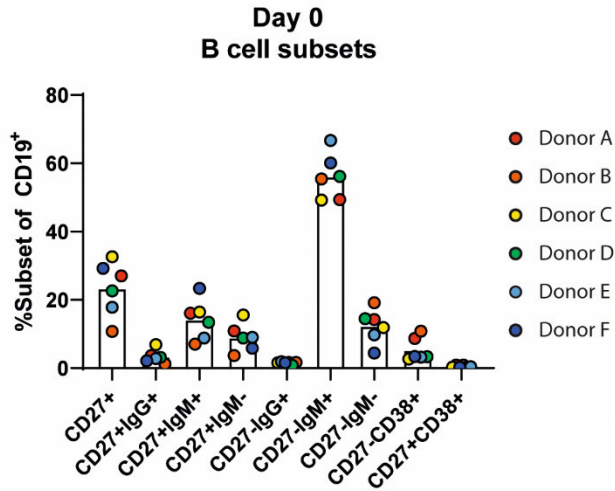


**Supplemental Figure 6. Proliferation, differentiation and antibody production primary human CD19<sup>+</sup> B cells after T cell independent *in vitro* stimulation and culturing of PBMCs. (A)** Schematic overview of the T cell independent (TI) culture system to induce B cell differentiation. A total of 25000, 2500 or 250 CD19<sup>+</sup> human B cells and PBMCs ( $n = 3$ ) were stimulated with CpG ( $1 \mu\text{M}$ ) and IL-2 ( $50 \text{ ng/ml}$ ) enabling condition IV.2 (dark blue), V.2 (cobalt blue) and VI.2 (light blue). Cells were analyzed at day 6 and day 9 by flow cytometry to evaluate plasmablast and plasma cell generation. The supernatant was collected at day 6 and day 9 to evaluate IgG, IgA and IgM production by ELISA. **(B)** The number of live CD19<sup>+</sup> events was analyzed using flow cytometry. A cut off of 1000 events was used to proceed with further analysis. **(C)** Representative histogram of CTY dilution (left panel) and quantification (right panel) of condition IV.2 and V.2 on day 6 compared to their unstimulated condition. **(D)** Analysis of proliferation by CTY dilution of CD3<sup>+</sup> T cells in condition IV.2 and V.2 on day 6. **(E)** The frequency of CD27<sup>+</sup>CD38<sup>+</sup> B cells and **(F)** CD27<sup>+</sup>CD38<sup>+</sup>CD138<sup>+</sup> B cells. **(G)** IgG, IgA and IgM production in culture supernatants was evaluated by ELISA after 6 and 9 days ( $n = 4$ ). Each data point represents the mean of an individual donor with duplicate culture measurements. Mean values are represented by bars and the error bars depict SEM. P values were calculated using two-way ANOVA with Sidak's multiple comparison test. \*  $P \leq 0.05$ , \*\*  $P \leq 0.01$ , \*\*\*  $P \leq 0.001$ , \*\*\*\*  $P \leq 0.0001$ .

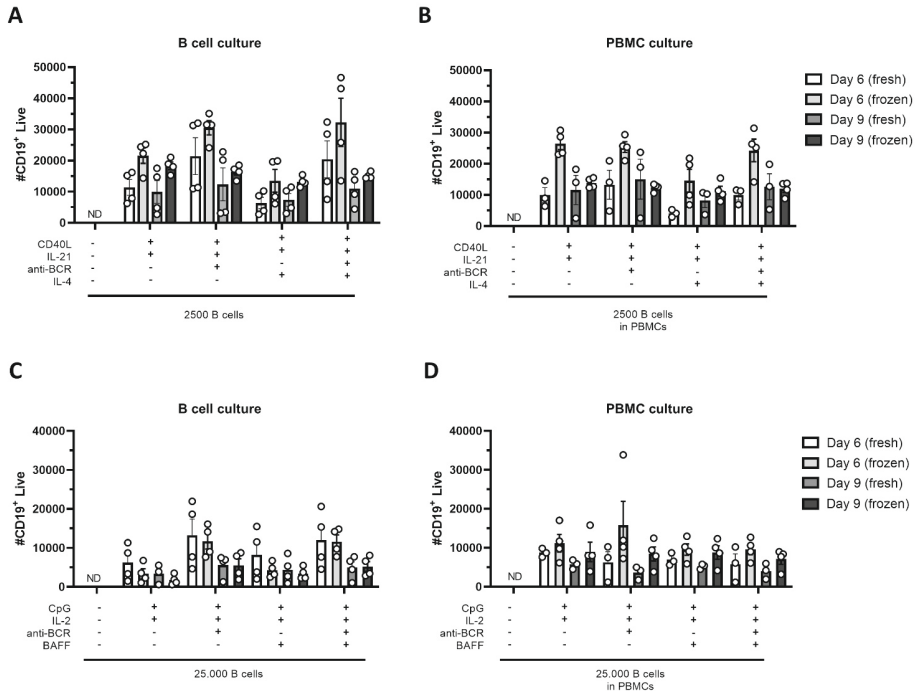


**Supplemental Figure 7. CD19<sup>+</sup> live cells in TI cultures with anti-BCR and BAFF. (A - B)** Frequencies of CD19<sup>+</sup> live cells on day 6 and day 9 in conditions described in Figure 3A (condition IV, V, VI) and Suppl. Fig. 6A (condition IV.2, V.2, VI.2) (PBMC cultures) with or without anti-BCR (anti-Ig F(ab)2 mix (5 µg/mL) targeting IgM, IgG and IgA) and/or BAFF (100 ng/mL). Frequencies of CD19<sup>+</sup> live cells on day 6 and day 9 in **(C)** condition IV (n=4) and **(D)** condition IV.2 (n=3) including statistics. Each data point represents the mean of an individual donor with duplicate culture measurements. Mean values are represented by bars and the error bars depict SEM. P values were calculated using two-way ANOVA with Sidak's multiple comparison test. \* P ≤ 0.05.

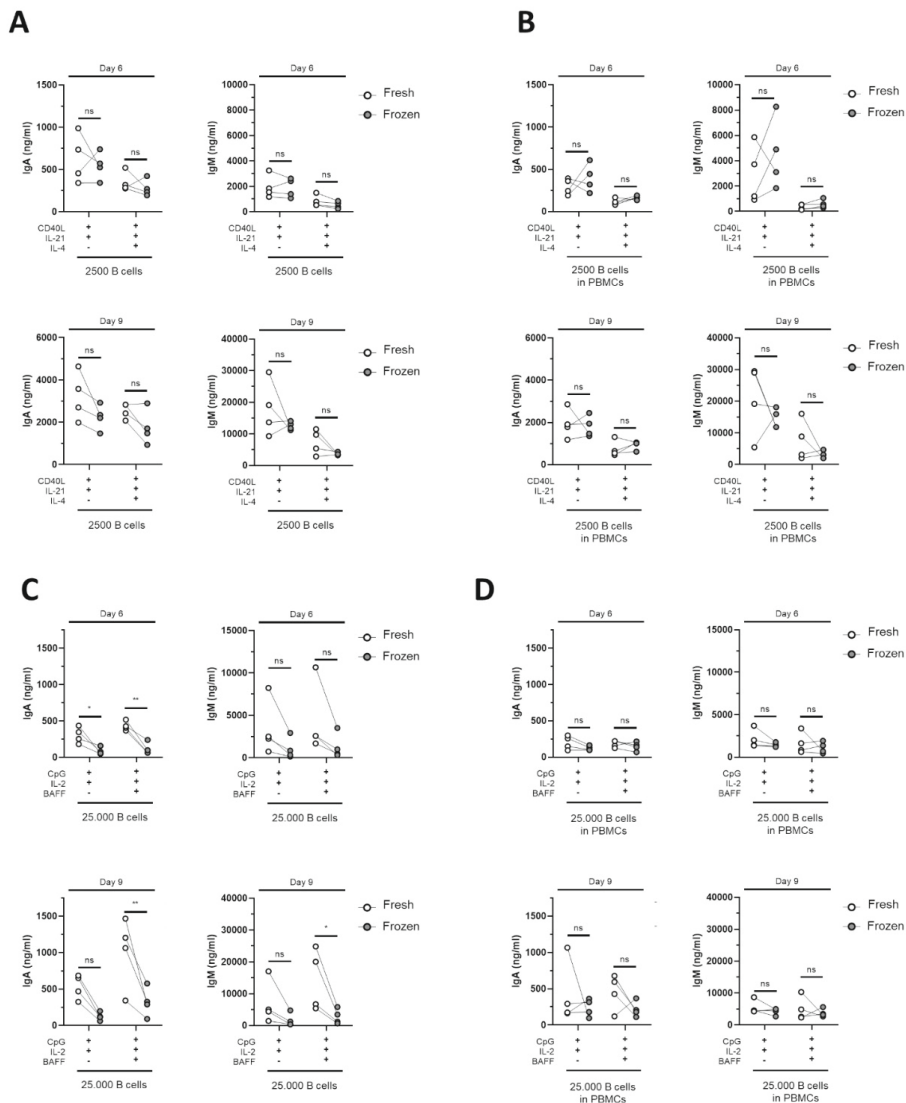
Donor	CD27+	CD27+IgG+	CD27+IgM+	CD27+IgM-	CD27-IgG+	CD27-IgM+	CD27-IgM-	CD27-CD38+	CD27+CD38+
<b>A</b>	27,066	3,688	16,117	10,884	1,732	49,383	14,219	8,676	0,881
<b>B</b>	10,779	1,214	7,017	3,699	1,690	55,441	19,192	10,826	0,904
<b>C</b>	32,601	6,886	16,463	15,582	1,574	49,220	11,932	2,669	0,294
<b>D</b>	22,632	3,190	13,462	8,857	0,831	56,180	14,488	3,365	0,305
<b>E</b>	17,830	2,855	8,827	9,047	1,933	66,667	9,750	3,206	0,439
<b>F</b>	29,227	2,189	23,347	5,837	1,545	60,085	4,421	3,433	0,300



**Supplemental Figure 8. Characterization of the B cell compartment at day 0.** On day 0 the initial characterization of the B cell compartment of donor A-F was performed (for gating strategy see Suppl. Fig. 1), including pre-existing CD27<sup>+</sup> CD38<sup>+</sup> plasmablasts, CD27<sup>-</sup> CD38<sup>+</sup> and CD27<sup>+</sup> B cells. IgM and IgG expression within the CD27<sup>+</sup> CD38<sup>-</sup> B cells was used to determine the naive, non-switched memory and switched memory distribution at baseline. These baseline % were used for correlation analysis (see Suppl. Table 1 and 2).

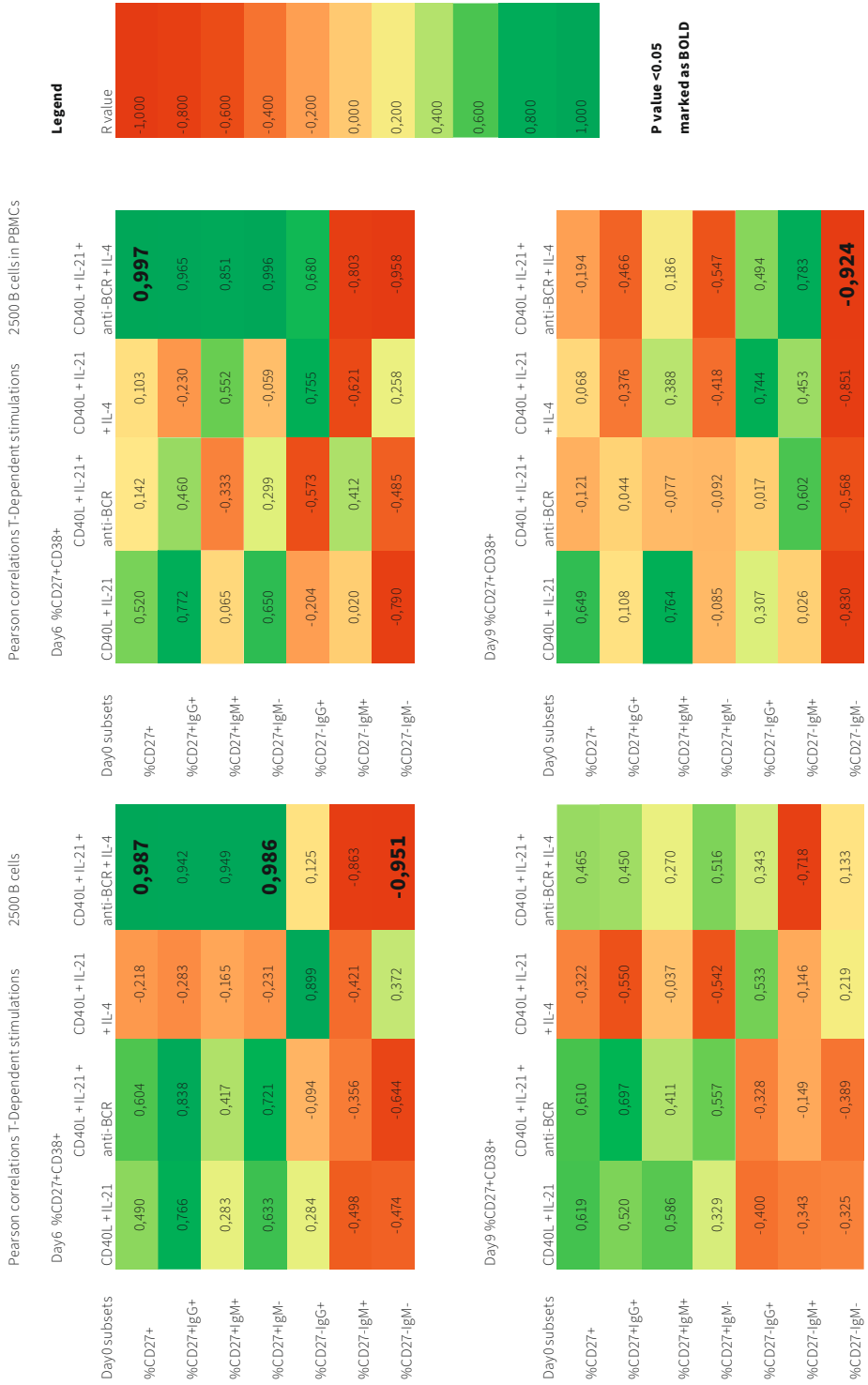


**Supplemental Figure 9. Frequencies of CD19<sup>+</sup> live cells in TD and TI cultures using cryopreserved and freshly isolated B cells.** Frequencies of CD19<sup>+</sup> live cells measured by flowcytometry from cultures with B cells isolated from fresh PBMCs or frozen PBMCs which were cultured for 6 and 9 (A-B) with TD stimuli with and without PBMCs (condition II and II.2) or (C-D) with TI stimuli (condition IV and IV.2). ND = not determined.



**Supplemental Figure 10. Cryopreserved and freshly isolated B cells produce similar amounts of antibodies in T cell dependent and independent assays.**

Comparison of IgA and IgM production of B cells isolated freshly from PBMCs or from cryopreserved PBMCs obtained from the same healthy donor ( $n=4$ ). Total human B cells were isolated from fresh PBMCs (indicated in white) or frozen PBMCs (indicated in gray) and cultured for 6 and 9 days. **(A-B)** Using T cell dependent (TD) stimuli (CD40L and IL-21 with/without IL-4) 2500 B cells (fresh and frozen) were cultured under conditions described previously **(A)** without PBMCs (condition II) and **(B)** with PBMCs (condition II.2). IgA (left panel) and IgM production (right panel) on day 6 (upper graphs) and day 9 (lower graphs) are shown. **(C-D)** Using T cell independent (TI) stimuli (CpG and IL-2 with/without BAFF) 25,000 B cells (fresh and frozen) were cultured under conditions described previously **(C)** without PBMCs (condition IV) and **(D)** with PBMCs (condition IV.2). IgA (left panel) and IgM production (right panel) on day 6 (upper graphs) and day 9 (lower graphs) are shown. Each data point represents the mean of an individual donor with duplicate culture measurements. Mean values are represented by bars and the error bars depict SEM. P values were calculated using two-way ANOVA with Sidak's multiple comparison test. \*  $P \leq 0.05$ , \*\*  $P \leq 0.01$ .



Day0 subsets	ELISA IgG Day6		ELISA IgG Day9		ELISA IgG Day9	
	CD40L + IL-21 + IL-4	CD40L + IL-21 + IL-4	CD40L + IL-21 + IL-4	CD40L + IL-21 + IL-4	CD40L + IL-21 + IL-4	CD40L + IL-21 + IL-4
%CD27+	-0,052	0,401	0,420	-0,100	0,410	0,876
%CD27+IgG+	-0,139	0,556	0,436	-0,450	-0,198	0,511
%CD27+IgM+	0,103	0,215	0,356	0,223	0,623	0,664
%CD27+IgM-	-0,269	0,450	0,282	-0,485	-0,225	0,414
%CD27+IgG+	-0,638	0,387	0,139	0,550	0,659	0,445
%CD27-IgM+	-0,578	-0,793	-0,774	-0,127	-0,057	-0,547
%CD27-IgM-	0,494	0,149	0,136	-0,047	-0,584	-0,314

Day0 subsets	ELISA IgM Day6		ELISA IgM Day9		ELISA IgM Day9	
	CD40L + IL-21 + IL-4	CD40L + IL-21 + IL-4	CD40L + IL-21 + IL-4	CD40L + IL-21 + IL-4	CD40L + IL-21 + IL-4	CD40L + IL-21 + IL-4
%CD27+	0,409	0,156	0,348	-0,354	0,870	-0,259
%CD27+IgG+	0,488	-0,356	-0,051	-0,734	0,415	-0,312
%CD27+IgM+	0,251	0,548	0,585	0,119	0,789	0,018
%CD27+IgM-	0,393	-0,457	-0,157	<b>-0,841</b>	0,211	-0,426
%CD27-IgG+	<b>-0,843</b>	0,365	-0,080	-0,319	0,121	0,189
%CD27-IgM+	-0,253	0,222	0,493	0,450	-0,317	0,815
%CD27-IgM-	-0,030	-0,586	<b>-0,842</b>	-0,177	-0,564	-0,791



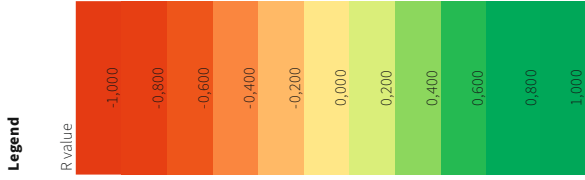
Day0 subsets	ELISA IgA Day6		ELISA IgA Day9		ELISA IgA Day9	
	CD40L + IL-21	CD40L + IL-21 + IL-4	CD40L + IL-21	CD40L + IL-21 + IL-4	CD40L + IL-21	CD40L + IL-21 + IL-4
%CD27+	0.708	0.862	0.520	0.411	0.520	0.411
%CD27+IgG+	0.609	0.853	0.731	-0.317	0.731	-0.317
%CD27+IgM+	0.327	0.420	0.143	0.806	0.143	0.806
%CD27+IgM-	0.638	0.716	0.577	-0.510	0.577	-0.510
%CD27-IgG+	0.369	0.092	0.017	0.113	0.017	0.113
%CD27-IgM+	-0.825	-0.603	-0.165	0.266	-0.165	0.266
%CD27-IgM-	0.266	-0.075	-0.214	<b>-0.930</b>	-0.214	<b>-0.930</b>

Pearson correlations T-independent stimulations 2500 B cells

Day0 subsets	Day6 %CD27+CD38+			
	CpG + IL-2	CpG + IL-2 + anti-BCR	CpG + IL-2 + BAFF	CpG + IL-2 + anti-BCR + BAFF
%CD27+	0,638	0,592	0,455	0,477
%CD27+IgG+	0,757	0,733	0,616	0,647
%CD27+IgM+	0,523	0,466	0,326	0,340
%CD27+IgM-	0,523	0,466	0,326	0,340
%CD27-IgG+	-0,552	-0,543	-0,616	-0,574
%CD27-IgM+	-0,118	-0,081	0,077	0,035
%CD27-IgM-	-0,738	-0,694	-0,573	-0,589

Pearson correlations T-independent stimulations 2500 B cells in PBMCs

Day0 subsets	Day6 %CD27+CD38+			
	CpG + IL-2	CpG + IL-2 + anti-BCR	CpG + IL-2 + BAFF	CpG + IL-2 + anti-BCR + BAFF
%CD27+	0,780	0,887	0,774	0,894
%CD27+IgG+	0,943	0,990	0,939	0,992
%CD27+IgM+	0,402	0,572	0,393	0,586
%CD27+IgM-	0,871	0,950	0,866	0,955
%CD27-IgG+	0,143	0,332	0,133	0,348
%CD27-IgM+	-0,322	-0,500	-0,313	-0,514
%CD27-IgM-	-0,952	-0,993	-0,949	-0,995



**P value <0.05 marked as BOLD**

Pearson correlations T-independent stimulations 2500 B cells

Day0 subsets	Day9 %CD27+CD38+			
	CpG + IL-2	CpG + IL-2 + anti-BCR	CpG + IL-2 + BAFF	CpG + IL-2 + anti-BCR + BAFF
%CD27+	0,464	0,721	0,415	0,388
%CD27+IgG+	<b>0,826</b>	<b>0,910</b>	0,737	<b>0,819</b>
%CD27+IgM+	0,059	0,331	0,066	-0,079
%CD27+IgM-	0,771	<b>0,884</b>	0,662	<b>0,824</b>
%CD27-IgG+	-0,380	-0,462	-0,640	-0,421
%CD27-IgM+	-0,803	-0,551	-0,528	-0,364
%CD27-IgM-	0,378	-0,070	0,230	0,170

Day0 subsets	Day9 %CD27+CD38+			
	CpG + IL-2	CpG + IL-2 + anti-BCR	CpG + IL-2 + BAFF	CpG + IL-2 + anti-BCR + BAFF
%CD27+	0,617	0,620	0,474	0,489
%CD27+IgG+	0,735	<b>0,947</b>	0,654	<b>0,889</b>
%CD27+IgM+	0,250	0,055	0,142	-0,049
%CD27+IgM-	0,578	0,860	0,517	0,808
%CD27-IgG+	0,131	0,111	0,275	0,194
%CD27-IgM+	-0,217	-0,491	-0,041	-0,313
%CD27-IgM-	-0,217	-0,491	-0,041	-0,313

ELISA IgG Day6		ELISA IgG Day9			ELISA IgM Day6			ELISA IgM Day9		
Day0 subsets	CpG + IL-2	CpG + IL-2 + BAFF	CpG + IL-2	CpG + IL-2 + BAFF	CpG + IL-2	CpG + IL-2 + BAFF	CpG + IL-2	CpG + IL-2 + BAFF	CpG + IL-2	CpG + IL-2 + BAFF
%CD27+	0,721	0,535	0,404	0,322	0,503	0,573	0,000	-0,088	0,594	0,544
%CD27+IgG+	<b>0,932</b>	0,557	0,776	0,634	0,799	0,597	-0,473	-0,718	<b>0,915</b>	0,340
%CD27+IgM+	0,373	0,271	0,035	0,022	0,097	0,386	-0,823	-0,295	-0,014	0,142
%CD27+IgM-	<b>0,826</b>	0,636	0,690	0,545	0,794	0,458	0,414	0,511	0,847	0,229
%CD27-IgG+	-0,082	-0,135	-0,363	-0,706	0,599	0,442	-0,612	-0,867	0,270	0,561
%CD27-IgM+	-0,558	-0,797	-0,191	-0,420	-0,460	-0,159	-0,823	-0,295	-0,390	0,270
%CD27-IgM-	-0,153	0,237	-0,056	0,226	-0,014	-0,487	-0,196	-0,736	0,046	-0,643
Day0 subsets <th>CpG + IL-2</th> <th>CpG + IL-2 + BAFF</th> <th>CpG + IL-2</th> <th>CpG + IL-2 + BAFF</th> <th>CpG + IL-2</th> <th>CpG + IL-2 + BAFF</th> <th>CpG + IL-2</th> <th>CpG + IL-2 + BAFF</th> <th>CpG + IL-2</th> <th>CpG + IL-2 + BAFF</th>	CpG + IL-2	CpG + IL-2 + BAFF	CpG + IL-2	CpG + IL-2 + BAFF	CpG + IL-2	CpG + IL-2 + BAFF	CpG + IL-2	CpG + IL-2 + BAFF	CpG + IL-2	CpG + IL-2 + BAFF
%CD27+	0,243	0,252	0,237	-0,257	0,503	0,573	0,000	-0,088	0,503	0,544
%CD27+IgG+	-0,320	-0,365	-0,316	-0,722	-0,263	-0,187	-0,473	-0,718	0,799	0,597
%CD27+IgM+	0,636	0,670	0,620	0,249	0,877	<b>0,903</b>	0,414	0,511	0,097	0,386
%CD27+IgM-	-0,420	-0,447	-0,420	-0,830	-0,476	-0,409	-0,612	-0,867	0,794	0,458
%CD27-IgG+	0,039	0,112	-0,410	0,076	-0,078	-0,134	-0,823	-0,295	0,599	0,442
%CD27-IgM+	0,429	0,369	0,367	0,257	0,133	0,045	0,146	0,557	-0,460	-0,159
%CD27-IgM-	-0,777	-0,758	-0,646	-0,207	-0,837	-0,784	-0,196	-0,736	-0,014	-0,487

Day0 subsets	ELISA IgA Day6			ELISA IgA Day9			ELISA IgA Day9		
	CpG + IL-2	CpG + IL-2 + BAFF	CpG + IL-2 + BAFF	CpG + IL-2	CpG + IL-2 + BAFF	CpG + IL-2	CpG + IL-2 + BAFF	CpG + IL-2 + BAFF	CpG + IL-2 + BAFF
%CD27+	0,270	0,406	0,503	0,402	0,402	0,520	0,520	-0,059	-0,059
%CD27+IgG+	<b>0,723</b>	<b>0,714</b>	<b>0,748</b>	<b>0,721</b>	<b>0,721</b>	<b>0,940</b>	<b>0,940</b>	0,257	0,257
%CD27+IgM+	-0,108	0,070	0,206	0,078	0,078	-0,055	-0,055	-0,205	-0,205
%CD27+IgM-	0,633	0,642	0,637	0,621	0,621	0,857	0,857	0,205	0,205
%CD27-IgG+	-0,358	-0,630	-0,459	-0,534	-0,534	-0,029	-0,029	0,566	0,566
%CD27-IgM+	-0,203	-0,314	-0,217	-0,265	-0,265	-0,452	-0,452	0,475	0,475
%CD27-IgM-	0,089	0,070	-0,157	0,008	0,008	0,202	0,202	-0,509	-0,509

**Appendix 1. T2B consortium members**

## PhD/Postdocs

Name	Institute
Mrs. Annabel Ruiten	LUMC
Mrs. Linda van der Weele	AMC
Mrs. Karoline Kielbassa	AMC
Mrs. Mariateresa Coppola	VUMC
Mrs. Dorit Verhoeven	AMC
Mrs. Jyaysi Desai	LUMC
Mrs. Mirjam van der Burg	LUMC
Mrs. Esther Vletter	LUMC
Mrs. Maaïke Braham	RIVM
Mr. Matthias Busch	MUMC
Mr. Carlo Bonasia	UMCG
Mrs. Elisabeth Raveling	UMCG
Mrs. Ruth Huizinga	ErasmusMC
Mr. Niels Verstegen	Sanquin
Mr. Casper Marsman	Sanquin
Mrs. Sabrina Pollastro	Sanquin
Mr. Koos van Dam	AMC
Mr. Laurent Paardekooper	LUMC
Mrs. Renée Ysermans	MUMC
Mrs. Odilia Corneth	ErasmusMC
Mrs. Annemarie Buisman	RIVM
Mr. Rob van Binnendijk	(RIVM)
Mrs Pauline van Schouwenburg	(LUMC)
Mr. Marvyn Koning	LUMC
Mr. Luuk Wieske	AMC

## Fundamental partners (Group leaders / division heads)

Name	Institute
Dr. Lisa van Baarsen	AMC
Prof. dr. Nico Bos	UMCG
Dr. Anja ten Brinke	Sanquin
Dr. Eric Eldering	AMC
Dr Cecile van Els	RIVM
Prof. dr. Marieke van Ham	Sanquin
Prof. dr. Peter Heeringa	UMCG
Prof. dr. Rudi Hendriks	ErasmusMC
Dr. Maartje Huijbers	LUMC
Dr. Ruth Huizinga	ErasmusMC

Prof. dr. Reina Mebius	VUMC
Dr. Theo Rispens	Sanquin
Prof. dr. Rene Toes	LUMC
Dr. Jelle de Wit	RIVM
Dr. Jan Damoiseaux	MUMC
Dr. Wayel Abdulahad	UMCG

## Clinical partners

Name	Institute
Dr. Filip Eftimov	AMC
Dr. Casper Franssen	UMCG
Prof. dr. Jaap Groothoff	AMC
Prof. dr. Bart Jacobs	ErasmusMC
Dr. Barbara Horvath	UMCG
Prof. dr. Arnon Kater	AMC
Dr. Joep Killestein	VUMC
Prof. dr. Taco Kuijpers	AMC
Dr. Karina de Leeuw	UMCG
Dr. L Oosten	LUMC
Dr. Pieter van Paassen	UMC Maastricht
Dr. Bram Rutgers	UMCG
Dr. Uli Scherer	LUMC
Dr. Maarten Titulaer	ErasmusMC
Prof. dr. Jan Verschuuren	LUMC
Dr. Niek de Vries	AMC
Dr. Diane van der Woude	LUMC
Dr. Josephine Vos	AMC
Prof. dr. Hendrik Veelken	LUMC







# CHAPTER 3

## Flow Cytometric Methods for the Detection of Intracellular Signaling Proteins and Transcription Factors Reveal Heterogeneity in Differentiating Human B Cell Subsets

Casper Marsman, Tineke Jorritsma, Anja ten Brinke and S. Marieke van Ham

*Cells (2020), 9(12):2633*

## ABSTRACT

Flow cytometric detection of intracellular (IC) signaling proteins and transcription factors (TFs) will help elucidate the regulation of B cell survival, proliferation and differentiation. However, simultaneous detection of signaling proteins or TFs, with membrane markers (MM) can be challenging as required fixation and permeabilization procedures can affect functionality of conjugated antibodies. Here, a phosphoflow method is presented for detection of activated NF- $\kappa$ B p65 and phosphorylated STAT1, STAT3, STAT5 and STAT6 together with B cell differentiation MM CD19, CD27 and CD38. Additionally, a TF-flow method is presented that allows detection of B cell TFs; PAX5, c-MYC, BCL6, AID and antibody-secreting cell (ASC) TFs BLIMP1 and XBP-1s together with MM. Applying these methods on *in vitro* induced human B cell differentiation cultures showed significantly different steady-state levels, and responses to stimulation, of phosphorylated signaling proteins in CD27-expressing B cell and ASC populations. The TF-flow protocol and UMAP analysis revealed heterogeneity in TF-expression within stimulated CD27 or CD38-expressing B cell subsets. The methods presented here allow for sensitive analysis of STAT and NF- $\kappa$ B p65 signaling and TFs together with B cell differentiation MM at single-cell resolution. This will aid further investigation of B cell responses in both health and disease.

## INTRODUCTION

One of the cornerstones of the adaptive immune system is the ability of B cells to respond to pathogens and differentiate into antibody-secreting cells. The generation of antibody-secreting cells (ASCs) is mainly regulated by follicular T helper cells [1, 2] ( $T_{FH}$ ) within germinal centers [3] (GCs) and are crucial for the development of high affinity antibodies [4, 5]. B cells are activated upon antigen recognition by the B cell receptor (BCR). Subsequently the antigen is internalized and presented on MHC-II in order to form a cognate interaction with the  $T_{FH}$  cell [6]. This interaction provides multiple stimuli indispensable for GC B cell proliferation and differentiation, such as membrane-bound CD40L that activates CD40 on the B cell [7, 8] and the  $T_{FH}$  hallmark cytokine IL-21 that binds to the IL-21 receptor [9–11]. Furthermore,  $T_{FH}$  cells are also able to produce IL-4 [12, 13] which contributes to class-switching and proper GC formation in combination with IL-21 [14–16]. When CD40L binds CD40 on the B cell surface, it induces activation of NF- $\kappa$ B p65 (canonical, heterodimerizes with NF- $\kappa$ B1) and NF- $\kappa$ B p52 (non-canonical, also known as NF- $\kappa$ B2) pathways [17–19]. The secreted cytokines IL-4 and IL-21 bind to their respective receptors and induce JAK-STAT pathways. IL-4 induces phosphorylation of STAT6 [20]–[22] whereas IL-21 mainly induces phosphorylation of STAT1, STAT3 and, to a lesser extent, STAT5 [22], [23]. After phosphorylation events, these signaling proteins translocate to the nucleus where they can regulate transcription [24, 25]. The induction of both NF- $\kappa$ B and STAT pathways are essential as mutations in involved genes are known to cause primary immunodeficiencies [10, 26].

Regulation of transcription factors (TFs) in B cell and GC responses is highly complex and dynamic [27–29]. B cell identity is maintained by high expression of PAX5 [30]. After stimulation by T cells, the GC is formed and BCL6 and AID expression is upregulated in B cells [31]. Within the GC, c-MYC is crucial for maintenance of the GC by regulating division capacity and cycling of GC B cells [32–34]. Differentiation into ASCs requires downregulation of PAX5, BCL6, AID and c-MYC and upregulation of BLIMP1 and XBP-1 [35, 36]. Additionally, XBP-1 transcripts are alternatively spliced into XBP-1s transcripts for efficient functioning of the unfolded-protein response [33, 37]. As the GC response and differentiation process is highly dynamic, a range of TFs have to be simultaneously measured with currently known membrane markers (MM) to allow further investigation of heterogeneity in these responses and to further investigate the effect of stimulatory signals on the expression of these TFs.

The regulation of TF-expression through intracellular signal transduction pathways activated by  $T_{FH}$ -cell provided CD40L, IL-21 and IL-4 are essential to the GC response and B cell differentiation. The ability to monitor both this signaling and transcriptional regulation is necessary to enable fundamental research on wanted B cell responses against pathogens and unwanted B cell responses as observed in autoimmune diseases [38–40] or during allo-antibody formation after blood transfusion [41]. Additionally,

transcriptional dysregulation and overactivated signaling pathways can lead to B cell malignancies [42, 43]. Finally, it can aid in the development and characterization of therapeutic inhibitors for a range of diseases [44].

Recently it was elegantly shown that detection of BCR signaling by flow cytometry has a clear advantage over the detection of the BCR downstream signaling molecules by western blot [45]. The authors clearly show that phosphoflow analysis allows for a precise detection of BCR signaling at a single-cell resolution in a range of human and mouse B cell subsets. The next steps to study or target B cell differentiation in health and disease is combining detection of NF- $\kappa$ B and p-STAT signaling pathways activated by T<sub>FH</sub> signals, with MM analysis, to elucidate crosstalk between BCR, CD40 and cytokine receptors. Detection of both MM and IC phospho-proteins has been optimized for analysis in murine lymphoid cells[46]. However, an optimized method for simultaneous analysis of both MM and signaling in specific human B cell subsets undergoing differentiation is still highly desired. Furthermore, detection of crucial TFs with MM expression during T-dependent stimulation of B cells will also allow further elucidation of human B cell differentiation.

Here we present two methods, one that allows monitoring of signaling via STAT molecules and NF- $\kappa$ B and one that allows for the detection of TFs dynamically expressed throughout *in vitro* T-cell dependent B cell differentiation. Both methods allow for sample processing in a 96-wells format and allow for analysis at the level of individual B cells in distinct B cell subpopulations, revealing a previously unappreciated heterogeneity in stimulated B cell subpopulations.

## **MATERIALS AND METHODS**

### **Cell lines**

NIH3T3 fibroblasts expressing human CD40L (3T3-CD40L<sup>+</sup>)[47] were cultured in IMDM (Lonza) containing 10% FCS (Serana), 100 U/ml penicillin (Invitrogen), 100  $\mu$ g/ml streptomycin (Invitrogen), 2mM L-glutamine (Invitrogen), 50  $\mu$ M  $\beta$ -mercaptoethanol (Sigma Aldrich) and 500  $\mu$ g/ml G418 (Life Technologies).

### **Isolation of peripheral blood mononucleated cells and B cells from human healthy donors**

Buffy coats of healthy human donors were obtained from Sanquin Blood Supply. All healthy donors provided written informed consent in accordance with the protocol of the local institutional review board, the Medical Ethics Committee of Sanquin Blood Supply, and conforms to the principles of the Declaration of Helsinki. Peripheral blood mononucleated cells (PBMCs) were isolated from buffy coats using a Lymphoprep (Axis-Shield PoCAS) density gradient. Afterwards, CD19<sup>+</sup> B cells were isolated using magnetic Dynabeads (Invitrogen) and DETACHaBEAD (Invitrogen) according to manufacturer's instructions.

### **In vitro B cell stimulation cultures**

3T3 -CD40L<sup>+</sup> were harvested, irradiated with 30 Gy and seeded in B cell medium (RPMI 1640 (Gibco) without phenol red containing 5% FCS, 100 U/ml penicillin, 100 µg/ml streptomycin, 2mM L-glutamine, 50 µM β-mercaptoethanol and 20 µg/ml human apo-transferrin (Sigma Aldrich; depleted for human IgG with protein G sepharose (GE Healthcare)) on 96-well flat-bottom plates (Nunc) to allow adherence overnight. 3T3 -CD40L<sup>+</sup> were seeded at 10.000 cells per 96-well. The next day, CD19<sup>+</sup> B cells were thawed from cryo-storage and washed with B cell medium. B cells were rested at 37°C for 1 h before counting. 5000 or 10.000 CD19<sup>+</sup> B cells were co-cultured with the irradiated 3T3-CD40L<sup>+</sup> fibroblast in the presence of F(ab')<sub>2</sub> fragment Goat Anti-Human IgA/G/M (5 µg/ml; Jackson ImmunoResearch), IL-4 (25 ng/ml; Cellgenix) and IL-21 (50 ng/ml; Peprotech) for up to six days. The B cell suspension, 3T3-CD40L<sup>+</sup> plates and stimulation mix were all heated to 37°C before mixing components together. After adding the B cells to the well the plate was centrifuged for 1 min at 400xg to force all B cells onto the 3T3-CD40L<sup>+</sup> layer.

### **Phosphoflow protocol**

#### *Flow cytometry antibodies*

Antibodies used here were first titrated and validated. This was done by using either the manufacturers advised positive controls or by using a known strong stimulus found in literature[48], [49]. During the validation and titration samples were compared to unstimulated and unstained controls. As conditions and flow cytometer settings differ per lab it is advised that these dilutions are taken as guidelines and that these are validated within each individual lab (Table 1).

**Table 1.** Antibodies used for phospho- and transcription factor- flow cytometry

<b>Antibody Target</b>	<b>Conjugate</b>	<b>Clone</b>	<b>Manufacturer</b>	<b>Dilutions*</b>	<b>Cat. No.</b>
<b>Membrane Markers</b>					
<b>CD19</b>	APC	SJ25C1	BD	1:400	345791
	BV510	SJ25C1	BD	1:100	562947
<b>CD27</b>	APC	L128	BD	1:50	337169
	PE	L128	BD	1:50	340425
	BUV395	L128	BD	1:100	563815
	BUV737	L128	BD	1:100	612829
<b>CD38</b>	V450	HB7	BD	1:100	646851
	FITC	T16	Beckman Coulter	1:50	A07778
<b>Phosphoflow</b>					
<b>pSTAT1</b>	Percp-Cy5.5	4a pY701	BD	1:5	560113
<b>pSTAT3</b>	PE	4/P-STAT3	BD	1:5	612569
<b>pSTAT5</b>	Pacific Blue	47/Stat5 (pY694)	BD	1:5	560311
<b>pSTAT6</b>	AF647	18/P-Stat6	BD	1:5	612601
<b>NF-κB p65</b>	PE-Cy7	K10-	BD	1:25	560335
		895.12.50			
<b>Transcription Factors</b>					
<b>PAX5</b>	PE	1H9	Biolegend	1:10.000	649708
<b>c-MYC</b>	AF647	D84C12	CST	1:150	13871S
<b>BCL6</b>	PE-Cy7	7D1	Biolegend	1:400	358512
<b>BLIMP1</b>	AF647	#646702	R&D	1:40	IC36081R-025
<b>XBP-1s</b>	AF647	Q3-695	BD	1:40	562821
<b>AID</b>	AF647	EK2-5G9	BD	1:150	565785

\*Optimal antibody dilutions as defined for the method and staining procedure used in this paper. As staining conditions and flow cytometer settings may differ per lab it is advised that these dilutions are taken as guidelines and that these are validated within each individual lab. See M&M for the full staining procedure.

#### *Harvesting, fixation and permeabilization*

At indicated timepoints wells were resuspended with a multichannel and transferred to 96-well V-bottom plates (Nunc). Multiple culture wells were pooled, up to a full 96-well plate per replicate. After harvest cells were kept on ice or at 4°C at all times. Cells were washed with 150 µl ice-cold PBS/0.1% bovine serum albumin (BSA; Sigma Aldrich), centrifuged at 600xg for 2 minutes and pooled. Samples were stained in a 25 µl staining mix with 1:1000 LIVE/DEAD Fixable Near-IR Dead cell stain kit (Invitrogen) and anti-CD19 and -CD38 antibodies (Table 1.) diluted in ice-cold PBS/0.1% BSA for 15 minutes on ice. Samples were washed once with 150 µl ice-cold PBS/0.1% BSA, centrifuged at 600xg for 2 minutes and fixed with 37°C 4% paraformaldehyde (PFA; Sigma) for 10 minutes at 37°C. After fixation, samples were centrifuged at 600xg for 2 minutes, washed once with

150 µl ice-cold PBS/0.1% BSA and permeabilized with 90% methanol from -20°C freezer. Samples were incubated for at least 30 minutes or stored at -20°C till day of FACS analysis.

#### *Intracellular stain and FACS analysis*

After permeabilization, samples were centrifuged at 600xg for 2 minutes followed by two consecutive washes with 150 µl ice-cold PBS/0.1% BSA. Samples were then stained in 25 µl staining mix containing anti-CD27, anti-NF-κBNF-κB p65, anti-p-STAT1, anti-p-STAT3, anti-p-STAT5 and anti-p-STAT6 (Table 1) diluted in PBS/0.1% BSA. Samples were incubated for 30 minutes on a plate shaker at room temperature. Samples were washed twice with 150 µl PBS/0.1% BSA. Finally, samples were resuspended in a volume of 150 µl and of which 100 µl was measured on a flow cytometer. The flow cytometer was calibrated by compensating for all conjugates using UltraComp eBeads compensation beads (Invitrogen). All measurements were performed on a BD FACSymphony machine and analyzed using FlowJo Software v10.6.2 (Treestar).

#### **Real-time semi-quantitative RT-PCR**

Different B cell subsets (as indicated) were sorted on FACS Aria III. After sorting, RT-PCR was performed as described before [50]. Briefly, cells were lysed in peqGOLD Trifast (PeQlab) and GlycoBlue (Ambion) was added as a carrier. Total RNA was extracted according to the manufacturer's instructions. First strand cDNA was reverse transcribed using random primers (Invitrogen) and SuperScript™ II Reverse Transcriptase (Invitrogen) according to the manufacturer's instructions. Primers were developed to span exon-intron junctions and then validated. Gene expression levels were measured in duplicate reactions for each sample in StepOnePlus (Applied Biosystems) using the SYBR green method with Power SYBR green (Applied Biosystems). Primers sets used were as followed:

c-MYC: F: 5'-TACAACCCGAGCAAGGAC-3'  
R: 5'GAGGCTGCTGGTTTTCCACT-3'

Published previously [23]:

PA5: F: 5'-ACGCTGACAGGGATGGTG-3';  
R: 5'-CCTCCAGGAGTCGTTGTACG-3'.

BCL6: F: 5'-GAGCTCTGTTGATTCTTAGAACTGG-3';  
R: 5'-GCCTTGCTTCACAGTCCAA-3'

BLIMP1: F: 5' -AACGTGTGGGTACGACCTTG-3';  
R: 5'-ATTTTCATGGTCCCCTTGGT-3'

XBP-1: F: 5'-CCGCAGCACTCAGACTACG-3';  
R: 5'-TGCCCAACAGGATATCAGACT-3'

AICDA: F: 5'-GACTTTGGTTATCTTCGCAATAAGA-3',  
R: 5'AGGTCCCAGTCCGAGATGTA-3'

Expression was normalized to the internal control of 18S rRNA [50]:

18S-rRNA: F: 5'-CGGCTACCACATCCAAGGAA-3',  
R: 5'-GCTGGAATTACCGCGGCT-3'

### **TF – flow protocol**

Cells were harvested, pooled and pelleted before washing twice with 10 ml PBS/0.1% BSA. Samples were counted and  $1 \times 10^6$  were added per well to a 96-well V-bottom plate. Samples were centrifuged at 600xg for 2 minutes and stained with 25  $\mu$ l staining mix with 1:1000 LIVE/DEAD Fixable Near-IR Dead cell stain kit, anti-CD19, anti-CD27 and anti-CD38 antibodies (Table 1) and incubated for 15 minutes in the fridge. Samples were washed once with 150  $\mu$ l ice-cold PBS/0.1% and centrifuged at 600xg for 2 minutes. Samples were then fixated with 100  $\mu$ l Foxp3 fixation buffer (eBioscience) for 30 minutes in the fridge. Next, 150  $\mu$ l Foxp3 permeabilization buffer (eBioscience) was added and samples were centrifuged at 600xg for 2 minutes. After removing the supernatant, samples were stained with 25  $\mu$ l staining mix containing anti-PAX5, anti-BCL6 and either anti-c-MYC, anti-BLIMP1, anti-XBP-1s or anti-AID (Table 1) diluted in Foxp3 permeabilization buffer and incubated for 30 minutes in the fridge. Samples were washed with 150  $\mu$ l Foxp3 permeabilization buffer. Finally, samples were resuspended in a volume of 140  $\mu$ l and of which 90  $\mu$ l was measured on a flow cytometer. The flow cytometer was calibrated by compensating for all conjugates using UltraComp eBeads compensation beads (Invitrogen). All measurements were performed on a BD FACSymphony machine and analyzed using FlowJo Software v10.6.2 (Treestar).

### **Multimarker analysis using UMAP**

Live CD19<sup>+</sup>B cells were gated on and duplicates from three donors were randomly down-sampled to 10.000 events and subsequently concatenated into a single 60.000 event FCS file using the DownSample plugin in FlowJo v10.6.2. Next, the concatenated sample was analyzed using the Uniform Manifold Approximation and Projection (UMAP) plugin v3.1 in FlowJo v10.6.2. UMAP is a machine learning algorithm used for dimensionality reduction to visualize high parameter datasets in a two-dimensional space. UMAP plugin settings were as followed: Distance function Euclidean; number of neighbors 30; minimal distance 0.5 and number of components 2. The UMAP dot plot generated can be manipulated as a standard dot plot and allows for multiple parameter and heatmap overlays in the FlowJo layout-editor. The DownSample and UMAP FlowJo plugins can be found on the FlowJo Exchange website.

### **Statistical analysis**

Statistical analysis was performed using GraphPad Prism (version 8; GraphPad Software). Phosphoflow data was analyzed with mixed-effects analysis with Tukey's multiple



comparison test. TF mRNA and flow data were analyzed with repeated-measures ANOVA with Tukey's multiple comparison test. Results were considered significant at  $p < 0.05$ . Significance was depicted as \*  $p < 0.05$ , \*\*  $p < 0.01$ , \*\*\*\*  $p < 0.0001$ .

## RESULTS

### In vitro stimulation of B cells

An *in vitro* stimulation system that mimics a T-cell dependent B cell stimulation (Fig. 1A) was used to functionally assess the NF- $\kappa$ B and STAT signaling and TF profiles during B cell differentiation within specific B cell and ASC subpopulations. In this culture system F(ab)<sub>2</sub> fragments targeting IgM, IgG and IgA were used to induce BCR signaling. Irradiated human-CD40L expressing 3T3-fibroblasts were used to mimic the T<sub>FH</sub>-mediated CD40 co-stimulation essential for B cell differentiation. Additionally, recombinant cytokines IL-21 and IL-4 were added to induce IL-21R and IL-4R signaling. B cells were cultured for up to 6 days and B cell differentiation was assessed based on the relative expression of CD27 and CD38 (Fig. 1B, full gating strategy in Suppl. Fig. 1). Relative expression of CD27 and CD38 (Fig. 1C-D) demonstrated significant B cell differentiation into the CD27<sup>+</sup>CD38<sup>+</sup> ASC-population started after 96 hours and increased over time.

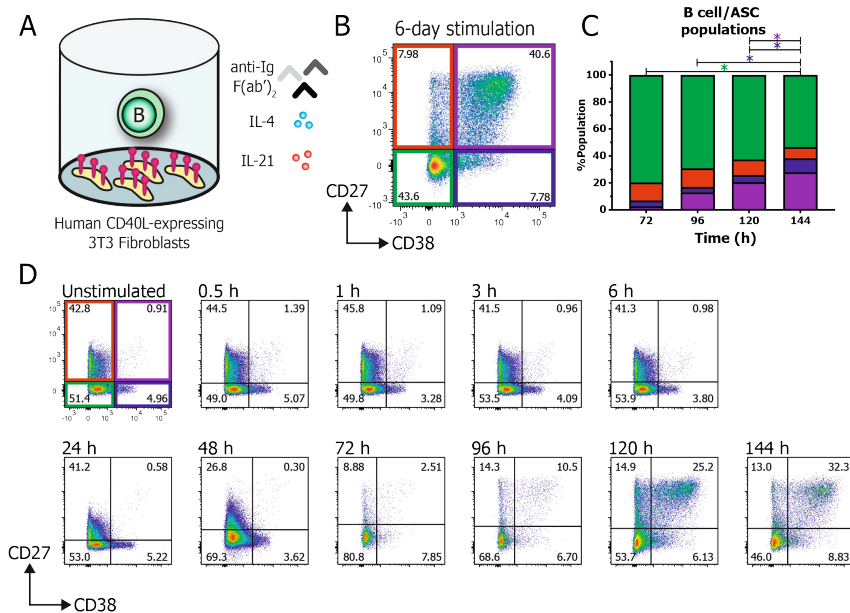


**Figure 1. Efficient *in vitro* generation of human B cell and antibody-secreting cell subpopulations.** Total human B cells ( $n=3$ ) were stimulated *in vitro* to generate multiple B cell and antibody-secreting cell (ASC) subpopulations. **(A)** Schematic overview of the culture system used to induce B cell differentiation. 5000 CD19<sup>+</sup> human B cells were stimulated with a human-CD40L expressing 3T3 feeder layer, an anti-Ig F(ab)<sub>2</sub> mix (5  $\mu$ g/ml) targeting IgM, IgG and IgA, and recombinant cytokines IL-4 (25 ng/ml) and IL-21 (50 ng/ml). **(B)** Representative FACS plot after 6 days of culture based on expression of CD27 and CD38. **(C)** Quantification of the relative percentage of CD27 and CD38 subpopulations in the total CD19<sup>+</sup> B cell population between 3 and 6 days of culture.  $N=4$ , P values were calculated by 2-way ANOVA with Tukey's multiple comparison test, \*  $p < 0.05$ . **(D)** Representative FACS plots of a time course experiment of B cell differentiation dynamics of one B cell donor, as measured over the course of 6 days culture.

### **Establishment of phosphoflow assay shows differences in phosphor-signaling profiles within B cell subpopulations**

To be able to investigate the dynamics of STAT and NF- $\kappa$ B signaling during B cell differentiation a phosphoflow protocol and panel were designed to allow simultaneous detection of differentiation MM together with intracellular signaling via p-STAT and activated NF- $\kappa$ B p65. Validation and titration of conjugated antibodies used here are listed in Table 1. Several antibodies directed against MMs for B cell differentiation and their conjugated fluorophores were tested for compatibility with the PFA-based fixation and methanol-based permeabilization protocol. Violet fluorophores like BV510 and V450, together with FITC and APC fluorophores survived permeabilization with only a slight loss in fluorescence (Suppl. Fig 2). Additionally, the anti-CD27 clone L128 was found to stain cells efficiently even after fixation and permeabilization. Even though some stains were significantly less after permeabilization or showed a significantly lower MFI, CD19, CD27 and CD38 populations were still easily distinguished. These antibodies and fluorophore properties combined allowed for an extensive panel to stain both MM and IC signaling proteins using the protocol presented here.

For detection of p-STAT and activated NF- $\kappa$ B signaling, B cells were stimulated as above. CD19<sup>+</sup> and CD27/CD38 subpopulations were gated (Fig 2A) and analyzed for expression of p-STAT1, p-STAT3, p-STAT5, p-STAT6 and activated NF- $\kappa$ B p65. Analysis of p-STAT1 per CD27/CD38 subpopulation showed clear induction of STAT1 signaling in all populations over time, with the CD27<sup>+</sup>CD38<sup>+</sup> ASC population reaching its maximum pSTAT1 value around 48 hours. In contrast, pSTAT1 peaked at 72 hours in the three B cell populations, with higher and more sustained p-STAT1 levels in the CD27<sup>+</sup>CD38<sup>+</sup> population.(Fig 2B).

p-STAT3 levels increased over time with a peak at 72 hours of stimulation (Fig 2C). There were significant differences between subpopulations with a tendency of higher phosphorylation of STAT3 in the CD27<sup>+</sup>CD38<sup>+</sup> population.

p-STAT6 levels in the B cell subpopulations were significantly different at start of the culture up until 6 hours of stimulation (Fig 2D). p-STAT6 increased in all subpopulations until 48 hours after stimulation. After this peak, the CD27<sup>+</sup>CD38<sup>-</sup> and CD27<sup>+</sup>CD38<sup>+</sup> populations remained higher and showed more sustained phosphorylation of STAT6 compared to the other populations.

NF- $\kappa$ B p65 was activated already after 30 minutes of stimulation followed by a second and higher peak of activation at 48 – 72 hours of stimulation. (Fig 2E). To accommodate differences in fluorescence intensity between donors (Suppl. Fig 4A), the fold change of NF- $\kappa$ B p65 was plotted to compare the dynamics of NF- $\kappa$ B p65 activation over time between the subpopulations. After 72 hours of stimulation NF- $\kappa$ B p65 levels declined in all subpopulations. There was a tendency of higher and more sustained NF- $\kappa$ B p65 activation in the CD27<sup>+</sup>CD38<sup>-</sup> and CD27<sup>+</sup>CD38<sup>+</sup> populations. The significant differences between pSTAT and NF- $\kappa$ B p65 levels in the CD27/CD38 subpopulations could not be attributed to differences in cell size (Suppl. Fig. 5A-B). Altogether, analysis showed that

this panel can be used to study dynamics of the combined pSTAT and NF- $\kappa$ B p65 signaling cascades during B cell to ASC differentiation.

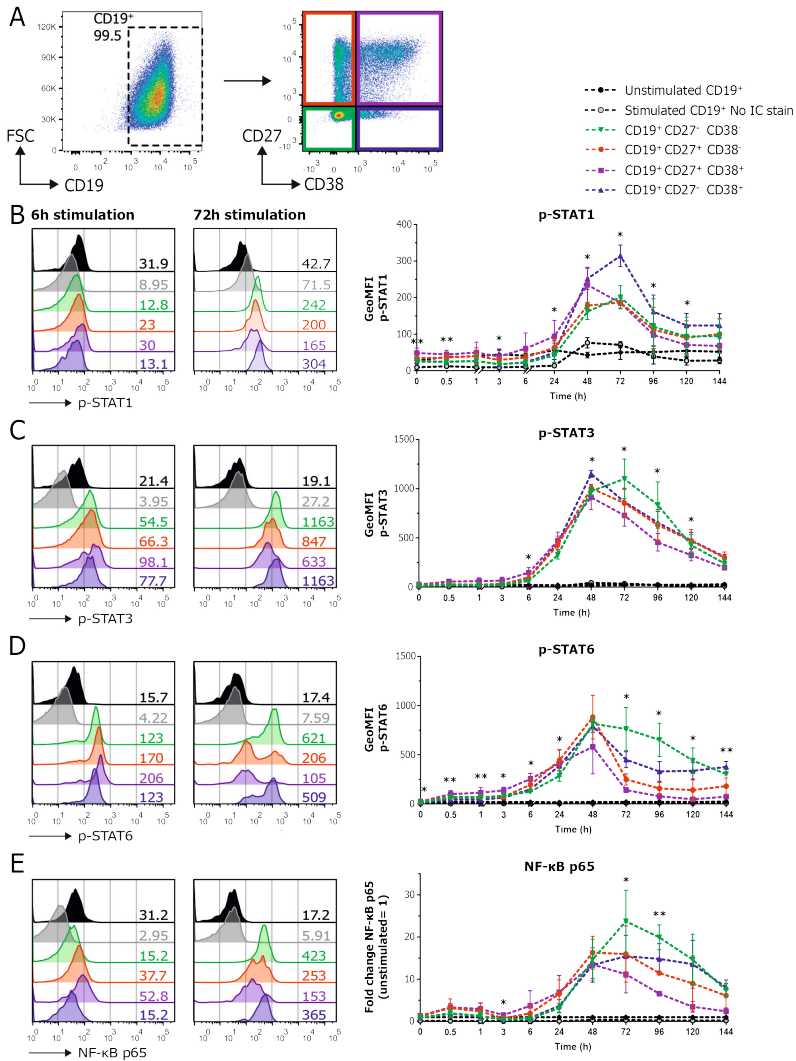
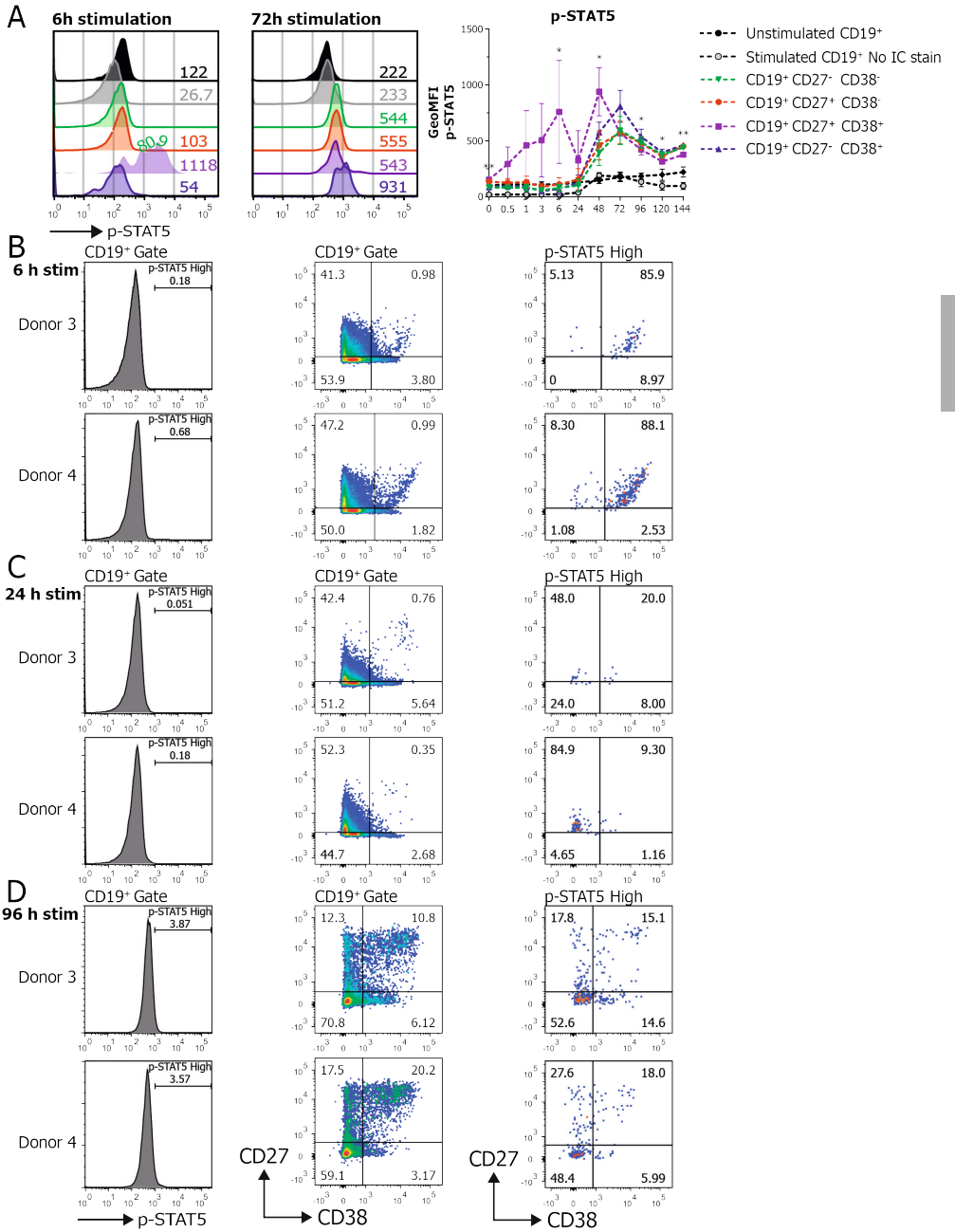


**Figure 2. Phosphoflow analysis of stimulated human B cells show differences between CD27/CD38 subpopulations.** Human B cells (n=3-4) were stimulated with human-CD40L expressing 3T3 feeder layer, an anti-Ig F(ab)<sub>2</sub> mix (5  $\mu$ g/ml) targeting IgM/IgG/IgA and recombinant cytokines IL-4 (25 ng/ml) and IL-21 (50 ng/ml) and multiple signaling proteins were analyzed by phosphoflow analysis over the course of 6-day culture. **(A)** Representative FACS plots show the gating strategy of CD19<sup>+</sup> and CD27/CD38 subpopulations by phosphoflow analysis after 96h stimulation. **(B-E)** Representative histogram overlays of p-STAT1 **(B)**, p-STAT3 **(C)**, p-STAT6 **(D)** or NF- $\kappa$ B p65 **(E)** staining in unstimulated and stimulated CD19<sup>+</sup> and CD27/CD38 subpopulations after 6 h and 72 h stimulation (left) and the quantification of GeoMFI within the different subpopulations over the course of 6 days culture (right). Values depicted next to histograms represent the corresponding GeoMFI. For NF- $\kappa$ B p65 **(E)** fold change was calculated by normalizing to the expression in unstimulated CD19<sup>+</sup> cells (set at value of 1). N = 3-4, P values were calculated using a mixed-effect analysis with Tukey's multiple comparison test, \* p < 0.05, \*\* p < 0.01, \*\*\*\* p < 0.0001. Significance\* is depicted if there is a significant difference between the green, red, purple or blue CD27/CD38 subpopulations.

p-STAT5 analysis in the B cell subpopulations showed a gradual and transient increase in STAT5 phosphorylation over time, with prominent early induction of in the CD27<sup>+</sup>CD38<sup>+</sup> ASC-population already after 6 hours of stimulation (Fig 3A). Interestingly, comparison of the four donors showed varying p-STAT5 profiles in the CD27<sup>+</sup>CD38<sup>+</sup> ASC-populations, resulting in the high deviation of GeoMFI (Suppl. Fig. 4B). To further investigate this the CD19<sup>+</sup> p-STAT5 high population (FI > 1000) was gated on in two donors at multiple timepoints (Fig 3B-D). Even though these two donors showed a different profile of p-STAT5 within subpopulations at a GeoMFI level, the p-STAT5<sup>high</sup> cells found in both donors at several timepoints had similar CD27/CD38 expression profiles (Fig 3B-D, right). This demonstrates that these p-STAT5<sup>high</sup> cells are indeed induced in both donors at early timepoints in the CD27<sup>+</sup>CD38<sup>+</sup> ASC-population, but that these can be overlooked when averaging values within subpopulations. Altogether, the data clearly shows that the simultaneous analysis of pSTAT5 and CD27 and CD38 differentiation markers in single cells allows for a more in-depth interrogation of B cell signaling across specific subpopulations, compared to using CD19 alone.

**Figure 3. Phosphoflow analysis of STAT5 phosphorylation unveils heterogeneity over time in CD27/CD38 subpopulations.** Human B cells (n=3-4) were stimulated with human-CD40L expressing 3T3 feeder layer, an anti-Ig F(ab)<sub>2</sub> mix (5 ug/ml) targeting IgM/IgG/IgA and recombinant cytokines IL-4 (25 ng/ml) and IL-21 (50 ng/ml) and multiple signaling proteins were analyzed by phosphoflow analysis over the course of 6-day culture. **(A)** Representative histogram overlays of p-STAT5 staining in CD19<sup>+</sup> and CD27/CD38 subpopulations after 6 h and 72 h stimulation (left) and the quantification of GeoMFI of p-STAT5 within the different subpopulations over the course of 6 days culture (right). Values depicted next to histograms represent the corresponding GeoMFI. N = 3-4, P values were calculated using a mixed-effect analysis with Tukey's multiple comparison test, \* p < 0.05, \*\* p < 0.01, \*\*\*\* p < 0.0001. Significance is shown if there is a significant difference between the green, red, purple or blue CD27/CD38 subpopulations. **(B-D)** Histograms of p-STAT5 expression in the CD19<sup>+</sup> population in donor 3 and donor 4 (left) and the corresponding of CD27/CD38 expression profile in the CD19<sup>+</sup> population (middle) and p-STAT5 high expressing population (right) after 6 h **(B)**, 24 h **(C)** or 96 h **(D)** of stimulation.



**Sorted naïve and memory B cells show significant differences in response to varying CD40L, IL-21 and/or IL-4 stimuli**

Next, naïve (CD19<sup>+</sup> CD27<sup>-</sup> IgD<sup>+</sup>) and memory B cells (CD19<sup>+</sup> CD27<sup>+</sup>) were sorted to further dissect intracellular signaling in naïve and memory B cells upon induction of B cell differentiation with various stimuli (Fig. 4A).

Clear p-STAT1 induction was observed through activation with CD40L in both naïve and memory B cells. The added presence of IL-21 further increase p-STAT1 levels in memory B cells (Fig. 4B). Although induction of p-STAT1 coincided with increased cell size, cell size alone did not fully account for p-STAT1 induction in memory B cells (Suppl. Fig. 5C-D).

Induction of p-STAT3 was the resultant of CD40L stimulation and amplified when IL-21 was also present in both naïve and memory B cells, irrespective of the presence of IL-4 (Fig. 4B-C).

Although BCR ligation yields p-STAT5 signaling, CD40L is the strongest inducer of p-STAT5 signaling, with naïve B cells being superior in p-STAT5 induction compared to memory B cells. (Fig. 4B-C).

In line with previous data[20]–[22]p-STAT6 is induced by IL-4, already after 30 minutes (Fig. 4C). This induction is amplified by CD40L. In addition, induction of p-STAT6 is significantly higher in naïve B cells compared to memory B cells. Activated NF-κB p65 was clearly induced when CD40L was present, already after 30 minutes of stimulation (Fig. 4B-C). In addition, activated NF-κB p65 was significantly higher in naïve B cells compared to memory B cells after 72 hours of stimulation. p-STAT3, 5 and 6 are induced by specific stimuli irrespective of cell size (Suppl. Fig. 5D). The higher induction of activated NF-κB p65 in naïve compared to memory B cells also indicates that this is induction that cannot fully be attributed to increased cell size. Altogether, these data show that the method presented here can be utilized to analyse the effects of crosstalk between BCR signaling and T<sub>FH</sub>-derived CD40 and cytokine co-stimulation on STAT and NF-κB signaling in both naïve and memory B cells.

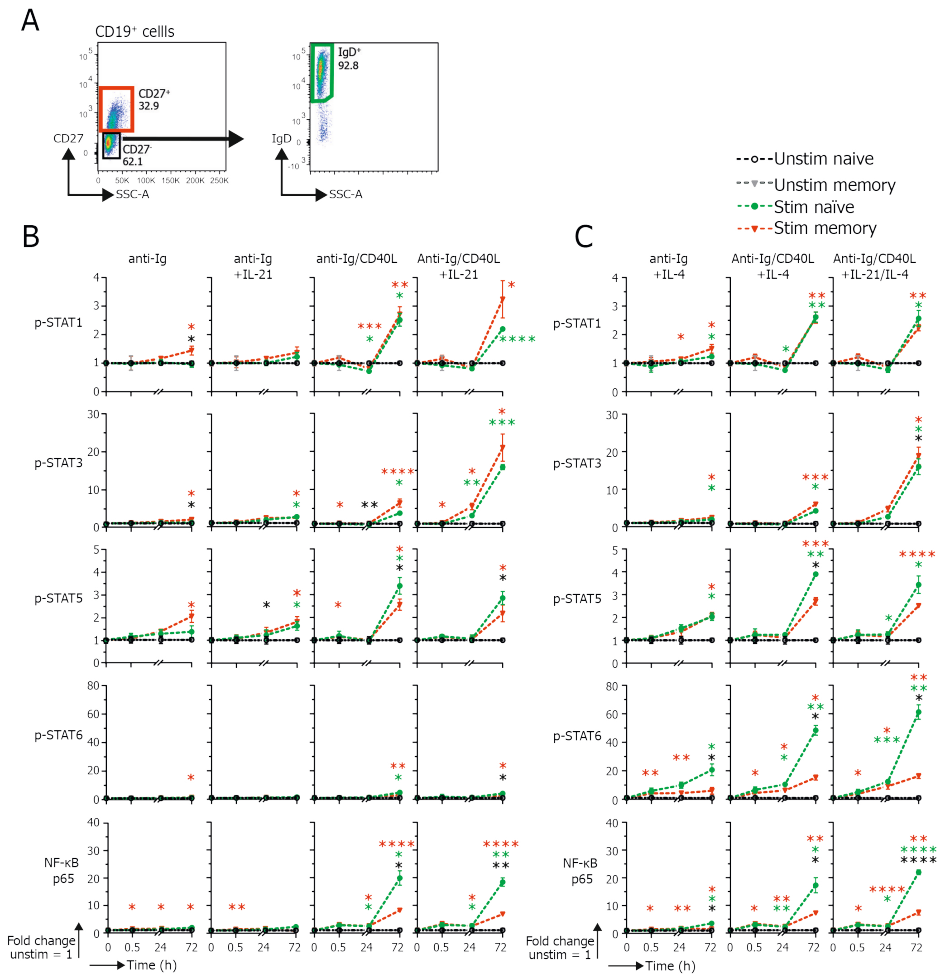


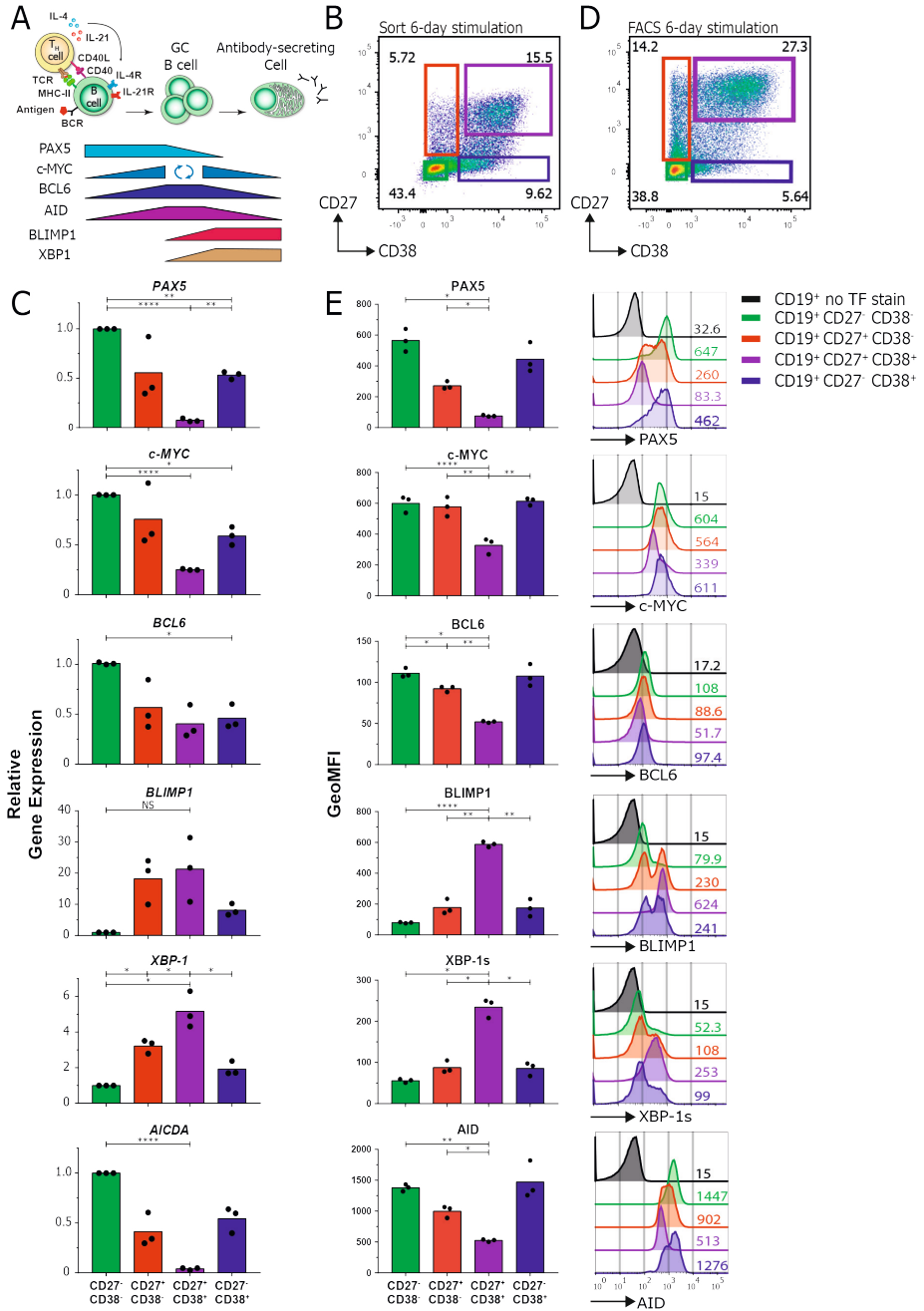
**Figure 4. pSTAT and NF- $\kappa$ B signaling in naive and memory B cells upon B cell activation via BCR, CD40 or IL4/IL-21.** 10,000 human naive (CD19<sup>+</sup> CD27<sup>-</sup> IgD<sup>+</sup>) or memory (CD19<sup>+</sup> CD27<sup>+</sup>) B cells (n=3) were stimulated after sorting with an anti-Ig F(ab)<sub>2</sub> mix (5  $\mu$ g/ml) either or not together with a CD40L expressing 3T3 cells, recombinant cytokines IL-4 (25 ng/ml) and/or IL-21 (50 ng/ml). Multiple signaling proteins were analyzed by phosphoflow analysis up to 72h of stimulation. **(A)** Representative FACS plots of the sorting strategy for purification of CD19<sup>+</sup> CD27<sup>+</sup> memory and CD19<sup>+</sup> CD27<sup>-</sup> IgD<sup>+</sup> naive B cells. **(B)** Quantification of GeoMFI of signaling proteins in stimulated sorted naive or memory B cells after 30min, 24h or 72h stimulation with varying IL-21 stimulations. Fold change was calculated normalizing expression to unstimulated condition. P values were calculated using a mixed-effect analysis with Tukey's multiple comparison test. \*  $p < 0.05$ , \*\*  $p < 0.01$ , \*\*\*\*  $p < 0.0001$ . Red\* shows significance of stimulated memory compared to unstimulated, green\* shows significance of stimulated naive compared to unstimulated and black\* shows significance of stimulated naive vs stimulated memory. **(C)** Quantification of GeoMFI of signaling proteins in stimulated sorted naive or memory B cells after 30min, 24h or 72h stimulation with varying IL-4 stimulations. Fold change was calculated normalizing the expression to the respective unstimulated condition. P values were calculated by using a mixed-effect analysis with Tukey's multiple comparison test. \*  $p < 0.05$ , \*\*  $p < 0.01$ , \*\*\*\*  $p < 0.0001$ . Red\* shows significance of stimulated memory compared to unstimulated, green\* shows significance of stimulated naive compared to unstimulated and black\* shows significance of stimulated naive vs stimulated memory.

### TF – flow assay allows for a high-resolution analysis of TFs within subpopulations

Next, a flow cytometric assay to detect known B cell transcription factors (Fig. 5A) within B cell subpopulations was set up. To validate TF – flow analyses, the TF protein expression levels measured by flow were compared to mRNA expression levels measured by semiquantitative PCR. First, after a 6-day stimulation the B cell subpopulations were sorted based on CD27 and CD38 expression (Fig. 5B). Subsequently, mRNA expression of the transcription factors PAX5, c-MYC, BCL6, BLIMP1, XBP-1 and AICDA were measured by semiquantitative PCR (Fig. 5C). As expected, mRNA expression of PAX5, c-MYC and AICDA was significantly downregulated in the CD27<sup>+</sup>CD38<sup>+</sup> population compared to other populations. Additionally, expression of BLIMP1 and XBP-1 was increased. Altogether indicating that the CD27<sup>+</sup>CD38<sup>+</sup> B cells have transitioned from a B cell mRNA expression profile to an ASC mRNA expression profile as the B cell signature gene PAX5 is downregulated and ASC-related genes BLIMP1 and XBP-1 are upregulated (Fig. 5A). Next, the same experiment was performed but now the transcription factors were stained within the different B cell subpopulations (Fig. 5C-D). As the reagents in the FcγR3 staining kit greatly reduce cell size (making it impossible to gate on a lymphocyte population) cells were first gated on live cells before doublet exclusion and gating for CD19 and CD27/CD38 subpopulations. The protein expression profiles of all transcription factors within subpopulations are highly comparable to the mRNA data. The expression of TFs was not dependent on cell size (Suppl. Fig. 6B). Furthermore, there is a clear downregulation of CD19 in the CD27<sup>+</sup>CD38<sup>+</sup> ASC population that coincides with a downregulation of PAX5 and an upregulation of BLIMP1 (Suppl. Fig. 6C). The clear advantage of these TF analyses by flow cytometry is that it allows for detection of protein instead of mRNA. Another advantage is the added depth of analyses, as demonstrated by the observed bimodal expression of PAX5 and BLIMP1 within the CD27<sup>+</sup>CD38<sup>-</sup> and CD27<sup>+</sup>CD38<sup>+</sup> populations (Fig. 5E, right), that could not be detected in the mRNA expression analysis.

**Figure 5. Transcription factor analysis in stimulated human B cells by flow cytometry.** Human B cells (n=3) were stimulated with an anti-Ig F(ab)<sub>2</sub> mix (5 µg/ml) and recombinant cytokines IL-4 (25 ng/ml) and IL-21 (50 ng/ml) for 6 days and analyzed for the mRNA and protein expression of multiple transcription factors. **(A)** Schematic representation of the expression of B cell-, GC cell- and ASC-defining transcription factors after T cell-dependent B cell stimulation. **(B)** Representative FACS plot of the sorting strategy of the CD27/CD38 subpopulations for analysis by semiquantitative RT-PCR. A more stringent gating strategy was used here to prevent contamination of subpopulations during sorting. **(C)** Quantification of relative gene expression of PAX5, c-MYC, BCL6, BLIMP1, XBP-1 and AICDA in different CD27/CD38 subpopulations as measured by semiquantitative RT-PCR. All results were normalized to the internal control 18S rRNA. Expression is calculated relatively to the CD27<sup>+</sup>CD38<sup>-</sup> subpopulation (set at value of 1). Each dot represents an independent donor and mean values are represented as bars (n=3). **(D)** Representative FACS plot of the CD27/CD38 subpopulations that were stained for transcription factors and analyzed by FACS. **(E)** Quantification of the GeoMFI of PAX5, c-MYC, BCL6, BLIMP1, XBP-1s (active spliced isoform) and AID stained for in different CD27/CD38 subpopulations (left) and corresponding histogram overlays (right). Values depicted next to histograms represent the corresponding GeoMFI. Each dot represents an independent donor and mean values are represented as bars (n=3). P values were calculated using Tukey's multiple comparison test, \* p < 0.05, \*\* p < 0.01, \*\*\*\* p < 0.0001.





**UMAP analysis unravels B cell subpopulation heterogeneity**

To further investigate the heterogeneous expression of transcription factors within B cell subpopulations on a single-cell level, a UMAP analysis was performed on the flow cytometric data (Fig. 6). Cells from either CD27<sup>+</sup>CD38<sup>-</sup> population or the CD27<sup>+</sup>CD38<sup>+</sup> population cluster together, as seen in the UMAP overlay of B cell subpopulations (Fig. 6A) and the heatmap expression plots (Fig. 6B). Neither the CD27<sup>+</sup>CD38<sup>-</sup> population or the CD27<sup>+</sup>CD38<sup>+</sup> population form a uniform cluster. Notably and in line with the mutual exclusive expression patterns of PAX5 (denoting B cell signature) and BLIMP1 (denoting ASC signature), the heatmaps of PAX5 and BLIMP1 clearly show a mirrored pattern, where PAX5 expression is down BLIMP1 expression is increased. Strikingly, the UMAP analyses bring to light a small cluster of BCL6 high expressing cells located on the border of the CD27<sup>+</sup>CD38<sup>+</sup> cluster (Fig. 6B, lower-right). As this population is not noted when plotting only the GeoMFI of CD27/CD38 subsets, these data show the clear added benefit of applying UMAP analyses on data generated with this TF flow method. As expression of PAX5 and BLIMP1 was bimodal in the CD27<sup>+</sup>CD38<sup>-</sup> and CD27<sup>+</sup>CD38<sup>+</sup> populations (Fig. 5E), this heterogeneity was further elucidated by comparing the heatmap expression of CD27, PAX5 and BLIMP1 (Fig. 6C). The data show that the expression of CD27 coincides with BLIMP1 expression (and therefore negatively coincides with PAX5 expression). Similar patterns are seen for CD38 in the CD27<sup>+</sup>CD38<sup>+</sup> population. Together, these heatmaps explain the bimodal expressions seen in Fig. 4E. Altogether this data shows that the TF – flow protocol can be used to efficiently stain TFs within B cell subpopulations. This technique allows for a relatively fast analysis of TF-expression at a single-cell resolution, a major advantage over mRNA-expression analysis where populations have to be sorted. In addition, this method and UMAP analysis allow for uncovering of small populations that have unique TF expression profiles.

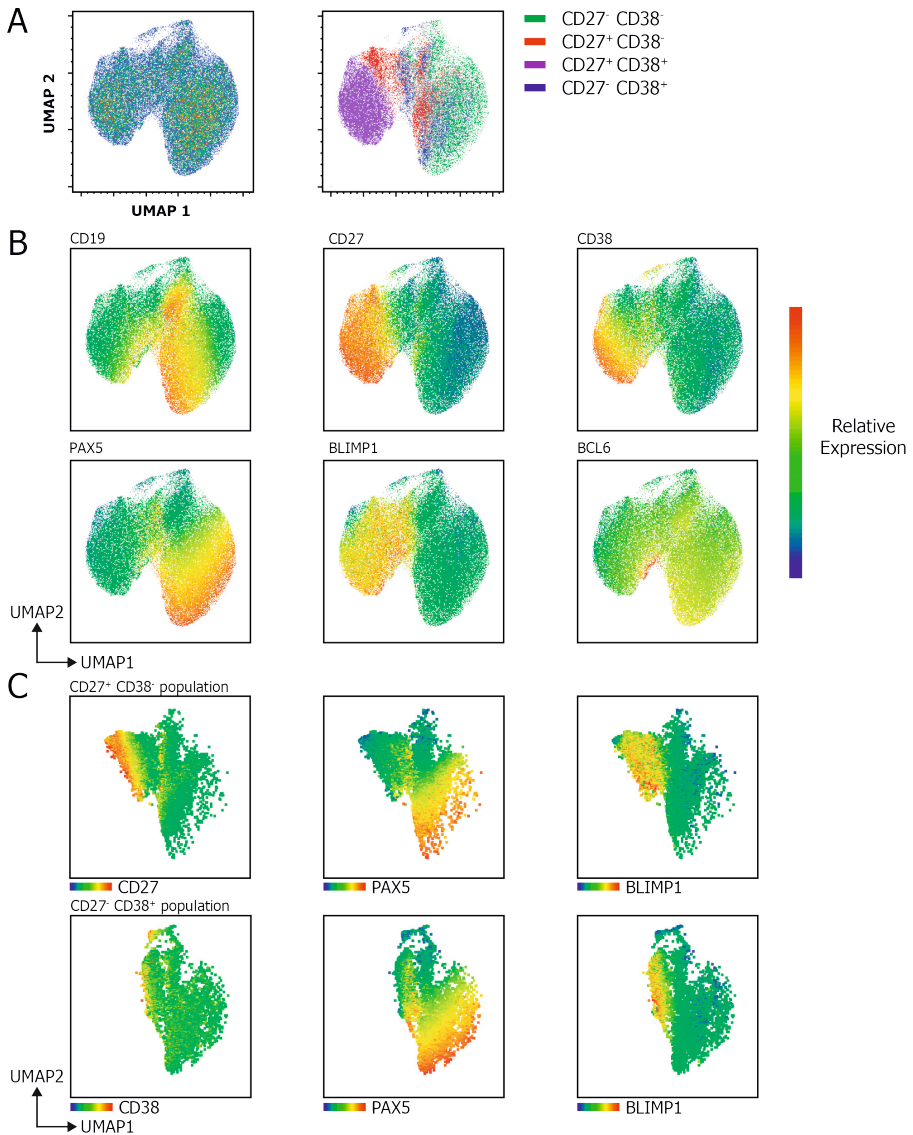


**Figure 6. UMAP analysis of combined membrane marker and TF marker analyses upon B cell differentiation.** UMAP clustering analysis on B cells stained for CD19, CD27, CD38, PAX5, BLIMP1 and BCL6 after 6-day culture with a human-CD40L expressing 3T3 feeder layer, an anti-Ig F(ab)<sub>2</sub> mix (5 ug/ml) targeting IgM/IgG/IgA and recombinant cytokines IL-4 (25 ng/ml) and IL-21 (50 ng/ml). **(A)** UMAP 2D scatter plot of 60,000 living single CD19<sup>+</sup> B cells from 3 donors (left) and the different CD27/CD38 subpopulations overlaid (right). UMAP settings were as followed: Distance function Euclidean; number of neighbours 30; minimal distance 0.5 and number of components 2. **(B)** Heatmap of the relative protein expression of CD19, CD27, CD38, PAX5, BLIMP1 and BCL6 included in the UMAP analysis overlaid on the UMAP 2D scatter plot. **(C)** Heatmap of the relative protein expression of PAX5 and BLIMP1 within the isolated CD27<sup>-</sup>CD38<sup>-</sup> population (top) and CD27<sup>+</sup>CD38<sup>+</sup> population (bottom) overlaid on the UMAP 2D scatter plot.

## DISCUSSION

Here we present a protocol for the detection and monitoring of signaling via phosphorylated STAT and activated NF- $\kappa$ B p65 within several B cell subpopulations. Furthermore, a second method is presented here that allows for detection of TFs within B cell subpopulations. Both flow cytometric-based methods provide a clear advantage over other techniques like western blotting or detection of mRNA. First, cells do not have to be purified prior to analysis and MM can be used to distinguish differentiated B cell subpopulations. Furthermore, these methods allow for analysis at a single-cell level for more in-depth analyses of cell signaling and TF expression in specific cellular subpopulations. In addition, these methods are optimized for sample processing in a 96-well format, allowing for a high throughput analysis. Finally, one major advantage of this methanol-based phosphoflow method is that samples can be stored in the freezer for prolonged periods of time [51]. This allowed for the harvesting of multiple timepoints over the course of a 6-day culture and staining intracellular phospho-proteins of multiple samples simultaneously. One drawback of these methods is the lack of commercially available conjugated antibodies with a wide range of fluorophores. Not all fluorophores or antibodies maintain reactivity under the phosphoflow protocol as also noted by others [45, 51, 52]. Additionally, antibodies directed against nuclear TFs are currently only available in a small selection of fluorophores. This makes it difficult to combine several TF-targeting antibodies into a single panel. When setting up the transcription flow within one's own lab it is advised to reserve the brightest fluorophores, like PE-Cy7 and AF647, for antibodies targeting the nuclear TFs. This ensures the highest resolution of detection of these, sometimes lowly expressed, TFs. Fortunately, the availability of antibodies and fluorophores is constantly expanding and this will most likely allow for a more extensive panel in the near future.

Using these phosphoflow and TF – flow methods several observations were made. First, B cell subsets showed significantly different steady state levels of phosphorylated STAT1 and STAT6. Mainly the CD27<sup>+</sup>CD38<sup>-</sup> subset, conventionally called memory B cells, and the CD27<sup>+</sup>CD38<sup>+</sup> ASC-population had significantly higher levels of phosphorylated STAT1 and STAT6. Furthermore, all the measured intracellular signaling proteins are more rapidly induced and also decline earlier in these subsets compared to the CD27<sup>-</sup>CD38<sup>-</sup> and CD27<sup>-</sup>CD38<sup>+</sup> populations. Interestingly, when naïve and memory B cells are compared, p-STAT6 induction is much higher in naïve B cells compared to memory B cell. In both subsets, p-STAT6 is induced by IL-4 as shown previously [20]–[22] and this induction is amplified if CD40L is present. In addition, p-STAT5 and activated NF- $\kappa$ B p65 levels are significantly higher in naïve B cells compared to memory B cells under specific stimuli. These data confirm previous findings that NF- $\kappa$ B p65 induction is higher in naïve compared to memory B cells[52]. Furthermore, in a different *in vitro* stimulation system it was shown that p-STAT 5 was more rapidly induced in naïve B cells compared to memory B cells [53]. However, in that paper IL-21 was used as a stimulus. The data presented

here show that IL-4 in fact induces and maintains higher levels of p-STAT5 compared to IL-21 as there was no dip in p-STAT5 at the 24-hour timepoint when IL-4 was present. Furthermore, it was previously shown that p-STAT1 and p-STAT3 induction is higher in naïve B cells and is induced mainly by IL-21[23], [53]. This contradicts the data presented here where p-STAT1 and p-STAT3 levels are higher in memory B cells compared to naïve B cells after stimulation. In addition, p-STAT1 is already induced by CD40L alone and further increased by IL-21 in memory B cells. Similarly, the data presented here shows that CD40L already induces p-STAT3 in both memory and naïve B cells and that this induction is amplified by IL-21. The main differences between the previously mentioned *in vitro* system[53] and the one utilized here is that the authors had to sort the splenic B cell subsets instead of circulating B cells and that these cells were pre-stimulated with anti-Ig/CD40L before adding cytokines and measuring phosphorylation of signaling proteins. Another observation is the rapid induction of p-STAT5 in the CD27<sup>+</sup>CD38<sup>+</sup> ASC-population in the first hours of stimulation. As these p-STAT5 high CD27<sup>+</sup>CD38<sup>+</sup> cells are almost all gone after 24 hours, it is likely that this induction is specific to *ex vivo* circulating plasmablasts present in the culture. These cells are however not sustained within this system. To the best of our knowledge this induction has not been shown before. The regulation of p-STAT5 in B cells remains largely unknown. It has been shown that p-STAT5 can induce but also inhibit BCL6 expression [54–56]. As BCL6 is tightly linked to survival and proliferation of B cells [57], this induction of p-STAT5 in the CD27<sup>+</sup>CD38<sup>+</sup> ASC-population could be linked to the survival of these cells after *in vitro* stimulation. Additionally, cells with high levels of p-STAT5 found throughout the culture may have a different capacity to survive and proliferate compared to the other cells. Combining the phosphoflow method here with cell trace proliferation dyes could help further elucidate this. To ensure that differences in signaling profiles in stimulated B cell subsets were not due differences in cell size, the FSC-A parameter was investigated as an indication of size. It was shown that indeed after prolonged culture and stimulation, the FSC-A increased. However, this increase does not correlate with the increases in p-STAT and NF-κB levels, showing that the induction was specific to the stimuli provided. As the increased cell size could lead to increased total-STAT levels these should be investigated and compared to p-STAT induction. This was not done here as the flow panel did not allow the addition of antibodies directed against all total-STAT proteins.

The TF – flow method revealed a previously unappreciated heterogeneity of PAX5 and BLIMP1 expression in the CD27<sup>+</sup>CD38<sup>+</sup> and CD27<sup>-</sup>CD38<sup>+</sup>. Furthermore, a high BCL6 expressing population was found that could not have been detected by measuring mRNA in bulk sorted populations. As high expression of BCL6 is a hallmark of GC B cells, this BCL6-high population could be *in vitro* induced GC B cells. Together this data shows that the single-cell resolution gained with this flow cytometric method will allow for further in-depth identification of distinct B cell subsets and elucidation of specific intracellular signaling and TF expression over time.

The methods presented here allow for a sensitive and efficient analysis of signaling proteins and TFs, together with MM. These methods allow for analysis at a single-cell resolution that can aid immunomonitoring of signaling and transcriptional regulation in healthy, and harmful B cell responses, like RA, lupus, vasculitis and allo-antibody formation [38–41]. Additionally, these techniques can aid in the development and characterization of therapeutic inhibitors [44]. Furthermore, as different B cell subsets have been known and shown here to have varying and dynamic regulation of signaling [53, 58], the methods presented here will help fundamental research further investigate this.

**Author Contributions:** C.M designed and performed all laboratory experiments, data analyses and generated all figures. T.J performed and analyzed all of the semiquantitative-PCR. A.t.B contributed to supervision. S.M.v.H main supervisor. All authors contributed to writing of the manuscript. All authors have read and agreed to the published version of the manuscript

**Funding:** This project was funded by the Landsteiner Foundation for Blood Transfusion Research, project grant number: LSBR 1609 and Sanquin Product and Process Development Call 2020.

**Acknowledgments:** We thank Simon Tol, Erik Mul, Mark Hoogenboezem and Tom Ebbes of the Sanquin central facility for cell sorting on the FACS AriaIII and maintenance and calibration of FACS machines.

**Conflicts of Interest:** The authors declare no conflict of interest. The funders had no role in the design of the study; in the collection, analyses, or interpretation of data; in the writing of the manuscript, or in the decision to publish the results.

## REFERENCES

1. C. King, S. G. Tangye, and C. R. Mackay, "T Follicular Helper (T<sub>FH</sub>) Cells in Normal and Dysregulated Immune Responses," *Annu. Rev. Immunol.*, vol. 26, no. 1, pp. 741–766, Apr. 2008, doi: 10.1146/annurev.immunol.26.021607.090344.
2. R. L. Reinhardt, H. E. Liang, and R. M. Locksley, "Cytokine-secreting follicular T cells shape the antibody repertoire," *Nat. Immunol.*, vol. 10, no. 4, pp. 385–393, 2009, doi: 10.1038/ni.1715.
3. Z. Shulman *et al.*, "Dynamic signaling by T follicular helper cells during germinal center B cell selection," *Science (80-. )*, vol. 345, no. 6200, pp. 1058–1062, Aug. 2014, doi: 10.1126/science.1257861.
4. K. Rajewsky, "Clonal selection and learning in the antibody system," *Nature*, vol. 381, no. 6585, pp. 751–758, Jun. 27, 1996, doi: 10.1038/381751a0.
5. A. D. Gitlin, Z. Shulman, and M. C. Nussenzweig, "Clonal selection in the germinal centre by regulated proliferation and hypermutation.," *Nature*, vol. 509, no. 7502, pp. 637–40, 2014, doi: 10.1038/nature13300.
6. L. J. McHeyzer-Williams, N. Pelletier, L. Mark, N. Fazilleau, and M. G. McHeyzer-Williams, "Follicular helper T cells as cognate regulators of B cell immunity," *Current Opinion in Immunology*, vol. 21, no. 3, Elsevier Current Trends, pp. 266–273, Jun. 01, 2009, doi: 10.1016/j.coi.2009.05.010.
7. Y. Takahashi, P. R. Dutta, D. M. Cerasoli, and G. Kelsoe, "In situ studies of the primary immune response to (4-hydroxy-3-nitrophenyl)acetyl. v. affinity maturation develops in two stages of clonal selection," *J. Exp. Med.*, vol. 187, no. 6, pp. 885–895, Mar. 1998, doi: 10.1084/jem.187.6.885.
8. F. J. Weisel, G. V. Zuccarino-Catania, M. Chikina, and M. J. Shlomchik, "A Temporal Switch in the Germinal Center Determines Differential Output of Memory B and Plasma Cells," *Immunity*, vol. 44, no. 1, pp. 116–130, 2016, doi: 10.1016/j.immuni.2015.12.004.
9. D. Zotos *et al.*, "IL-21 regulates germinal center B cell differentiation and proliferation through a B cell-intrinsic mechanism.," *J. Exp. Med.*, vol. 207, no. 2, pp. 365–78, Feb. 2010, doi: 10.1084/jem.20091777.
10. B. B. Ding, E. Bi, H. Chen, J. J. Yu, and B. H. Ye, "IL-21 and CD40L Synergistically Promote Plasma Cell Differentiation through Upregulation of Blimp-1 in Human B Cells," *J. Immunol.*, vol. 190, no. 4, pp. 1827–1836, Feb. 2013, doi: 10.4049/jimmunol.1201678.
11. L. Moens and S. G. Tangye, "Cytokine-mediated regulation of plasma cell generation: IL-21 takes center stage," *Frontiers in Immunology*, vol. 5, no. FEB, Frontiers Research Foundation, p. 65, Feb. 18, 2014, doi: 10.3389/fimmu.2014.00065.
12. I. Yusuf *et al.*, "Germinal Center T Follicular Helper Cell IL-4 Production Is Dependent on Signaling Lymphocytic Activation Molecule Receptor (CD150)," *J. Immunol.*, vol. 185, no. 1, pp. 190–202, Jul. 2010, doi: 10.4049/jimmunol.0903505.
13. J. S. Weinstein *et al.*, "TFH cells progressively differentiate to regulate the germinal center response," *Nat. Immunol.*, vol. 17, no. 10, pp. 1197–1205, 2016, doi: 10.1038/ni.3554.
14. H. Gascan, J. F. Gauchat, M. G. Roncarolo, H. Yssel, H. Spits, and J. E. De Vries, "Human B cell clones can be induced to proliferate and to switch to IgE and IgG4 synthesis by interleukin 4 and a signal provided by activated CD4+ T cell clones," *J. Exp. Med.*, vol. 173, no. 3, pp. 747–750, 1991, doi: 10.1084/jem.173.3.747.

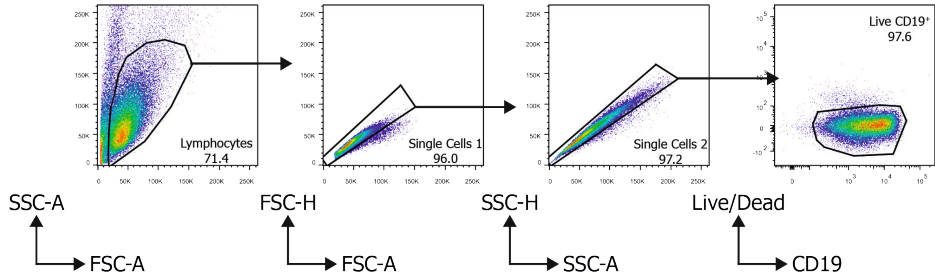
15. D. T. Avery, V. L. Bryant, C. S. Ma, R. de Waal Malefyt, and S. G. Tangye, "IL-21-Induced Isotype Switching to IgG and IgA by Human Naive B Cells Is Differentially Regulated by IL-4," *J. Immunol.*, vol. 181, no. 3, pp. 1767–1779, Aug. 2008, doi: 10.4049/jimmunol.181.3.1767.
16. D. G. Gonzalez *et al.*, "Nonredundant Roles of IL-21 and IL-4 in the Phased Initiation of Germinal Center B Cells and Subsequent Self-Renewal Transitions," *J. Immunol.*, p. j1500497, 2018, doi: 10.4049/jimmunol.1500497.
17. A. Craxton, G. Shu, J. D. Graves, J. Saklatvala, E. G. Krebs, and E. A. Clark, "p38 MAPK is required for CD40-induced gene expression and proliferation in B lymphocytes," *J. Immunol.*, vol. 161, no. 7, pp. 3225–36, Oct. 1998, Accessed: May 10, 2020. [Online]. Available: <http://www.ncbi.nlm.nih.gov/pubmed/9759836>.
18. D. Chen *et al.*, "CD40-Mediated NF- $\kappa$ B Activation in B Cells Is Increased in Multiple Sclerosis and Modulated by Therapeutics," *J. Immunol.*, vol. 197, no. 11, pp. 4257–4265, Dec. 2016, doi: 10.4049/jimmunol.1600782.
19. S. C. Sun, "The non-canonical NF- $\kappa$ B pathway in immunity and inflammation," *Nature Reviews Immunology*, vol. 17, no. 9. Nature Publishing Group, pp. 545–558, Sep. 01, 2017, doi: 10.1038/nri.2017.52.
20. M. B. Harris *et al.*, "Transcriptional Repression of Stat6-Dependent Interleukin-4-Induced Genes by BCL-6: Specific Regulation of I $\epsilon$  Transcription and Immunoglobulin E Switching," *Mol. Cell. Biol.*, vol. 19, no. 10, pp. 7264–7275, Oct. 1999, doi: 10.1128/mcb.19.10.7264.
21. A. L. Wurster, V. L. Rodgers, M. F. White, T. L. Rothstein, and M. J. Grusby, "Interleukin-4-mediated protection of primary B cells from apoptosis through Stat6-dependent up-regulation of Bcl-xL," *J. Biol. Chem.*, vol. 277, no. 30, pp. 27169–27175, 2002, doi: 10.1074/jbc.M201207200.
22. D. T. Avery *et al.*, "STAT3 is required for IL-21 induced secretion of IgE from human naive B cells," *Blood*, vol. 112, no. 5, pp. 1784–1793, Sep. 2008, doi: 10.1182/blood-2008-02-142745.
23. D. T. Avery *et al.*, "B cell-intrinsic signaling through IL-21 receptor and STAT3 is required for establishing long-lived antibody responses in humans," *J. Exp. Med.*, vol. 207, no. 1, pp. 155–171, 2010, doi: 10.1084/jem.20091706.
24. J. E. Darnell, I. M. Kerr, and G. R. Stark, "Jak-STAT pathways and transcriptional activation in response to IFNs and other extracellular signaling proteins," *Science (80- )*, vol. 264, no. 5164, pp. 1415–1421, 1994, doi: 10.1126/science.8197455.
25. A. Oeckinghaus and S. Ghosh, "The NF-kappaB family of transcription factors and its regulation," *Cold Spring Harbor perspectives in biology*, vol. 1, no. 4. Cold Spring Harbor Laboratory Press, 2009, doi: 10.1101/cshperspect.a000034.
26. P. Tuijnenburg *et al.*, "Loss-of-function nuclear factor  $\kappa$ B subunit 1 (NFKB1) variants are the most common monogenic cause of common variable immunodeficiency in Europeans," *J. Allergy Clin. Immunol.*, vol. 142, no. 4, pp. 1285–1296, Oct. 2018, doi: 10.1016/j.jaci.2018.01.039.
27. G. D. Victora and M. C. Nussenzweig, "Germinal Centers," doi: 10.1146/annurev-immunol-020711-075032.
28. L. Mesin, J. Ersching, and G. D. Victora, "Germinal Center B Cell Dynamics," *Immunity*, vol. 45, no. 3, pp. 471–482, 2016, doi: 10.1016/j.immuni.2016.09.001.
29. N. S. De Silva and U. Klein, "Dynamics of B cells in germinal centres," *Nat. Rev. Immunol.*, vol. 15, no. 3, pp. 137–148, 2015, doi: 10.1038/nri3804.
30. C. Cobaleda, A. Schebesta, A. Delogu, and M. Busslinger, "Pax5: The guardian of B cell identity and function," *Nature Immunology*, vol. 8, no. 5. pp. 463–470, May 2007, doi: 10.1038/ni1454.



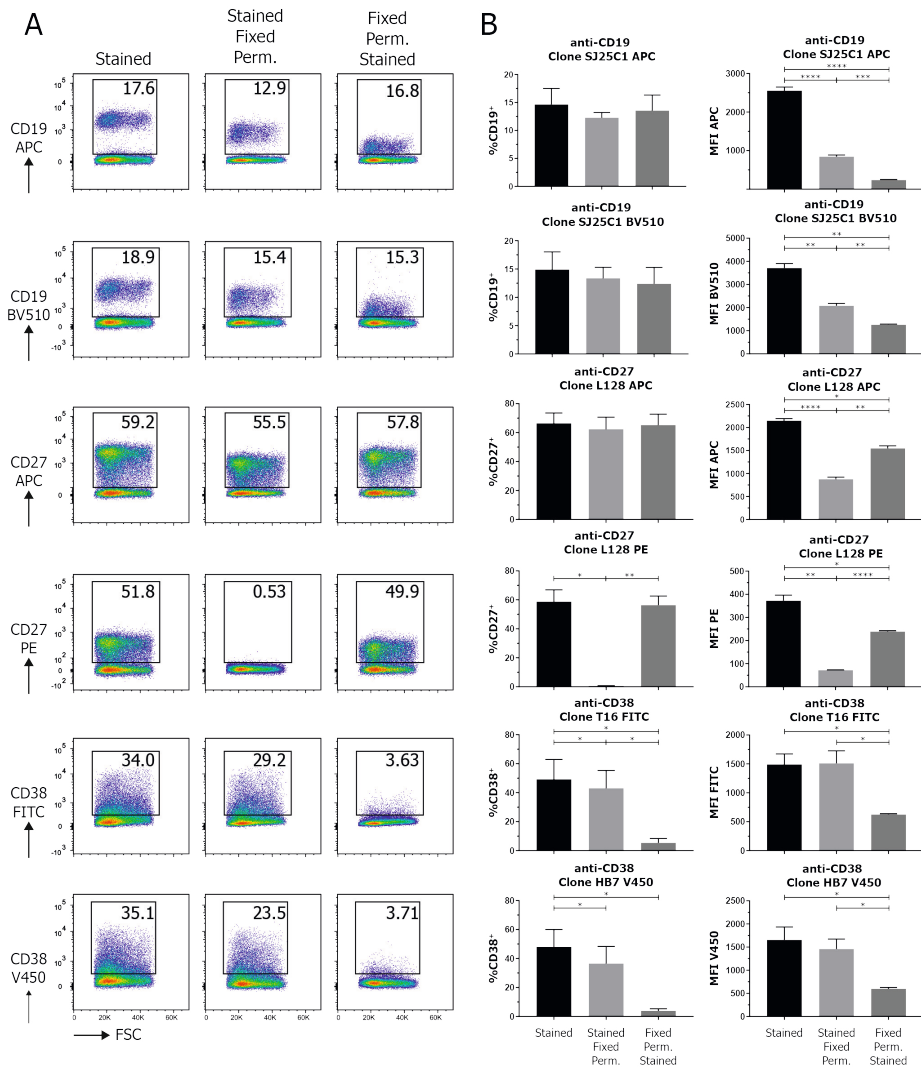
31. H. L. Chang *et al.*, “Regulation of the germinal center gene program by interferon (IFN) regulatory factor 8/IFN consensus sequence-binding protein,” *J. Exp. Med.*, vol. 203, no. 1, pp. 63–72, Jan. 2006, doi: 10.1084/jem.20051450.
32. D. Pedro Calado *et al.*, “MYC is essential for the formation and maintenance of germinal centers HHS Public Access,” *Nat Immunol*, vol. 13, no. 11, pp. 1092–1100, 2012, doi: 10.1038/ni.2418.
33. S. L. Nutt, P. D. Hodgkin, D. M. Tarlinton, and L. M. Corcoran, “The generation of antibody-secreting plasma cells,” *Nat. Rev. Immunol.*, vol. 15, no. 3, pp. 160–171, Mar. 2015, doi: 10.1038/nri3795.
34. S. Finkin, H. Hartweger, T. Y. Oliveira, E. E. Kara, and M. C. Nussenzweig, “Protein Amounts of the MYC Transcription Factor Determine Germinal Center B Cell Division Capacity,” *Immunity*, vol. 51, no. 2, pp. 324–336.e5, 2019, doi: 10.1016/j.immuni.2019.06.013.
35. S. L. Nutt, P. D. Hodgkin, D. M. Tarlinton, and L. M. Corcoran, “The generation of antibody-secreting plasma cells,” *Nat. Rev. Immunol.*, vol. 15, no. 3, pp. 160–171, 2015, doi: 10.1038/nri3795.
36. J. Tellier and S. L. Nutt, “Plasma cells: The programming of an antibody-secreting machine,” *Eur. J. Immunol.*, vol. 49, no. 1, pp. 30–37, Jan. 2019, doi: 10.1002/eji.201847517.
37. H. Yoshida, T. Matsui, A. Yamamoto, T. Okada, and K. Mori, “XBP1 mRNA is induced by ATF6 and spliced by IRE1 in response to ER stress to produce a highly active transcription factor,” *Cell*, vol. 107, no. 7, pp. 881–891, Dec. 2001, doi: 10.1016/S0092-8674(01)00611-0.
38. S. Bugatti, B. Vitolo, R. Caporali, C. Montecucco, and A. Manzo, “B cells in rheumatoid arthritis: From pathogenic players to disease biomarkers,” *Biomed Res. Int.*, vol. 2014, 2014, doi: 10.1155/2014/681678.
39. D. Y. H. Yap and T. M. Chan, “B cell abnormalities in systemic lupus erythematosus and lupus nephritis—role in pathogenesis and effect of immunosuppressive treatments,” *International Journal of Molecular Sciences*, vol. 20, no. 24, MDPI AG, Dec. 02, 2019, doi: 10.3390/ijms20246231.
40. M. McClure, S. Gopaluni, D. Jayne, and R. Jones, “B cell therapy in ANCA-associated vasculitis: current and emerging treatment options,” *Nature Reviews Rheumatology*, vol. 14, no. 10, Nature Publishing Group, pp. 580–591, Oct. 01, 2018, doi: 10.1038/s41584-018-0065-x.
41. K. Pavenski, J. Freedman, and J. W. Semple, “HLA alloimmunization against platelet transfusions: pathophysiology, significance, prevention and management,” *Tissue Antigens*, vol. 79, no. 4, pp. 237–245, Apr. 2012, doi: 10.1111/j.1399-0039.2012.01852.x.
42. O. de Barrios, A. Meler, and M. Parra, “MYC’s Fine Line Between B Cell Development and Malignancy,” *Cells*, vol. 9, no. 2, p. 523, Feb. 2020, doi: 10.3390/cells9020523.
43. A. L. Shaffer, R. M. Young, and L. M. Staudt, “Pathogenesis of Human B Cell Lymphomas,” *Annu. Rev. Immunol.*, vol. 30, no. 1, pp. 565–610, Apr. 2012, doi: 10.1146/annurev-immunol-020711-075027.
44. Y. Jamilloux, T. El Jammal, L. Vuitton, M. Gerfaud-Valentin, S. Kerever, and P. Sève, “JAK inhibitors for the treatment of autoimmune and inflammatory diseases,” *Autoimmunity Reviews*, vol. 18, no. 11, Elsevier B.V., Nov. 01, 2019, doi: 10.1016/j.autrev.2019.102390.
45. J. Rip, M. J. W. de Bruijn, A. Kaptein, R. W. Hendriks, and O. B. J. Corneth, “Phosphoflow Protocol for Signaling Studies in Human and Murine B Cell Subpopulations,” *J. Immunol.*, p. j1901117, 2020, doi: 10.4049/jimmunol.1901117.
46. P. O. Krutzik, M. R. Clutter, and G. P. Nolan, “Coordinate Analysis of Murine Immune Cell Surface Markers and Intracellular Phosphoproteins by Flow Cytometry 1,” 2005.

47. M. Urashima, D. Chauhan, H. Uchiyama, G. J. Freeman, and K. C. Anderson, "CD40 ligand triggered interleukin-6 secretion in multiple myeloma," *Blood*, vol. 85, no. 7, pp. 1903–1912, 1995, doi: 10.1182/blood.v85.7.1903.bloodjournal8571903.
48. T. Karonitsch *et al.*, "Activation of the interferon-gamma signaling pathway in systemic lupus erythematosus peripheral blood mononuclear cells," *Arthritis Rheum.*, vol. 60, no. 5, pp. 1463–71, 2009, doi: 10.1002/art.24449.
49. N. Schmitt *et al.*, "The cytokine TGF- $\beta$  2 co-opts signaling via STAT3-STAT4 to promote the differentiation of human T FH cells," *Nat. Immunol.*, vol. 15, no. 9, pp. 856–865, 2014, doi: 10.1038/ni.2947.
50. Y. Souwer *et al.*, "Detection of aberrant transcription of major histocompatibility complex class II antigen presentation genes in chronic lymphocytic leukaemia identifies *HLA-DOA* mRNA as a prognostic factor for survival," *Br. J. Haematol.*, vol. 145, no. 3, pp. 334–343, May 2009, doi: 10.1111/j.1365-2141.2009.07625.x.
51. P. O. Krutzik and G. P. Nolan, "Intracellular phospho-protein staining techniques for flow cytometry: Monitoring single cell signaling events," *Cytometry*, vol. 55A, no. 2, pp. 61–70, Oct. 2003, doi: 10.1002/cyto.a.10072.
52. K. Huse *et al.*, "Human Germinal Center B Cells Differ from Naïve and Memory B Cells in CD40 Expression and CD40L-Induced Signaling Response," *Cytom. Part A*, vol. 95, no. 4, pp. 442–449, Apr. 2019, doi: 10.1002/cyto.a.23737.
53. E. K. Deenick *et al.*, "Naive and memory human B cells have distinct requirements for STAT3 activation to differentiate into antibody-secreting plasma cells," *J. Exp. Med.*, vol. 210, no. 12, pp. 2739–53, 2013, doi: 10.1084/jem.20130323.
54. F. A. Scheeren *et al.*, "STAT5 regulates the self-renewal capacity and differentiation of human memory B cells and controls Bcl-6 expression," *Nat. Immunol.*, vol. 6, no. 3, pp. 303–313, 2005, doi: 10.1038/ni1172.
55. S. A. Diehl *et al.*, "STAT3-mediated up-regulation of BLIMP1 Is coordinated with BCL6 down-regulation to control human plasma cell differentiation.," *J. Immunol.*, vol. 180, no. 7, pp. 4805–15, Apr. 2008, Accessed: Mar. 28, 2017. [Online]. Available: <http://www.ncbi.nlm.nih.gov/pubmed/18354204>.
56. L. M. Heltemes-Harris and M. A. Farrar, "The role of STAT5 in lymphocyte development and transformation," *Current Opinion in Immunology*, vol. 24, no. 2. NIH Public Access, pp. 146–152, Apr. 2012, doi: 10.1016/j.coi.2012.01.015.
57. K. Basso and R. Dalla-Favera, "Roles of BCL6 in normal and transformed germinal center B cells," *Immunol. Rev.*, vol. 247, no. 1, pp. 172–183, May 2012, doi: 10.1111/j.1600-065X.2012.01112.x.
58. W. Luo, F. Weisel, and M. J. Shlomchik, "B Cell Receptor and CD40 Signaling Are Rewired for Synergistic Induction of the c-Myc Transcription Factor in Germinal Center B Cells," *Immunity*, vol. 48, no. 2, pp. 313–326.e5, 2018, doi: 10.1016/j.immuni.2018.01.008.

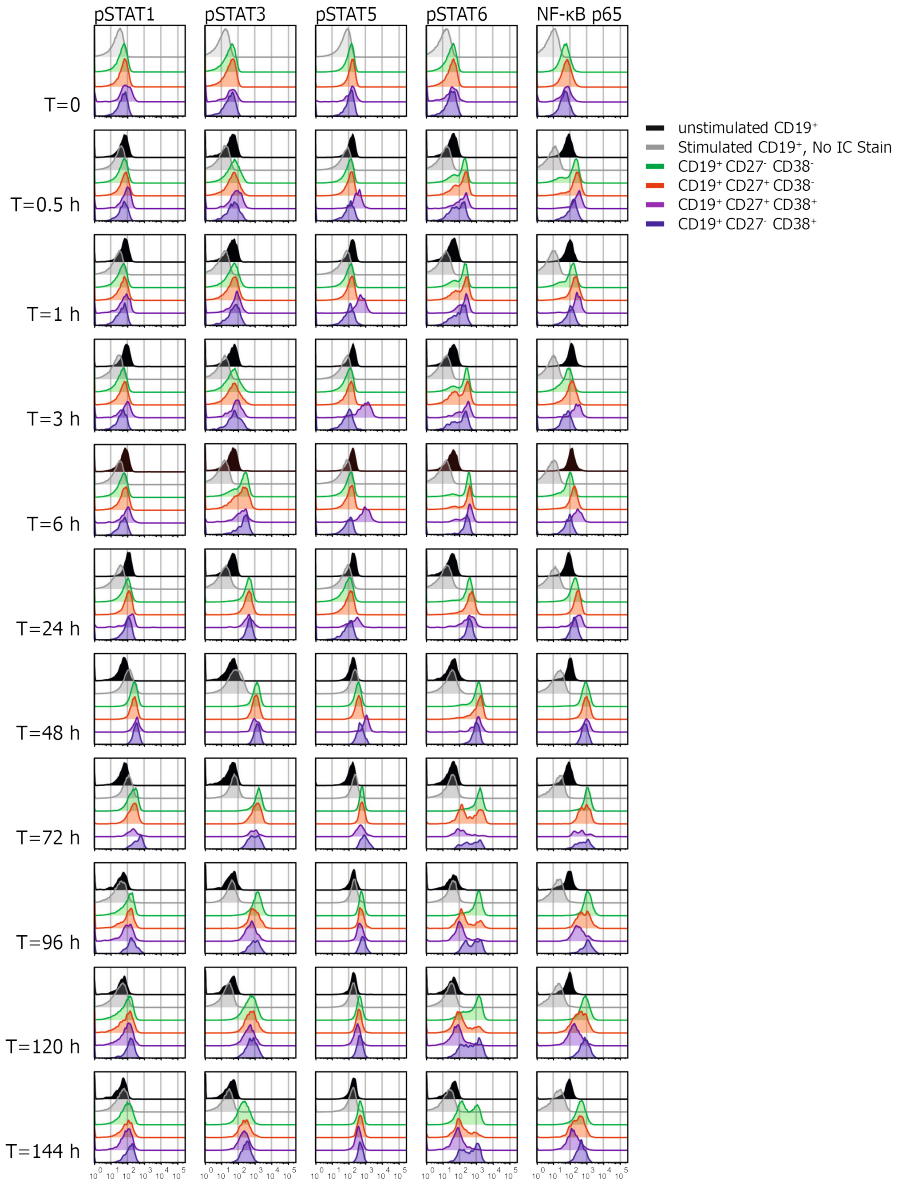
## SUPPLEMENTARY MATERIAL



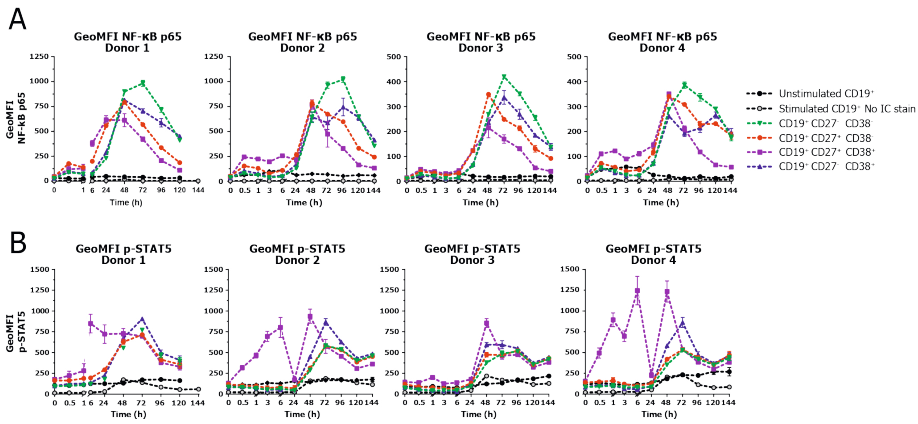
**Supplementary Figure 1. Preservation of antibody reactivity against MM for B cell differentiation upon fixation and permeabilization of PBMCs.** Thawed human PBMCs from  $-80^{\circ}\text{C}$  storage were washed and were either stained for MM, stained for MM before fixation with 4% PFA and permeabilization with 90% methanol or stained for MM after fixation with 4% PFA and permeabilization with 90% methanol. **(A)** Representative FACS plots of PBMCs comparing antibody reactivity of anti-CD19, -CD27 and -CD38 antibodies stained directly without fixation and permeabilization (left), stained before fixation and permeabilization (middle) or stained after fixation and permeabilization (right). **(B)** Quantification of percentage positive cells stained with the respective anti-CD19, -CD27 and -CD38 antibodies (left) and MFI of positive cells (right) stained directly without fixation and permeabilization, stained before fixation and permeabilization or stained after fixation and permeabilization. N = 3



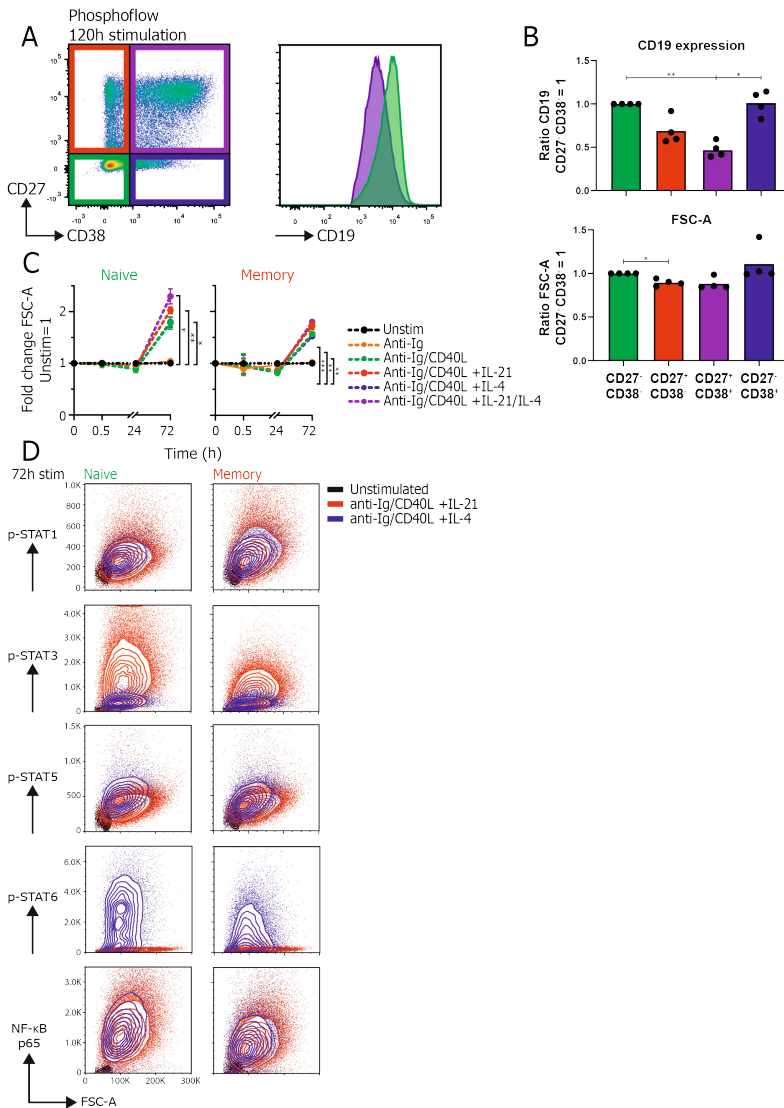
**Supplementary Figure 2. Representative gating strategy for the gating of CD19<sup>+</sup> B cells.** Live single CD19<sup>+</sup> B cells were gated on as depicted. First a FSC/SSC gate is set for the lymphocyte population that contains the CD19<sup>+</sup> B cells. Doublets were excluded by setting two single cell gates on both the FSC-A/FSC-H and SSC-A/SSC-H parameters. Dead cells were excluded using a live/dead fixable viability stain and CD19<sup>+</sup> cells were gated on.



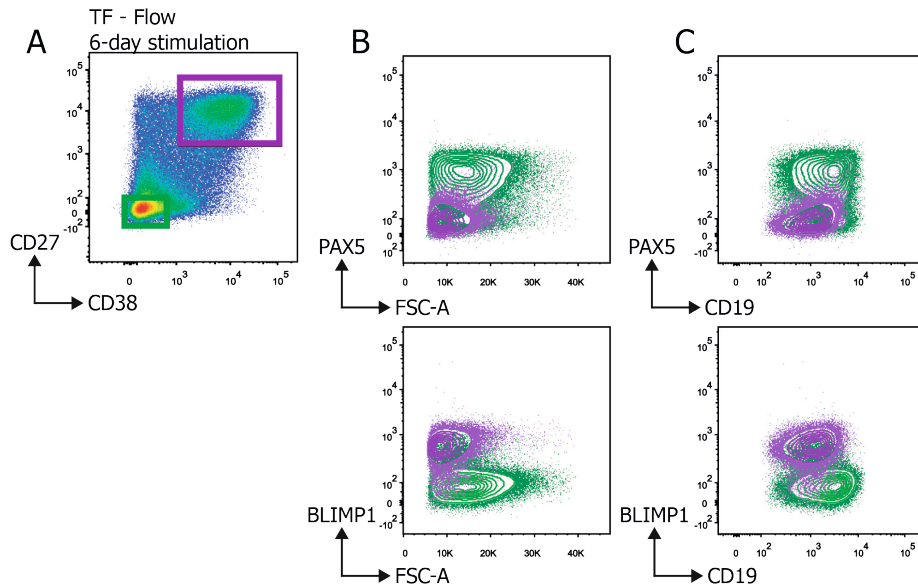
**Supplementary Figure 3. Representative histograms of phosphoflow analysis at different time points of B cell differentiation.** Human B cells ( $n=3-4$ ) were stimulated with human-CD40L expressing 3T3 feeder layer, an anti-Ig F(ab)<sub>2</sub> mix (5  $\mu\text{g}/\text{ml}$ ) targeting IgM/IgG/IgA and recombinant cytokines IL-4 (25  $\text{ng}/\text{ml}$ ) and IL-21 (50  $\text{ng}/\text{ml}$ ) and analyzed for the expression multiple signaling proteins by phosphoflow analysis over the course of 6-day culture. Representative histogram overlays of p-STAT1, p-STAT3, p-STAT5, p-STAT6 and NF- $\kappa\text{B}$  p65 in the different CD27/CD38 subpopulations. All time points are shown ( $t=0$ , 30min, 60min, 3h, 6h, 24h-144h)



**Supplementary Figure 4. NF- $\kappa$ B p65 and p-STAT5 expression of 4 individual donors.** Human B cells ( $n=4$ ) were stimulated with human-CD40L expressing 3T3 feeder layer, an anti-Ig F(ab)<sub>2</sub> mix (5  $\mu$ g/ml) targeting IgM/IgG/IgA and recombinant cytokines IL-4 (25 ng/ml) and IL-21 (50 ng/ml) and analyzed for the expression multiple signaling proteins by phosphoflow analysis over the course of 6-day culture. **(A)** Quantification of the GeoMFI of NF- $\kappa$ B p65 within CD27/CD38 subpopulations in 4 individual donors over the course of 6 days culture. Max y-axis = 1250 for the two left donors and max y-axis = 500 for the right two donors. **(B)** Quantification of the GeoMFI of p-STAT5 within CD27/CD38 subpopulations in 4 individual donors in 4 individual donors over the course of 6 days culture.



**Supplementary Figure 5. Relationship between pSTAT/NF-kB p65 signals and cell size during B cell differentiation.** Human B cells were stimulated with human-CD40L expressing 3T3 feeder layer, an anti-Ig F(ab)<sub>2</sub> mix (5 ug/ml) targeting IgM/IgG/IgA and recombinant cytokines IL-4 (25 ng/ml) and IL-21 (50 ng/ml) and multiple signaling proteins were analyzed by phosphoflow analysis over the course of 6-day culture. **(A)** Representative dot plot of CD27/CD38 subpopulations after 120h of stimulation (left) and representative histogram of CD19 expression of CD27<sup>+</sup>CD38<sup>-</sup> and CD27<sup>+</sup>CD38<sup>+</sup> subpopulations during phosphoflow analysis. **(B)** Quantification of CD19 expression (top) and FSC-A (bottom) of CD27/CD38 subpopulations after 120h of stimulation during phosphoflow analysis. Fold change was calculated by normalizing to the CD27<sup>+</sup>CD38<sup>-</sup> population. Each dot represents an independent donor and mean values are represented as bars (n=4). P values were calculated using Tukey's multiple comparison test, \* p < 0.05, \*\* p < 0.01, \*\*\*\* p < 0.0001. **(C)** Quantification of FSC-A of sorted naive or memory B cells after stimulation up to 72h with anti-Ig F(ab)<sub>2</sub> alone or together with CD40L, IL-21 and/or IL-4. Fold change was calculated by normalizing FSC-A to the unstimulated control condition (n=3). P values were calculated comparing stimulated conditions versus the unstimulated control condition using a mixed-effect analysis with Dunnett's multiple comparison test. \* p < 0.05, \*\* p < 0.01, \*\*\*\* p < 0.0001. **(D)** Representative contour plot overlays of stimulated naive or memory B cells after 72h either or not stimulated with anti-Ig F(ab)<sub>2</sub>, CD40L, IL-21 or IL-4. The FSC-A parameter is plotted against measured signaling proteins.



**Supplementary Figure 6. Stimulated CD27/CD38 subpopulations show significant differences in CD19 expression and FSC-A during TF-flow analysis.** Human B cells (n=3) were stimulated with an anti-Ig F(ab)2 mix (5 ug/ml) and recombinant cytokines IL-4 (25 ng/ml) and IL-21 (50 ng/ml) for 6 days and analyzed for the protein expression of transcription factors. **(A)** Representative dot plot of CD27/CD38 expression after 6 days of stimulation and gating of CD27<sup>+</sup>CD38<sup>-</sup> and CD27<sup>+</sup>CD38<sup>+</sup> subpopulations during TF-flow analysis. **(B)** Representative contour plot overlay of CD27<sup>+</sup>CD38<sup>-</sup> and CD27<sup>+</sup>CD38<sup>+</sup> subpopulations and PAX5 (top) and BLIMP1 (bottom) expression compared to FSC-A parameter. **(C)** Representative contour plot overlay of CD27<sup>+</sup>CD38<sup>-</sup> and CD27<sup>+</sup>CD38<sup>+</sup> subpopulations and PAX5 (top) and BLIMP1 (bottom) expression compared to the expression of CD19.







# CHAPTER 4

## Soluble FAS ligand enhances suboptimal CD40L/IL-21 mediated human memory B cell differentiation into antibody-secreting cells

Saskia D. van Asten, Peter-Paul Unger\*, Casper Marsman\*, Sophie Bliss, Tineke Jorritsma, Nicole M. Thielens, S. Marieke van Ham and Robbert M. Spaapen

*Journal of Immunology* (2021), 207 (2) 449-458

\*Both authors contributed equally

## **ABSTRACT**

Differentiation of antigen-specific B cells into class-switched, high affinity antibody-secreting cells provides protection against invading pathogens but is undesired when antibodies target self-tissues in autoimmunity, beneficial non-self blood transfusion products or therapeutic proteins. Essential T cell factors have been uncovered that regulate T cell-dependent B cell differentiation. We performed a screen using a secreted protein library to identify novel factors that promote this process and may be used to combat undesired antibody formation. We tested the differentiating capacity of 756 secreted proteins on human naive or memory B cell differentiation in a setting with suboptimal T cell help *in vitro* (suboptimal CD40L and IL-21). High-throughput flow cytometry screening and validation revealed that type I IFNs and soluble FAS ligand (sFASL) induce plasmablast differentiation in memory B cells. Furthermore, sFASL induces robust secretion of IgG1 and IgG4 antibodies, indicative of functional plasma cell differentiation. Our data suggest a mechanistic connection between elevated sFASL levels and the induction of autoreactive antibodies, providing a potential therapeutic target in autoimmunity. Indeed, the modulators identified in this secretome screen are associated with systemic lupus erythematosus and may also be relevant in other autoimmune diseases and allergy.

## INTRODUCTION

The immune response against a wide variety of pathogens is critically dependent on antigen-specific, high affinity antibodies generated upon natural infection or through vaccination. In contrast, antibodies are detrimental when induced against self-antigens in autoimmune disorders or against allergens, therapeutic proteins, blood products or transplants. Protective and pathogenic antibodies are produced by antibody-secreting plasmablasts or plasma cells (ASCs) that originate from B cells. T cell help consisting of CD40L/CD40 costimulation and the secretion of specific cytokines is essential for the generation of long-lived plasma cells that produce high-affinity, class switched antibodies. Short-lived plasmablasts differentiated from B cells without T cell help mostly secrete low-affinity antibodies.

T cell-dependent B cells differentiate in secondary lymphoid organs after being activated by their cognate antigen (1). Upon activation they migrate to the border of the B and T cell zones where they present antigen-derived peptides to activated T helper cells. After receiving T cell help, B cells migrate back into the B cell follicles while undergoing class switching. They initiate so called germinal center (GC) reactions by alternating between stages of proliferation in GC dark zones (DZ) and reacquisition of antigen to receive additional help from GC-resident antigen-specific follicular T helper ( $T_{fh}$ ) cells in GC light zones (LZ) (2, 3). Expression of the chemokine receptor CXCR4 allows migration into the DZ, whereas absence of CXCR4 favors LZ localization. During this cycling process, somatic hypermutation of the B cell receptor (BCR) occurs followed by affinity maturation, where B cells with the highest affinity BCRs for the antigen selectively proliferate. Ultimately, these B cells differentiate into memory B cells ( $CD38^-CD27^+$ ) and later into ASCs consisting of plasmablasts ( $CD38^+CD27^+CD138^-$ ) and terminally differentiated plasma cells ( $CD38^+CD27^+CD138^+$ ) (1, 4–7). A subset of memory B cells expresses CXCR3 to migrate into inflamed tissue, while others remain in lymphoid organs or circulates in the peripheral blood (8). Upon reinfection and antigen recall, memory B cells may reengage in GC reactions (8, 9). Plasma cell migration to the bone marrow for long-term survival is directed by CXCR4 (10).

Essential for driving B cell differentiation are membrane-bound interactions between receptor-ligand pairs on B cells and  $T_{fh}$ , such as CD40/CD40L (11–13). Furthermore, it is clear that soluble factors like  $T_{fh}$  cytokines IL-21 and IL-4 are key  $T_{fh}$  cytokines for effective B cell differentiation and that IFN- $\gamma$  promotes, among other things, migration to inflamed tissue (11, 14, 15). Yet, several other secreted proteins such as IL-10 and type I IFNs affect B cell differentiation in humans, indicating that the role of soluble factors to modulate this process is underexplored (16–18).

To study B cell differentiation *in vitro*, T cell help may be mimicked using a CD40L-expressing cell line and recombinant IL-21 and IL-4. This system is well-suited to study which additional signals modulate differentiation of naive or memory B cells into ASCs. Here, we used a previously generated secreted protein library to identify soluble B cell differentiation modulators (19). We designed the library to contain immune-related and

non-immune human proteins including cytokines, growth factors, peptide hormones and enzymes, because factors from non-hematopoietic cells may also modulate B cell differentiation. Using this diverse library, we identified few additional factors affecting naive B cell differentiation but several molecules with a strong impact on memory B cell differentiation. More specifically, type I IFNs, MAp19 (mannan-binding lectin-associated protein of 19 kDa, transcript variant of complement enzyme MASP-2)(20) and soluble FASL (sFASL) induced plasmablast differentiation in IgG<sup>+</sup> memory B cells. Moreover, sFASL promoted the secretion of substantial amounts of IgG<sub>1</sub> and IgG<sub>4</sub>, showing that FASL drives the formation of ASCs. The different modulators identified in our screens improve the understanding of B cell differentiation and may represent new targets for modulation of B cells and antibody production during disease.

## **METHODS**

### **Generation of CD40L expressing 3T3 cell line**

NIH3T3 fibroblast cells (3T3) cells were cultured in IMDM medium (Lonza, Basel, Switzerland) supplemented with 10% FCS (Bodinco, Alkmaar, The Netherlands), 100 U/ml penicillin (Thermo Fisher Scientific, Waltham, Massachusetts), 100 µg/ml streptomycin (Thermo Fisher Scientific), 2mM L-glutamine (Thermo Fisher Scientific) and 50 µM β-mercaptoethanol (Sigma Aldrich, St. Louis, Missouri). The 3T3 cells were transfected with Fsp I linearized CD40L plasmid (a kind gift from G. Freeman (21, 22)) and Pvu I linearized pcDNA3-Neomycin plasmid using Lipofectamine 2000 Reagent (Thermo Fisher Scientific) according to manufacturer's protocol. Three days after transfection, the 3T3 culture medium was supplemented with 500 µg/ml G418 (Thermo Fisher Scientific) to select successfully transfected cells. The 3T3 cells were FACS sorted four times for expression of CD40L using an anti-CD40L antibody (clone TRAP1, BD Biosciences, San Jose, California). This resulted in a stable CD40L-expressing cell line that was cultivated in G418 containing selection media to maintain expression. The same batch of 3T3 CD40L-expressing cells was used for all experiments.

### **Secreted protein library**

The arrayed secreted protein library was generated previously (19). Additional conditioned media were generated using the exact same protocol. In brief, HEK293T cells were individually transfected with plasmids encoding for secreted proteins (OriGene Technologies, Rockville, Maryland and GE Health Care, Chicago, Illinois) using polyethylenimine (Polysciences, Warrington, Pennsylvania). Six hours after transfection, medium was replaced with fresh medium (IMDM supplemented with 10% FCS, 100 U/ml penicillin and 100 µg/ml streptomycin). Three days after transfection, conditioned media were collected and stored in ready-to-screen 96 well plates at -80°C.

### Isolation of human B cells

Buffy coats were obtained from healthy volunteers upon written informed consent in conformity with the protocol of the local institutional review board, the Medical Ethics Committee of Sanquin Blood Supply (Amsterdam, The Netherlands). PBMCs were isolated by density gradient centrifugation using Lymphoprep (Axis-Shield PoC AS, Oslo, Norway). CD19<sup>+</sup> cells were isolated from PBMCs using CD19 Pan B Dynabeads and DETACHaBEAD (Thermo Fisher Scientific) according to manufacturer's protocol with purity >99% and cryopreserved.

### In vitro differentiation culture of human naive and IgG memory B cells

One day ahead of B cell culture, CD40L<sup>+</sup> 3T3 cells were irradiated with 30 Gy and plated at a density of 10,000 cells/well in a 96 flat-bottom plate (Nunc, Roskilde, Denmark) in B cell culture medium, which is RPMI-1640 without phenol-red (Thermo Fisher Scientific) supplemented with 5% FCS, 100 U/ml penicillin, 100 µg/ml streptomycin, 2mM L-glutamine, 50 µM β-mercapthoethanol and 20 µg/ml human apotransferrin (Sigma Aldrich, St. Louis, Missouri; depleted for human IgG with protein G sepharose). The following day thawed human B cells were stained with CD19-BV510 (clone 5J25C1, BD Biosciences), CD27-PE-Cy7 (clone 0323, Thermo Fisher Scientific) and IgG-DyLight 650 (clone MH16-1, Sanquin Reagents, Amsterdam, The Netherlands; conjugated using DyLight 650 NHS Ester (Thermo Fisher Scientific) according to manufacturer's protocol). CD19<sup>+</sup>CD27<sup>+</sup>IgG<sup>+</sup> memory or CD19<sup>+</sup>CD27<sup>-</sup>IgG<sup>-</sup> naive B cells were isolated using an Aria II sorter (BD Biosciences). The sorted B cells were then added to the irradiated CD40L<sup>+</sup> 3T3 cells at a density of 500-25000 cells/well, in the presence of 5 or 50 ng/ml IL-21 (Thermo Fisher Scientific) as indicated. Conditioned medium from the secreted protein library was added at a 1:12 dilution. For the screens, four wells of empty vector and two wells of IL-21 conditioned media were added to each of the 14 plates. Purified recombinant IFN-α, soluble FAS ligand (both PeproTech, London, United Kingdom) and MAP19 were added at indicated concentrations (23). After 9-10 days, B cells were analyzed by flow cytometry. The culture supernatants were used for ELISA.

### Flow cytometry

B cells were stained with LIVE/DEAD fixable near-IR dye (Thermo Fisher Scientific), and CD19-BV510, CD27-PE-Cy7, CD38-V450 (clone HB7, BD Biosciences), CD138-FITC (clone MI15, BD Biosciences), or CD95-PE-CF594 (BD Biosciences) for 30 minutes at 4 °C. After staining, cells were washed twice with and taken up in PBS containing 1% BSA and 0.01% azide to be measured on an LSRII (BD Biosciences). Data was analyzed using FlowJo software (BD Biosciences).

### ELISA

Levels of total IgG1 and IgG4 in culture supernatants were determined by sandwich ELISA. Maxisorp ELISA plates (Nunc) were coated overnight with anti-IgG1 or anti-IgG4 (2 µg/ml clones MH161-1, MH161-1, MH164-4 respectively, Sanquin Reagents) in PBS. Plates were

washed five times with 0.02% Tween-20 (Avantor, Radnor Township, Pennsylvania) in PBS (Fresenius Kabi, Bad Homburg, Germany), and incubated with culture supernatants (diluted in high-performance ELISA buffer, Sanquin Reagents). Plates were again washed five times and incubated for one hour with horseradish peroxidase-conjugated mouse-anti-human-IgG (1 µg/ml, clone MH16-1, Sanquin Reagents). After a final five-times wash, the ELISA was developed with 100 µg/ml tetramethylbenzidine (Interchim, Montluçon, France) in 0.11 mol/L sodium acetate (pH 5.5) containing 0.003% (v/v) H<sub>2</sub>O<sub>2</sub> (all from Merck, Darmstadt, Germany). The reaction was stopped with 2M H<sub>2</sub>SO<sub>4</sub> (Merck). IgG concentrations were determined from the 450 nm minus background 540 nm absorption (Synergy2; BioTek, Winooski, Vermont) in comparison to a serial diluted serum pool standard in each plate.

### Screen analysis

The Z-factor (Z') can be calculated to determine whether an assay is suitable for high-throughput screening (24). The Z' for multiple parameters was calculated from empirical data of 27 replicates of negative (empty vector conditioned medium) and positive control (IL-21 conditioned medium) B cell cultures as indicated using the following formula:  $Z' = 1 - \frac{3 \times (\sigma_{\text{empty vector}} + \sigma_{\text{IL-21}})}{|\mu_{\text{empty vector}} - \mu_{\text{IL-21}}|}$  in which  $\sigma$  represents the measured standard deviation, and  $\mu$  the measured mean. For each parameter, the screen data were normalized per plate by B-score normalization using R as described by Malo *et al* (25). This method normalizes for column and row confounding effects by three iterative subtractions of median row and column values (excluding IL-21 controls) from each individual well value. After performing this median polish, the B-score for each well was determined by division of the median absolute deviation (MAD = median {|well – median(plate)|}). The screen was performed twice, using B cells from two different healthy donors. The final B-score per secreted protein per condition was the mean of these two screens. The cut-off for hit selection was set at 3 times standard deviation of all conditions, excluding IL-21 controls.

### Proliferation assay

Sorted B cells were washed twice with 10 ml PBS and resuspended to a concentration of 2x10<sup>7</sup> cells/ml in PBS. Cells and 40 µM CellTrace Yellow (Thermo Fisher Scientific) were mixed at a 1:1 ratio and incubated 15 minutes at RT in the dark, vortexing the tube every 5 minutes to ensure uniform staining. Cells were washed twice using a 10 times volume of cold culture medium to end labeling. Thereafter, B cells were cultured according to the protocol described above. At day 4 and day 10 of culture B cells were mixed with at least 2000 Cyto-Cal counting beads (Thermo Fisher Scientific) or CountBright Absolute counting beads (Thermo Fisher Scientific) and prepared for flow cytometry analysis as described above. Absolute B cell counts were determined according to the formula:

$$\frac{\# \text{Live CD19}}{\# \text{beads measured}} \times \# \text{beads added}.$$



### Transcription factor staining

Transcription factor detection assays were performed as previously described (26). In short, at day 4 of culture in the B cell differentiation assay, B cells were harvested and stained with LIVE/DEAD fixable near-IR dye (Thermo Fisher Scientific), and CD19-BV510 (BD Biosciences), CD27-BUV395 (BD Biosciences) and CD38-FITC (Beckman Coulter) in 0.1% BSA in PBS for 15 minutes on ice. Cells were washed with 0.1% BSA in PBS, followed by fixation in Foxp3 fixation buffer (FoxP3 Transcription Factor staining buffer set, eBioscience) for 30 minutes at 4 °C. Cells were washed with permeabilization buffer (FoxP3 Transcription Factor staining buffer set) and stained with PAX5-PE (Biolegend), BLIMP1-AF647 (R&D) antibodies in permeabilization buffer for 30 minutes at 4 °C. The stained cells were again washed with permeabilization buffer before measurement on the BD FACSymphony (BD Biosciences).

### Statistics

Statistical analysis was performed using R and GraphPad prism 8.2.1 (GraphPad Software, San Diego, California). *P*-values were determined by indicated statistical tests and depicted using the following symbols:  $p < 0.05 = *$ ,  $p < 0.01 = **$ ,  $p < 0.001 = ***$ , n.s. = not significant.

## RESULTS

### An *in vitro* assay allows for unbiased large-scale evaluation of factors required for B cell differentiation into plasmablasts

Because CD40 stimulation and IL-21 signaling seem to be minimal requirements to induce differentiation into antibody secreting cells (27), we set out to identify soluble factors that cooperate or act in synergy with these  $T_{fh}$  signals. To discover new soluble factors that coregulate human B cell differentiation into antibody-secreting cells, we set up *in vitro* B cell cultures suitable for arrayed secreted protein screening. IgG<sup>+</sup> memory B cells or naive B cells were cultured with irradiated CD40L-expressing cells in the presence of IL-21 (Fig. 1A). After nine days, the B cell differentiation state was analyzed by flow cytometry using antibodies against CD27, CD38, CD138 and surface-bound IgG (gating in Fig. S1A). The chemokine receptors CXCR3 and CXCR4 were included in the analysis as they are essential for LZ-DZ cycling and migration to inflamed tissue or bone marrow (Fig. S1A). The B cell differentiation factor IL-21 was titrated to minimize memory and naive B cell differentiation into CD27<sup>+</sup>CD38<sup>+</sup> ASCs and IgG<sup>+</sup> B cells respectively, while still supporting B cell survival (Fig. 1B and C). Comparison of the effects of different B cell starting numbers on the efficacy of differentiation into IgG<sup>+</sup> B cells and CD27<sup>+</sup>CD38<sup>+</sup> ASCs demonstrated similar trajectories of the IL-21 titration curves (Fig. 1B and C, right panels). Culture initiation with 500 memory B cells per well yielded too few cells for reliable endpoint measurements. Therefore, we chose to start the ensuing differentiation cultures with 1000 memory B cells per well in presence of 5 ng/ml IL-21. For naive B cells, culture initiation

with 10,000 cells and 5 ng/ml of IL-21 provided sufficient survival signal for the nine-day culture period, while inducing only few cells to class switch to IgG (Fig. 1C).

The screen was executed using a library of arrayed conditioned media each enriched for a single soluble protein secreted by cDNA-transfected HEK293T cells (19). This library contains 756 secreted proteins with a broad variety of biological functions, such as neuropeptides, hormones, growth factors and cytokines. To determine the optimal dilution of the library to use in the B cell differentiation screen, we generated IL-21 and empty vector conditioned positive and negative control media respectively. Titrations of both control media showed that the IL-21 conditioned medium was more effective at inducing CD27<sup>+</sup>CD38<sup>+</sup> ASC differentiation from IgG<sup>+</sup> memory B cells at lower concentrations, possibly because of supra-optimal IL-21 levels in the conditioned medium (Fig. S1B). While the IL-21 concentration in the supernatant was in the mg/ml range as determined by ELISA (data not shown), we previously found that several other conditioned media in the library contained lower (functional) levels of secreted protein (19). For naive B cells, the optimal IL-21 conditioned medium dilution to promote IgG class switching was 1:12 (Fig. S1C). For the library screen on naive and memory B cells, a 1:12 dilution was subsequently used, as it induced no measurable background signal with empty vector (EV) and was sufficient to distinguish IL-21 differentiation effects (Fig. S1B, C dashed line). Finally, we analyzed whether this optimized assay was applicable for screening by determining the dynamic range between 48 negative and positive controls. We found that for several parameters (including the CD27<sup>+</sup>CD38<sup>+</sup> population and CXCR4 expression) Z' was higher than zero, indicating that the assay was suitable for large scale screening (Fig. S1D, E).

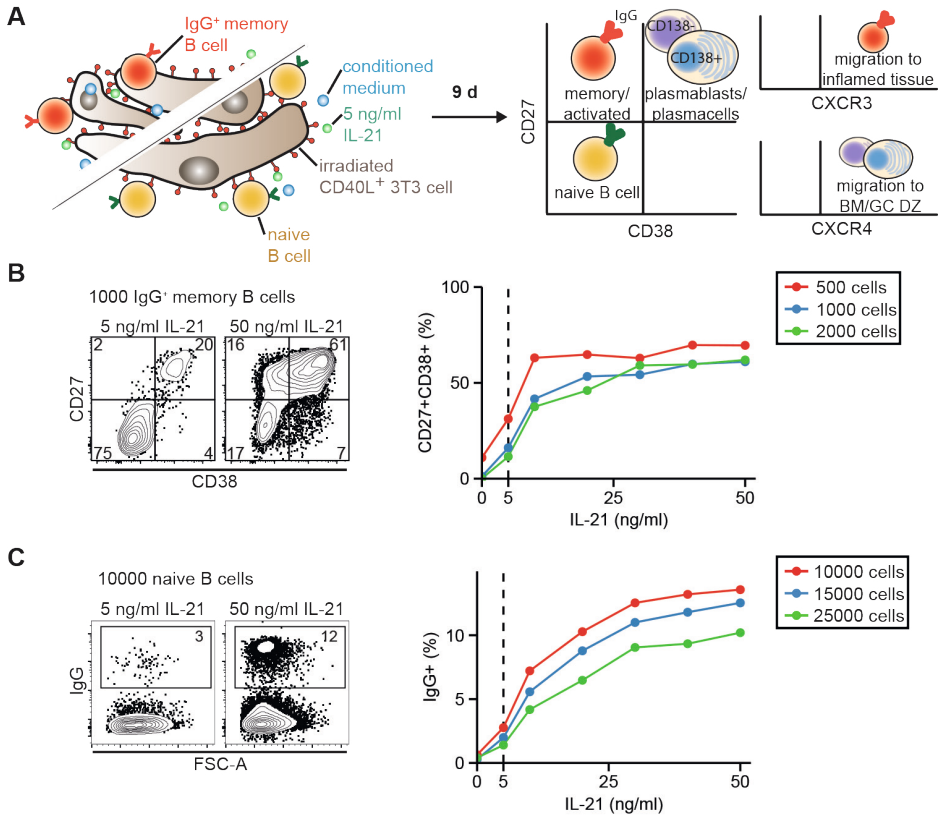


**Figure 1. Setup of a suitable assay for arrayed secreted protein screening.** (A) Schematic overview of the B cell differentiation assay used in Figures 2-5. Isolated CD27<sup>+</sup>IgG<sup>+</sup> memory B cells or CD27<sup>+</sup>IgG<sup>+</sup> naive B cells were cultured for nine days in the presence of irradiated 3T3 cells, 5 ng/ml IL-21 (see B and C) and the individual conditioned media of the secreted protein library. B cells were analyzed by flow cytometry for expression of CD27, CD38, CD138, surface IgG (red), CXCR3 and CXCR4. (B and C) Determination of a suboptimal concentration of IL-21 to culture different indicated starting amounts of memory (B) or naive (C) B cells (n=1). Left panels contain example flow cytometry plots of CD27/CD38 (B) and IgG (C) at the indicated concentrations. Right panels show quantification of the percentage of positive cells in the depicted gates. Dashed line indicates 5 ng/ml IL-21. BM = bone marrow, GC DZ = germinal center dark zone.

### IFN- $\gamma$ induces CXCR3 expression in naive and memory B cells

After setting up a suitable assay, the complete secreted protein library was screened for factors that alter chemokine receptor expression or induce differentiation of B cells. Data from two screens using two different healthy donors were averaged after per plate B-score normalization, which accounts for row and column effects within a single plate as well as variation between plates. Most conditioned media resulted in similar phenotypes compared to empty conditioned media with a B score close to zero (Fig. 2). Positive control IL-21 conditioned medium significantly altered surface CXCR3 and CXCR4 expression in memory B cells and CXCR4 in naive B cells, showing that the library IL-21 conditioned medium was biologically active (Fig. 2A, E, G). The threshold for hit

selection was set at three times standard deviation of all conditioned media except the IL-21 positive control (Fig. 2). IFN- $\gamma$  conditioned medium was the strongest CXCR3 inducer in both memory and naive B cell screens (Fig. 2A-D), in line with previous reports (14). In memory B cells, CXCR3 expression was also upregulated by IFN- $\beta$ 1, but not by IFN- $\alpha$ 2 (Fig. 2A). Both type I IFNs failed to induce CXCR3 expression in naive B cells (Fig. 2C). In addition, sFASL, FGF5, RLN2, IL15RA and MMP24 conditioned media led to slightly increased CXCR3 levels in memory B cells. None of the conditioned media clearly reduced CXCR4 expression in memory B cells compared to EV (Fig. 2E), yet naive B cells exposed to IFNs, C8B, NRG1, EBI3 and SERPINF1 had lower CXCR4 levels compared to EV (Fig. 2G). HPR, CLC and IL-2 led to marginally enhanced CXCR4 upregulation in memory B cells, and sFASL in both memory and naive B cells (Fig. 2E-H).

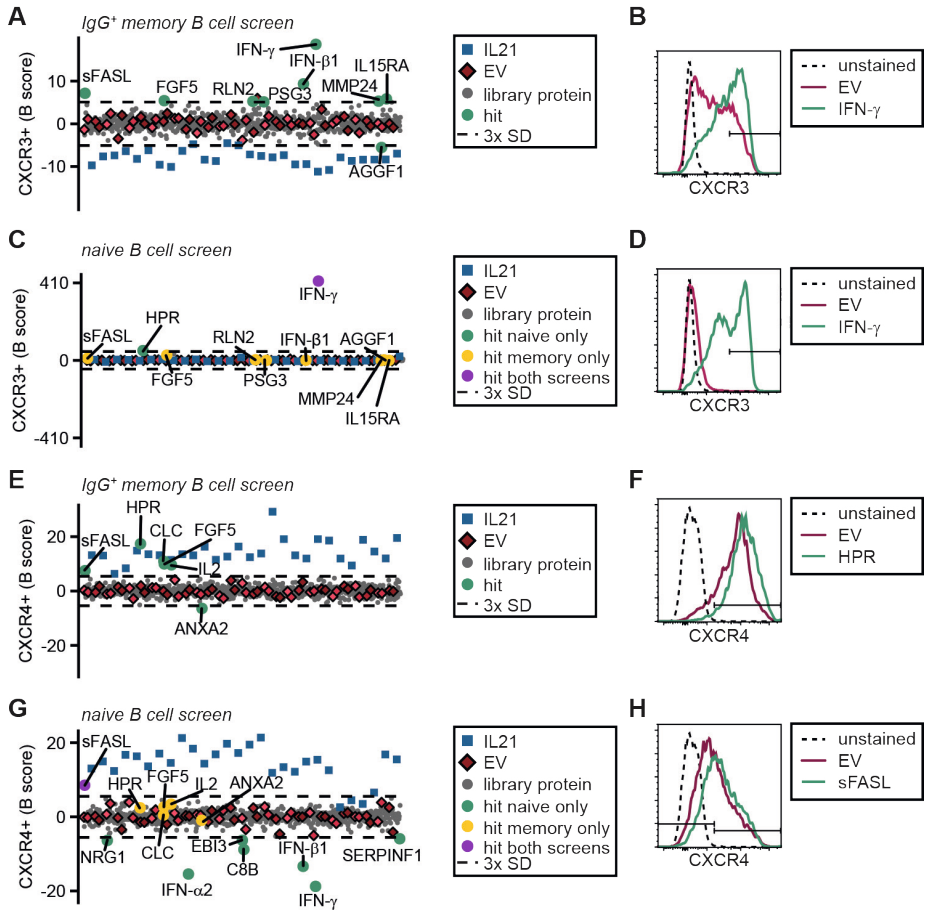


**Figure 2. The secreted protein screen identifies several proteins to affect the chemokine receptors CXCR3 and CXCR4.** The entire secreted protein library was screened on B cells of two healthy donors. (A-D) Data of CXCR3 expression on IgG<sup>+</sup> memory (A and B) and naive B cells (C and D). (E-H) Data of CXCR4 expression on IgG<sup>+</sup> memory (E and F) and naive B cells (G and H). (A, C, E and G) Pooled B score normalized percentages of each phenotype were averaged. For each readout the threshold for hit selection was set at three times SD (dashed line). Controls, hits and other secreted proteins are annotated in the legend boxes. EV is empty vector. (B, D, F and H) Example histograms of the secreted proteins inducing the highest indicated receptor expression on IgG<sup>+</sup> memory and naive B cells.

**Type I IFNs induce plasmablast differentiation**

We next analyzed the capacity of individual secreted proteins to differentiate B cells into CD27<sup>+</sup>CD38<sup>+</sup> ASCs. Control conditioned medium containing biologically active IL-21 (see Fig. 2) did not greatly induce CD27<sup>+</sup>CD38<sup>+</sup> ASCs, possibly because of supra-optimal IL-21 levels similar as found during the screen set up (Fig. S1B). Type I IFNs, MAb19 and sFASL all induced memory B cell differentiation into CD27<sup>+</sup>CD38<sup>+</sup> ASCs, with IFN- $\alpha$ 2 and IFN- $\beta$ 1 being the strongest hits (Fig. 3A-C). In addition, naive B cells cultured with type I IFNs differentiated into CD27<sup>+</sup>CD38<sup>+</sup> B cells (35%), while hardly any CD27<sup>+</sup> B cells were formed (Fig. 3D-G). The naive B cell differentiation into CD27<sup>+</sup> B cells was stimulated by IL-2, HPR, CLC, ADAMTS10 and FGF5 conditioned media, but these conditioned media largely failed to drive CD38<sup>+</sup> plasmablast differentiation.

Since type I IFNs were the most potent inducers of B cell differentiation in our screens, we validated these findings using serial dilutions of recombinant purified IFN- $\alpha$ . At all tested concentrations (starting at 0.1 ng/ml), IFN- $\alpha$  significantly directed IgG<sup>+</sup> memory B cells towards CD27<sup>+</sup>CD38<sup>+</sup> ASCs (Fig. 3H). IFN- $\alpha$  was also effective in inducing CD38 and CD27 expression in naive B cells, suggesting that the capacity of type I IFN signaling is similar between naive and memory B cells (Fig. 2I-J). Together, our screens reveal that a variety of secreted proteins can stimulate B cell differentiation and support the fact that naive B cells require different signals compared to memory B cells to differentiate into ASCs.

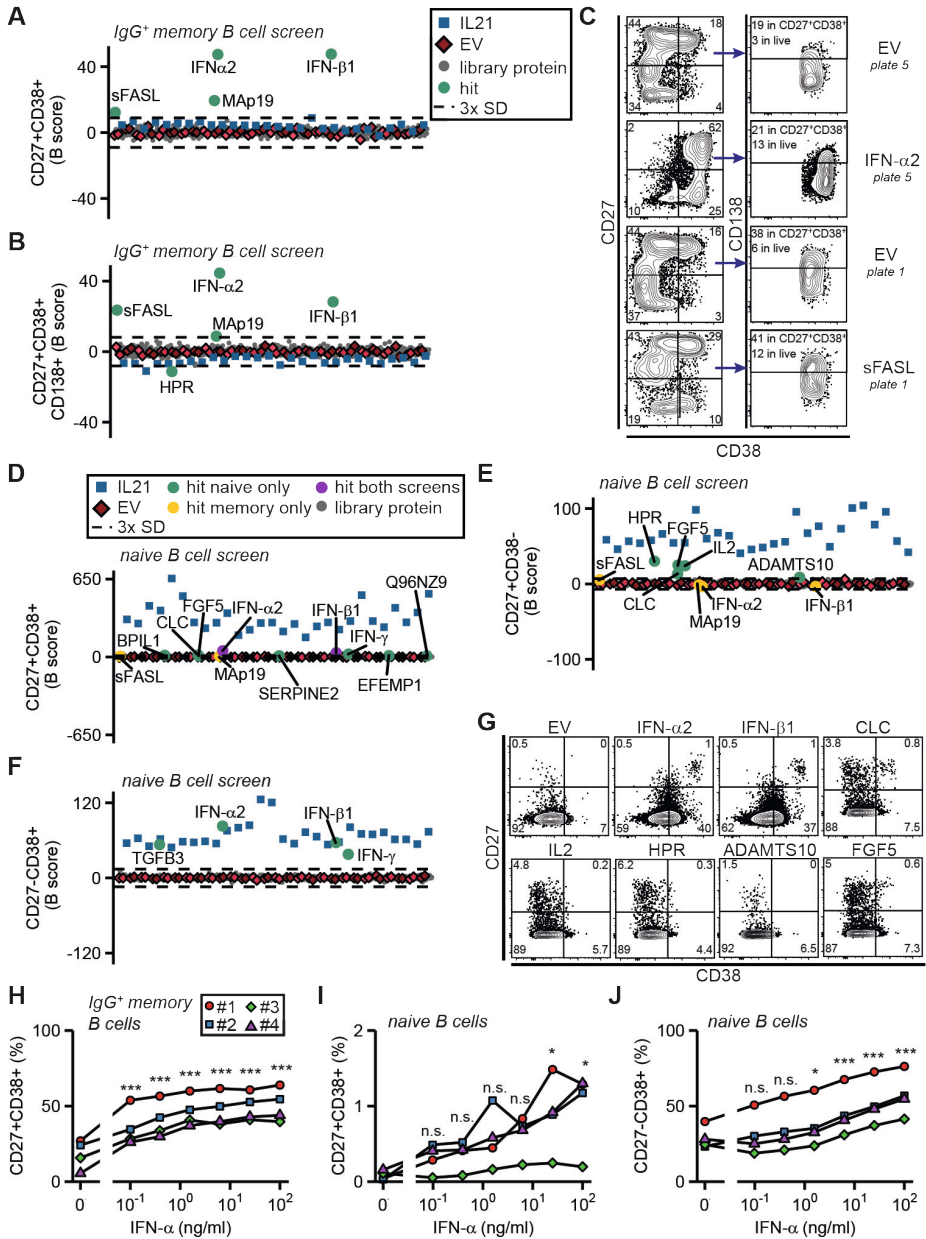


**Figure 3. Secretome screening reveals multiple plasmablast differentiation inducing factors.** (A, B, and D-F) Mean B scores of screen readouts for various differentiation stages of IgG<sup>+</sup> memory and naive B cells from two healthy donors. Legend boxes contain annotation of controls, hits and other secreted proteins. EV is empty vector. Differentiation stage was based on CD27, CD38 and CD138 expression as indicated and gated as shown in the contour plots (C and G) for controls and the most prominent hits (hit threshold is three times SD; dashed lines). IgG<sup>+</sup> memory (H) or naive (I and J) B cells from four different healthy donors were cultured as in Figure 1A using serial dilutions of purified recombinant IFN- $\alpha$  instead of conditioned medium. Significance compared to 0 ng/ml IFN- $\alpha$  is shown as determined by ANOVA with Tukey's post hoc test.

**sFASL induces ASC differentiation**

Our screens identified known and unknown secreted proteins to drive naive and memory B cells into various stages of differentiation. As the largest effects were witnessed upon differentiation of memory B cells, we validated these results for two additional donors using newly generated conditioned media. These confirmed that IFN- $\alpha$ 2, IFN- $\beta$ 1, MAp19 and sFASL conditioned media induced plasmablast differentiation from memory B cells (Fig. S2A). We further continued investigating MAp19 and sFASL, because to our knowledge these factors were unknown to promote B cell differentiation. MAp19 is a splice variant of MASP-2 (28). The function of MAp19 is unknown as it lacks the MASP-2 catalytic domain which is responsible for activating complement by cleaving C2 and C4 and may not be sufficiently expressed to compete with MASP-2 for binding to mannan-binding lectin (20). FASL is known as an inducer of apoptosis in many (embryonic) developmental and immunological processes (29, 30). In addition, occasional reports have described cell death independent functions of FASL (31). The FASL cDNA in our library encodes for a membrane-bound protein, which may be cleaved to obtain soluble FASL (sFASL) (32). As we used the conditioned medium of FASL transfected cells, we hypothesized that sFASL was present in the conditioned media.

Our validation assays showed that the conditioned media containing MAp19 or sFASL significantly induced CD27<sup>+</sup>CD38<sup>+</sup> B cells in IgG<sup>+</sup> memory B cells from four different donors (Fig. 4A). To further pinpoint the activity of these proteins, we repeated the assay with purified recombinant MAp19 or sFASL. MAp19 failed to reproduce the conditioned medium effect on B cell differentiation (Fig. 4B). In contrast, sFASL induced B cell differentiation into CD27<sup>+</sup>CD38<sup>+</sup> B cells starting at 10 ng/ml (Fig. 4C).



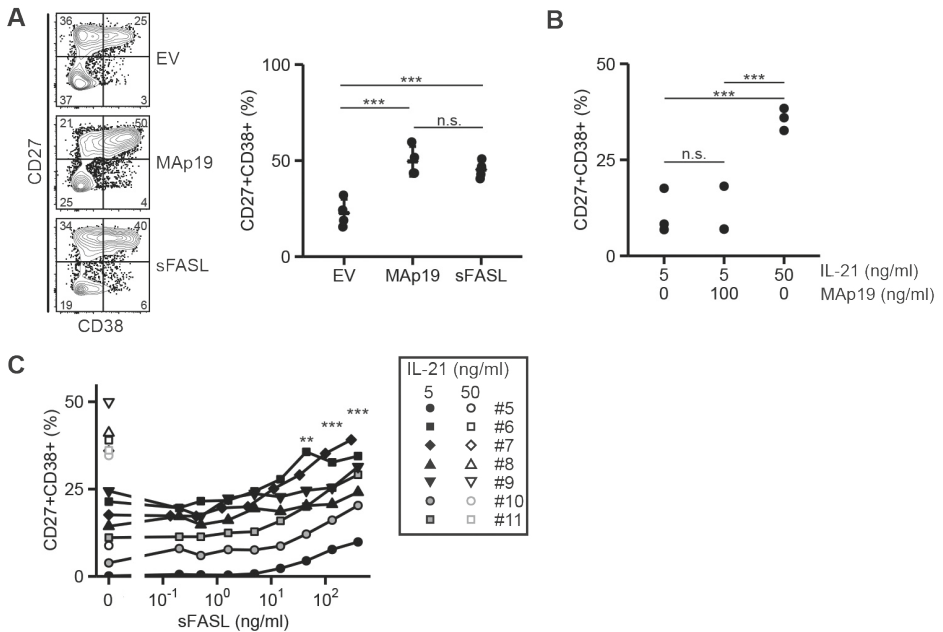


**Figure 4. sFASL induces differentiation into ASCs.** (A) Newly prepared conditioned media for MAp19 and sFASL were tested for CD27<sup>+</sup>CD38<sup>+</sup> ASC induction potential on IgG<sup>+</sup> memory B cells of four different healthy donors (two are the same as in Fig. S2). (B and C) IgG<sup>+</sup> memory B cell differentiation into CD27<sup>+</sup>CD38<sup>+</sup> ASCs in the presence of purified recombinant MAp19 (n=3) (B) or a serial dilution of commercially available recombinant sFASL (n=7) (C). Statistical significance was determined by ANOVA with Tukey's post hoc test. In panel only C statistical significance compared to 0 ng/mL FASL is shown.

FASL signals via the FAS receptor, also known as CD95. During germinal center reactions, B cells express this receptor due to stimulation with CD40L (33). In line with these data, the vast majority of B cells in our B cell differentiation assay express FAS after one day of culture in the presence of CD40L costimulation (Fig. S2B). The broad FAS receptor upregulation on B cells in our culture system is therefore not correlated with sFASL-mediated differentiation of a fraction of these B cells.

There are multiple possible explanations for sFASL-driven plasmablast differentiation. sFASL may cause the death of non-differentiating cells, it could encourage the proliferation of differentiating cells or finally, sFASL could drive differentiation into ASCs. To gain more insight into the mechanism, we analyzed the effect of sFASL on cell survival and proliferation by flow cytometry four days after culture initiation (gating in Fig. S3A). sFASL-treated B cells were still in an early stage of ASC differentiation, and had proliferated at a similar speed as the control without sFASL. Similar B cell numbers were present in sFASL-stimulated cultures compared to the control on both day 4 and day 10, indicating that sFASL does not promote plasmablast differentiation by affecting B cell apoptosis or proliferation (Fig. 5A-C).

Differentiation of B cells into ASCs is regulated by multiple transcription factors including the key molecules PAX5 and BLIMP-1 (34). Accordingly, PAX5 was downregulated in the presence of high amounts of IL-21 at day 4 of differentiation into ASCs, while expression of BLIMP-1 was increased (Fig. 5D). sFASL also induced more cells with a BLIMP-1<sup>+</sup>PAX5<sup>low</sup> phenotype compared to the control condition without sFASL (Fig. 5D), suggesting that sFASL supports B cell differentiation in a similar manner as IL-21. To investigate if these differentiated B cells could secrete antibodies, we measured the amounts of IgG1 and IgG4 in the culture supernatants. sFASL induced secretion of IgG1 and IgG4 in a concentration-dependent manner (normalized data in Fig. 5E, absolute values in S3C-S3D). The levels of produced IgG1 and IgG4 corresponded with the degree of CD27<sup>+</sup>CD38<sup>+</sup> cell differentiation for each donor (Fig. 4C, S3C-S3D). In conclusion, sFASL induced differentiation of IgG<sup>+</sup> memory B cells into antibody-secreting CD27<sup>+</sup>CD38<sup>+</sup> cells.

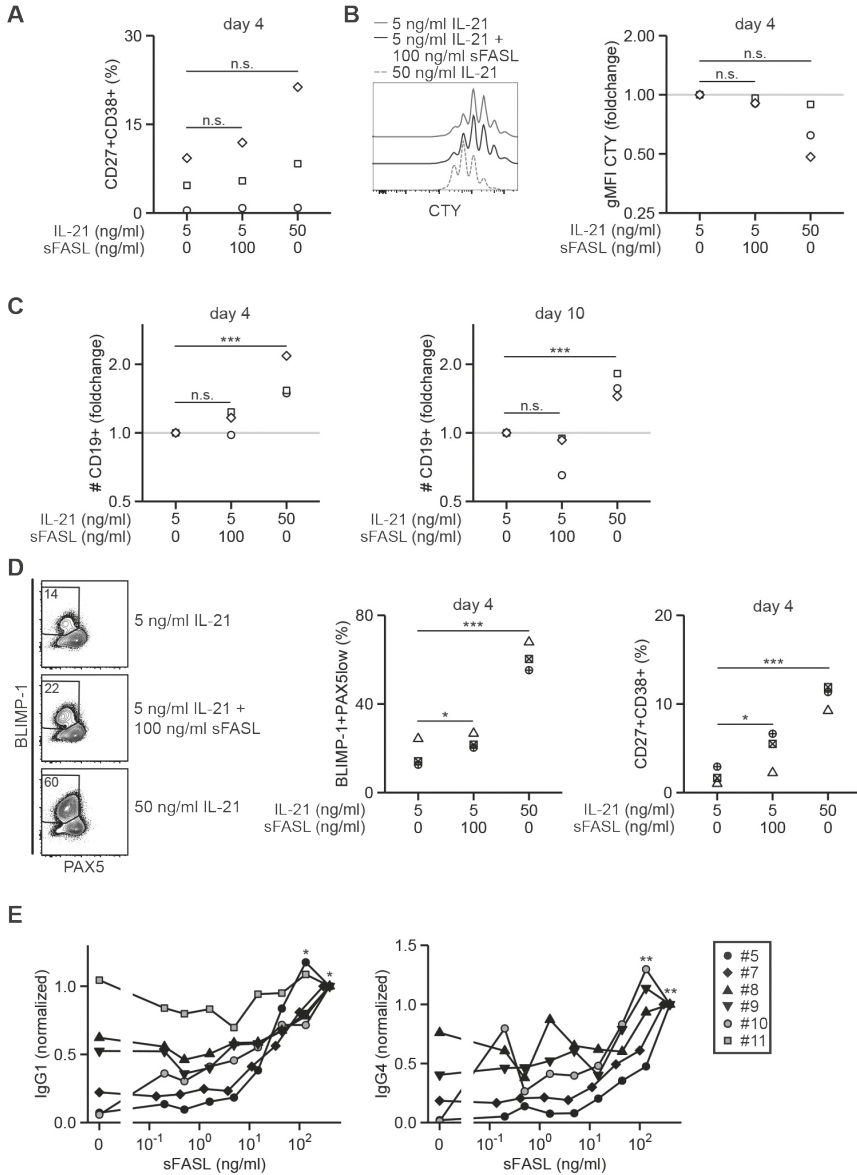


**Figure 5. sFASL affects differentiation and not proliferation into IgG1- and IgG4-secreting cells.** (A) CD27<sup>+</sup>CD38<sup>+</sup> expression analysis at day 4 of IgG<sup>+</sup> memory B cell culture in the presence of purified recombinant sFASL (n=3). (B) Histogram of cell trace yellow (CTY) dilution at day 4 after labeling (left panel) and geometric mean fluorescence intensity quantification of CTY dilution from three healthy donors (right panel) (n=3). (C) Counting bead normalized amount of CD19<sup>+</sup> B cells after 4-day (left panel) and 10-day (right panel) culture of IgG<sup>+</sup> memory B cells with indicated conditions (n=3). (D) PAX5<sup>low</sup>BLIMP-1<sup>+</sup> and CD27<sup>+</sup>CD38<sup>+</sup> analysis at day 4 (n=3). (E) IgG1 (n=6) and IgG4 (n=5) levels were determined by ELISA in the culture supernatants obtained at the end of IgG<sup>+</sup> memory B cell cultures in the presence of serial dilutions of sFASL. Data were normalized to the highest sFASL concentration per donor. Donor numbers (#) correspond to Figure 4C. For donor 11 IgG4 levels were below detection for all conditions including 50 ng/mL IL-21, therefore these data were excluded from analysis. Raw data are plotted in Fig. S3. Statistical significance was determined by ANOVA with Tukey's post hoc test for panels A-D. In E the Friedman test followed by Dunn's posttest was applied to determine statistical significance between 0 ng/ml sFASL and the individual serial dilutions of sFASL.

## DISCUSSION

The germinal center reaction is a dynamic process where activated B cells differentiate into ASCs upon receiving the appropriate signals. By employing a secreted protein library, we successfully identified multiple proteins that promote T cell-dependent differentiation of naive or memory B cells in the presence of CD40L and IL-21.

The strongest inducers of B cell differentiation in our screens are the well-studied type I IFNs. These multipotent proinflammatory cytokines signal through the Interferon-alpha/beta receptor (IFNAR) to inhibit viral replication by inducing an anti-viral state in non-immune cells and by activating immune cells including B cells. Type I IFNs induce upregulation of CD69, CD86 and CD40 in murine B cells, promote antibody secretion during influenza infection in mice, and can induce antibody secretion in human B cells *in vitro* (18, 35–38). Although the pro-inflammatory effects of type I IFNs are beneficial during viral infection, type I IFNs may also promote auto-reactive B cells in autoimmune diseases such as systemic lupus erythematosus (SLE) as reviewed by Kiefer *et al* (39).

While IFN- $\alpha$  and sFASL directly stimulate differentiation of memory B cells into CD27<sup>+</sup>CD38<sup>+</sup>CD138<sup>+</sup> plasma cells, purified MAp19 does not. A possible explanation as to why MAp19 conditioned medium induces B cell differentiation and its purified form does not may be that MAp19 stimulates HEK293T cells to secrete another protein or metabolic products. Alternatively, there may be structural differences between the freshly secreted and purified MAp19. Currently MAp19 has no known function (20), yet the fact that it is a spliced variant of the complement factor MASP-2 warrants future research on potential regulation of B cell differentiation through the complement system.

It is relevant to consider physiological concentrations when using soluble proteins in *in vitro* systems. Nonetheless, many soluble proteins have higher local than systemic concentrations, for example when they are secreted in immunological synapses. Such soluble proteins include the cytokine IL-21 (here used at 50 ng/mL for optimal B cell differentiation) and sFASL. In both of these cases, the physiological concentration is difficult to determine. Still, the role of IL-21 in B cell differentiation is beyond question because of the overwhelming amount of physiological relevance generated over the last years (e.g. using IL-21<sup>-/-</sup> mice) (40–42). We here provide the first data that in principle sFASL can play a role in human B cell differentiation.

FASL is well-known for its apoptosis-inducing capacity. For example, membrane-bound FASL is expressed by activated T cells to kill infected or malignant target cells by binding to and oligomerizing its receptor FAS present on these cells. Apoptosis plays a central role in selection of B cells during affinity maturation. CD40 ligation stimulates FAS expression and sensitizes B cells for FAS-mediated apoptosis, although IL-4 protects B cells from cell death (43, 44). Yet, *in vivo* studies showed that FAS signaling is dispensable for GC B cell selection in mice (45, 46).

The function of sFASL is still under debate as it is less effective in inducing apoptosis than membrane-bound FASL. sFASL may compete with membrane-bound FASL for FAS-binding thereby blocking apoptosis and even promoting proliferation (32, 47). We did not

observe a role of sFASL in the induction of apoptosis. Our results rather highlight a novel function of sFASL, which is to directly induce differentiation of CD40-activated memory B cells into ASCs.

sFASL may partake in the pathogenesis of several autoimmune diseases. Increased sFASL levels have been found in the serum of SLE patients and saliva of Sjögren's syndrome patients compared to healthy individuals. In addition, patients with more severe rheumatoid arthritis have higher sFASL levels in synovial fluid compared to those with less severe pathology (48–50). These autoimmune diseases are all characterized by the presence of autoantibodies, produced by ASCs originating from self-reactive B cells. So far, it remains unclear if the relationship between sFASL levels and autoimmunity is causal. Our data now demonstrates a direct role for sFASL in promoting B cell differentiation. It therefore opens the way for novel research exploring if sFASL initiates or worsens immune-mediated diseases by promoting differentiation of detrimental, autoreactive B cells.

### **Acknowledgments**

The authors thank the Sanquin Research Facility for their assistance with flow cytometry. IBS acknowledges integration into the Interdisciplinary Research Institute of Grenoble (IRIG, CEA).

## REFERENCES

1. Mesin, L., J. Ersching, and G. D. Victora. 2016. Germinal Center B Cell Dynamics. *Immunity* 45: 471–482.
2. Roco, J. A., L. Mesin, S. C. Binder, C. Nefzger, P. Gonzalez-Figueroa, P. F. Canete, J. Ellyard, Q. Shen, P. A. Robert, J. Cappello, H. Vohra, Y. Zhang, C. R. Nowosad, A. Schiepers, L. M. Corcoran, K. M. Toellner, J. M. Polo, M. Meyer-Hermann, G. D. Victora, and C. G. Vinuesa. 2019. Class-Switch Recombination Occurs Infrequently in Germinal Centers. *Immunity* 51: 337–350.e7.
3. Bannard, O., R. M. Horton, C. D. C. Allen, J. An, T. Nagasawa, and J. G. Cyster. 2013. Germinal center centroblasts transition to a centrocyte phenotype according to a timed program and depend on the dark zone for effective selection. *Immunity* 39: 912–924.
4. Kräutler, N. J., D. Suan, D. Butt, K. Bourne, J. R. Hermes, T. D. Chan, C. Sundling, W. Kaplan, P. Schofield, J. Jackson, A. Basten, D. Christ, and R. Brink. 2017. Differentiation of germinal center B cells into plasma cells is initiated by high-affinity antigen and completed by Tfh cells. *J. Exp. Med.* 214: 1259–1267.
5. Lau, A. W., and R. Brink. 2020. Selection in the germinal center. *Curr. Opin. Immunol.* 63: 29–34.
6. Bannard, O., and J. G. Cyster. 2017. Germinal centers: programmed for affinity maturation and antibody diversification. *Curr. Opin. Immunol.* 45: 21–30.
7. Weisel, F. J., G. V. Zuccarino-Catania, M. Chikina, and M. J. Shlomchik. 2016. A Temporal Switch in the Germinal Center Determines Differential Output of Memory B and Plasma Cells. *Immunity* 44: 116–130.
8. McHeyzer-Williams, L. J., C. Dufaud, and M. G. McHeyzer-Williams. 2017. Do Memory B Cells Form Secondary Germinal Centers? Impact of Antibody Class and Quality of Memory T-Cell Help at Recall. *Cold Spring Harb. Perspect. Biol.* 16: a029116.
9. Riedel, R., R. Addo, M. Ferreira-Gomes, G. A. Heinz, F. Heinrich, J. Kummer, V. Greiff, D. Schulz, C. Klaeden, R. Cornelis, U. Menzel, S. Kröger, U. Stervbo, R. Köhler, C. Haftmann, S. Kühnel, K. Lehmann, P. Maschmeyer, M. McGrath, S. Naundorf, S. Hahne, Ö. Sercan-Alp, F. Siracusa, J. Stefanowski, M. Weber, K. Westendorf, J. Zimmermann, A. E. Hauser, S. T. Reddy, P. Durek, H.-D. Chang, M.-F. Mashreghi, and A. Radbruch. 2020. Discrete populations of isotype-switched memory B lymphocytes are maintained in murine spleen and bone marrow. *Nat. Commun.* 11: 2570.
10. Hauser, A. E., G. F. Debes, S. Arce, G. Cassese, A. Hamann, A. Radbruch, and R. A. Manz. 2002. Chemotactic responsiveness toward ligands for CXCR3 and CXCR4 is regulated on plasma blasts during the time course of a memory immune response. *J. Immunol.* 169: 1277–82.
11. Ding, B. B., E. Bi, H. Chen, J. J. Yu, and B. H. Ye. 2013. IL-21 and CD40L Synergistically Promote Plasma Cell Differentiation through Upregulation of Blimp-1 in Human B Cells. *J. Immunol.* 190: 1827–1836.
12. Liu, D., H. Xu, C. Shih, Z. Wan, X. Ma, W. Ma, D. Luo, and H. Qi. 2015. T-B-cell entanglement and ICOSL-driven feed-forward regulation of germinal centre reaction. *Nature* 517: 214–218.
13. Good-Jacobson, K. L., C. G. Szumilas, L. Chen, A. H. Sharpe, M. M. Tomayko, and M. J. Shlomchik. 2010. PD-1 regulates germinal center B cell survival and the formation and affinity of long-lived plasma cells. *Nat. Immunol.* 11: 535–542.
14. Muehlinghaus, G., L. Cigliano, S. Huehn, A. Peddinghaus, H. Leyendeckers, A. E. Hauser, F. Hiepe, A. Radbruch, S. Arce, and R. A. Manz. 2005. Regulation of CXCR3 and CXCR4 expression during terminal differentiation of memory B cells into plasma cells. *Blood* 105: 3965–3971.

15. Gonzalez, D. G., C. M. Cote, J. R. Patel, C. B. Smith, Y. Zhang, K. M. Nickerson, T. Zhang, S. M. Kerfoot, and A. M. Haberman. 2018. Nonredundant Roles of IL-21 and IL-4 in the Phased Initiation of Germinal Center B Cells and Subsequent Self-Renewal Transitions. *J. Immunol.* 201: 3569–3579.
16. Laidlaw, B. J., Y. Lu, R. A. Amezcua, J. S. Weinstein, J. A. Vander Heiden, N. T. Gupta, S. H. Kleinstein, S. M. Kaeck, and J. Craft. 2017. Interleukin-10 from CD4+ follicular regulatory T cells promotes the germinal center response. *Sci. Immunol.* 2.
17. Guthmiller, J. J., A. C. Graham, R. A. Zander, R. L. Pope, and N. S. Butler. 2017. Cutting Edge: IL-10 Is Essential for the Generation of Germinal Center B Cell Responses and Anti-Plasmodium Humoral Immunity. *J. Immunol.* 198: 617–622.
18. Jego, G., A. K. Palucka, J.-P. Blanck, C. Chalouni, V. Pascual, and J. Banchereau. 2003. Plasmacytoid dendritic cells induce plasma cell differentiation through type I interferon and interleukin 6. *Immunity* 19: 225–34.
19. van Asten, S. D., M. Raaben, B. Nota, and R. M. Spaapen. 2018. Secretome Screening Reveals Fibroblast Growth Factors as Novel Inhibitors of Viral Replication. *J. Virol.* 92: JVI.00260-18.
20. Degn, S. E., S. Thiel, O. Nielsen, A. G. Hansen, R. Steffensen, and J. C. Jensenius. 2011. MAP19, the alternative splice product of the MASP2 gene. *J. Immunol. Methods* 373: 89–101.
21. Urashima, M., D. Chauhan, H. Uchiyama, G. J. Freeman, and K. C. Anderson. 1995. CD40 ligand triggered interleukin-6 secretion in multiple myeloma. *Blood* 85: 1903–12.
22. Schultze, J. L., A. A. Cardoso, G. J. Freeman, M. J. Seamon, J. Daley, G. S. Pinkus, J. G. Gribben, and L. M. Nadler. 1995. Follicular lymphomas can be induced to present alloantigen efficiently: A conceptual model to improve their tumor immunogenicity. *Proc. Natl. Acad. Sci. U. S. A.* 92: 8200–8204.
23. Thielens, N. M., S. Cseh, S. Thiel, T. Vorup-Jensen, V. Rossi, J. C. Jensenius, and G. J. Arlaud. 2001. Interaction Properties of Human Mannan-Binding Lectin (MBL)-Associated Serine Proteases-1 and -2, MBL-Associated Protein 19, and MBL. *J. Immunol.* 166: 5068–5077.
24. Zhang, J., T. D. Y. Chung, and K. R. Oldenburg. 1999. A Simple Statistical Parameter for Use in Evaluation and Validation of High Throughput Screening Assays. *J. Biomol. Screen.* 4: 67–73.
25. Malo, N., J. A. Hanley, S. Cerquozzi, J. Pelletier, and R. Nadon. 2006. Statistical practice in high-throughput screening data analysis. *Nat. Biotechnol.* 24: 167–75.
26. Marsman, C., T. Jorritsma, A. ten Brinke, and S. M. van Ham. 2020. Flow Cytometric Methods for the Detection of Intracellular Signaling Proteins and Transcription Factors Reveal Heterogeneity in Differentiating Human B Cell Subsets. *Cells* 9: 2633.
27. Tangye, S. G., and C. S. Ma. 2020. Regulation of the germinal center and humoral immunity by interleukin-21. *J. Exp. Med.* 217.
28. Takahashi, M., Y. Endo, T. Fujita, and M. Matsushita. 1999. A truncated form of mannose-binding lectin-associated serine protease (MASP)-2 expressed by alternative polyadenylation is a component of the lectin complement pathway. *Int. Immunol.* 11: 859–863.
29. French, L. E., M. Hahne, I. Viard, G. Radlgruber, R. Zanone, K. Becker, C. Müller, and J. Tschopp. 1996. Fas and Fas ligand in embryos and adult mice: ligand expression in several immune-privileged tissues and coexpression in adult tissues characterized by apoptotic cell turnover. *J. Cell Biol.* 133: 335–43.
30. Waring, P., and A. Müllbacher. 1999. Cell death induced by the Fas/Fas ligand pathway and its role in pathology. *Immunol. Cell Biol.* 77: 312–317.
31. Suzuki, I., and P. J. Fink. 2000. The dual functions of Fas ligand in the regulation of peripheral CD8+ and CD4+ T cells. *Proc. Natl. Acad. Sci. U. S. A.* 97: 1707–1712.

32. Schneider, P., N. Holler, J.-L. Bodmer, M. Hahne, K. Frei, A. Fontana, and J. Tschopp. 1998. Conversion of Membrane-bound Fas(CD95) Ligand to Its Soluble Form Is Associated with Downregulation of Its Proapoptotic Activity and Loss of Liver Toxicity. *J. Exp. Med.* 187: 1205–1213.
33. Schattner, E. J., K. B. Elkon, D. H. Yoo, J. Tumang, P. H. Krammer, M. K. Crow, and S. M. Friedman. 1995. CD40 ligation induces apo-1/fas expression on human B lymphocytes and facilitates apoptosis through the apo-1/fas pathway. *J. Exp. Med.* 182: 1557–1565.
34. Nutt, S. L., N. Taubenheim, J. Hasbold, L. M. Corcoran, and P. D. Hodgkin. 2011. The genetic network controlling plasma cell differentiation. *Semin. Immunol.* 23: 341–349.
35. Coro, E. S., W. L. W. Chang, and N. Baumgarth. 2006. Type I IFN receptor signals directly stimulate local B cells early following influenza virus infection. *J. Immunol.* 176: 4343–51.
36. Braun, D., I. Caramalho, and J. Demengeot. 2002. IFN-alpha/beta enhances BCR-dependent B cell responses. *Int. Immunol.* 14: 411–9.
37. Peters, M., L. Ambrus, A. Zheleznyak, J. A. Y. H. Hoofnagle, and F. Washington. 1986. Effect of interferon-alpha on immunoglobulin synthesis by human B cells. *J. Immunol.* 137: 3153–3157.
38. Klarquist, J., R. Cantrell, M. A. Lehn, K. Lampe, C. M. Hennies, K. Hoebe, and E. M. Janssen. 2020. Type I IFN Drives Experimental Systemic Lupus Erythematosus by Distinct Mechanisms in CD4 T Cells and B Cells. *ImmunoHorizons* 4: 140–152.
39. Kiefer, K., M. A. Oropallo, M. P. Cancro, and A. Marshak-Rothstein. 2012. Role of type I interferons in the activation of autoreactive B cells. *Immunol. Cell Biol.* 90: 498–504.
40. Zotos, D., J. M. Coquet, Y. Zhang, A. Light, K. D’Costa, A. Kallies, L. M. Corcoran, D. I. Godfrey, K.-M. Toellner, M. J. Smyth, S. L. Nutt, and D. M. Tarlinton. 2010. IL-21 regulates germinal center B cell differentiation and proliferation through a B cell-intrinsic mechanism. *J. Exp. Med.* 207: 365–78.
41. Ozaki, K., R. Spolski, C. G. Feng, C.-F. Qi, J. Cheng, A. Sher, H. C. Morse, C. Liu, P. L. Schwartzberg, and W. J. Leonard. 2002. A critical role for IL-21 in regulating immunoglobulin production. *Science* 298: 1630–4.
42. Ozaki, K., R. Spolski, R. Ettinger, H.-P. Kim, G. Wang, C.-F. Qi, P. Hwu, D. J. Shaffer, S. Akilesh, D. C. Roopenian, H. C. Morse, P. E. Lipsky, and W. J. Leonard. 2004. Regulation of B Cell Differentiation and Plasma Cell Generation by IL-21, a Novel Inducer of Blimp-1 and Bcl-6. *J. Immunol.* 173: 5361–5371.
43. Garrone, P., E. M. Neidhardt, E. Garcia, L. Galibert, C. Van Kooten, and J. Banchereau. 1995. Fas ligation induces apoptosis of CD40-activated human B lymphocytes. *J. Exp. Med.* 182: 1265–1273.
44. Nakanishi, K., K. Matsui, S. Kashiwamura, Y. Nishioka, J. Nomura, Y. Nishimura, N. Sakaguchi, S. Yonehara, K. Higashino, and S. Shinka. 1996. IL-4 and anti-CD40 protect against Fas-mediated B cell apoptosis and induce B cell growth and differentiation. *Int. Immunol.* 8: 791–8.
45. Butt, D., T. D. Chan, K. Bourne, J. R. Hermes, A. Nguyen, A. Statham, L. A. O’Reilly, A. Strasser, S. Price, P. Schofield, D. Christ, A. Basten, C. S. Ma, S. G. Tangye, T. G. Phan, V. K. Rao, and R. Brink. 2015. FAS Inactivation Releases Unconventional Germinal Center B Cells that Escape Antigen Control and Drive IgE and Autoantibody Production. *Immunity* 42: 890–902.
46. Smith, K. G. C., G. J. V. Nossal, and D. M. Tarlinton. 1995. FAS is highly expressed in the germinal center but is not required for regulation of the B-cell response to antigen. *Proc. Natl. Acad. Sci. U. S. A.* 92: 11628–11632.



47. Audo, R., F. Calmon-Hamaty, L. Papon, B. Combe, J. Morel, and M. Hahne. 2014. Distinct Effects of Soluble and Membrane-Bound Fas Ligand on Fibroblast-like Synoviocytes From Rheumatoid Arthritis Patients. *Arthritis Rheumatol.* 66: 3289–3299.
48. Vincent, F. B., R. Kandane-Rathnayake, R. Koelmeyer, J. Harris, A. Y. Hoi, F. MacKay, F. MacKay, and E. F. Morand. 2020. Associations of serum soluble Fas and Fas ligand (FasL) with outcomes in systemic lupus erythematosus. *Lupus Sci. Med.* 7: 375.
49. Nakamura, H., A. Kawakami, M. Izumi, T. Nakashima, Y. Takagi, H. Ida, T. Nakamura, T. Nakamura, and K. Eguchi. 2005. Detection of the soluble form of Fas ligand (sFasL) and sFas in the saliva from patients with Sjögren's syndrome. *Clin. Exp. Rheumatol.* 23: 915.
50. Hashimoto, H., M. Tanaka, T. Suda, T. Tomita, K. Hayashida, E. Takeuchi, M. Kaneko, H. Takano, S. Nagata, and T. Ochi. 1998. Soluble fas ligand in the joints of patients with rheumatoid arthritis and osteoarthritis. *Arthritis Rheum.* 41: 657–662.

## Footnotes

**Grant support:** This research was supported by Sanquin Product and Process Development of Cellular Products grants PPOC-14-46 to Dr. Robbert Spaapen, and both the PPOC-17-34 and the Landsteiner Foundation for Blood Transfusion Research (LSBR) grant 1609 to Dr. Marieke van Ham.

**Abbreviations used in this article:** ASC, antibody secreting cell; BCR, B cell receptor; CTY, cell trace yellow; DZ, dark zone; EV, empty vector; GC, germinal center; IFN, interferon; IFNAR, Interferon-alpha/beta receptor; LZ, light zone; M $\alpha$ p19, mannan-binding lectin-associated protein of 19 kDa; SD, standard deviation; SLE, systemic lupus erythematosus; sFASL, soluble FAS ligand; Tfh, T follicular helper;

## SUPPLEMENTARY MATERIAL

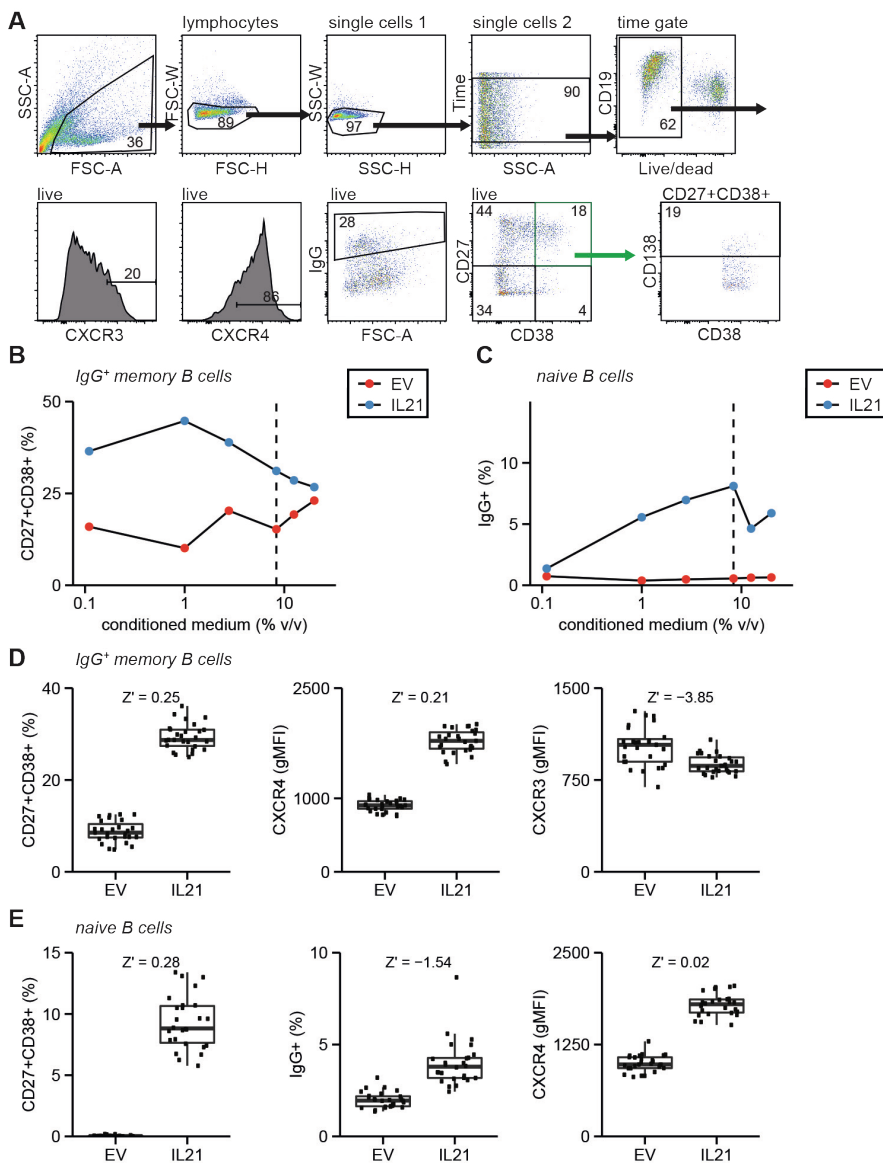


**Figure S1. Optimization of B cell differentiation assay for arrayed screening.** (A) Strategy at the end of the B cell differentiation assay to gate live, single CD19<sup>+</sup> B cells. Markers of interest within these B cells include CXCR3, CXCR4, IgG and also CD27/CD38 to allow gating on plasmablasts and plasma cells. Plasma cells were identified by gating for CD138 within CD27<sup>+</sup> CD38<sup>+</sup> B cells. Percentages of CD27<sup>+</sup> CD38<sup>+</sup> CD138<sup>+</sup> cells were calculated within live B cells. (B and C) IgG<sup>+</sup> memory (B) and naive B cells (C) were cultured as depicted in Figure 1A in the presence of a serial dilution of conditioned medium derived from empty vector (EV) or IL-21 cDNA transfected HEK293T cells in addition to 5 ng/ml IL-21. 1:12 (8.3 % v/v) was chosen as the preferred conditioned medium dilution for the secreted protein screen, here indicated with a dashed line. (D-E) 24 replicates of control empty vector and IL-21 conditioned media were assayed according to the optimized conditions. Depicted parameters were readout at the end of IgG<sup>+</sup> memory (D) and naive B cell (E) cultures. Z' scores are shown, Z'<sup>2</sup>>0 indicates suitability of the assay for arrayed screening

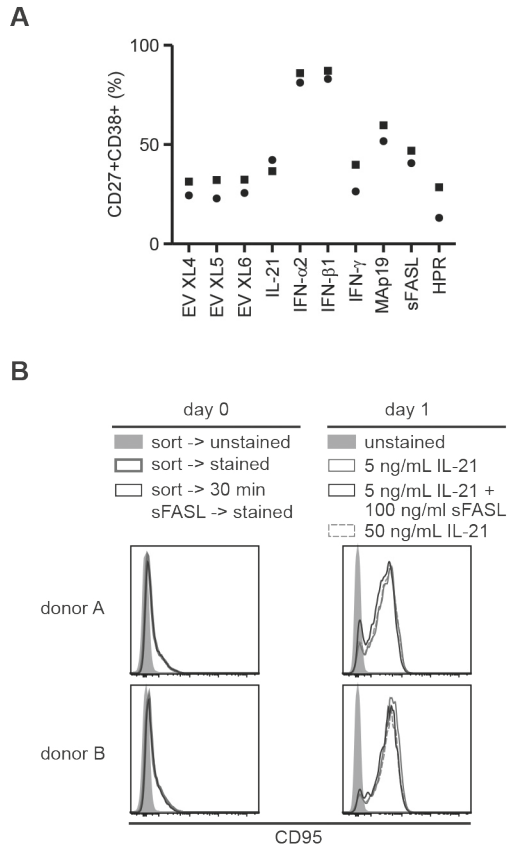


**Figure S2. Type I IFNs, sFASL and Map19 induce the formation of CD27+ CD38+ ASCs.** (A) Newly prepared conditioned media from indicated cDNAs and empty vectors (XL4, XL5 and XL6 backbones) were tested for CD27+ CD38+ ASC induction potential on IgG+ memory B cells of two different healthy donors (part of the data is also included in Fig. 4A). (B) IgG+ memory B cells from two donors were stained for CD95 immediately after the sort (left panel), after 30 minutes of incubation with sFASL (left panel) or after 1 day in the B cell differentiation assay (right panel).

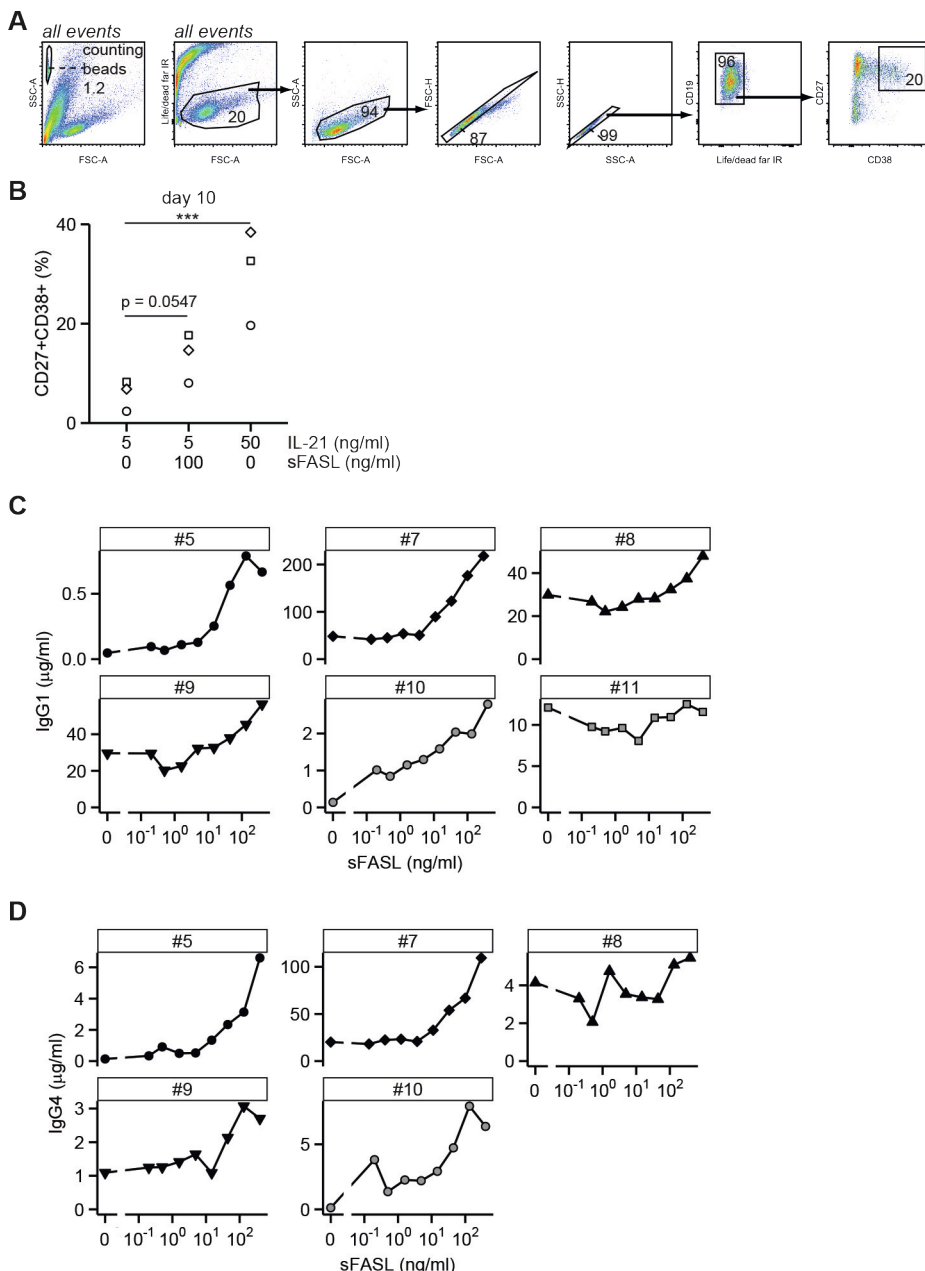


**Figure S3. Gating strategy of B cell proliferation assay.** (A) Strategy to gate on counting beads, CD19+ live cells and CD27+ CD38+ ASCs on both day 4 and day 10 of the proliferation assay. (B) Quantification of CD27+ CD38+ ASCs within live CD19+ B cells on day 10. Statistical significance was determined by ANOVA with Tukey's post hoc test. (C and D) IgG1 (C) and IgG4 (D) levels in culture supernatants of IgG+ memory B cells cultured in the presence of sFASL serial dilutions.





# CHAPTER 5

## Termination of CD40L co-stimulation promotes human B cell differentiation into antibody-secreting cells

Casper Marsman, Niels J.M. Verstegen, Marij Streutker, Tineke Jorritsma, Louis Boon, Anja ten Brinke, S. Marieke van Ham

*European Journal of Immunology (2022), 0: 1-14*

**ABSTRACT**

Human naïve B cells are notoriously difficult to differentiate into antibody-secreting cells (ASCs) in vitro while maintaining sufficient cell numbers to evaluate the differentiation process. Insights in factors controlling this process are needed to boost protective humoral immunity or to prevent harmful antibody formation in autoimmunity. B cells require T follicular helper ( $T_{FH}$ ) cell-derived signals like CD40L and IL-21 during germinal center (GC) responses to undergo differentiation into ASCs. The cognate interaction between B and  $T_{FH}$  cells are transient; after  $T_{FH}$  contact, B cells cycle between GC light and dark zones where  $T_{FH}$  contact is present and absent, respectively. Here, we elucidated that efficacy of naïve B cell into ACS differentiation in vitro is dramatically enhanced by release of CD40L stimulation. Multiparameter phospho-flow and transcription factor (TF)-flow cytometry revealed that termination of CD40L stimulation downmodulates NF- $\kappa$ B and STAT3 signaling. Furthermore, Termination of CD40 signaling downmodulates C-MYC, while promoting ASC TFs BLIMP1 and XBP-1s. While IRF4 is downmodulated in the differentiating B cells by termination of CD40 signaling, IRF4 is maintained at high levels in BLIMP1 expressing cells. Reduced levels of C-MYC in the differentiating B cells is later associated with crucial downmodulation of the B cell signature TF PAX5 specifically upon termination of CD40 signaling, resulting in the differentiation of BLIMP1 high expressing cells into ASCs. The data presented here are the first steps to provide further insights how the transient nature of CD40 signaling is in fact needed for efficient human naïve B cell differentiation to ASCs.



## INTRODUCTION

One key aspect of humoral immunity is the ability of B cells to respond to pathogens and differentiate into antibody-secreting cells (ASCs). Essential to generation of high-affinity antibody production are follicular T helper cells ( $T_{FH}$ ) that regulate germinal center (GC) formation and B cell differentiation by providing cognate B cells with co-stimulatory signals and specific cytokines<sup>1-4</sup>. Naïve B cells are activated when antigen is recognized by the B cell receptor (BCR). Antigen is subsequently phagocytosed, degraded, loaded onto MHC class II molecules and presented to  $T_{FH}$  cells to allow cognate recognition<sup>5</sup>. Positive recognition results in strong synapse formation between B and  $T_{FH}$  cells and allows  $T_{FH}$  cells to stimulate B cells through membrane-bound CD40L that activates CD40 on the B cell surface<sup>6,7</sup>. Additionally,  $T_{FH}$  cells secrete cytokines that promote B cell differentiation. Of these the  $T_{FH}$  hallmark cytokine IL-21, which triggers the IL-21 receptor, is indispensable for B cell differentiation<sup>8,9</sup>.

The timing and regulation of CD40L and IL-21 stimulation within GC responses is highly complex and dynamic<sup>10,11</sup>. Interactions between  $T_{FH}$  cells and B cells are spatio-dynamically regulated and therefore temporary<sup>12</sup>. B cells actively move away from initial cognate T cell interactions at the B/T cell border in secondary lymphoid organs to form GC dark zones. Here, B cells expand rapidly and can undergo class-switch recombination (CSR) and somatic hyper-mutation (SHM). Subsequently, B cells migrate out of the GC dark zones to establish GC light zones where the B cells re-acquire antigen, followed by reacquisition of  $T_{FH}$  help, consisting of additional CD40L and (among others) IL-21-mediated  $T_{FH}$  cell stimulation<sup>13</sup>. After  $T_{FH}$  cell interactions, differentiating B cells may migrate back to the GC dark zone to undergo more proliferation, SHM and/or CSR or undergo early B memory formation. After several rounds of GC cycling and memory formation, B cells differentiate into ASCs. Still, questions remain how exactly the latter process is regulated. CD40L stimulation induces activation of NF- $\kappa$ B pathways while IL-21R stimulation mainly induces phosphorylation of STAT3 (p-STAT3)<sup>14-16</sup>. These signaling pathways subsequently regulate an intricate network of transcription factors (TFs) governing B cell identity, GC cell regulation and ASC differentiation<sup>11,17</sup>. Expression of PAX5 maintains B cell identity and is induced by CD40L stimulation<sup>18</sup>. Additionally, CD40L stimulation and NF- $\kappa$ B signaling induce expression of C-MYC<sup>19</sup>, which regulates proliferation and cycling of GC B cells<sup>20,21</sup>, and IRF4<sup>22</sup>, which at low levels promotes GC B cell development<sup>23</sup>. Differentiation of B cells into ASCs requires the downregulation of PAX5 and C-MYC and the concomitant upregulation of BLIMP1, master regulator of ASC differentiation<sup>17,24,25</sup>. BLIMP1 expression is mainly induced by IL-21 mediated p-STAT3 signaling<sup>1,9,26,27</sup> while CD40L co-stimulation has been shown to inhibit BLIMP1 expression<sup>6</sup> but both CD40L and IL-21 however, are essential for ASC differentiation<sup>1</sup>. Additionally, alternative splicing of XBP1 into XBP-1s is required for the maintenance of the unfolded-protein response (UPR), allowing the massive production of antibodies<sup>28</sup>. Within this complicated network, TFs can also positively and negatively feedback on expression of

other TFs in the network. Most well-known is the fact that PAX5 and BLIMP1 inhibit each other<sup>17</sup>. However, PAX5 has also been shown to inhibit C-MYC<sup>29,30</sup> and XBP1 expression, possibly through downregulation of BLIMP1<sup>31</sup>. Additionally, high levels of IRF4 promote expression of BLIMP1 and thus downregulation of PAX5<sup>23,32</sup>.

As the T-dependent B cell response is complex and still not fully elucidated, insights into factors determining B cell to ASC differentiation are highly desired. Over the years *in vitro* cultures have been applied to study human ASC generation with varying success<sup>33-36</sup>. Most cultures rely on continued CD40L and IL-21 stimulation over the course of several days. Based on the *in vivo* situation of spatiotemporal regulation of B cell to ASC differentiation and intermittent T<sub>FH</sub> cell help, we hypothesized that temporal instead of continued T<sub>FH</sub> stimulation contributes to the T-dependent B cells response. Recently, a similar mechanism was found for the IL-4 / STAT6 pathway for which it was demonstrated that ASC differentiation requires the downregulation of this pathway<sup>37</sup>. Additionally, we have shown that phospho- STAT1, -STAT3, -STAT6 and activated NF- $\kappa$ B p65 signaling in *in vitro* generated ASC is also downregulated compared to other B cell subsets<sup>38</sup>. Here we demonstrate that targeted termination of CD40L stimulation with continuous IL-21 stimulation, promotes human B cell to ASC differentiation. Interestingly, abrogation of CD40L stimulation both extinguished NF- $\kappa$ B and STAT3 signaling during B cell differentiation. Our data show that even though BLIMP-1 expression may be induced independently of termination of CD40L stimulation, both downregulation of the B cell identity TF PAX5 and upregulation of the ASC-associated TF XBP-1s are dependent on termination of CD40L stimulation and extinguishment the NF- $\kappa$ B signaling pathway. Termination of CD40L stimulation during B cell differentiation is therefore a direct factor involved in B cell differentiation into ASCs.

## RESULTS

### **Termination of CD40L co-stimulation inhibits B cell proliferation and expansion while promoting differentiation**

The effect of termination of CD40L co-stimulation on human naive B cell proliferation and differentiation was investigated by activating naive human B cells via CD40L-expressing 3T3 cells and IL-21 and addition of CD40L blocking antibodies at several points in time during. When CD40L blocking antibodies were present before activation almost no proliferation occurred, showing that, in accordance with literature<sup>36</sup>, B cell proliferation is highly reliant on CD40L and IL-21 stimulation (Fig 1A, Suppl Fig 1B). Proliferation was also significantly reduced when CD40L blocking antibodies were added at later time points during stimulation (Fig 1A), showing that CD40L blocking antibodies efficiently inhibit CD40L induced proliferation even after an initial stimulation. Termination of CD40L co-stimulation at all timepoints also significantly reduced actual expansion of CD19<sup>+</sup> cells in culture (Fig 1B). These data demonstrate that termination of CD40L co-stimulation

inhibits proliferation and expansion of CD19<sup>+</sup> naïve B cells even when CD40L stimulation is blocked at a later stage of the culture.

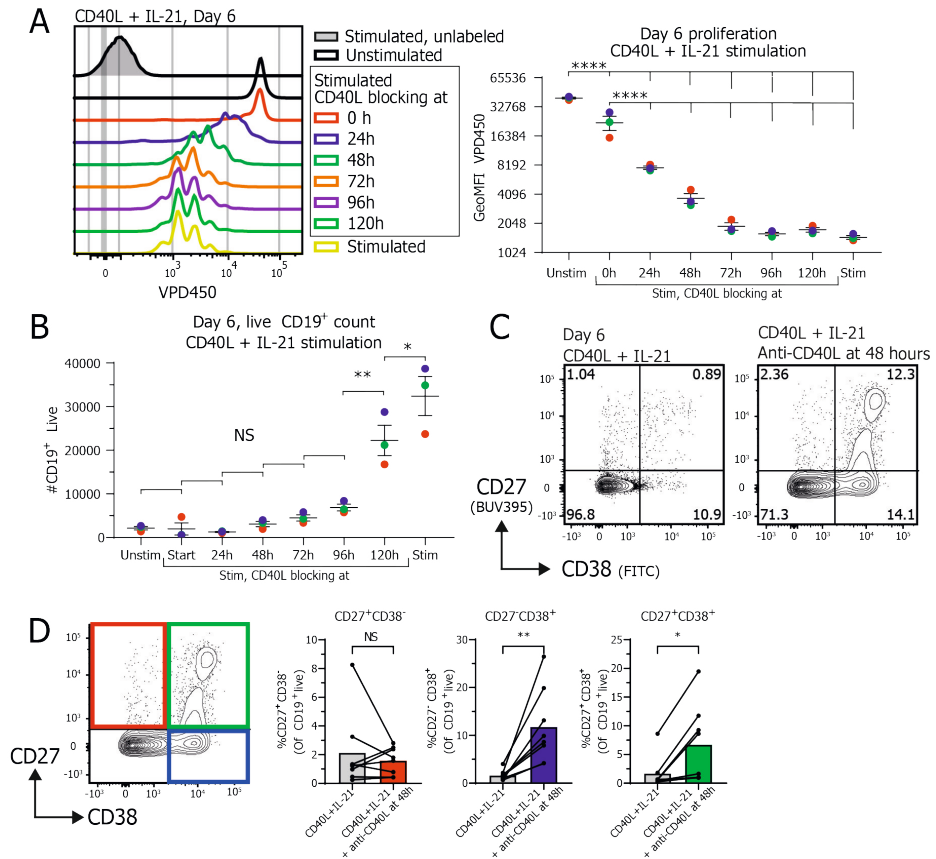


**Figure 1. Termination of CD40L stimulation after CD40L and IL-21 stimulation inhibits proliferation and promotes differentiation into ASCs.** Naïve B cells were sorted and 25,000 cells were stimulated with a human-CD40L expressing 3T3 feeder layer and recombinant IL-21 (50 ng/ml). After the indicated culture duration CD40L blocking antibodies (13 µg/ml) were added and cells were analyzed at day 6 by flow cytometry. **(A)** Naïve B cells were labelled with proliferation dye VPD450 prior to culture. Representative histogram overlay (left) and quantification of VPD450 GeoMFI after 6 days of culture under indicated conditions. Data from a single independent experiment with the mean of 3 individual donors replicates marked as red, green or blue dots with triplicate measurements (n=3). **(B)** Number of live CD19<sup>+</sup> cells were analyzed at day 6 after adding CD40L blocking antibodies at indicated time points (n=3). Data from a single independent experiment with the mean of 3 individual donors marked as red, green or blue dots with triplicate measurements (n=3), scatter plots show mean +/- SD, P-values were calculated using one-way ANOVA with Tukey's multiple comparison test. **(C)** Representative contour plot of CD27 and CD38 expression profiles after 6 days of culture with the indicated conditions. **(D)** Quantification of the relative percentages of CD27 and CD38 subpopulations after 6 days of culture with the indicated conditions (n=8). Combined data from 7 independent experiments, each performed with 1-2 donors. Each data point represents the mean of an individual donor with duplicate or triplicate measurements. Mean values are represented as bars. P-values were calculated using paired t-test \* P ≤ 0.05, \*\* P ≤ 0.01, \*\*\* P ≤ 0.001, \*\*\*\* P ≤ 0.0001.

Further investigation of effects of termination of CD40L stimulation on naïve B cell differentiation showed that naïve B cell differentiation into CD27<sup>+</sup>CD38<sup>+</sup> ASC was prominently induced upon termination of CD40L co-stimulation after 2 to 4 days of culture, while ASC differentiation was nearly absent when stimulated continuously with CD40L and IL-21 (Fig 1C, suppl Fig 1C). In order to mimic the *in vivo* situation as close as possible, by aiming to terminate CD40L stimulation as early as possible after the initial stimulus, while maintaining sufficient numbers of CD19<sup>+</sup> cells for differentiation analysis, CD40L stimulation was blocked after 48 hours in the rest of the experiments. Termination of CD40L co-stimulation after 48 hours significantly increased differentiation into both CD38<sup>+</sup> B cells and CD27<sup>+</sup>CD38<sup>+</sup> ASCs at day 6 (Fig 1D).

To further elucidate the effect of CD40L co-stimulation and termination thereof in more detail, cultures were analyzed for proliferation, expansion and differentiation every 24 hours during continued or terminated CD40L stimulation. Unstimulated naïve B cells were analyzed as controls and did not proliferate or expand and were therefore not analyzed after the 72-hour time point in any further analyses (Fig 2A). Termination of CD40L co-stimulation after 48 hours resulted in significantly reduced B cell expansion, compared to continued stimulation, after 120 hours of culture (Fig 2A). This observation is in line with the fact that proliferation stagnated at 96 hours and later time points compared to continued stimulation (Fig 2B). These data interestingly also demonstrate that B cells continue to proliferate in the first days after termination of the CD40L stimulation.

Additionally, the effect of CD40L blockade on dynamics of CD27<sup>+</sup>CD38<sup>+</sup> ASC differentiation was investigated. Remarkably, termination of CD40L co-stimulation after 48 hours significantly increased differentiation into CD27<sup>+</sup>CD38<sup>+</sup> ASCs already within 48 hours after CD40L stimulation was blocked (Fig 2C – D). These data demonstrate that the B cell differentiation in CD40L terminated cultures is not only elevated but also that differentiation is quicker and already detectable at 96 hours of culture and reaches a peak after 120 hours. After this time point however, CD27<sup>+</sup>CD38<sup>+</sup> ASCs numbers declined indicating that these differentiated cells do not survive in longer cultures. Utilizing Uniform Manifold Approximation and Projection (UMAP) analyses of expression of TFs regulating B cell identity and ASC differentiation revealed that termination of CD40L co-stimulation strongly induced relatively high expression of ASC TFs IRF4, BLIMP1 and XBP-1s and relatively low expression of B cell identity TF PAX5 in the CD27<sup>+</sup>CD38<sup>+</sup> compartment (Fig 2E, below the black arrow). Finally, measuring secreted antibodies in culture supernatant demonstrated that termination of CD40L stimulation also promotes secretion of both IgM and IgG (Suppl 2). Altogether, these data clearly show that termination of CD40L co-stimulation with continuous IL-21 inhibits B cell proliferation and expansion while promoting rapid differentiation of stimulated B cells into CD27<sup>+</sup>CD38<sup>+</sup> ASCs.

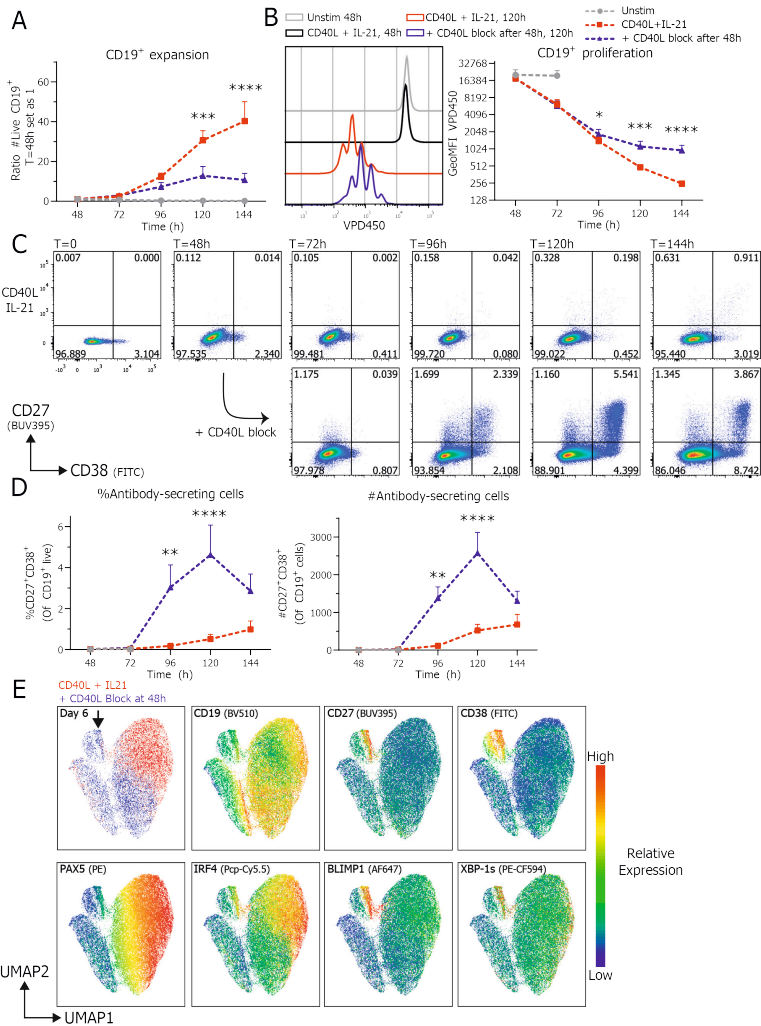


**Figure 2. Termination of CD40L stimulation inhibits CD19<sup>+</sup> expansion and proliferation and results in efficient ASC differentiation.** Naïve B cells were sorted, labelled with VPD450 and 25,000 cells were stimulated with a human-CD40L expressing 3T3 feeder layer and recombinant IL-21 (50 ng/ml). After the 48 hours CD40L blocking antibodies (13 µg/ml) were added or not. At indicated timepoints cultures were harvested, stained for membrane markers, fixed and stored until day 6 when all samples were analyzed by flow cytometry. **(A)** Quantification of live CD19<sup>+</sup> cells per day (n=8) **(B)** Representative histogram overlay (left) and quantification (right) of VPD450 GeoMFI per day (n=8). Combined data from 4 independent experiments, each performed with 2 donors. Symbols represent the mean and error bars show +/- SEM. **(C)** Representative pseudocolor dot plots of CD27 and CD38 expression profiles per day under indicated conditions. **(D)** Quantification of relative percentages (left) and absolute counts (right) of CD27<sup>+</sup>CD38<sup>+</sup> ASC per day (n=6). Combined data from 3 independent experiments, each performed with 2 donors. Symbols represent the mean and error bars show +/- SEM. P-values were calculated by comparing the red CD40L + IL-21 condition and the blue CD40L stimulation terminated after 48h condition, using two-way ANOVA with Sidak's multiple comparison test. \* P ≤ 0.05, \*\* P ≤ 0.01, \*\*\* P ≤ 0.001, \*\*\*\* P ≤ 0.0001. **(E)** UMAP clustering analysis on day 6 cultured B cells stained for CD19, CD27, CD38, PAX5, IRF4, BLIMP1 and XBP-1s. The different conditions (red and blue) are shown overlaid at the top left, the ASC population is marked by a black arrow and relative protein expressions are represented as a heatmap. UMAP settings were as follows: distance function, Euclidean; number of neighbors, 30; minimal distance, 0.5; and number of components, 2. UMAP generated with data from a single representative donor measured in duplicate.

**Termination of CD40L stimulation results in downregulation of activated NF- $\kappa$ B p65 and p-STAT3 pathways**

To elucidate in more detail how termination of CD40L co-stimulation leads to ASC differentiation intracellular (phospho) signaling pathways were investigated. Stimulation by CD40L is known to activate NF- $\kappa$ B signaling and this subsequently leads to survival and proliferation of B cells<sup>15</sup>. Additionally, IL-21 is known to mainly induce phosphorylation of STAT3 which in turn is crucial for the induction of BLIMP1<sup>27</sup>. Therefore, activated NF- $\kappa$ B p65 and (phosphorylated) STAT3 by CD40L and IL-21 stimulation (Fig 3A) were analyzed over time during continued stimulation or in cultures with terminated CD40L co-stimulation after 48 hours. Continued CD40L and IL-21 stimulation induced high levels of activated NF- $\kappa$ B p65 after 72 hours, after which it decreased again (Fig 3B). Termination of CD40L stimulation with continued IL-21 stimulation however, resulted in an immediate and clear inhibition of activated NF- $\kappa$ B p65 induction (Fig 3B). The activated NF- $\kappa$ B p65 levels after CD40L termination declined to a level that is higher than the unstimulated condition, indicating that residual active NF- $\kappa$ B p65 signaling remains after termination of CD40L co-stimulation. Partly this residual staining could be attributed to an increased cell size after stimulation (Suppl Fig 3). Remarkably, termination of CD40L stimulation with continued IL-21 stimulation also resulted in significant inhibition of both STAT3 and p-STAT3 levels (Fig 3C-D), indicating crosstalk between the CD40 / NF- $\kappa$ B and IL-21R pathways. After termination of CD40L stimulation p-STAT3/STAT3 signaling was not reduced to baseline levels, again indicating that a low level of signaling remains even without CD40L stimulation present. This could however not be attributed to increased cell size as with the residual activated NF- $\kappa$ B p65 and STAT3 expression (Suppl Fig 3). Together these data show that termination of CD40L stimulation rapidly inhibits not only NF- $\kappa$ B but also downmodulates STAT3 signaling.

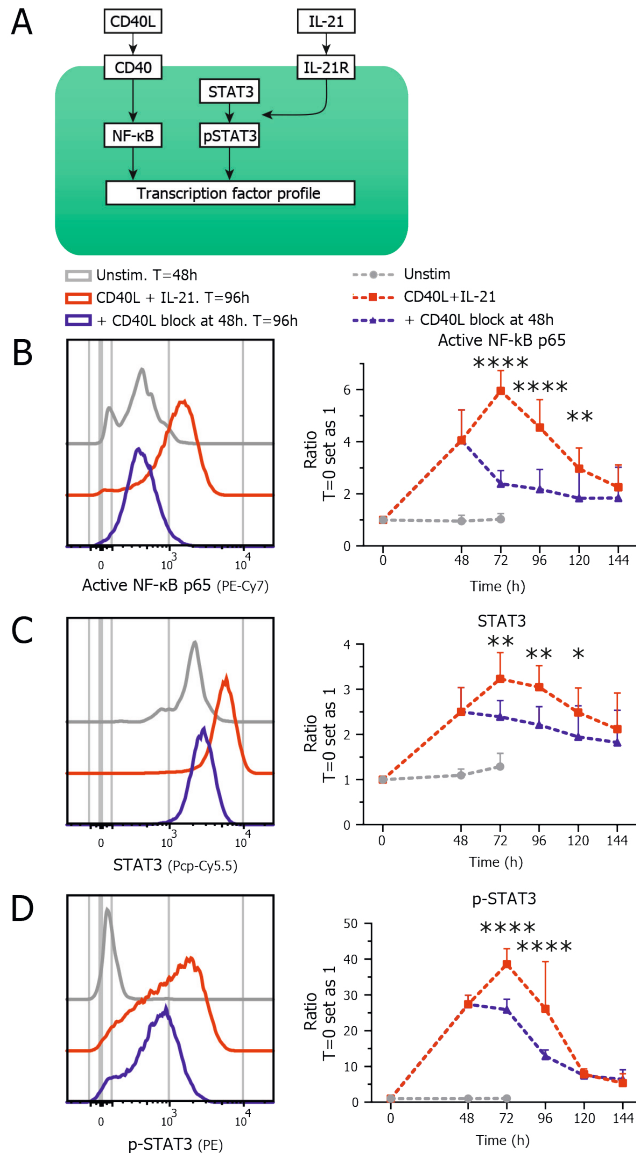


**Figure 3. Termination of CD40L stimulation results in downregulation of NF- $\kappa$ B and pSTAT3 / STAT3 signaling.** Naïve B cells were sorted and 25,000 cells were stimulated with a human-CD40L expressing 3T3 feeder layer and recombinant IL-21 (50 ng/ml). After 48 hours CD40L blocking antibodies (13  $\mu$ g/ml) were added or not. At indicated timepoints cultures were harvested, stained for membrane markers, fixed and stored until day 6 when all samples were stained intracellularly and analyzed by flow cytometry. **(A)** Schematic representation of CD40L and IL-21 signaling pathways. **(B)** Representative histogram overlay (left) and quantification (right) of activated NF- $\kappa$ B p65 GeoMFI per day under indicated conditions (n=4). **(C)** Representative histogram overlay (left) and quantification (right) of STAT3 GeoMFI per day under indicated conditions (n=4). **(D)** Representative histogram overlay (left) and quantification (right) of p-STAT3 GeoMFI per day under indicated conditions (n=4). P-values were calculated by comparing the red CD40L + IL-21 condition and the blue CD40L stimulation terminated after 48h condition, using two-way ANOVA with Sidak's multiple comparison test. Combined data from 2 independent experiments, each performed with 2 donors. Symbols represent the mean and error bars show  $\pm$  SEM. \*  $P \leq 0.05$ , \*\*  $P \leq 0.01$ , \*\*\*  $P \leq 0.001$ , \*\*\*\*  $P \leq 0.0001$ .

**Termination of CD40L stimulation inhibits proliferation through downregulation of C-MYC and promotes differentiation by promoting a true ASC transcriptional program**

B cell to ASC differentiation is tightly regulated by a complex network of multiple inducible transcriptional regulators, as summarized in Fig 4A<sup>11</sup>. Analysis of these transcriptional regulators during CD40L stimulation and termination shows that CD40L and IL-21 stimulation induced increased IRF4 expression (Fig 4B). Interestingly, while termination of CD40L co-stimulation does reduce expression of IRF4 significantly, a high IRF4 expressing population remained at 96 hours of culture (Fig 4B, left) coinciding with the generation of CD27<sup>+</sup>CD38<sup>+</sup> ASCs (Fig 2D). Secondly, the regulator of GC maintenance and B cell proliferation C-MYC was rapidly induced upon CD40L and IL-21 stimulation in CD19<sup>+</sup> cells. Similarly to activated NF- $\kappa$ B p65, C-MYC expression was significantly inhibited after termination of CD40L stimulation (Fig 3B & 4C). CD40L and IL-21 stimulation steadily induced PAX5 expression over the course of the culture (Fig 4D). Termination of CD40L co-stimulation first stabilized expression of PAX5 until 96 hours of culture, after which PAX5 expression was significantly decreased. Strikingly, the downregulation of PAX5 occurred after downregulation of IRF4, indicating that these two TFs are regulated differently upon termination of CD40L stimulation. In addition, termination of CD40L stimulation with continued IL-21 stimulation resulted in a prominent increase in the percentage of BLIMP1<sup>High</sup> expressing cells (Fig 4E, middle). This increase in BLIMP1<sup>High</sup> expressing cells already occurred after 72 hours of culture, preceding the downregulation of PAX5 and the generation of CD27<sup>+</sup>CD38<sup>+</sup> ASCs (Fig 2D). However, even though differentiation into CD27<sup>+</sup>CD38<sup>+</sup> ASCs in both percentages and absolute counts is significantly higher in the CD40L blocked condition (Fig 2D) this is not the case for the absolute counts of BLIMP1<sup>High</sup> expressing cells (Fig 4E, right) indicating that high BLIMP1 expression alone is not sufficient for ASC differentiation. Altogether these data demonstrate that termination of CD40L co-stimulation reduces proliferation and expression of C-MYC while subsequently PAX5 expression is downregulated and B cell differentiation into ASCs is enhanced. However, as high levels of IRF4 are found in both CD40L stimulated and terminated conditions and that absolute numbers of BLIMP1<sup>High</sup> expressing cells are the same for both conditions, we next investigated these high BLIMP1 expressing cells in more detail as these are expected to differentiate into ASCs.



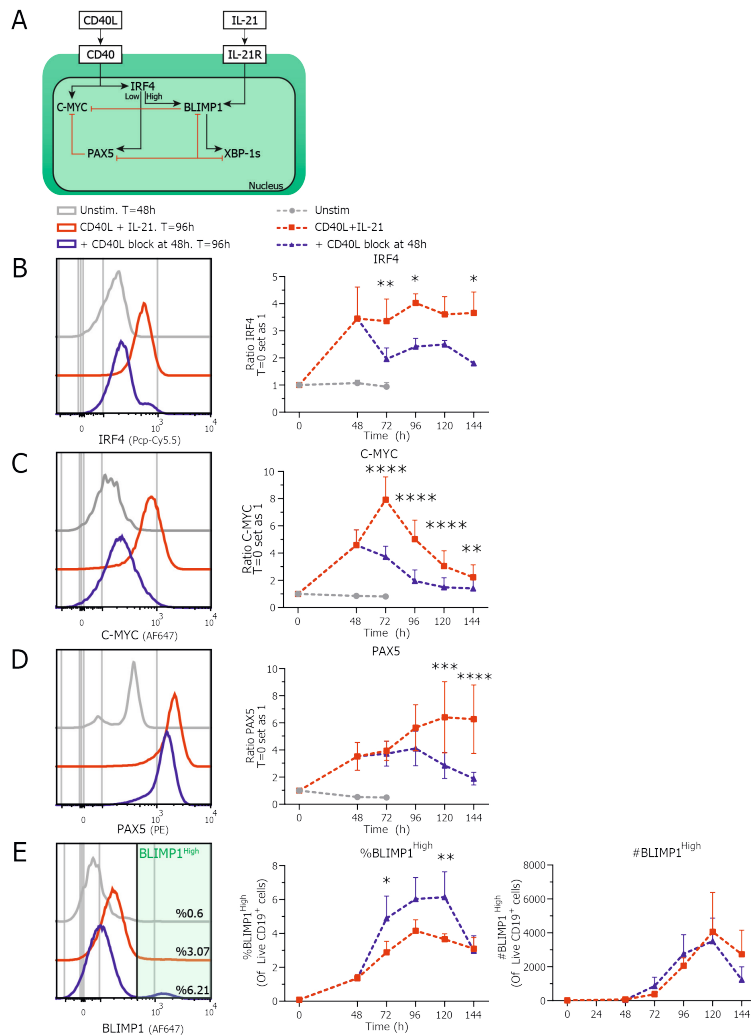


**Figure 4. Termination of CD40L stimulation inhibits expression of C-MYC, IRF4 and PAX5.** Naïve B cells were sorted and 25,000 cells were stimulated with a human-CD40L expressing 3T3 feeder layer and recombinant IL-21 (50 ng/ml). After 48 hours CD40L blocking antibodies (13 µg/ml) were added or not. At indicated timepoints cultures were harvested, stained for membrane markers, fixed and stored until day 6 when all samples were stained for TFs and analyzed by flow cytometry. **(A)** Schematic representation of CD40L and IL-21 induced TF network. CD40L stimulation induces expression of IRF4, PAX5 and proliferation regulator C-MYC while IL-21 induces expression of BLIMP1 which is the crucial regulator of ASC differentiation. BLIMP1 expression inhibits and is inhibited by PAX5. Depending on the level of IRF4 expression either PAX5 or BLIMP1 expression is promoted. Additionally, TF XBP-1s is expressed by PAX5 and promoted by BLIMP1. While B cells are known to express high levels of PAX5, ASCs express high levels of IRF4, BLIMP1 and XBP-1s. **(B)** Representative histogram overlay (left) and quantification (right) of C-MYC GeoMFI per day under indicated conditions (n=4). **(C)** Representative histogram overlay (left) and quantification (right) of IRF4 GeoMFI per day under indicated conditions (n=4). Combined data from 2 independent experiments, both performed with 2 donors. Symbols represent the mean and error bars show +/- SEM. **(D)** Representative histogram overlay (left) and quantification (right) of PAX5 GeoMFI per day under indicated conditions (n=6). **(E)** Representative histogram overlay (left), relative percentages (middle) and absolute counts (right) of BLIMP1<sup>High</sup> expressing cells under indicated conditions (n=6). Combined data from 3 independent experiments, each performed with 2 donors. Symbols represent the mean and error bars show +/- SEM. P-values were calculated by comparing the red CD40L + IL-21 condition and the blue CD40L stimulation terminated after 48h condition, using two-way ANOVA with Sidak's multiple comparison test. \* P ≤ 0.05, \*\* P ≤ 0.01, \*\*\* P ≤ 0.001, \*\*\*\* P ≤ 0.0001

The phenotype of the BLIMP1<sup>High</sup> cells was analyzed to determine the CD27<sup>+</sup>CD38<sup>+</sup> ASCs within this population (Fig 5A, left). This clearly demonstrates that termination of CD40L stimulation results in significantly more differentiation of BLIMP1<sup>High</sup> cells into CD27<sup>+</sup>CD38<sup>+</sup> ASCs (Fig 5A, right). In addition, differentiation into CD27<sup>+</sup>CD38<sup>+</sup> cells was preceded by significantly increased differentiation into CD27<sup>+</sup>CD38<sup>-</sup> cells after 72 hours of culture (Suppl Fig 4). Next to increased differentiation, significantly more XBP-1s<sup>High</sup> expressing cells were found in BLIMP1<sup>High</sup> cells when CD40L stimulation was terminated. Increased secretion of antibodies (Suppl 2) in CD40L terminated cultures was observed, in line with the function of XBP-1s as a crucial regulator of the UPR that is required for efficient production of antibodies. Next, analysis of expression of IRF4 and PAX5 within CD19<sup>+</sup> and BLIMP1<sup>High</sup> expressing cells (Fig 5C) revealed that induction of high levels of IRF4 is similar in continuous CD40L and IL-21 stimulated and CD40L terminated conditions within BLIMP1<sup>High</sup> expressing cells (Fig 5D). However, negative regulator of ASC differentiation PAX5 is prominently downregulated in BLIMP1<sup>High</sup> expressing cells when CD40L co-stimulation is terminated (Fig 5C and E). These data demonstrate that termination of CD40L stimulation with continued IL-21 stimulation reduced PAX5 expression in BLIMP1<sup>High</sup> expressing cells which maintained high expression of IRF4 and increasing XBP-1s expression, ultimately leading to the inhibition of the B cell program and promotion of a true ASC differentiation program resulting in the efficient generation of CD27<sup>+</sup>CD38<sup>+</sup> ASCs.

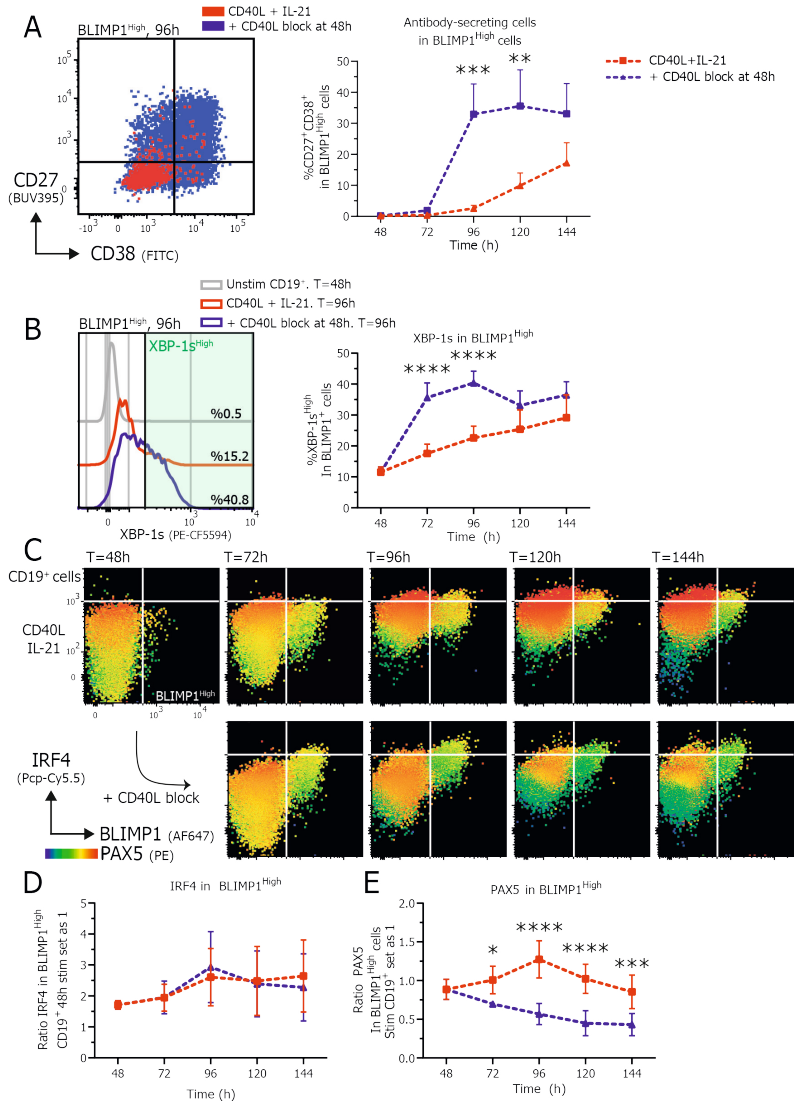


**Figure 5. Termination of CD40L stimulation promotes differentiation of BLIMP1<sup>High</sup> B cells which express XBP-1s while inhibiting PAX5 expression.** Naïve B cells were sorted and 25,000 cells were stimulated with a human-CD40L expressing 3T3 feeder layer and recombinant IL-21 (50 ng/ml). After 48 hours CD40L blocking antibodies (13 µg/ml) were added or not. At indicated timepoints cultures were harvested, stained for membrane markers, fixed and stored until day 6 when all samples were stained for TFs and analyzed by flow cytometry. **(A)** Representative overlay of CD27 and CD38 expression profiles (left) of BLIMP1<sup>High</sup> gated cells under indicated conditions after 96 hours of culture and quantification (right) of the relative percentages of CD27<sup>+</sup>CD38<sup>+</sup> ASCs within BLIMP1<sup>High</sup> gated cells per day (n=6). **(B)** Representative histogram overlay (left) and quantification (right) of the relative percentages of XBP-1s<sup>High</sup> expressing cells within BLIMP1<sup>High</sup> gated cells per day (n=6). **(C)** Representative heatmap dot plots of IRF4, BLIMP1 and PAX5 expression profiles per day under indicated conditions gated on CD19<sup>+</sup> cells. **(D)** Quantification of IRF4 GeoMFI per day under indicated conditions in BLIMP1<sup>High</sup> expressing cells (n=4). **(E)** Quantification of PAX5 GeoMFI per day under indicated conditions in BLIMP1<sup>High</sup> expressing cells (n=6). Combined data from 2 or 3 independent experiments, each performed with 2 donors. Symbols represent the mean and error bars show +/- SEM. P-values were calculated by comparing the red CD40L + IL-21 condition and the blue CD40L stimulation terminated after 48h condition, using two-way ANOVA with Sidak's multiple comparison test. \* P ≤ 0.05, \*\* P ≤ 0.01, \*\*\* P ≤ 0.001, \*\*\*\* P ≤ 0.0001

## DISCUSSION

During T-cell dependent B cell responses, naïve B cells require stimulation from T<sub>FH</sub> cells in the form of CD40L and IL-21 and this stimulation has often been mimicked *in vitro*<sup>33-36</sup>. However, a key limitation in *in vitro* studies is that the duration of stimulation has never been investigated. It has been shown that the T-B cell interactions are short-lived and B cells actively move away from T cell stimulation<sup>12,39,40</sup> and thus we hypothesized that the termination of T cell stimulation contributes to B cell differentiation. In this study we show that after CD40L and IL-21 stimulation, termination of CD40L stimulation promotes efficient and rapid differentiation of human naïve B cells into ASCs *in vitro*. These data are of importance as in mice, CD40L termination did not result in more ASC formation<sup>41</sup>. This discrepancy could also be explained by the differences in experimental setup, rather than being a difference in human-versus-mouse B cell responses, and requires additional investigation. Here, by using in depth analysis of intracellular signaling pathways and TF expression profiles<sup>38</sup> during culture we assessed the mechanism underlying the increased ASC differentiation after CD40L stimulation termination of human differentiating naïve B cells. These findings are summarized in Figure 6 where our observed expression profiles are depicted in a model in which direct connections between signaling pathways and transcription factors are depicted based on extensive literature<sup>11,17,42</sup>.

As shown before<sup>14-16</sup>, CD40L and IL-21 induced high levels of NF-κB and p-STAT3 signaling. Analysis of NF-κB p65 and pSTAT3/STAT3 pathways demonstrated that release of CD40L co-stimulation not only downregulates NF-κB but also pSTAT3/STAT3 signaling, indicating a link between CD40 and STAT3 pathways as there was continued IL-21 stimulation present in culture (Fig 6, dashed line). One possible explanation is that CD40L co-stimulation promotes expression of IL-21R<sup>1</sup>, release of CD40L stimulation could subsequently lead to downregulation of IL-21R and thus downregulation STAT3 phosphorylation. As CD40L stimulation induces expression of PAX5<sup>31</sup> and, through NF-κB induction, C-MYC<sup>19</sup>, it was to be expected that both PAX5 and C-MYC are downregulated upon release of CD40L stimulation. As C-MYC drives a proliferative state instead of a differentiative state, downregulation of C-MYC is required for terminal differentiation to occur<sup>43</sup>. This alone is not sufficient however, as PAX5 must also be downregulated in order to reach a true ASC transcriptional profile<sup>42,44-46</sup>. Interestingly it has also been shown that during B cell development, C-MYC expression is able to regulate PAX5 expression indirectly<sup>47</sup>. Although these separate findings are in agreement with the data presented here, we are the first to show that termination of CD40L co-stimulation instigates first the required downregulation of C-MYC and subsequently PAX5. Furthermore, a higher proportion of BLIMP1<sup>High</sup> expressing cells was found in CD40L stimulation terminated cultures. However, as there was no increase in absolute count of BLIMP1<sup>High</sup> expressing cells this warranted further investigation.

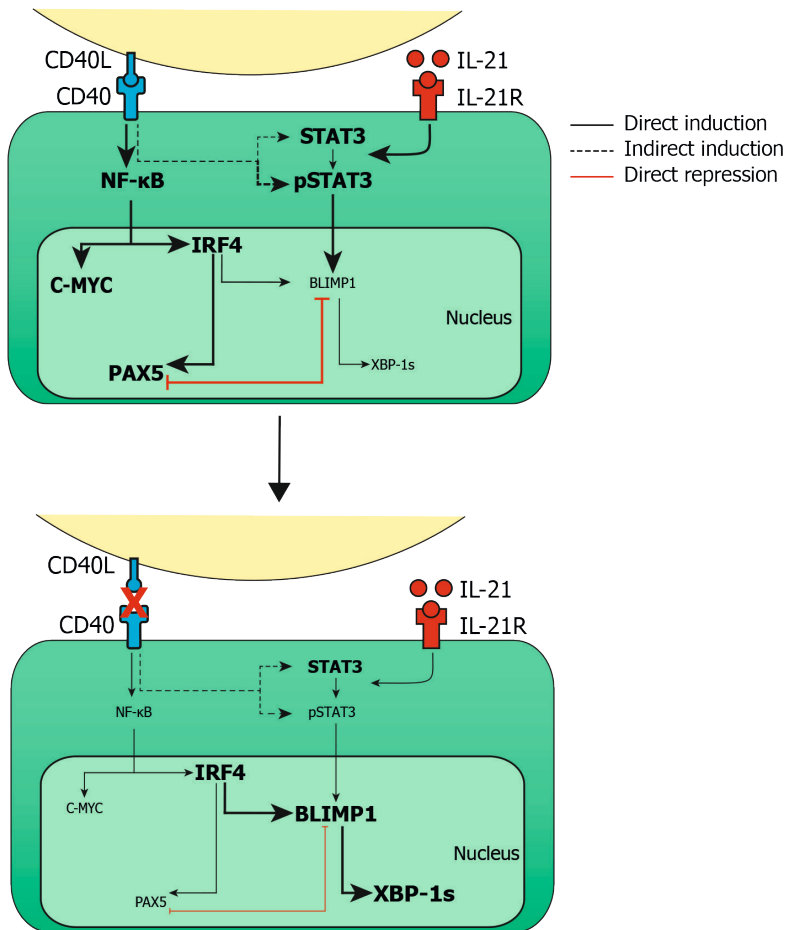


**Figure 6. Schematic overview of CD40L stimulated and CD40L stimulation terminated B cells with phospho-signaling and transcription factor profiles**

Analysis into BLIMP1<sup>High</sup> cells showed that upon termination of CD40L co-stimulation IRF4 expression was maintained, while PAX5 was downmodulated. In line with these findings, termination of CD40 signaling efficiently increased differentiation of these cells into CD27<sup>+</sup>CD38<sup>+</sup> ASCs. Actual antibody secretion was observed, in line with increased expression of XBP-1s (Fig 6, below). Together these data demonstrate that termination of CD40L stimulation with continued IL-21 stimulation induces a true ASC transcriptional profile, explaining the increased generation of both ASCs and Igs in these cultures. Furthermore, BLIMP1 and PAX5 are known to be mutually inhibitory and as a consequence, it is often assumed that upregulation of BLIMP1 is always accompanied by downregulation of PAX5 and that upregulation of BLIMP1 is leading induction of ASC differentiation. Our data show that cells that do not exhibit an CD27<sup>+</sup>CD38<sup>+</sup> ASC phenotype, and are still in the B cell state, can show upregulation of BLIMP1. In this

case however, they still express PAX5. Only upregulation of BLIMP1 with concomitant downregulation of PAX5 leads to the CD27<sup>+</sup>CD38<sup>+</sup> ASC phenotype with accompanying elevated expression of XBP-1s. Although cyclic migration of B cells to and away from T<sub>FH</sub> cell stimulation is a hallmark of *in vivo* GC reactions<sup>10,12,39,40</sup>, the importance of termination of T cell stimulation has always been overlooked in *in vitro* B cell cultures. We show efficient ASC differentiation in this culture where naïve B cells only receive and are released from CD40L stimulation once. Potentially, ASC differentiation can be further increased by introducing multiple rounds of stimulation, and termination thereof, as *in vivo* this cyclic stimulation also occurs multiple times<sup>10</sup>. Indeed, our previous work demonstrated that secondary CD40L and IL-21 stimulation induces downregulation of B cell identity gene PAX5 and thus promotes ASC differentiation<sup>36</sup>. Additionally, *in vivo* T-B cell interactions only last for a few minutes and can occur multiple times over several hours<sup>12,39</sup>. Thus, future *in vitro* cultures should allow for dynamic control of B cell stimulation in order to investigate how specific timing and duration of stimulation impacts formation of ASCs. Our data already demonstrates that prolonged stimulation promotes proliferation of B cells while inhibiting ASC differentiation and others have shown that in mice, constitutive CD40L stimulation in fact promotes ASC differentiation<sup>41</sup> while transient release of T-cell help promotes GC B cell transition<sup>48</sup>. In addition, prolonged (IL-4) stimulation in human B cells impairs differentiation<sup>37</sup>. These findings clearly show that dynamic B cell stimulation and termination of stimulation are key in controlling B cell fate decision. Finally, several groups have sought to quantitatively model signal integration in order to interrogate what transcriptional thresholds are in place that control B cell differentiation<sup>49-51</sup> and several descriptive models have been proposed that explain B cell fate decision making<sup>52</sup>. Each model still requires a deeper investigation into underlying mechanisms of how signaling integration results in crossing a transcriptional threshold in order to undergo ASC differentiation. In the future, dynamically controlled *in vitro* systems can contribute to these models and will improve our understanding of the temporal requirements for B cell to ASC differentiation. Altogether, literature and data presented here demonstrate that the next step for *in vitro* human B cell differentiation studies should be the generation of an *in vitro* system that allows for transient and controlled B cell stimulation, in combination with secondary or even cyclic stimulation in order to mimic *in vivo* T<sub>FH</sub> stimulation dynamics as closely as possible. This system could lead to even more B cell to ASC differentiation and that system could then be interrogated to determine what temporal factors drive this differentiation. This will ultimately result in better understanding of how desired B cell responses can be promoted and how undesired responses, such as auto- and allo-immunity<sup>53-56</sup>, can be inhibited.

The generation of ASC from naïve B cells by T<sub>FH</sub> cell stimulation remains incompletely understood and insights in the mechanisms underlying this response are highly required as secreted antibodies form a crucial layer of immune protection. The data presented here show, for the first time, that termination of the initially essential CD40L stimulation is required in order to downregulate signaling and proliferation and subsequently

reach a true ASC transcription factor profile where termination specifically lowers PAX5 and C-MYC, in a background where IRF4, BLIMP1 and XBP-1s are highly induced and maintained by initial CD40 signaling. These insights will aid future research on T-dependent B cell responses both for improving vaccination strategies and treating B cell mediated diseases.

**Author contributions:** CM, NV, AtB and SMvH designed research. CM, MS and TJ performed research. CM analyzed data. LB provided reagents. All authors critically reviewed the manuscript, gave final approval of the version to be published and agreed to be accountable for all aspects of the work ensuring that questions related to the accuracy or integrity of any part of the work are appropriately investigated and resolved.

**Funding:** This project was funded by the Landsteiner Foundation for Blood Transfusion Research, project grant number: LSBR 1609 and Sanquin Product and Process Development Call 2020.

**Acknowledgments:** We thank Simon Tol, Erik Mul, Mark Hoogenboezem and Tom Ebbes of the Sanquin central facility for cell sorting on the FACS AriaIII and maintenance and calibration of FACS machines. We thank Gijs van Schijndel and Ninotska Derksen for their help with ELISA assays.

**Conflicts of Interest:** The authors declare no conflict of interest. The funders had no role in the design of the study; in the collection, analyses, or interpretation of data; in the writing of the manuscript, or in the decision to publish the results.

## MATERIALS AND METHODS

### Cell lines

NIH3T3 fibroblasts expressing human CD40L (3T3-CD40L)<sup>57</sup> were cultured in IMDM (Lonza) containing 10% FCS (Serana), 100 U/ml penicillin (Invitrogen), 100 µg/ml streptomycin (Invitrogen), 2mM L-glutamine (Invitrogen), 50 µM β-mercaptoethanol (Sigma Aldrich) and 500 µg/ml G418 (Life Technologies).

### Isolation of B Cells from Human Healthy Donors

Buffy coats were collected from voluntary, non-remunerated, adult healthy blood donors (Sanquin Blood Supply, Amsterdam, the Netherlands), who provided written informed consent for the use of remainders of their donation for research as part of routine donor selection and blood collection procedures. Peripheral blood mononucleated cells (PBMCs) were isolated from buffy coats using a Lymphoprep (Axis-Shield PoC AS, Dundee, Scotland) density gradient. Afterward, CD19<sup>+</sup> B-cells were separated using magnetic anti-CD19 Dynabeads and DETACHaBEAD (Invitrogen, Carlsbad, CA, USA) according to manufacturer's instructions with purity > 99%.

### **In vitro B cell stimulation cultures**

B cell cultures were carried out as described before<sup>36</sup> with a few adjustments. In short, 3T3 -CD40L<sup>+</sup> were harvested, irradiated with 30 Gy and seeded in B cell medium (RPMI 1640 (Gibco) without phenol red containing 5% FCS, 100 U/ml penicillin, 100 µg/ml streptomycin, 2 mM L-glutamine, 50 µM β-mercaptoethanol and 20 µg/ml human apo-transferrin (Sigma Aldrich; depleted for human IgG with protein G sepharose (GE Healthcare)) on 96-well flat-bottom plates (Nunc) to allow adherence overnight. 3T3 -CD40L<sup>+</sup> were seeded at 10.000 cells per 96-well. The next day, CD19<sup>+</sup> B cells were thawed after cryopreservation and CD19<sup>+</sup>CD27<sup>-</sup>IgG<sup>-</sup> naive B cells were sorted on a FACSAria II.  $2.5 \times 10^4$  naive B cells were cultured on the irradiated CD40L-expressing 3T3 fibroblasts in the presence of IL-21 (50 ng/mL; Peprotech, London W6 8LL, UK) for 6 days. After 48 hours or at indicated timepoints either medium or anti-CD40L clone 5C8 antibodies (13 µg/ml) were added to the cultures.

### **Violet Proliferation Dye 450 labeling**

B cells were labelled according to manufacturer's instructions. In short, sorted B cells were washed with 10 ml PBS twice and resuspended to a concentration of  $2 \times 10^7$  cells/ml in PBS. Cells and 4 µM Violet Proliferation Dye 450 (VPD450, BD Biosciences) in PBS were mixed at a 1:1 ratio and incubated 15 minutes in a 37°C water bath in the dark, vortexing the tube every 5 minutes to ensure uniform staining. Cells were washed twice using a 10 times volume of cold culture medium to end labeling. Thereafter, B cells were cultured according to the protocol described above.

### **Phosphoflow analysis**

Flow cytometric samples were prepared as described previously<sup>38</sup> with a few adjustments. In short, wells were harvested at indicated time points and multiple culture wells were pooled, up to a full 96-well plate per replicate, in 96-well V-bottom plates. After harvest cells were kept on ice or at 4°C at all times. Cells were washed with ice-cold PBS/0.1% bovine serum albumin (BSA; Sigma Aldrich), centrifuged and pooled. Samples were stained in with LIVE/DEAD Fixable Near-IR Dead cell stain kit (Invitrogen) and anti-CD19 BV510 (BD) and anti-CD38 FITC (Beckman Coulter) diluted in ice-cold PBS/0.1% BSA for 15 minutes on ice. Samples were washed once with ice-cold PBS/0.1% BSA, centrifuged and fixed with 37 °C 4% paraformaldehyde (PFA; Sigma) for 10 minutes at 37°C. After fixation, samples were centrifuged, washed once with PBS/0.1% BSA and permeabilized with 90% methanol from a -20°C freezer. Samples were incubated for at least 30 minutes or stored at -20°C till day of FACS analysis. After permeabilization, samples were centrifuged followed by two consecutive washes with PBS/0.1% BSA. Samples were then stained with anti-CD27 BUV395 (BD), anti-NF-κB p65 (pS529) PE-Cy7 (BD), anti-STAT3 Percp-Cy5.5 (BD), anti-p-STAT3 PE (BD) and anti-C-MYC AF647 (CST) diluted in PBS/0.1% BSA. Samples were incubated for 30 minutes on a plate shaker at room temperature. Samples were washed and resuspended in PBS/0.1%BSA before measuring on a BD FACSymphony A5 machine and analyzed using FlowJo Software v10.8. (Treestar). Cells were pre-gated on live cells,



lymphocytes, two single cells gates and live CD19<sup>+</sup> gate unless stated otherwise (Suppl fig 1A). We adhered to the 'Guidelines for the use of flow cytometry and cell sorting in immunological studies'<sup>58</sup>.

### **Transcription factor flow analysis**

Flow cytometric samples were prepared as described previously<sup>38</sup> with a few adjustments. In short, wells were harvested at indicated time points and multiple culture wells were pooled, up to 20 wells per replicate, in 96-well V-bottom plates. After harvest cells were kept on ice or at 4°C at all times. Samples were centrifuged and stained with 25 µl staining mix LIVE/DEAD Fixable Near-IR Dead cell stain kit, anti-CD19, anti-CD27 and anti-CD38 antibodies and incubated for 15 minutes at 4 °C. Samples were washed with ice-cold PBS/0.1% and centrifuged. Samples were then fixated with 100 µl Foxp3 fixation buffer (eBioscience) for 30 minutes at 4 °C. Next, Foxp3 permeabilization buffer (eBioscience) was added, samples were centrifuged and stored in PBS/0.1%BSA at 4 °C till the day of FACS analysis. After permeabilization or storage, samples were centrifuged and washed with Foxp3 permeabilization buffer. After removing the supernatant, samples were stained with anti-PAX5 PE, anti-IRF4 PercpCy5.5, anti-BLIMP1 AF647 and anti-XBP-1s PE-CF594 diluted in Foxp3 permeabilization buffer and incubated for 30 minutes in the fridge. Samples were washed with Foxp3 permeabilization buffer and resuspended in PBS/0.1%BSA before measuring on a BD FACSymphony A5 machine and analyzed using FlowJo Software v10.8. (Treestar). Cells were pre-gated on live cells, lymphocytes, two single cells gates and live CD19<sup>+</sup> gate unless stated otherwise (Suppl fig 1A). We adhered to the 'Guidelines for the use of flow cytometry and cell sorting in immunological studies'<sup>58</sup>.

### **Multimarker analysis using UMAP**

After gating for live CD19<sup>+</sup> B cells, samples were randomly down sampled to 25.000 events and subsequently stimulated and CD40L stimulation terminated samples were concatenated into a single 50.000 event FCS file using the DownSample plugin in FlowJo v10.8.0. Next, the concatenated sample was analyzed using the Uniform Manifold Approximation and Projection (UMAP) plugin v3.1 in FlowJo v10.8.0. UMAP is a machine learning algorithm used for dimensionality reduction to visualize high parameter datasets in a two-dimensional space. UMAP plugin settings were as followed: Distance function Euclidean; number of neighbors 30; minimal distance 0.5 and number of components 2. The UMAP dot plot generated can be manipulated as a standard dot plot and allows for multiple parameter and heatmap overlays in the FlowJo layout-editor. The DownSample and UMAP FlowJo plugins can be found on the FlowJo Exchange website.

### **IgM and IgG ELISA of Culture Supernatants**

IgM and IgG levels in supernatants were measured as previously described<sup>59</sup>. In short, plates were coated with monoclonal anti-IgM or anti-IgG (2 µg/mL; clone MH15-1 and MH16-1, respectively; Sanquin Reagents, Amsterdam, the Netherlands) and for detection, horseradish peroxidase-conjugated mouse-anti-human-IgM or mouse-anti-human- IgG (1

$\mu\text{g/mL}$  in HPE; clone MH15-1 and MH16-1, respectively; Sanquin Reagents, Amsterdam, the Netherlands) were used. The ELISA was developed with  $100 \mu\text{g/mL}$  tetramethylbenzidine in  $0.11 \text{ M/L}$  sodium acetate (pH 5.5) containing  $0.003\%$  (v/v)  $\text{H}_2\text{O}_2$ . The reaction was stopped with  $2 \text{ M H}_2\text{SO}_4$ . Absorption at  $450$  and  $540 \text{ nm}$  was measured with a Synergy 2 microplate reader (Biotek, Winooski, VT, USA). Results were related to a titration curve of a serum pool in each plate. The lower-limit detection levels of IgM and IgG ELISA were  $3 \text{ ng/mL}$  and  $2.8 \text{ ng/mL}$ , respectively.

### **Data Availability Statement**

The data that support the findings of this study are available from the corresponding author upon reasonable request.

### **Statistical analysis**

Statistical analysis was performed using GraphPad Prism (version 8; GraphPad Software). Data were analyzed using t-tests, Repeated Measures one-way ANOVA with Tukey's multiple comparison test, Repeated Measures two-way ANOVA with Sidak's multiple comparison test or mixed-effects analysis with Dunnett's multiple comparison test where appropriate. Results were considered significant at  $p < 0.05$ . Significance was depicted as \* ( $p < 0.05$ ) or \*\* ( $p < 0.01$ ), \*\*\* ( $p < 0.001$ ) or \*\*\*\* ( $p < 0.0001$ ).

## REFERENCES

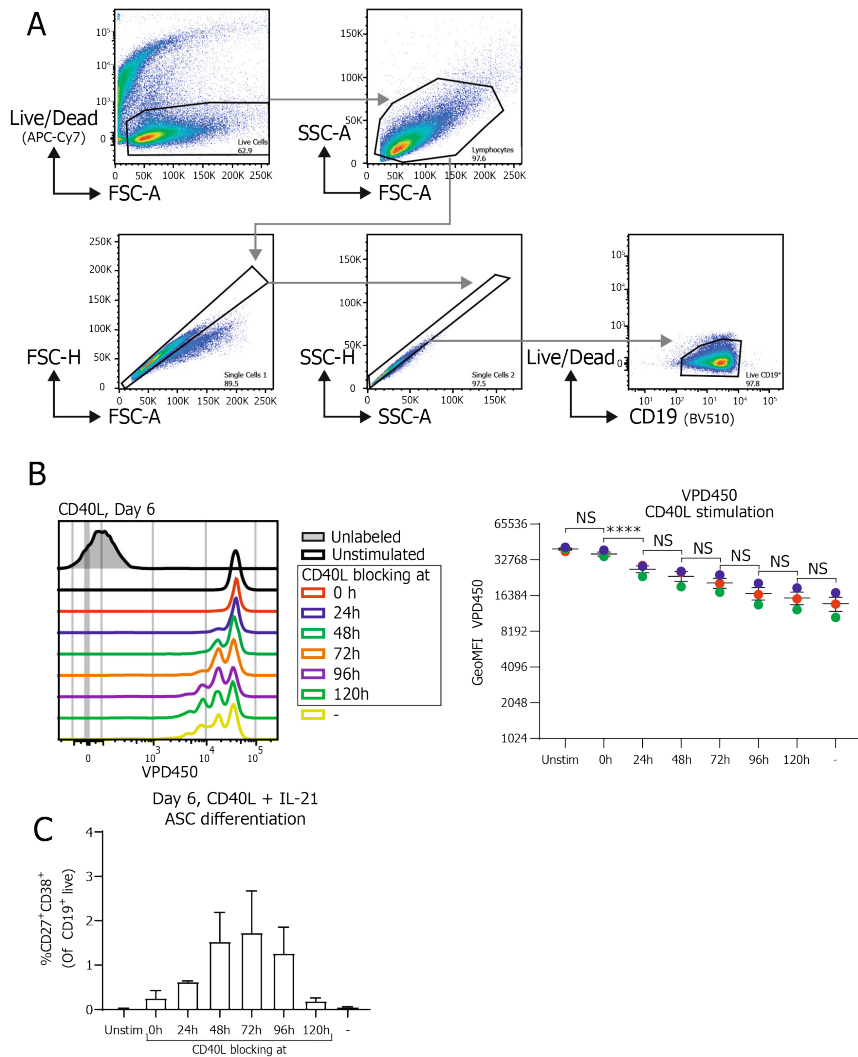
1. Ding BB, Bi E, Chen H, Yu JJ, Ye BH. IL-21 and CD40L Synergistically Promote Plasma Cell Differentiation through Upregulation of Blimp-1 in Human B Cells. *The Journal of Immunology*. 2013;190(4):1827-1836. doi:10.4049/jimmunol.1201678
2. Moens L, Tangye SG. Cytokine-mediated regulation of plasma cell generation: IL-21 takes center stage. *Front Immunol*. 2014;5(FEB):1-13. doi:10.3389/fimmu.2014.00065
3. Weinstein JS, Herman EI, Lainez B, et al. TFH cells progressively differentiate to regulate the germinal center response. *Nat Immunol*. 2016;17(10):1197-1205. doi:10.1038/ni.3554
4. Weisel FJ, Zuccarino-Catania G v., Chikina M, Shlomchik MJ. A Temporal Switch in the Germinal Center Determines Differential Output of Memory B and Plasma Cells. *Immunity*. 2016;44(1):116-130. doi:10.1016/j.immuni.2015.12.004
5. McHeyzer-Williams LJ, Pelletier N, Mark L, Fazilleau N, McHeyzer-Williams MG. Follicular helper T cells as cognate regulators of B cell immunity. *Curr Opin Immunol*. 2009;21(3):266-273. doi:10.1016/j.coi.2009.05.010
6. Upadhyay M, Priya GK, Ramesh P, et al. CD40 signaling drives B lymphocytes into an intermediate memory-like state, poised between naïve and plasma cells. *J Cell Physiol*. 2014;229(10):1387-1396. doi:10.1002/JCP.24572
7. Luo W, Weisel F, Shlomchik MJ. B Cell Receptor and CD40 Signaling Are Rewired for Synergistic Induction of the c-Myc Transcription Factor in Germinal Center B Cells. *Immunity*. 2018;48(2):313-326.e5. doi:10.1016/j.immuni.2018.01.008
8. Avery DT, Ma CS, Bryant VL, et al. STAT3 is required for IL-21 induced secretion of IgE from human naïve B cells. *Blood*. 2008;112(5):1784-1793. doi:10.1182/blood-2008-02-142745
9. Avery DT, Deenick EK, Ma CS, et al. B cell-intrinsic signaling through IL-21 receptor and STAT3 is required for establishing long-lived antibody responses in humans. *J Exp Med*. 2010;207(1):155-171. doi:10.1084/jem.20091706
10. Mesin L, Ersching J, Victora GD. Germinal Center B Cell Dynamics. *Immunity*. 2016;45(3):471-482. doi:10.1016/j.immuni.2016.09.001
11. Verstegen NJM, Ubels V, Westerhoff H v., van Ham SM, Barberis M. System-Level Scenarios for the Elucidation of T Cell-Mediated Germinal Center B Cell Differentiation. *Front Immunol*. 2021;12(September):1-19. doi:10.3389/fimmu.2021.734282
12. Shulman Z, Gitlin AD, Weinstein JS, et al. Dynamic signaling by T follicular helper cells during germinal center B cell selection. *Science (1979)*. 2014;345(6200):1058-1062. doi:10.1126/science.1257861
13. Victora GD, Nussenzweig MC. Germinal Centers. doi:10.1146/annurev-immunol-020711-075032
14. Craxton A, Shu G, Graves JD, Saklatvala J, Krebs EG, Clark EA. p38 MAPK is required for CD40-induced gene expression and proliferation in B lymphocytes. *J Immunol*. 1998;161(7):3225-3236. Accessed May 10, 2020. <http://www.ncbi.nlm.nih.gov/pubmed/9759836>
15. Chen D, Ireland SJ, Remington G, et al. CD40-Mediated NF- $\kappa$ B Activation in B Cells Is Increased in Multiple Sclerosis and Modulated by Therapeutics. *The Journal of Immunology*. 2016;197(11):4257-4265. doi:10.4049/jimmunol.1600782
16. Deenick EK, Avery DT, Chan A, et al. Naive and memory human B cells have distinct requirements for STAT3 activation to differentiate into antibody-secreting plasma cells. *J Exp Med*. 2013;210(12):2739-2753. doi:10.1084/jem.20130323

17. Nutt SL, Hodgkin PD, Tarlinton DM, Corcoran LM. The generation of antibody-secreting plasma cells. *Nat Rev Immunol*. 2015;15(3):160-171. doi:10.1038/nri3795
18. Merluzzi S, Moretti M, Altamura S, et al. CD40 stimulation induces Pax5/BSAP and EBF activation through a APE/Ref-1-dependent redox mechanism. *J Biol Chem*. 2004;279(3):1777-1786. doi:10.1074/JBC.M305418200
19. Grumont RJ, Strasser A, Gerondakis S. B cell growth is controlled by phosphatidylinositol 3-kinase-dependent induction of Rel/NF-kappaB regulated c-myc transcription. *Mol Cell*. 2002;10(6):1283-1294. doi:10.1016/S1097-2765(02)00779-7
20. Dominguez-Sola D, Victora GD, Ying CY, et al. c-MYC is required for germinal center selection and cyclic re-entry HHS Public Access. *Nat Immunol*. 2012;13(11):1083-1091. doi:10.1038/ni.2428
21. Finkin S, Hartweger H, Oliveira TY, Kara EE, Nussenzweig MC. Protein Amounts of the MYC Transcription Factor Determine Germinal Center B Cell Division Capacity. *Immunity*. 2019;51(2):324-336.e5. doi:10.1016/j.immuni.2019.06.013
22. Grumont RJ, Gerondakis S. Rel induces interferon regulatory factor 4 (IRF-4) expression in lymphocytes: modulation of interferon-regulated gene expression by rel/nuclear factor kappaB. *J Exp Med*. 2000;191(8):1281-1291. doi:10.1084/JEM.191.8.1281
23. Sciammas R, Shaffer AL, Schatz JH, Zhao H, Staudt LM, Singh H. Graded Expression of Interferon Regulatory Factor-4 Coordinates Isotype Switching with Plasma Cell Differentiation. *Immunity*. 2006;25(2):225-236. doi:10.1016/j.immuni.2006.07.009
24. Fairfax KA, Kallies A, Nutt SL, Tarlinton DM. Plasma cell development: From B-cell subsets to long-term survival niches. *Semin Immunol*. 2008;20(1):49-58. doi:10.1016/j.smim.2007.12.002
25. Méndez A, Mendoza L. A Network Model to Describe the Terminal Differentiation of B Cells. *PLoS Comput Biol*. 2016;12(1):1-26. doi:10.1371/journal.pcbi.1004696
26. Scheeren FA, Naspetti M, Diehl S, et al. STAT5 regulates the self-renewal capacity and differentiation of human memory B cells and controls Bcl-6 expression. *Nat Immunol*. 2005;6(3):303-313. doi:10.1038/ni1172
27. Kwon H, Thierry-Mieg D, Thierry-Mieg J, et al. Analysis of Interleukin-21-Induced Prdm1 Gene Regulation Reveals Functional Cooperation of STAT3 and IRF4 Transcription Factors. *Immunity*. 2009;31(6):941-952. doi:10.1016/j.immuni.2009.10.008
28. Tellier J, Shi W, Minnich M, et al. Blimp-1 controls plasma cell function through the regulation of immunoglobulin secretion and the unfolded protein response. *Nat Immunol*. 2016;17(3):323-330. doi:10.1038/ni.3348
29. Chung EY, Psathas JN, Yu D, Li Y, Weiss MJ, Thomas-Tikhonenko A. CD19 is a major B cell receptor-independent activator of MYC-driven B-lymphomagenesis. *J Clin Invest*. 2012;122(6):2257-2266. doi:10.1172/JCI45851
30. Somasundaram R, Jensen CT, Tingvall-Gustafsson J, et al. EBF1 and PAX5 control pro-B cell expansion via opposing regulation of the Myc gene. *Blood*. 2021;137(22):3037-3049. doi:10.1182/BLOOD.2020009564
31. Reimold AM, Ponath PD, Li YS, et al. Transcription factor B cell lineage-specific activator protein regulates the gene for human X-box binding protein 1. *Journal of Experimental Medicine*. 1996;183(2):393-401. doi:10.1084/JEM.183.2.393
32. Ochiai K, Maienschein-Cline M, Simonetti G, et al. Transcriptional Regulation of Germinal Center B and Plasma Cell Fates by Dynamical Control of IRF4. *Immunity*. 2013;38(5):918-929. doi:10.1016/j.immuni.2013.04.009

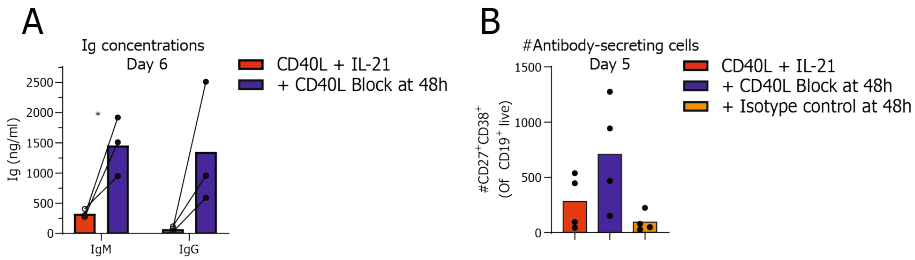
33. Ettinger R, Sims GP, Fairhurst AM, et al. IL-21 Induces Differentiation of Human Naive and Memory B Cells into Antibody-Secreting Plasma Cells. *The Journal of Immunology*. 2005;175(12):7867-7879. doi:10.4049/JIMMUNOL.175.12.7867
34. Marasco E, Farroni C, Cascioli S, et al. B-cell activation with CD40L or CpG measures the function of B-cell subsets and identifies specific defects in immunodeficient patients. *Eur J Immunol*. 2017;47(1):131-143. doi:10.1002/eji.201646574
35. Tuijnenburg P, aan de Kerk DJ, Jansen MH, et al. High-throughput compound screen reveals mTOR inhibitors as potential therapeutics to reduce (auto)antibody production by human plasma cells. *Eur J Immunol*. 2020;50(1):73-85. doi:10.1002/EJI.201948241/FORMAT/PDF
36. Unger PPA, Verstegen NJM, Marsman C, et al. Minimalistic In Vitro Culture to Drive Human Naive B Cell Differentiation into Antibody-Secreting Cells. *Cells*. 2021;10(5). doi:10.3390/cells10051183
37. Pignarre A, Chatonnet F, Caron G, Haas M, Desmots F, Fest T. Plasmablasts derive from CD23- activated B cells after the extinction of IL-4/STAT6 signaling and IRF4 induction. *Blood*. 2021;137(9):1166-1180. doi:10.1182/BLOOD.2020005083
38. Marsman C, Jorritsma T, ten Brinke A, van Ham SM. Flow Cytometric Methods for the Detection of Intracellular Signaling Proteins and Transcription Factors Reveal Heterogeneity in Differentiating Human B Cell Subsets. *Cells 2020, Vol 9, Page 2633*. 2020;9(12):2633. doi:10.3390/CELLS9122633
39. Victora GD, Schwickert TA, Fooksman DR, et al. Germinal center dynamics revealed by multiphoton microscopy with a photoactivatable fluorescent reporter. *Cell*. 2010;143(4):592-605. doi:10.1016/j.cell.2010.10.032
40. Shulman Z, Gitlin AD, Targ S, et al. T follicular helper cell dynamics in germinal centers. *Science (1979)*. 2013;341(6146):673-677. doi:10.1126/science.1241680
41. Bolduc A, Long E, Stapler D, et al. Constitutive CD40L Expression on B Cells Prematurely Terminates Germinal Center Response and Leads to Augmented Plasma Cell Production in T Cell Areas. *The Journal of Immunology*. 2010;185(1):220-230. doi:10.4049/JIMMUNOL.0901689
42. Song S, Matthias PD. The transcriptional regulation of germinal center formation. *Front Immunol*. 2018;9(SEP):2026. doi:10.3389/fimmu.2018.02026
43. Lin KI, Lin Y, Calame K. Repression of c- myc Is Necessary but Not Sufficient for Terminal Differentiation of B Lymphocytes In Vitro . *Mol Cell Biol*. 2000;20(23):8684-8695. doi:10.1128/MCB.20.23.8684-8695.2000/ASSET/827CA3E4-92E2-43A7-8182-6EF72FFD5350/ASSETS/GRAPHIC/MB2300887008.JPEG
44. Reimold AM, Iwakoshi NN, Manis J, et al. Plasma cell differentiation requires the transcription factor XBP-1. *Nature 2001 412:6844*. 2001;412(6844):300-307. doi:10.1038/35085509
45. Lin KI, Angelin-Duclos C, Kuo TC, Calame K. Blimp-1-Dependent Repression of Pax-5 Is Required for Differentiation of B Cells to Immunoglobulin M-Secreting Plasma Cells . *Mol Cell Biol*. 2002;22(13):4771-4780. doi:10.1128/MCB.22.13.4771-4780.2002/ASSET/C0A381FC-DC4F-4BB5-9595-7057F5B0B81A/ASSETS/GRAPHIC/MB1321807005.JPEG
46. Nutt SL, Tarlinton DM. Germinal center B and follicular helper T cells: siblings, cousins or just good friends? *Nat Immunol*. 2011;12(6):472-477. doi:10.1038/ni.2019
47. Vallespinós M, Fernández D, Rodríguez L, et al. B Lymphocyte Commitment Program Is Driven by the Proto-Oncogene c-myc. *The Journal of Immunology*. 2011;186(12):6726-6736. doi:10.4049/JIMMUNOL.1002753

48. Zhang T ting, Gonzalez DG, Cote CM, et al. Germinal center B cell development has distinctly regulated stages completed by disengagement from T cell help. *Elife*. 2017;6:1-20. doi:10.7554/eLife.19552
49. Martínez MR, Corradin A, Klein U, et al. Quantitative modeling of the terminal differentiation of B cells and mechanisms of lymphomagenesis. *Proc Natl Acad Sci U S A*. 2012;109(7):2672-2677. doi:10.1073/PNAS.1113019109/-/DCSUPPLEMENTAL
50. Merino Tejero E, Lashgari D, García-Valiente R, et al. Multiscale Modeling of Germinal Center Recapitulates the Temporal Transition From Memory B Cells to Plasma Cells Differentiation as Regulated by Antigen Affinity-Based Tfh Cell Help. *Front Immunol*. 2021;11. doi:10.3389/FIMMU.2020.620716/FULL
51. Merino Tejero E, Lashgari D, García-Valiente R, et al. Coupled Antigen and BLIMP1 Asymmetric Division With a Large Segregation Between Daughter Cells Recapitulates the Temporal Transition From Memory B Cells to Plasma Cells and a DZ-to-LZ Ratio in the Germinal Center. *Front Immunol*. 2021;12:3185. doi:10.3389/FIMMU.2021.716240/BIBTEX
52. Laidlaw BJ, Cyster JG. Transcriptional regulation of memory B cell differentiation. *Nature Reviews Immunology* 2020 21:4. 2020;21(4):209-220. doi:10.1038/s41577-020-00446-2
53. Zimring JC, Hudson KE. Cellular immune responses in red blood cell alloimmunization. *Hematology Am Soc Hematol Educ Program*. 2016;2016(1):452-456. doi:10.1182/ASHEDUCATION-2016.1.452
54. Bugatti S, Vitolo B, Caporali R, Montecucco C, Manzo A. B cells in rheumatoid arthritis: From pathogenic players to disease biomarkers. *Biomed Res Int*. 2014;2014. doi:10.1155/2014/681678
55. Yap DYH, Chan TM. B cell abnormalities in systemic lupus erythematosus and lupus nephritis—role in pathogenesis and effect of immunosuppressive treatments. *Int J Mol Sci*. 2019;20(24). doi:10.3390/ijms20246231
56. McClure M, Gopaluni S, Jayne D, Jones R. B cell therapy in ANCA-associated vasculitis: current and emerging treatment options. *Nat Rev Rheumatol*. 2018;14(10):580-591. doi:10.1038/s41584-018-0065-x
57. Urashima M, Chauhan D, Uchiyama H, Freeman GJ, Anderson KC. CD40 ligand triggered interleukin-6 secretion in multiple myeloma. *Blood*. 1995;85(7):1903-1912. doi:10.1182/blood.v85.7.1903.bloodjournal8571903
58. Cossarizza A, Chang HD, Radbruch A, et al. Guidelines for the use of flow cytometry and cell sorting in immunological studies (third edition). *Eur J Immunol*. 2021;51(12):2708-3145. doi:10.1002/eji.202170126
59. Souwer Y, Griekspoor A, Jorritsma T, et al. B Cell Receptor-Mediated Internalization of Salmonella : A Novel Pathway for Autonomous B Cell Activation and Antibody Production . *The Journal of Immunology*. 2009;182(12):7473-7481. doi:10.4049/jimmunol.0802831

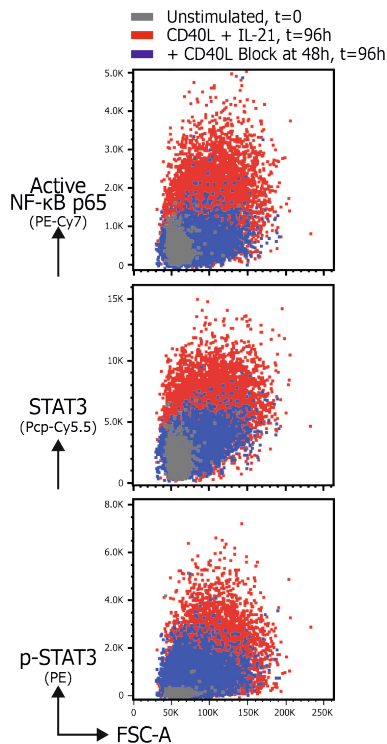
## SUPPLEMENTARY MATERIAL



**Supplementary Figure 1. CD40L blocking antibodies efficiently inhibit CD40L induced proliferation and promote differentiation after CD40L and IL-21 stimulation.** Naïve B cells were sorted and 25,000 cells were stimulated with a human-CD40L expressing 3T3 feeder layer with or without recombinant IL-21 (50 ng/ml). After the indicated culture duration CD40L blocking antibodies (13 µg/ml) were added and cells were analyzed at day 6 by flow cytometry. **(A)** Representative gating strategy for the gating of Live CD19<sup>+</sup> B cells as depicted. First, dead cells were excluded using a live/dead fixable viability stain. FSC/SSC gate is set for lymphocyte population that contains the CD19<sup>+</sup> B cells. Doublets were excluded by setting two single cell gates on both the FSC-A/FSC-H and SSC-A/SSC-H parameters. Finally, Live CD19<sup>+</sup> cells were gated on. **(B)** Naïve B cells were labelled with proliferation dye VPD450 prior to culture. Representative histogram overlay (left) and quantification of VPD450 GeoMFI after 6 days of culture under indicated conditions (n=3). Data from a single independent experiment with the mean of 3 individual donors marked as red, green or blue dots with triplicate measurements (n=3), scatter plots show mean  $\pm$  SD **(C)** Quantification of relative percentages of CD27<sup>+</sup>CD38<sup>+</sup> ASC at day 6 under indicated conditions (n=3). Data from a single independent experiment with 3 individual donors, bar indicate mean  $\pm$  SD P-values were calculated using one-way ANOVA with Tukey's multiple comparison test. \*\*\*\* P  $\leq$  0.0001

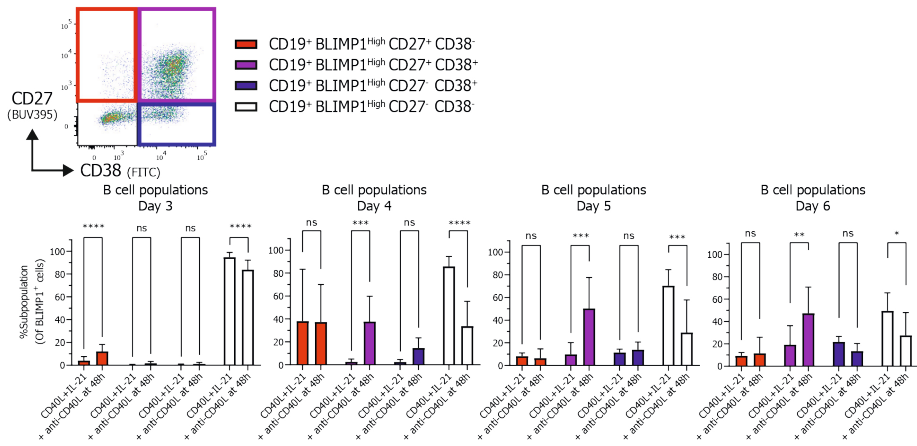


**Supplementary Figure 2. Termination of CD40L stimulation promotes secretion of immunoglobulins.** Naïve B cells were sorted and 25,000 cells were stimulated with a human-CD40L expressing 3T3 feeder layer and recombinant IL-21 (50 ng/ml). **(A)** After 48 hours CD40L blocking antibodies (13 ug/ml) were added or not. Quantification of secreted IgM and IgG measured by ELISA in day 6 culture supernatants. Combined data from 2 independent experiments performed with 1-2 donors. Symbols represent the mean of an individual with triplicate measurements, bars indicate mean. P-values were calculated by student t-test. \*  $P \leq 0.05$ . **(B)** After 48 hours CD40L blocking antibodies (13 ug/ml) or isotype control antibodies were added or not. Quantification of absolute counts of CD27<sup>+</sup>CD38<sup>+</sup> ASC at day 5. Data from a single independent experiment with 4 individual donors, bar indicate mean and dots represent individual donors.



**Supplementary Figure 3. Relationship between cell size and reduced phospho-signaling in CD40L blocked cultures.** Naïve B cells were sorted and 25,000 cells were stimulated with a human-CD40L expressing 3T3 feeder layer and recombinant IL-21 (50 ng/ml). After 48 hours CD40L blocking antibodies (13 ug/ml) were added or not. Representative dot plot overlays of unstimulated B cells (Grey) and stimulated (Red) and CD40L blocked B cells (Blue) after 96 hours. The FSC-A parameter is plotted against measured phospho-signaling proteins.





**Supplementary Figure 4. Termination of CD40L stimulation promotes differentiation of BLIMP1<sup>High</sup> cells into CD27<sup>+</sup>CD38<sup>-</sup> and CD27<sup>+</sup>CD38<sup>+</sup> populations.** Naïve B cells were sorted and 25,000 cells were stimulated with a human-CD40L expressing 3T3 feeder layer and recombinant IL-21 (50 ng/ml). Representative pseudocolor dot plot of CD27 and CD38 expression profiles after 120 hours of culture in CD19<sup>+</sup>BLIMP1<sup>High</sup> cells (Top) and quantification of the relative percentages of CD27<sup>+</sup> and CD38<sup>+</sup> subpopulations per day within BLIMP1<sup>High</sup> expressing cells under indicated conditions (bottom). Combined data from 3 independent experiments, each performed with 2 donors. Bars indicate the mean  $\pm$  SD. P-values were calculated using two-way ANOVA with Sidak's multiple comparison test. \*  $P \leq 0.05$ , \*\*  $P \leq 0.01$ , \*\*\*  $P \leq 0.001$ , \*\*\*\*  $P \leq 0.0001$



# CHAPTER 6

## Oxygen level is a critical driver of human B cell differentiation and IgG class switch recombination

Jana Koers\*, Casper Marsman\*, Juulke Steuten\*, Simon Tol, Ninotska I.L. Derksen, Anja ten Brinke, S. Marieke van Ham<sup>§</sup> and Theo Rispens<sup>§</sup>

*In press, Frontiers in Immunology*

\*/§ These authors contributed equally

## ABSTRACT

The generation of high-affinity antibodies requires an efficient germinal center (GC) response. As differentiating B cells cycle between GC dark and light zones they encounter different oxygen pressures ( $pO_2$ ). However, it is essentially unknown if and how variations in  $pO_2$  affect B cell differentiation. Using optimized *in vitro* cultures together with in-depth assessment of B cell phenotype and signaling pathways, we show that oxygen is a critical regulator of human naive B cell differentiation and class switch recombination. Normoxia promotes differentiation into functional antibody secreting cells, while a population of CD27<sup>+</sup> B cells was uniquely generated under hypoxia. Moreover, time-dependent transitions between hypoxic and normoxic  $pO_2$  during culture - reminiscent of *in vivo* GC cyclic re-entry - steer different human B cell differentiation trajectories and IgG class switch recombination. Taken together, we identified oxygen pressure as an important variable governing human B cell differentiation.

## INTRODUCTION

Development of an effective long-lasting immune response implies development of high-affinity, class-switched antibodies, the result of B cell differentiation within so-called germinal centers (GC), specialized substructures in secondary lymphoid tissues. Upon initiation of the humoral immune responses, initial T cell-dependent B cell activation leads to generation of a GC response, which is preceded by a short period of extrafollicular B cell activation. During the initial extrafollicular response, an early wave of naive B cells differentiate into plasma blasts and early memory B cells. These cells display limited levels of somatic hypermutation and affinity maturation (1–4). The GC forms approximately one week after antigen exposure and becomes organized into two histologically distinct regions; the dark zone, where B cells undergo extensive proliferation and somatic hypermutation, and the light zone, where high-affinity B cells compete for antigen in order to undergo affinity selection. Class switch recombination may occur as early as the pre-GC stages and ensues in the GC reactions (5–7). GC B cells cycle repeatedly through the light zone and dark zone. After initial fate decision, differentiation may proceed towards affinity-matured late memory B cells or antibody secreting cells (i.e., plasmablasts and plasma cells) with accumulating affinity maturation (8–10).

Previous studies by ourselves and others using *in vitro* cultures of human or mouse B cells demonstrated that a GC-like B cell response can be faithfully reproduced, including generation of mature memory B cells and antibody secreting cells (11, 12). Similar to what has been reported *in vivo*, CD40 ligation together with the availability of Tfh-associated cytokines IL-4 and IL-21 is required to promote B cell proliferation, isotype switching and generation of antibody secreting cell *in vitro* (2, 13–15). The combined action of Tfh-derived CD40L, IL-21, and IL-4, results in activation of NF $\kappa$ B and JAK-STAT pathways. These are vital for, amongst others, upregulation of BLIMP1 and XBP-1s, transcription factors necessary for initiation of antibody secreting cell differentiation and antibody production (16–20), as well as C-Myc and IRF4 upregulation (18, 21–23). C-Myc is required for the survival of GC B cells and is strongly upregulated upon antigen-specific selection in the GC light zone, allowing for dark zone (re-) entry (24–27). A central role in orchestrating these events is the transcriptional repressor BCL6, which regulates expression of amongst others c-Myc and BLIMP1 (24, 28, 29) (For more detail, see Fig. S4A).

The partial pressure of oxygen ( $pO_2$ ) in healthy human tissues is around 3-6%, (30, 31) but within lymphoid tissues, distinctive hypoxic regions exist ( $pO_2$  ~0.5-1%), as specifically observed in GC light zone regions (32–34). However, the role of variations in  $pO_2$  on human B cell differentiation, and fate decision into memory B cells and antibody secreting cells has not been studied. In fact, the vast majority of *in vitro* studies is carried out at atmospheric oxygen levels ( $pO_2$  ~21%), which is much higher than proliferating B cells will encounter *in vivo*.

Variations in  $pO_2$  are likely to affect the amplitude of B cell differentiation, due to profound effects of cellular metabolism as well as direct effects on transcriptional regulation (30, 31, 35–38). Previous studies in mice on the effect of hypoxic  $pO_2$  on the GC B cell response report contrasting effects. Some reports claim hypoxia to be beneficial for an efficient GC response increasing class switch recombination, plasma cell formation and antibody production, whereas impaired proliferation and class switch recombination has also been reported (32, 34). Others observed increased Tfh function induced by upregulation of HIF-1a, a major transcription factor involved in the cellular sensing of  $pO_2$  (33). Interestingly, GC B cells were previously described to not have increased HIF-1a expression, suggesting hypoxia may regulate B cell function independent of HIF-1a (39). Another study comparing hypoxic (1%) and venous (5%)  $pO_2$  reported decreased class switch recombination and altered cellular metabolism upon culture at hypoxic  $pO_2$  (32). Overall, oxygen pressure appears an important but as yet poorly understood variable in B cell differentiation.

In the present study, we systematically investigated the effect of atmospheric (21%), normoxic, tissue-associated (3%), and hypoxic (1%)  $pO_2$  on human B cell differentiation in our highly optimized system for human primary B cell culture. Moreover, in line with varying oxygen pressures during B cell cycling in the GC dark zone and light zone, we studied time-dependent transitions in  $pO_2$  during culture and its effects on B cell differentiation trajectories and IgG class switch recombination. We show that oxygen forms another critical regulator of human naive B cell differentiation and class switch recombination.

## RESULTS

### **Differential $pO_2$ controls human B cell differentiation into CD27<sup>+</sup> and antibody secreting cell compartments**

The contribution of  $pO_2$  on human naive B cell differentiation was investigated in B cell differentiation cultures while maintaining constant  $pCO_2$ . Resting naive B cells (CD19<sup>+</sup>IgD<sup>+</sup>CD27<sup>+</sup>IgG<sup>+</sup>IgA<sup>-</sup>) from human peripheral blood were stimulated under atmospheric ( $pO_2 = 21\%$ ), normoxic ( $pO_2 = 3\%$ ) or hypoxic ( $pO_2 = 1\%$ ) conditions, using a combination of CD40L-expressing 3T3 cells (12), IL-4 and IL-21, known to facilitate class switch recombination, memory B cell and antibody secreting cell formation (Fig. 1A) (12, 40, 41). Alterations in  $pO_2$  did not affect CD40L expression levels on 3T3 cells used for stimulation (Fig. S2I, subtype high). Up until day 7 B cell survival was similar among  $pO_2$  conditions, but at day 11 hypoxic cultures contained fewer cells (Fig. S2A,B). In all cultures a rapid upregulation of activation marker CD80 was observed (Fig. S2C). Remarkably, naive B cell differentiation, as determined by the formation of antibody secreting cells (CD27<sup>+</sup>CD38<sup>-</sup>) and CD27<sup>+</sup> (CD27<sup>+</sup>CD38<sup>+</sup>) B cells, was dramatically altered by differential  $pO_2$ . Hypoxia induced a 5 to 10-fold induction of CD27<sup>+</sup> B cells as compared to atmospheric ( $p < 0.0001$ ) and normoxic cultures ( $p < 0.0001$ ) at day 7 (Fig. 1B, C, and absolute cell no. in Fig. S2D), at the expense of antibody secreting cell formation at day 11. In addition,

in normoxic cultures, the relative numbers of CD138<sup>+</sup> antibody secreting cells were 2 to 4-fold increased relative to atmospheric ( $p < 0.001$ ) and hypoxic cultures ( $p < 0.0001$ , Fig. 1D), in line with increased concentration of secreted IgM and IgG in normoxic culture supernatant at day 11 (Fig. 1E). Naive B cells poorly survived and differentiated when cultured under extreme hypoxic conditions ( $pO_2 = 0.5\%$ , Fig. S2E, F). Furthermore, using 3T3 cells with higher or lower expression of CD40L resulted in reduced proliferation, especially at reduced oxygen pressures (resp. 'VH', and 'Low', vs 'High'; Fig. S2H, I). The addition of anti-IgM F(ab')<sub>2</sub>s to the cultures, as additional BCR stimulation, did not alter *in vitro* B cell survival and differentiation at differential  $pO_2$ s (Fig. S2J). Next, we assessed the effect of  $pO_2$  on antibody class switching and Ig production. Protein expression of DNA-editing enzyme AID –indispensable for class switch recombination and somatic hypermutation– were substantially elevated over time regardless of oxygen pressure, but significantly lower at low  $pO_2$  at day 7 and 11 (Fig. 1F), in accordance with previous studies in mice (32), reflecting the overall larger fraction of differentiated cells under these conditions (Fig. 1B-C; Fig. S2K). In line with AID expression levels, IgG<sup>+</sup> B cell frequencies were higher in atmospheric cultures ( $p < 0.001$ , Fig. 1F) with minimal switch to IgA<sup>+</sup> overall, as was expected by the IgG promoting culture conditions (CD40L + IL-21 + IL-4, Fig. S2L). Altogether, these data illustrate a profound regulation of human naive B cell differentiation by oxygen levels and show that normoxia promotes differentiation into potent antibody secreting cells while hypoxia promotes differentiation into CD27<sup>+</sup> B cells.

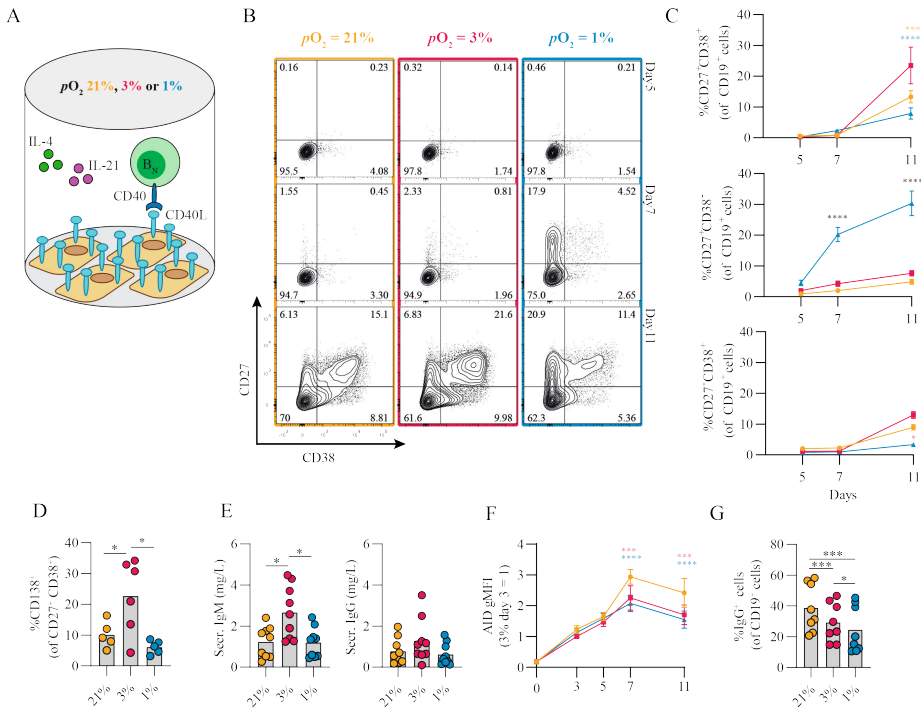


**Figure 1. Differential pO<sub>2</sub> controls human B cell differentiation into CD27<sup>+</sup> and antibody secreting cell compartments.** (A) Schematic overview of B cell *in vitro* culture system. 250 resting human naive B cells (CD19<sup>+</sup>CD27<sup>+</sup>IgD<sup>+</sup>) were stimulated using a human CD40L-expressing feeder cell layer (subtype ‘High’, (12)); recombinant human IL-4 (25ng/ml) and IL-21 (50ng/ml) and cultured at 5% pCO<sub>2</sub> and 21, 3, or 1% pO<sub>2</sub> for a maximum of 11 days. (B) Representative biaxial CD27/CD38 FACS plots after 5, 7, and 11 days of culture at 21, 3, or 1% pO<sub>2</sub>. (C) Quantification of the percentages of CD27<sup>+</sup> and CD38<sup>+</sup> subpopulations within total CD19<sup>+</sup> B cells over time ( $n = 9$ ). (D) CD138 expression within the CD27<sup>+</sup>CD38<sup>+</sup> antibody secreting cell population ( $n = 6$ ). (E) Cumulative secretion of IgM and IgG measured in culture supernatants after 11 days ( $n = 9$ ). (F) gMFI of AID expression over time ( $n = 3$ ). (G) Percentage of IgG<sup>+</sup> cells within CD19<sup>+</sup> B cells, combined surface and intracellular staining ( $n = 8$ ). Bars represent means of biological replicates each composed of 2 technical replicates in (D, F) 2, (E, G) 3 or (C) 4 independent experiments. Statistical differences were determined using (C, F) mixed-effects analysis using Tukey’s test for multiple comparisons (D, E, G) repeated measures one-way ANOVA using Tukey’s test for multiple comparisons. \*  $p < 0.05$ , \*\*\*  $p < 0.001$ , \*\*\*\*  $p < 0.0001$ .

### Proliferative human B cells adopt glycolysis and mitochondrial-associated ROS levels are increased in hypoxic cultures

Given that cellular metabolism has been reported to be linked to gene expression and B cell differentiation (42), we assessed the metabolic status of B cells that were cultured at different pO<sub>2</sub>s. Using flow cytometry, HIF1 $\alpha$  levels were increased throughout hypoxic cultures compared to normoxic and atmospheric cultures (Fig. 2A). After 7 days of *in vitro* stimulation B cells showed similar increase in cell size in all conditions compared to unstimulated cells (Fig. S3A). Dividing lymphocytes typically rely on aerobic glycolysis, fermenting imported glucose into lactate rather than oxidizing it in the mitochondria for energy. Glycolytic activity was assessed by uptake of 2-NBDG, a fluorescent analog of glucose, and production of lactate as an end product of glycolysis. Uptake of 2-NBDG



and lactate production were not significantly different between different  $pO_2$  culture conditions, but overall higher compared to resting naive B cells suggesting that indeed stimulated B cells require more glucose but demands did not change considerably upon differential  $pO_2$  environments (Fig. 2B). Also expression of GLUT1, a glucose transporter, varied minimally between culture conditions (Fig. S3B). To assess mitochondrial oxidative metabolism we analyzed mitochondrial mass, potential and formation of reactive oxygen species (ROS) by flow cytometry at day 7. Mitochondrial mass, potential and mitochondrial ROS were higher in B cells cultured at hypoxic conditions (Fig. 2C), suggesting that these cells exhibit elevated mitochondrial activity. Uptake of a fluorescent fatty acid probe was reduced in B cells under hypoxic conditions (Fig. 2D), suggesting these cells rely less on oxidation of fatty acids. At day 11 metabolic markers yielded similar result among different  $pO_2$  conditions, except for ROS levels that were significantly higher in hypoxic cultures compared to atmospheric cultures (Fig. S3C). Taken together, these results indicate that highly proliferative B cells adopt glycolysis independent of local  $pO_2$  levels and mitochondrial-associated ROS levels are elevated in hypoxic cultures.

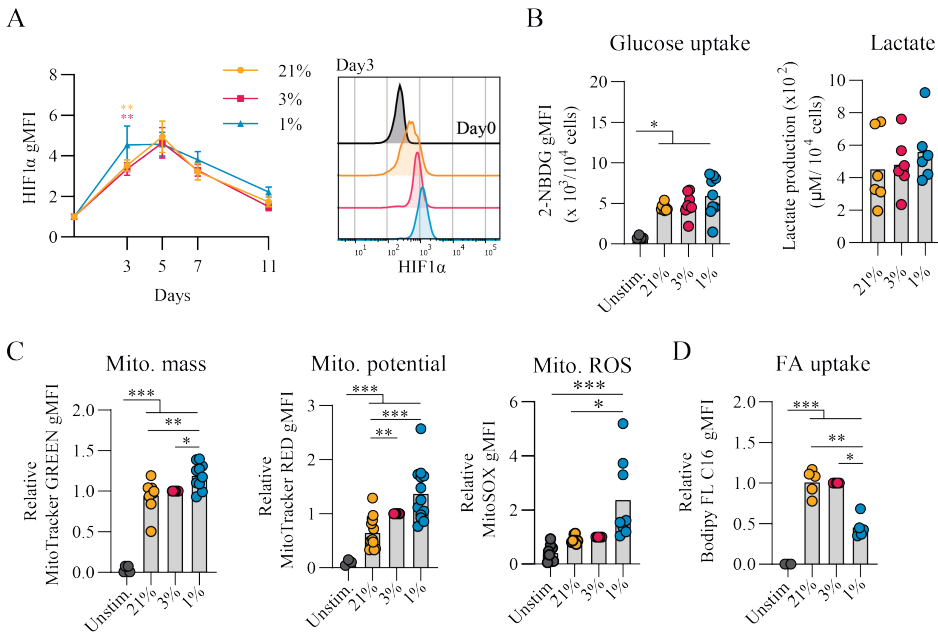


**Figure 2. Proliferative human B cells adopt glycolysis and mitochondrial-associated ROS levels are increased in hypoxic cultures** (A) gMFI of HIF1 $\alpha$  expression over time ( $n = 6$ ) and histogram overlay at day 3. (B) Glucose uptake (2-NBDG; (2-(N-(7-nitrobenz-2-oxa-1,3-diazol-4-yl)amino)-2-deoxyglucose) by B cells cultured for 7 days ( $n = 9$ ). Lactate production measured in supernatants at day 11 in  $\mu$ M per  $10^4$  cultured B cells ( $n = 6$ ). (C) gMFI of MitoTracker GREEN, MitoTracker RED, and MitoSOX after 7 days of culture ( $n = 8$ ) indicative for mitochondrial mass, potential and ROS production, respectively. (D) Fatty acid (FA) uptake by B cells cultured for 7 days ( $n = 5$ ). Bars represent means of biological replicates each composed of two technical replicates of (E) 1, (A, C) 2 or (B, D) 3 independent experiments. Statistical differences were determined using a repeated measures one-way ANOVA using Tukey's test for multiple comparisons. \*  $p < 0.05$ , \*\*  $p < 0.01$ , \*\*\*  $p < 0.001$ , \*\*\*\*  $p < 0.0001$ .

### **$pO_2$ steers canonical signaling pathways that direct naive B cell differentiation pathways**

The amplitude of B cell proliferation and differentiation is regulated by a complex interplay of signaling pathways induced by antigen recognition, CD40 ligation and reception of Tfh-derived cytokines IL-4 and IL-21 (summarized in Fig. S4A) (8, 43). Upregulation of BCL6 as well as IRF4 expression suggests differentiation of cells with a GC-like phenotype (Fig. 3A and B, respectively). In line, PNA positivity, indicative for expression of GC-specific glycans, and CD95 expression was observed early on in culture and decreased prior to the generation of CD27<sup>+</sup> B cells and antibody secreting cells (Fig. 3C and D). PNA binding was reduced for B cells cultured at hypoxic  $pO_2$  at day 3 and 5 potentially due to the accelerated CD27<sup>+</sup> differentiation in hypoxic cultures. Expression of CD86, an activation marker highly expressed on light zone B cells (44, 45), increased rapidly during culture and remained significantly higher expressed on B cells cultured at hypoxic  $pO_2$  (Fig. 3E). CD40 signaling primarily shapes the magnitude of B cell expansion and survival through induction of NF $\kappa$ B p65 and c-Myc (21, 22, 46). Moreover, NF $\kappa$ B p65 and c-Myc

are reported to maintain cellular GC commitment (47). B cells cultured at hypoxic  $pO_2$  showed a reduction in NF $\kappa$ B p65 (Fig. 3F) and c-Myc (Fig. 3G) expression from day 5 onwards, supporting the concomitant differentiation into CD27<sup>+</sup> cells, and to a lesser extent antibody secreting cells, at day 7 and reduced B cells numbers observed in hypoxic cultures thereafter (Fig. S2B).

Next, the effect of  $pO_2$  on the IL-4R/IL-21R signaling pathways to regulate B cell and antibody secreting cell transcriptional programs was analyzed. Increased phosphorylation of STAT6 (pSTAT6), a signaling protein downstream of the IL-4R, was observed in B cells cultured at hypoxic  $pO_2$ , peaking at day 3 and 5 ( $p < 0.01$  at day 5) (Fig. 3H and Fig S4B). This coincided with higher expression of XBP-1s, a transcription factor (TF) downstream of pSTAT6, at day 7 (Fig. 3J, right panel), and was not the result of variable IL-4R expression levels, determined by RT-qPCR (Fig. S4C). Peak levels of pSTAT3 on day 3 and 5, with minor differences when comparing the different  $pO_2$  conditions (Fig. 3I and Fig. S4D), coincided with upregulation of BLIMP1, directly downstream of pSTAT3, and repression of PAX5, most prominently in B cells cultured at hypoxic  $pO_2$  (Fig. 3J and Fig. S4E). PAX5 supports B cell identity. Consistent with this activity, B cells cultured at atmospheric  $pO_2$  retained highest PAX5 levels throughout culture, and thus overall a lower fraction of differentiated cells under this conditions (Fig. S4E and Fig. 1C) (48). Expression of BLIMP1 and XBP-1s was higher under hypoxic conditions (Fig 3J), and did not differ within the CD27<sup>+</sup>CD38<sup>-</sup> population at varying  $pO_2$  at day 7 (Fig. S4F), suggesting elevated BLIMP1 and XBP-1s expression in B cells cultured at hypoxic  $pO_2$  arises from the expanded CD27<sup>+</sup> compartment (Fig. 1C). This CD27<sup>+</sup> population did not secrete more Ig at day 7 compared to cells cultured at normoxic or atmospheric  $pO_2$  despite elevated XBP-1s expression, which is essential for the unfolded protein response in antibody secreting cells (Fig S4G). At day 11, naive B cells differentiation into antibody secreting cells in normoxic cultures outperformed atmospheric cultures in which B cells retained higher PAX5 levels and repression of BLIMP1 and XBP-1s (Fig. S4H). Furthermore, cells in normoxic cultures had highest XBP-1s levels in line with higher Ig production observed in these cultures ( $p < 0.05$ ) (Fig. 1G). Overall, B cell culture at different  $pO_2$  affects CD40-, IL-21R- and IL-4R-dependent signaling pathways essential for efficient B cell survival and differentiation. Expression dynamics of B differentiation-associated TFs PAX5, BLIMP1 and XBP1 were influenced by local  $pO_2$ , skewing the formation of CD27<sup>+</sup> and/or antibody secreting cell populations at hypoxic or normoxic  $pO_2$ , respectively.

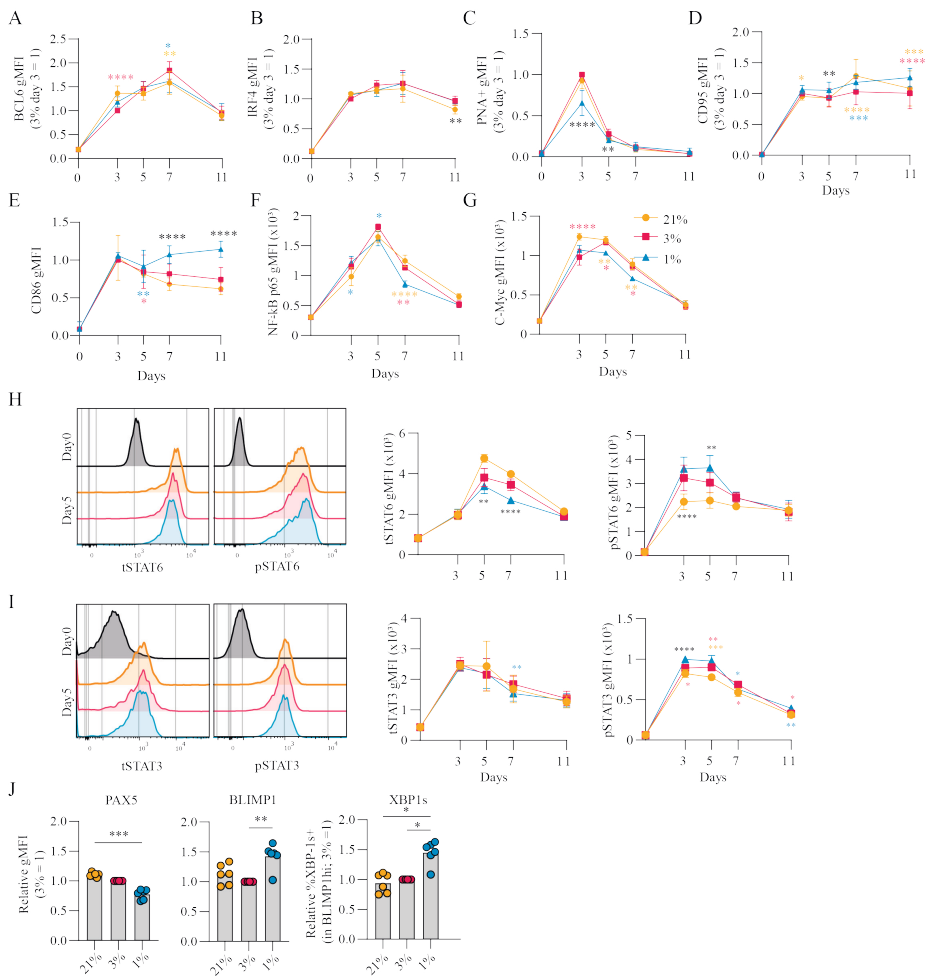


**Figure 3.  $pO_2$  steers canonical signaling pathways that direct naive B cell differentiation pathways (A-D)** gMFI of (A) BCL-6 ( $n = 6$ ) (B) IRF4 ( $n = 6$ ) (C) PNA+ ( $n = 6$ ) (D) CD95 ( $n = 6$ ) (E) CD86 ( $n = 6$ ) (F) NFkB active subunit p65 ( $n = 9$ ) (G) c-Myc ( $n = 9$ ) (H-I) gMFI of (H) tSTAT6 and pSTAT6 and (I) tSTAT3 and pSTAT3 over time in culture ( $n = 6$ ) and (left panels) representative histogram overlays of pSTAT and tSTAT expression on day 5 of culture ( $n = 6$ ) and (right panels) representative histogram overlays of pSTAT and tSTAT expression on day 7 of culture ( $n = 6$ ) (J) gMFI of PAX5, BLIMP1 and %XBP1s+ in BLIMP1hi cells ( $n = 6$ ) on day 7 (A-J) Bars represent means of biological replicates each composed of two technical replicates of 2 (H-J) or (A-G) 3 independent experiments (A-I) Differences in gMFI were determined using mixed-effects analysis using Tukey's test for multiple comparisons. (J) Differences in gMFI were determined using repeated measures one-way ANOVA using Tukey's tests for multiple comparisons. \*  $p < 0.05$ , \*\*  $p < 0.01$ , \*\*\*  $p < 0.001$ , \*\*\*\*  $p < 0.0001$ .

**Hypoxic  $pO_2$  drives generation of a unique CD27<sup>++</sup> B cell population, with enhanced antibody secreting cell differentiation capacity and Ig production upon restimulation**

Culturing B cells at hypoxic  $pO_2$  resulted in a remarkable increase in CD27<sup>+</sup> B cells which emerged earlier as compared to atmospheric and normoxic cultures (Fig. 1C). Interestingly, there was not only enlargement of this compartment but also formation of a population of CD27<sup>++</sup> cells (4.4% of CD19<sup>+</sup> population), absent in normoxic and atmospheric cultures at day 7 ( $p < 0.05$ ) (Fig. 4A, Fig S5). To assess the phenotype of these CD27<sup>++</sup> B cells, transcription factor profiles directing B cell differentiation were compared between CD27<sup>-</sup>, CD27<sup>+/-</sup>, CD27<sup>+/+</sup> and CD27<sup>++</sup>CD38<sup>++</sup> populations that developed under hypoxic  $pO_2$  at day 7 (Fig. 4B). PAX5 expression was lower and BLIMP1 expression higher in CD27<sup>+/+</sup> cells compared to CD27<sup>-</sup>CD38<sup>-</sup> B cells, with PAX5 and BLIMP1 expression being similar between CD27<sup>++</sup> and CD27<sup>++</sup>CD38<sup>++</sup> populations (Fig. 4C, upper and middle panel). Expression of XBP-1s increased as differentiation progressed, being highest in the CD27<sup>++</sup>CD38<sup>++</sup> population (Fig. 4C, lower panel). Moreover, a rise in the frequency of IgG<sup>+</sup> B cells coincided with increasing CD27 expression, being highest in the CD27<sup>++</sup> population (Fig. 4D).

As the CD27<sup>++</sup> showed a distinct transcriptional profile compared to CD27<sup>+/-</sup> and CD27<sup>-</sup> B cells, we assessed whether this translated into functional differences with regard to antibody secreting cell differentiation and Ig production. To this end naive B cells were cultured for 7 days under hypoxia, after which different CD27 expressing populations were sorted and subsequently cultured at antibody secreting cell-promoting normoxic  $pO_2$  for an additional 4 or 7 days (Fig. 4E). CD27<sup>++</sup> cells showed a significant increase in antibody secreting cell differentiation and antibody production as compared to the CD27<sup>+/-</sup> and CD27<sup>-</sup> subsets ( $p < 0.05$ ) (Fig. 4F), indicating that with the same level of stimulation the CD27<sup>++</sup> cells had enhanced capacity to differentiate towards functional antibody secreting cells. In summary, a population of CD27<sup>++</sup> B cells emerged exclusively in hypoxic cultures, with the potential to rapidly differentiate into antibody secreting cells and produce Ig after restimulation.

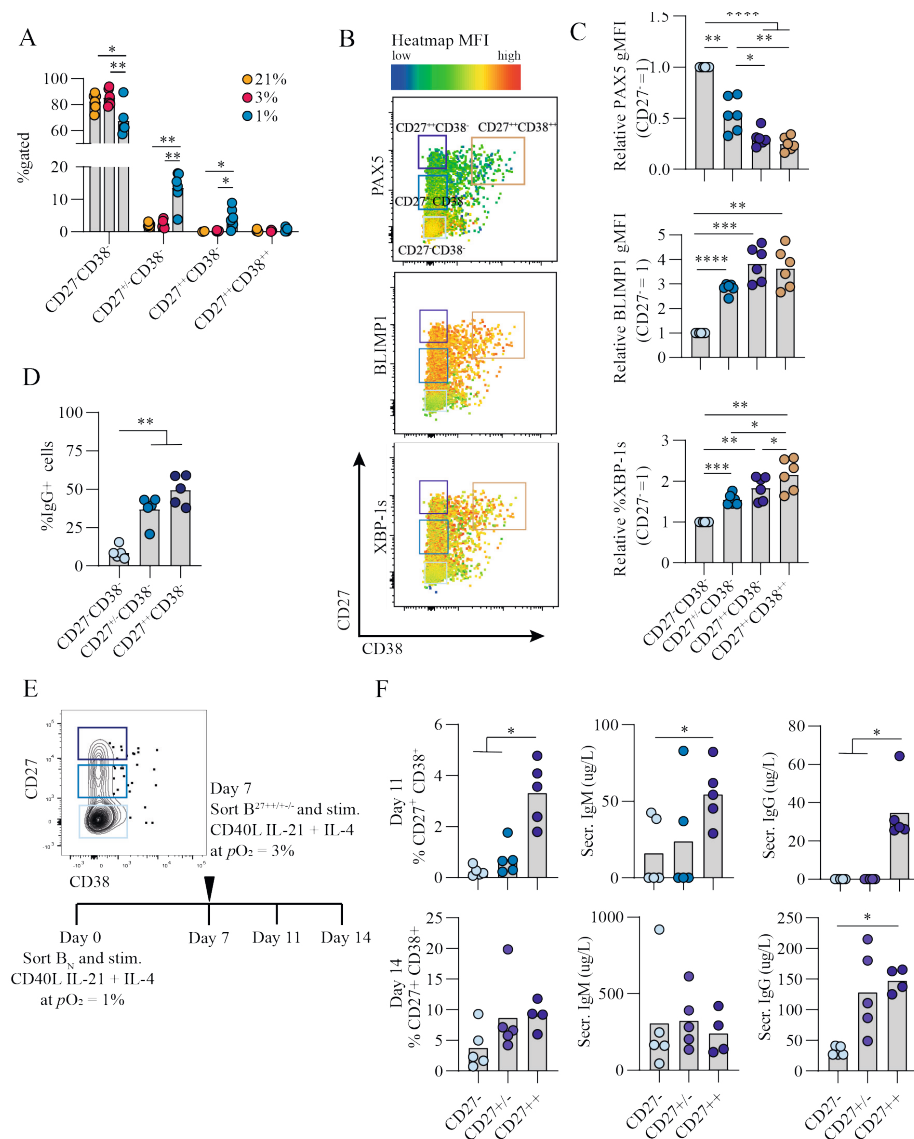


**Figure 4. Hypoxic  $pO_2$  drives generation of a unique  $CD27^{+}$  B cell population, with enhanced antibody secreting cell differentiation capacity and Ig production upon restimulation (A)** Quantification of percentage of  $CD27^{+}CD38^{-}$ ,  $CD27^{+}CD38^{+}$ ,  $CD27^{-}CD38^{-}$  and  $CD27^{-}CD38^{+}$  cells on day 7 of culture ( $n = 5$ ) **(B)** Representative biaxial flow cytometry plot of  $CD27$  and  $CD38$  expression, with heatmap depicting MFI expression of  $PAX5$ ,  $BLIMP1$  and  $XBP-1s$  on day 7. **(C)** gMFI of  $PAX5$ ,  $BLIMP1$  and  $XBP-1s$  in respective populations of  $CD27^{+}CD38^{-}$ ,  $CD27^{+}CD38^{+}$ ,  $CD27^{-}CD38^{-}$  and  $CD27^{-}CD38^{+}$  cells on day 7 ( $n = 6$ ) **(D)** Percentage of  $IgG^{+}$  B cells on day 7 of culture at 1%  $pO_2$  within  $CD27^{+}CD38^{-}$ ,  $CD27^{+}CD38^{+}$  or  $CD27^{-}CD38^{+}$  populations. ( $n = 5$ ) **(E)** Representative example of FACS sort gating strategy on day 7 to isolate  $CD27^{+}CD38^{-}$ ,  $CD27^{+}CD38^{+}$  or  $CD27^{-}CD38^{+}$  B cells with schematic experimental time line. **(F)** Quantification of % $CD27^{+}CD38^{+}$  cells by flow cytometry and  $IgM$  and  $IgG$  secretion by ELISA, 4 or 7 days after sort (day 11 or 14 of culture) ( $n = 5$ ). **(A-F)** Bars represent means of biological replicates each composed of two technical replicates of **(A, C, D)** 2 or **(F)** 1 independent experiment **(A)** Differences in %gated cells were determined using mixed-effects analysis using Tukey's test for multiple comparisons. **(C, D, F)** Differences in gMFI and % gated cells were determined using repeated measures one-way ANOVA using Tukey's test for multiple comparisons.

**Time-dependent  $pO_2$  transitions alter B cell differentiation dynamics and promote class switch recombination to IgG**

Given that during an *in vivo* GC reaction B cells cycle between the hypoxic light zone and normoxic dark zone, we assessed the effect of a  $pO_2$  transition on B cell differentiation and class switch recombination *in vitro*. To this end, naive B cells were cultured at either hypoxic or normoxic  $pO_2$  and transferred at stated time points to normoxic or hypoxic  $pO_2$ , respectively. Independent of timing, a transition from hypoxic to normoxic  $pO_2$  increased antibody secreting cell differentiation concomitant with decreased CD27<sup>+</sup> cell formation (Fig. 5A and B). Transition from hypoxic to normoxic  $pO_2$  at day 3 of culture enhanced antibody secreting cell differentiation at day 11 compared to continued culture at hypoxic  $pO_2$  and was similar to continuous culture under normoxic  $pO_2$  (Fig. 5A and B), with BLIMP1 expression lower compared to hypoxic cultures and similar to levels observed in normoxic cultures (Fig. 5C). A transition from 1 to 3%  $pO_2$  at day 5 led to a moderate generation of CD27<sup>+</sup> B cells and reduced antibody secreting cells formation in line with continuous hypoxic cultures. When hypoxic cultures were transitioned to normoxic  $pO_2$  at day 7, this induced an efficient formation of antibody secreting cells at day 11. Different from cultures at hypoxic  $pO_2$  on day 3 and 5, at day 7 hypoxic cultures consist for a significant proportion (~20%) of CD27<sup>+/++</sup> B cells, which efficiently differentiate to antibody secreting cells upon restimulation and transition to normoxic  $pO_2$  as was shown in Fig 4F. Overall this suggests time-dependent transitions in  $pO_2$  steer B cell differentiation, where early (day 3) transitions from hypoxic to normoxic  $pO_2$  lead to antibody secreting cell formation comparable to continuous normoxic cultures whereas a  $pO_2$  transition later on during culture (day 7) induces antibody secreting cell formation - in part - via the CD27<sup>++</sup> compartment. These data show that *in vitro* B cell differentiation can occur via distinct trajectories steered by differential  $pO_2$ , where hypoxia drives differentiation via a CD27<sup>++</sup> population and atmospheric and normoxic  $pO_2$  via CD38<sup>+</sup> or directly towards antibody secreting cells (Fig. S6A). Remarkably, transitions from hypoxic to normoxic  $pO_2$  at day 3 and 5 enhanced class switch recombination to IgG<sup>+</sup> B cells concomitant with a reduction in IgM<sup>+</sup> B cells (Fig. 5D). Even though the percentage of CD138<sup>+</sup> antibody secreting cells was similar (Fig. 5E) and lower compared to continuous normoxic cultures (Fig. 1D), transition of hypoxic to normoxic  $pO_2$  at day 3 and 5 resulted in higher quantities of secreted IgM and IgG in culture supernatants (Fig. 5F). Enhanced IgG class switch recombination and Ig production were no longer observed when the  $pO_2$  transition was made at day 7.

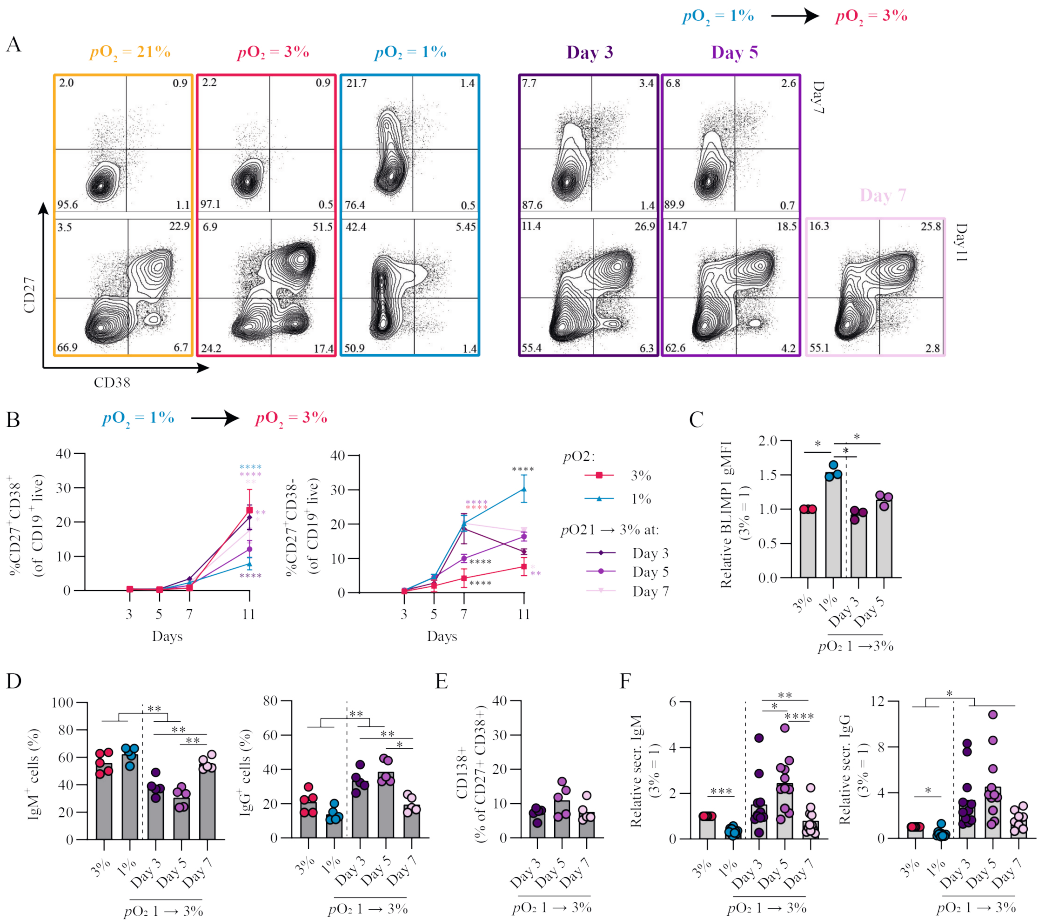


**Figure 5. Time-dependent  $pO_2$  transitions alter naive B cell differentiation and IgG class switch recombination.** (A) Representative biaxial CD27/CD38 FACS plots of 21, 3, 1%  $pO_2$  cultures and 1 – 3%  $pO_2$  transition cultures at day 3, 5 or 7 shown for day 7 and 11 of culture. (B) Quantification of CD27<sup>+</sup>CD38<sup>+</sup> and CD27<sup>+</sup>CD38<sup>-</sup> B cells over time in culture ( $n = 11$ ) (C) gMFI of BLIMP1 on day 7 ( $n = 3$ ) (D) Frequency of IgM<sup>+</sup> and IgG<sup>+</sup> B cells on day 11 ( $n = 5$ ). (E) CD138 expression within the CD27<sup>+</sup>CD38<sup>+</sup> population ( $n = 5$ ). (F) IgM and IgG levels were measured by ELISA in culture supernatant after 11 days ( $n = 11$ ). Bars represent means of biological replicates each composed of two technical replicates of (B, F) 3, (D) 2 or (C, E) 1 independent experiment. (B) Statistical differences were determined using mixed-effects analysis using Tukey’s test for multiple comparisons (C-F) Differences in gMFI, % gated cells and Ig production were determined using repeated measures one-way ANOVA using Tukey’s test for multiple comparisons.

Vice versa, transition from normoxic to hypoxic  $pO_2$  at day 3 and 5 enhanced CD27<sup>+</sup> B cell formation and BLIMP1 expression compared to continuous normoxic cultures and was more similar to continuous hypoxic cultures (Fig. S6B, C and D). A transition at day 7 from normoxic to hypoxic  $pO_2$  was deleterious for both CD27<sup>+</sup> B cell and antibody secreting cell differentiation. class switch recombination to IgG<sup>+</sup> B cells and Ig production levels ranged between those found in continuous normoxic and hypoxic cultures (Fig. S6E, F and G).



Overall, time-dependent transitions between hypoxic and normoxic  $pO_2$  during culture govern different human B cell differentiation trajectories and IgG class switch recombination *in vitro*.

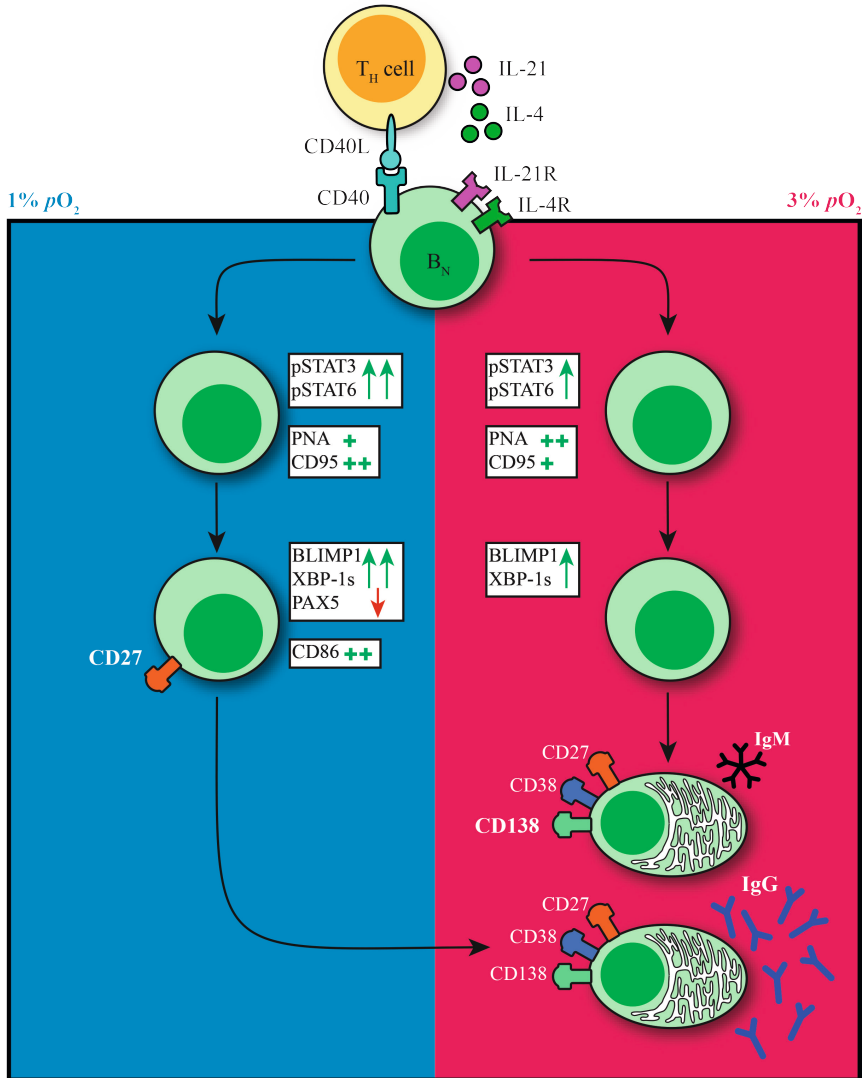


**Figure 6.  $pO_2$  as a critical driver of B cell differentiation *in vitro*.** Schematic representation of the effect of differential  $pO_2$  on B cell differentiation and underlying signaling pathways.

## DISCUSSION

The GC reaction is at the heart of the humoral immune response. Both extrafollicular and GC B cell responses take place within human tissues where oxygen pressure may range from 0.5-6%  $pO_2$  with hypoxic regions (0.5-1%  $pO_2$ ) described within GC light zone regions. Preciously little information is available about the potential role of local  $pO_2$  on human B cell fate decision during their cycling between dark zone and light zone, typically characterized by dissimilar oxygen pressures. Here we studied the effect of atmospheric (21%), tissue associated (normoxia, 3%) and hypoxic (1%)  $pO_2$  on human B cell differentiation. We observe profound differences in B cell differentiation, dynamics of emergence of various cell populations, class switch, and Ig production under these different oxygen pressures. Figure 6 summarizes our key findings on the contribution of  $pO_2$  on human naive B cell differentiation. In both hypoxic and normoxic cultures, naive B cells differentiated into a GC-like phenotype as evidenced by the expression of BCL6 and IRF4, as well as increased expression of CD95 and PNA binding. Similar to light zone B cell phenotype and function *in vivo* (8), B cells cultured at hypoxic  $pO_2$  showed high expression of CD86 and differentiated rapidly into CD27<sup>+</sup> B cells. Moreover, culture at hypoxic  $pO_2$  generated a unique population of CD27<sup>+</sup> B cells efficient in antibody secreting cell differentiation and Ig production upon restimulation. In normoxic cultures, naive B cells predominantly differentiated into antibody secreting cells, which occurred less rapidly compared to CD27<sup>+</sup> B cell formation at hypoxic  $pO_2$  in line with time-dependent waves of memory B cell and antibody secreting cell formation *in vivo* (2). Finally, time-dependent transitions from hypoxic to normoxic  $pO_2$  during culture changes B cell differentiation trajectories and promotes IgG class switch recombination and Ig production. This indicates during *in vivo* B cell cycling between GC light zone and GC dark zone, the dynamic variation in  $pO_2$  is also likely to form another regulatory layer for human B cell differentiation. Overall, our results identify oxygen as a critical factor in dictating human B cell differentiation and demonstrate the necessity of incorporating GC-like physiological  $pO_2$  variations rather than continuous atmospheric  $pO_2$  to study human B cell responses *in vitro*.

*In vivo*, antigen-specific triggering of the BCR is required for the generation of an efficient GC response. We did not observe an effect on B cell survival or differentiation by addition of a BCR stimulus to the B cell cultures at different  $pO_2$ , in line with previous reports showing limited additional effects of BCR triggers in *in vitro* cultures (12). Despite the absence of a BCR trigger, we saw a clear upregulation of c-Myc expression which is normally upregulated upon positive selection in the GC, in line with previous reports indicating CD40L ligation to be sufficient to induce c-Myc expression (25). We observed a reduction of c-Myc and NFkB expression in cells cultured at hypoxic  $pO_2$  after an initial surge upon culture initiation. c-Myc and NFkB signaling play a major role in transcriptional regulation of GC B cell proliferation and cell survival, thereby correlating with our observations regarding reduced cell numbers towards the end of cultures at

hypoxic  $pO_2$ . Naive B cell survival was abrogated upon culture at 0.5%  $pO_2$  and upon higher CD40L co-stimulation (subtype VH) at low  $pO_2$ , but not atmospheric  $pO_2$ , due to impaired proliferation. Hence, the level of CD40L co-stimulation impacts B cell survival at physiological  $pO_2$ .

Highly proliferative lymphocytes have been described to adopt glycolysis (49), which -although not comprehensively studied- is in line with the increase in glycolysis-associated metabolic traits observed in our cultures independent of *in vitro*  $pO_2$ . B cells cultured under hypoxic  $pO_2$  carried out mitochondrial oxidative metabolism, in addition to glycolysis. The difference in B cell differentiation trajectories and expansion of the CD27<sup>+</sup> compartment in hypoxic cultures may explain the expanded metabolic program towards mitochondrial oxidative metabolism at day 7. Much of the research on crosstalk between immune responses and  $pO_2$  has focused on the TF HIF1 $\alpha$ . We observe upregulation of HIF1 $\alpha$  expression throughout all culture conditions not only at hypoxic  $pO_2$ . HIF1 $\alpha$  can also be induced by signaling through CD40L, BCRs as well as TLR ligands, probably explaining the increase in HIF1 $\alpha$  also in non-hypoxic cultures (50). Furthermore, a recent study could not identify expression of hypoxia-induced genes in *ex vivo* analyzed mouse GC B cells (39), indicating HIF1 $\alpha$  is not the sole regulator of hypoxia-associated responses.

Clear differences were observed in the expansion of CD27<sup>+</sup> B cell and/or antibody secreting cell compartments in human naive B cells cultures at hypoxic and normoxic  $pO_2$ , respectively, driven by differences in the underlying molecular pathways regulating B cell survival and differentiation. It has been shown that there is a time-dependent developmental switch in the output of the GCs, such that it first dedicates itself to memory B cell generation and later switches to mainly producing antibody secreting cells (2). During culture of naive B cells at hypoxic  $pO_2$  a hypoxia-dependent CD27<sup>++</sup> population emerged early during culture. The question arises whether these CD27<sup>++</sup> cells may resemble memory B cell generated early within a GC response. Albeit unanswered in this study, it did become clear that these CD27<sup>++</sup> cells did not secrete Igs, whereas upon restimulation they swiftly differentiated into antibody secreting cells and exhibited efficient Ig secretion, in line with functionalities of memory B cells (51). Nevertheless, these cells clearly expressed a transcription factor signature of increased BLIMP1 and XBP-1s expression concomitant with a reduction of the B cell identity TF PAX5, similar to antibody secreting cells and different from memory B cells (16, 19). In line with varying  $pO_2$  during a GC response, where B cells cycle between hypoxic light zone to normoxic dark zone, we observed time-dependent effects of  $pO_2$  transitions on human B cell differentiation trajectories. Taken together, hypoxic  $pO_2$  primes B cells for efficient antibody secreting cell differentiation from a CD27<sup>+</sup> phenotype that, in order to occur, favors a transition to a normoxic environment. Besides B cell differentiation trajectories, also IgG class switch recombination was influenced by  $pO_2$  transitions. When cultured at continuous  $pO_2$ , atmospheric  $pO_2$  yielded the highest proportion of IgG<sup>+</sup> B cells (albeit not corroborated with equally elevated levels of IgG antibody production). Similar numbers of IgG<sup>+</sup> B cells

could be generated in cultures that transitioned from hypoxic to normoxic  $pO_2$  at day 3 or 5. Overall, our *in vitro* studies demonstrate the necessity of incorporating GC-like physiological  $pO_2$  variations rather than continuous atmospheric  $pO_2$  to study human B cell responses *in vitro*, as it more closely resembles the *in vivo* GC microenvironment and recapitulates time-dependent regulation of B cell fate decisions.

Besides local  $pO_2$ , other factors such as availability of nutrients, migratory and physical signals such as shear stress are also likely to contribute to B cell fate decision during both extrafollicular and GC B cell responses, warranting the need for 3D culture systems or organoids that more closely resemble the GC microenvironment to facilitate human *in vitro* B cell differentiation studies. In addition, several pathological conditions have been described to be related to hypoxia, such as myocardial ischemia (52), metabolic diseases (53), chronic heart and kidney diseases (54), and reproductive diseases (55). Moreover,  $pO_2$  has been measured and found to be significantly reduced in the majority of tumors, and sensitivity to chemotherapeutic agents changed dramatically under hypoxic conditions (56–58), highlighting the importance to adopt hypoxic cultures also for other avenues such as cancer-related drug testing and *in vitro* disease models.

In summary, we demonstrate that oxygen is an important regulator of human naive B cell differentiation by promoting oxygen-dependent differentiation trajectories and IgG class switch recombination.

## **MATERIALS & METHODS**

### **Isolation of human naive B cells**

Buffy coats were obtained from anonymized healthy donors with written informed consent in accordance to the guidelines established by the Sanquin Medical Ethical Committee and in line with the Declaration of Helsinki. Human Peripheral blood mononucleated cells (PBMCs) were isolated from fresh buffy coats using Ficoll gradient centrifugation (lymphoprep; Axis-Shield PoC AS). CD19<sup>+</sup> cells were isolated by positive selection using magnetic Dynabeads (Invitrogen). Cryopreserved CD19<sup>+</sup> cells were resuspended in PBA (PBS supplemented with 0.1% bovine serum albumin) and stained for surface markers 30 minutes in the dark at 4 °C. Viable, singlet naive B cells (CD19<sup>+</sup>IgD<sup>+</sup>CD27<sup>-</sup>IgG<sup>-</sup>IgA<sup>-</sup>) were sorted on a FACS Aria II/III.

### **Human B cell cultures**

3T3 mouse fibroblast cells expressing human CD40L (subtype: high), described previously (12), were harvested and irradiated with 30 Gy and seeded  $10 \times 10^3$  cells/well on 96-well plates for overnight adherence in B cell culture medium (RPMI medium supplemented with FCS (5%, Bodinco), penicillin (100 U/mL, Invitrogen), streptomycin (100 µg/mL, Invitrogen), β-mercaptoethanol (50 µM, Sigma-Aldrich), L-glutamine (2mM, Invitrogen), human apo-transferrin (20 µg/mL, Sigma-Aldrich) depleted for IgG using protein A sepharose (GE

Healthcare). The next day, naive B cells were sorted and 250 naive B cells/well were co-cultured with the seeded 3T3-CD40L expressing cells in the presence of IL-4 (25ng/ml; Peprotech) and IL-21 (50ng/ml; Peprotech) for 3 – 11 days to determine proliferation, isotype switching, GC, memory and plasma cell formation and Ig production. Cultures were maintained at 37 °C in an atmosphere with 5%  $p\text{CO}_2$  and 21%, 3% or 1%  $p\text{O}_2$ . For some cultures after 3, 5 or 7 days cultures were moved from 1 to 3%  $p\text{O}_2$  and vice versa.

## Flow cytometry

### *Extracellular staining of surface markers*

Cultured cells were washed with PBA and extracellular staining was performed at 4 °C for 30 minutes using the following antibody conjugates; CD19 (562947), CD38 (646851), IgD (561315), and IgM (562977), CD138 (552723), CD21 (561372 or 740395), FAS/CD95 (762346), CD80 (750440 or 558226), CD86 (748375 or 562433), CXCR4 (563924) from BD Biosciences. IgG (M1268) from Sanquin Reagents. IgA (2050-09) from SouthernBiotech. CD27 (25-0279-42) from ThermoFisher. PNA (FL-1071-5) from VectorLabs. Glut1 (FAB1418A) from R&D. LIVE/DEAD Fixable Near-IR from Invitrogen.

### *Intracellular staining of signaling and transcription factors*

Staining procedures were performed as previously described (59). In short, harvested and pooled cultures were kept on melting ice at all times. After washing, cultures were stained for membrane markers in a 25 $\mu$ l staining mix containing the Live/Dead stain, anti-CD19 and anti-CD38 antibodies. TF stain procedure also contained anti-CD27 antibodies during membrane marker staining. After staining, samples were washed once with ice-cold PBA and centrifuged. Samples were fixed with either paraformaldehyde (PFA; Sigma) or Foxp3 fixation buffer (eBioscience). PFA fixed samples were subsequently washed once and permeabilized with 90% methanol. Samples were incubated at -20°C till day of FACS analysis. Foxp3-fixed samples were washed once with Foxp3 permeabilization buffer and kept in ice-cold PBA in the dark till day of FACS analysis.

Before FACS analysis, all samples were retrieved from -20 °C or 4 °C storage and washed once with ice-cold PBA. Methanol permeabilized samples were washed once more before adding 25 $\mu$ l staining mix containing antibodies against STAT3 (564133, BD), pSTAT3 (612569, BD), NF $\kappa$ B p65 (565446, BD), STAT6 (IC2167T, R&D), pSTAT6 (612600, BD) and C-MYC (13871S, CST), NF $\kappa$ B p65, HIF1 $\alpha$  (359706, Biolegend) diluted in PBA. Samples were incubated for 45 minutes on a plate shaker at room temperature. Afterwards, samples were washed once with PBA and measured on a flow cytometer.

Foxp3 fixed samples were washed once with Foxp3 permeabilization buffer. Samples were stained in 25 $\mu$ l staining mix containing antibodies against PAX5 (649708, Biolegend), BCL6 (358512, Biolegend), IRF4 (646416, Biolegend) and AID (565785, BD) or PAX5, BCL6, IRF4, BLIMP1 (IC36081R-025, R&D) and XBP-1s (562820, BD) diluted in Foxp3 permeabilization

buffer and incubated for 30 minutes in the fridge. Samples were washed once with Foxp3 permeabilization buffer and measured on a flow cytometer.

#### *Proliferation assays*

B cells were labelled with proliferation dye according to manufacturer's instructions. In short, sorted B cells were washed with 10 ml PBS twice and resuspended to a concentration of  $2 \times 10^7$  cells/ml in PBS. Cells and  $4 \mu\text{M}$  Violet Proliferation Dye 450 (VPD450, BD Biosciences) in PBS were mixed at a 1:1 ratio and incubated 15 minutes in a  $37^\circ\text{C}$  water bath in the dark, vortexing the tube every 5 minutes to ensure uniform staining. Cells were washed twice using a 10 times volume of cold culture medium to end labeling. Thereafter, B cells were cultured according to the protocol described above.

#### *Assessment of B cell metabolic status*

To monitor B cell metabolic activity, cells were cultured as described and loaded with  $50\text{nM}$  MitoTracker Red CMXRos (M7512, Invitrogen) and  $25\text{nM}$  MitoTracker Green FM (M7514, Invitrogen),  $20\text{nM}$  BODIPY™ FL C12 (4,4-Difluoro-5,7-Dimethyl-4-Bora-3a,4a-Diaza-s-Indacene-3-Dodecanoic Acid) (D3822, Invitrogen) or  $200\mu\text{M}$  2-NBDG (2-(N-(7-Nitrobenz-2-oxa-1,3-diazol-4-yl)Amino)-2-Deoxyglucose) (N13195, Invitrogen) for 30 minutes or  $2.5\mu\text{M}$  MitoSOX (M36008, Invitrogen) for 10 minutes at  $37^\circ\text{C}$   $5\%$   $\text{CO}_2$  in pre-warmed Hank's Buffered Salt Solution (HBSS, 14025050, Gibco) on day 0 and 7 of culture. Cells were washed, stained for membrane markers as described above and measured on a flow cytometer.

All antibodies and reagents were titrated to optimal staining concentration using PBMCs and samples were measured on the BD LSR Fortessa or BD FACSymphony and analyzed using Flowjo V10.8. For representative gating strategy, see Fig. S1.

#### *Cell counts*

Before FACS analysis samples were mixed with at least 10.000 CountBright Absolute counting beads (Thermo Fisher Scientific) and prepared for flow cytometry analysis as described above. Absolute B cell counts were determined according to the formula:

$$\frac{\#LiveCD19 +}{\#Beadsmeasured} \times \#beadsadded$$

#### **Ig ELISAs of culture supernatants**

IgM, IgA, IgG, and IgG1 and IgG4 expression levels were measured in culture supernatants at day 7, 11 and 14. 96-well maxisorb plates were coated with monoclonal mouse anti-human IgM ( $2\mu\text{g/ml}$ , MH15-1), anti-IgA ( $1\mu\text{g/ml}$ , MH14-01), anti-IgG ( $2\mu\text{g/ml}$ , MH16-1), anti-IgG1 ( $1\mu\text{g/ml}$ , MH161-01), and IgG4 ( $1\mu\text{g/ml}$ , MH164-01) in PBS all provided by Sanquin Reagents. Culture supernatants were incubated for 1h and secreted Igs were detected using  $1\mu\text{g/ml}$  HRP-conjugated mouse anti-human IgM, IgA, IgG, IgG1, or IgG4 (Sanquin

Reagents) in HPE (Sanquin Reagents). The ELISA was developed using TMB substrate, stopped by addition of 2M H<sub>2</sub>SO<sub>4</sub> and absorbance was measured at 450 and 540 nm. OD values were normalized to values of a titration curve of a serum pool that was included in each plate.

### **Lactate production**

L(+)-lactate production was measured in B cell culture supernatant using L-lactate Assay Kit (ab65331, Abcam) according to manufacturer's instructions. Lactate production was corrected for cell counts as measured by flow cytometry.

### **Real-time semi-quantitative RT-PCR**

RNA isolation was performed as described elsewhere (60). Primers were developed to span exon-intron junctions and then validated (IL-4R: 5'- CCCTGAAGTCTGGGATTCCT -3'). Gene expression levels were measured in duplicate reactions for each sample in StepOnePlus (Applied Biosystems, Foster City, CA, USA) using the SYBR green method (Applied Biosystems, Foster City, CA, USA). Expression of housekeeping gene 16S was used for normalization.

### **Statistical analysis**

Statistical analysis was performed using GraphPad Prism 8. Data were analyzed using Repeated Measures one-way ANOVA with Tukey's multiple comparison test, Repeated Measures two-way ANOVA with Sidak's multiple comparison test or mixed-effects analysis with Dunnett's multiple comparison test where appropriate. Results were considered significant at  $p < 0.05$ . Significance was depicted as \* $p < 0.05$  or \*\* $p < 0.01$ , \*\*\* $p < 0.001$  or \*\*\*\* $p < 0.0001$ . To show significance between specific datasets within a graph containing multiple datasets, the \* shows the significance between the dataset matching the color of \* and the dataset closest to the \*.

## REFERENCES

1. R. A. Elsner, M. J. Shlomchik, Germinal Center and Extrafollicular B Cell Responses in Vaccination, Immunity, and Autoimmunity. *Immunity* 53, 1136–1150 (2020).
2. F. J. Weisel, G. V. Zuccarino-Catania, M. Chikina, M. J. Shlomchik, A Temporal Switch in the Germinal Center Determines Differential Output of Memory B and Plasma Cells. *Immunity* 44, 116–130 (2016).
3. B. J. Laidlaw, J. G. Cyster, Transcriptional regulation of memory B cell differentiation. *Nat. Rev. Immunol.* 21, 209–220 (2021).
4. D. Suan, *et al.*, CCR6 Defines Memory B Cell Precursors in Mouse and Human Germinal Centers, Revealing Light-Zone Location and Predominant Low Antigen Affinity. *Immunity* 47, 1142-1153.e4 (2017).
5. A. F. Cunningham, *et al.*, Salmonella Induces a Switched Antibody Response without Germinal Centers That Impedes the Extracellular Spread of Infection. *J. Immunol.* 178, 6200–6207 (2007).
6. J. L. Marshall, *et al.*, Early B blasts acquire a capacity for Ig class switch recombination that is lost as they become plasmablasts. *Eur. J. Immunol.* 41, 3506–3512 (2011).
7. J. A. Roco, *et al.*, Class Switch Recombination Occurs Infrequently in Germinal Centers. *Immunity* 51, 337–350 (2019).
8. G. D. Victora, M. C. Nussenzweig, Germinal centers. *Immunol. Rev.* 247, 5–10 (2022).
9. R. Shinnakasu, *et al.*, Regulated selection of germinal-center cells into the memory B cell compartment. *Nat. Immunol.* 17, 861–869 (2016).
10. B. J. Laidlaw, *et al.*, The Eph-related tyrosine kinase ligand Ephrin-B1 marks germinal center and memory precursor B cells. *J. Exp. Med.* 214, 639–649 (2017).
11. Y. Takahashi, P. R. Dutta, D. M. Cerasoli, G. Kelsoe, “In Situ Studies of the Primary Immune Response to (4-Hydroxy-3-Nitrophenyl)Acetyl. V. Affinity Maturation Develops in Two Stages of Clonal Selection” (1998).
12. P. P. A. Unger, *et al.*, Minimalistic In Vitro Culture to Drive Human Naive B Cell Differentiation into Antibody-Secreting Cells. *Cells* 10 (2021).
13. M. A. Linterman, *et al.*, IL-21 acts directly on B cells to regulate Bcl-6 expression and germinal center responses. *J. Exp. Med.* 207, 353–363 (2010).
14. S. G. Tangye, A. Ferguson, D. T. Avery, C. S. Ma, P. D. Hodgkin, Isotype Switching by Human B Cells Is Division-Associated and Regulated by Cytokines. *J. Immunol.* 169, 4298–4306 (2002).
15. D. Zotos, *et al.*, IL-21 regulates germinal center B cell differentiation and proliferation through a B cell-intrinsic mechanism. *J. Exp. Med.* 207, 365–378 (2010).
16. J. Tellier, S. L. Nutt, Plasma cells: The programming of an antibody-secreting machine. *Eur. J. Immunol.* 49, 30–37 (2019).
17. S. L. Nutt, P. D. Hodgkin, D. M. Tarlinton, L. M. Corcoran, The generation of antibody-secreting plasma cells. *Nat. Rev. Immunol.* 15, 160–171 (2015).
18. U. Klein, *et al.*, Transcription factor IRF4 controls plasma cell differentiation and class-switch recombination. *Nat. Immunol.* 7, 773–782 (2006).
19. B. B. Ding, E. Bi, H. Chen, J. J. Yu, B. H. Ye, IL-21 and CD40L Synergistically Promote Plasma Cell Differentiation through Upregulation of Blimp-1 in Human B Cells. *J. Immunol.* 190, 1827–1836 (2013).



20. D. T. Avery, *et al.*, B cell-intrinsic signaling through IL-21 receptor and STAT3 is required for establishing long-lived antibody responses in humans. *J. Exp. Med.* 207, 155–171 (2010).
21. A. Craxton, *et al.*, p38 MAPK is required for CD40-induced gene expression and proliferation in B lymphocytes. *J. Immunol.* 161, 3225–36 (1998).
22. S. C. Sun, The non-canonical NF- $\kappa$ B pathway in immunity and inflammation. *Nat. Rev. Immunol.* 17, 545–558 (2017).
23. D. Chen, *et al.*, CD40-Mediated NF- $\kappa$ B Activation in B Cells Is Increased in Multiple Sclerosis and Modulated by Therapeutics. *J. Immunol.* 197, 4257–4265 (2016).
24. S. Finkin, H. Hartweiger, T. Y. Oliveira, E. E. Kara, M. C. Nussenzweig, Protein Amounts of the MYC Transcription Factor Determine Germinal Center B Cell Division Capacity. *Immunity* 51, 324–336.e5 (2019).
25. W. Luo, F. Weisel, M. J. Shlomchik, B Cell Receptor and CD40 Signaling Are Rewired for Synergistic Induction of the c-Myc Transcription Factor in Germinal Center B Cells. *Immunity* 48, 313–326.e5 (2018).
26. D. P. Calado, *et al.*, The cell-cycle regulator c-Myc is essential for the formation and maintenance of germinal centers. *Nat. Immunol.* 13, 1092–1100 (2012).
27. D. Dominguez-Sola, *et al.*, The proto-oncogene MYC is required for selection in the germinal center and cyclic reentry. *Nat. Immunol.* 13, 1083–1091 (2012).
28. M. Kitano, *et al.*, Bcl6 Protein Expression Shapes Pre-Germinal Center B Cell Dynamics and Follicular Helper T Cell Heterogeneity. *Immunity* 34, 961–972 (2011).
29. M. B. Harris, *et al.*, Transcriptional Repression of Stat6-Dependent Interleukin-4-Induced Genes by BCL-6: Specific Regulation of I $\epsilon$  Transcription and Immunoglobulin E Switching. *Mol. Cell. Biol.* 19, 7264–7275 (1999).
30. K. R. Atkuri, L. A. Herzenberg, L. A. Herzenberg, Culturing at atmospheric oxygen levels impacts lymphocyte function. *Proc. Natl. Acad. Sci. U. S. A.* 102, 3756–3759 (2005).
31. N. Burrows, P. H. Maxwell, Hypoxia and B cells. *Exp. Cell Res.* 356, 197–203 (2017).
32. S. H. Cho, *et al.*, Germinal centre hypoxia and regulation of antibody qualities by a hypoxia response system. *Nature* 537, 234–238 (2016).
33. S. H. Cho, *et al.*, Hypoxia-inducible factors in CD4<sup>+</sup> T cells promote metabolism, switch cytokine secretion, and T cell help in humoral immunity. *Proc. Natl. Acad. Sci. U. S. A.* 116, 8975–8984 (2019).
34. R. K. Abbott, *et al.*, Germinal Center Hypoxia Potentiates Immunoglobulin Class Switch Recombination. *J. Immunol.* 197, 4014–4020 (2016).
35. N. Burrows, *et al.*, Dynamic regulation of hypoxia-inducible factor-1 $\alpha$  activity is essential for normal B cell development. *Nat. Immunol.* 21, 1408–1420 (2020).
36. J. Jellusova, *et al.*, Gsk3 is a metabolic checkpoint regulator in B cells. *Nat. Immunol.* 18, 303–312 (2017).
37. D. N. Halligan, S. J. E. Murphy, C. T. Taylor, The hypoxia-inducible factor (HIF) couples immunity with metabolism. *Semin. Immunol.* 28, 469–477 (2016).
38. L. Li, *et al.*, Regulation of humoral immune response by HIF-1 $\alpha$ -dependent metabolic reprogramming of the germinal center reaction. *Cell. Immunol.* 367 (2021).
39. F. J. Weisel, *et al.*, Germinal center B cells selectively oxidize fatty acids for energy while conducting minimal glycolysis. *Nat. Immunol.* 21, 331–342 (2020).

40. J. Koers, *et al.*, CD45RB Glycosylation and Ig Isotype Define Maturation of Functionally Distinct B Cell Subsets in Human Peripheral Blood. *Front. Immunol.* 13, 891316 (2022).
41. C. Marsman, D. Verhoeven, J. Koers, T. Rispens, Optimized protocols for in vitro T cell-dependent and T cell-independent activation for B cell differentiation studies using limited cells (2022) <https://doi.org/10.20944/preprints202111.0365.v2>.
42. E. L. Pearce, E. J. Pearce, Metabolic pathways in immune cell activation and quiescence. *Immunity* 38, 633–643 (2013).
43. N. J. M. Versteegen, V. Ubels, H. V. Westerhoff, S. M. van Ham, M. Barberis, System-Level Scenarios for the Elucidation of T Cell-Mediated Germinal Center B Cell Differentiation. *Front. Immunol.* 12, 1–19 (2021).
44. G. D. Victora, *et al.*, Germinal center dynamics revealed by multiphoton microscopy with a photoactivatable fluorescent reporter. *Cell* 143, 592–605 (2010).
45. C. D. C. Allen, *et al.*, Germinal center dark and light zone organization is mediated by CXCR4 and CXCR5. *Nat. Immunol.* 5, 943–952 (2004).
46. D. Chen, *et al.*, CD40-Mediated NF- $\kappa$ B Activation in B Cells Is Increased in Multiple Sclerosis and Modulated by Therapeutics. *J. Immunol.* 197, 4257–4265 (2016).
47. N. Heise, *et al.*, Germinal center B cell maintenance and differentiation are controlled by distinct NF- $\kappa$ B transcription factor subunits. *J. Exp. Med.* 211, 2103–2118 (2014).
48. C. Cobaleda, A. Schebesta, A. Delogu, M. Busslinger, Pax5: The guardian of B cell identity and function. *Nat. Immunol.* 8, 463–470 (2007).
49. M. G. Vander Heiden, L. C. Cantley, C. B. Thompson, Understanding the Warburg effect: the metabolic requirements of cell proliferation. *Science* 324, 1029–1033 (2009).
50. D. N. Halligan, S. J. E. Murphy, C. T. Taylor, The hypoxia-inducible factor (HIF) couples immunity with metabolism. *Semin. Immunol.* 28, 469–477 (2016).
51. E. K. Deenick, *et al.*, Naive and memory human B cells have distinct requirements for STAT3 activation to differentiate into antibody-secreting plasma cells. *J. Exp. Med.* 210, 2739–2753 (2013).
52. H. Abe, H. Semba, N. Takeda, The Roles of Hypoxia Signaling in the Pathogenesis of Cardiovascular Diseases. *J. Atheroscler. Thromb.* 24, 884–894 (2017).
53. P. Trayhurn, B. Wang, I. S. Wood, Hypoxia in adipose tissue: a basis for the dysregulation of tissue function in obesity? *Br. J. Nutr.* 100, 227–235 (2008).
54. K. Sun, *et al.*, Sphingosine-1-phosphate promotes erythrocyte glycolysis and oxygen release for adaptation to high-altitude hypoxia. *Nat. Commun.* 7, 12086 (2016).
55. S. Zamudio, *et al.*, Maternal and fetoplacental hypoxia do not alter circulating angiogenic growth effectors during human pregnancy. *Biol. Reprod.* 90, 42 (2014).
56. A. Carreau, B. El Hafny-Rahbi, A. Matejuk, C. Grillon, C. Kieda, Why is the partial oxygen pressure of human tissues a crucial parameter? Small molecules and hypoxia. *J. Cell. Mol. Med.* 15, 1239–1253 (2011).
57. L. Schito, G. L. Semenza, Hypoxia-Inducible Factors: Master Regulators of Cancer Progression. *Trends in cancer* 2, 758–770 (2016).
58. J. M. Brown, Exploiting tumour hypoxia and overcoming mutant p53 with tirapazamine. *Br. J. Cancer* 77 Suppl 4, 12–14 (1998).

59. C. Marsman, T. Jorritsma, A. Ten Brinke, S. M. van Ham, Flow Cytometric Methods for the Detection of Intracellular Signaling Proteins and Transcription Factors Reveal Heterogeneity in Differentiating Human B Cell Subsets. *Cells 2020, Vol. 9, Page 2633 9, 2633* (2020).
60. Y. Souwer, *et al.*, Detection of aberrant transcription of major histocompatibility complex class II antigen presentation genes in chronic lymphocytic leukaemia identifies HLA-DOA mRNA as a prognostic factor for survival. *Br. J. Haematol.* 145, 334–343 (2009).

## SUPPLEMENTARY MATERIAL

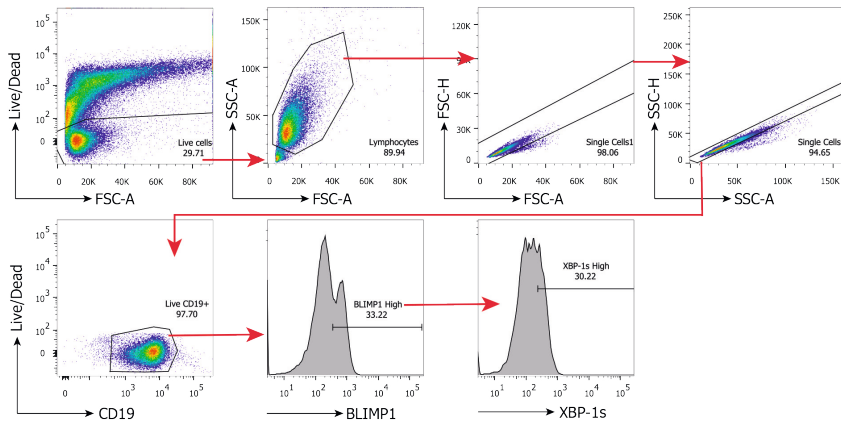


**Figure S1.** Representative gating strategy of B cells after culture. First live cells are gated based on viability dye and FSC-A, subsequently lymphocytes are gated using FSC-A and SSC-A, two gates to select singles, based on FSC and SSC and H parameters. Finally cells were gated as live, CD19+ whereupon specific phenotyping and transcription factor markers were gated. Example gating strategy for BLIMP1 and XBP-1s gates.

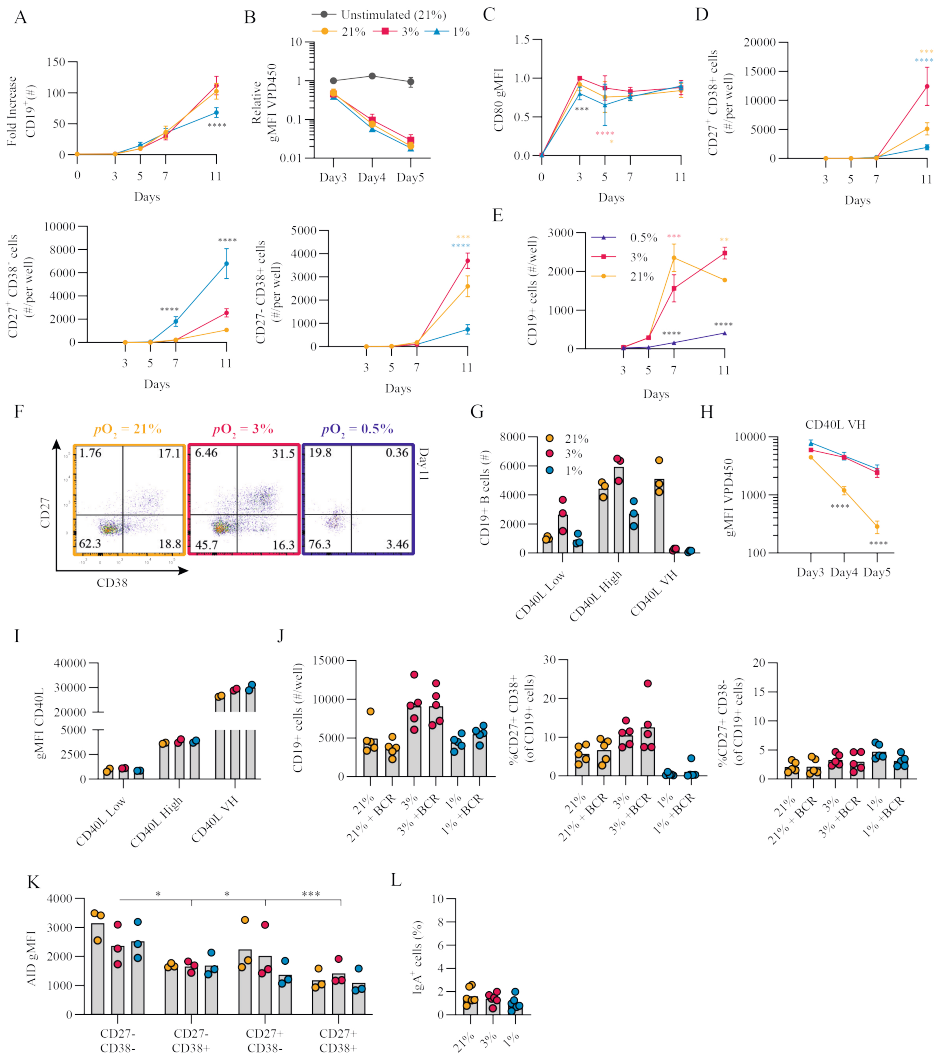


**Figure S2.** Hypoxia promotes human B cell differentiation *in vitro*. **(A)** Fold increase in number of CD19<sup>+</sup> cells over the course of the culture compared to day 0 (250 cells/well,  $n = 9$ ). **(B)** Proliferation (area = 3). **(C)** gMFI CD80 ( $n = 6$ ). **(D)** The number of CD19<sup>+</sup> cells retrieved per well within the CD27/CD38 quadrants ( $n = 9$ ). **(E)** Number of live CD19<sup>+</sup> cells present in cultures using 0.5%, 3 and 21% pO ( $n = 3$ ). **(F)** Representative CD27/CD38 biaxial plot showing the differentiation of naive B cells at 0.5, 3 and 21% pO at day 11 of culture. **(G)** Number of live CD19<sup>+</sup> cells in cultures stimulated with IL-4 + IL-21 and human CD40L low, high or very high (VH) co-stimulation cultured at 21, 3 and 1% pO, for 11 days ( $n = 3$ ). **(H)** As in **(G)** for proliferation at day 3, 4 and 5 ( $n = 3$ ) **(I)** Expression levels of human CD40L low, high and very high (VH) expressed on mice 3T3 fibroblast cells cultured at 21, 3 and 1% pO for 5 days ( $n = 2$ ). **(J)** Number of live CD19<sup>+</sup> cells, percentage of CD27<sup>+</sup>CD38<sup>+</sup> and CD27<sup>+</sup>CD38<sup>-</sup> cells in cultures with and without 1 $\mu$ g/ml anti-IgM F(ab')<sub>2</sub> cultured for 11 days. ( $n = 5$ ) **(K)** AID expression within the different CD27/CD38 quadrants ( $n = 3$ ). **(L)** IgA<sup>+</sup> B cells after 11 days of culture ( $n = 6$ ). Bars represent means of biological replicates each composed of two technical replicates of **(F-I, K)** 1, **(A, B, J, L)** 2 or **(C-E)** 3 independent experiments. Statistical differences were determined using **(B-F)** mixed effects model using Tukey's test for multiple comparisons. **(H-J)** repeated measures one-way

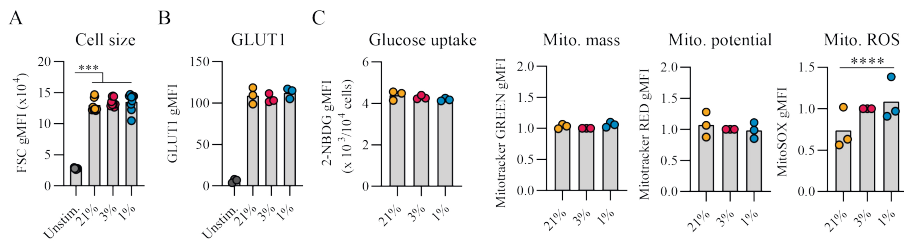


**Figure S3.** B cell cultured at hypoxic  $pO_2$  alter their metabolic program. At day 7 of culture **(A)** Cell size determined as gMFI of the forward scatter (FSC,  $n=14$ ), **(B)** gMFI of GLUT1 expression, and **(C)** gMFI of 2-NBDG, MitoTracker GREEN, MitoTracker RED, and MitoSOX in cells cultured at differential  $pO_2$  for 11 days ( $n=3$ ). Bars represent means of biological replicates each composed of two technical replicates of **(A)** 2 **(B-C)** or 1 independent experiments. Statistical differences were determined using repeated measures one-way ANOVA using Tukey's test for multiple comparisons. \*\*\*  $p < 0.001$ , \*\*\*\*  $p < 0.0001$ .

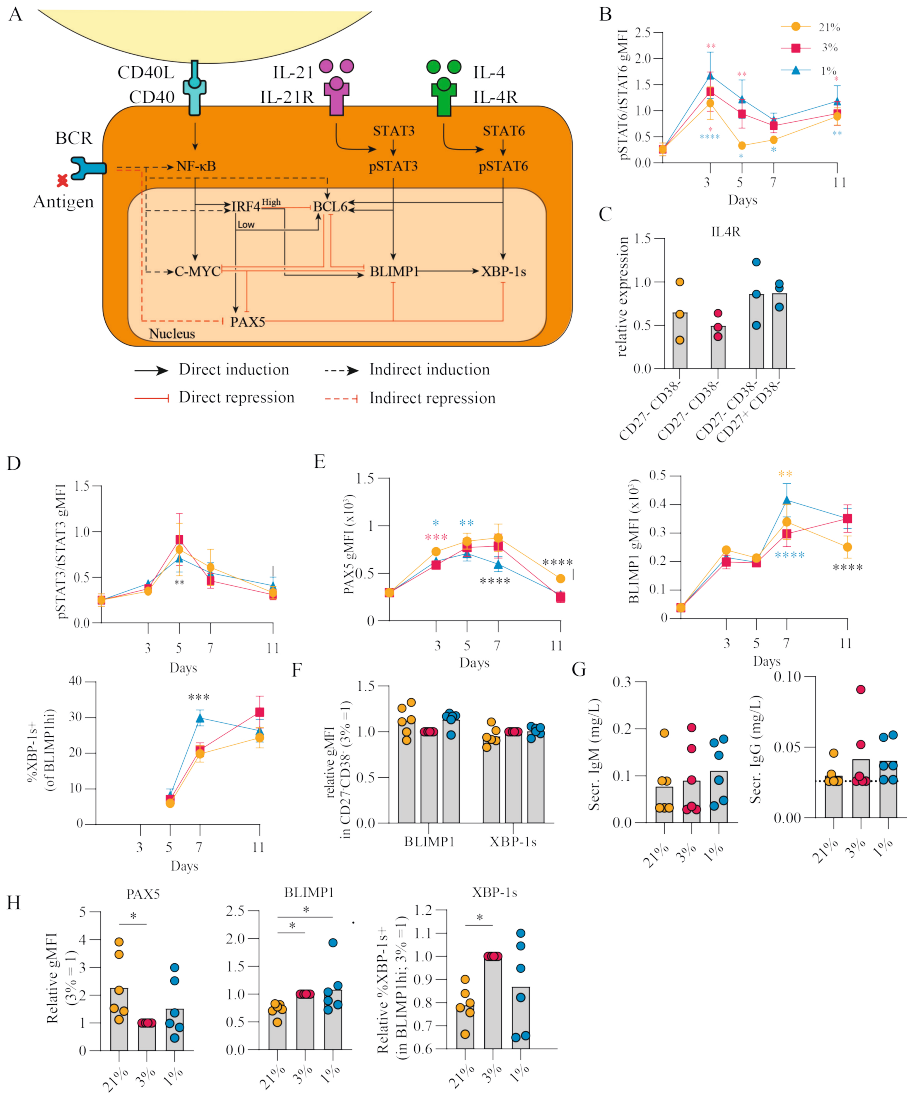


**Figure S4.** *pO2* steers molecular signaling underlying B cell differentiation **(A)** Schematic representation of intracellular signaling events leading to TF expression regulation upon B cell stimulation with typical Tfh signals including CD40L, IL-21 and IL-4. **(B)** ratio of pSTAT6/tSTAT6 gMFI ( $n = 6$ ). **(C)** Relative expression of IL-4R mRNA as determined by RT-qPCR ( $n = 3$ ). **(D)** ratio of pSTAT3/tSTAT3 gMFI ( $n = 6$ ) **(E)** gMFI of PAX5, BLIMP1 and %XBP-1s over time ( $n = 6$ ) **(F)** gMFI of BLIMP1 and XBP-1s within CD27<sup>+</sup>CD38<sup>-</sup> population. ( $n = 6$ ) **(G)** secreted IgM and IgG as measured by ELISA on day 7 of culture ( $n = 6$ ) **(H)** gMFI of PAX5, BLIMP1 and %XBP-1s at day 11 ( $n = 6$ ). Bars represent means of biological replicates each composed of two technical replicates of **(B, D-H)** 2 or **(C)** 1 independent experiments. Statistical differences were determined using **(B, D-E)** mixed-effects analysis using Tukey's test for multiple comparisons or **(C, F-H)** using repeated measures one-way ANOVA using Tukey's test for multiple comparisons. \*  $p < 0.05$ , \*\*  $p < 0.01$ , \*\*\*  $p < 0.001$ , \*\*\*\*  $p < 0.0001$ .

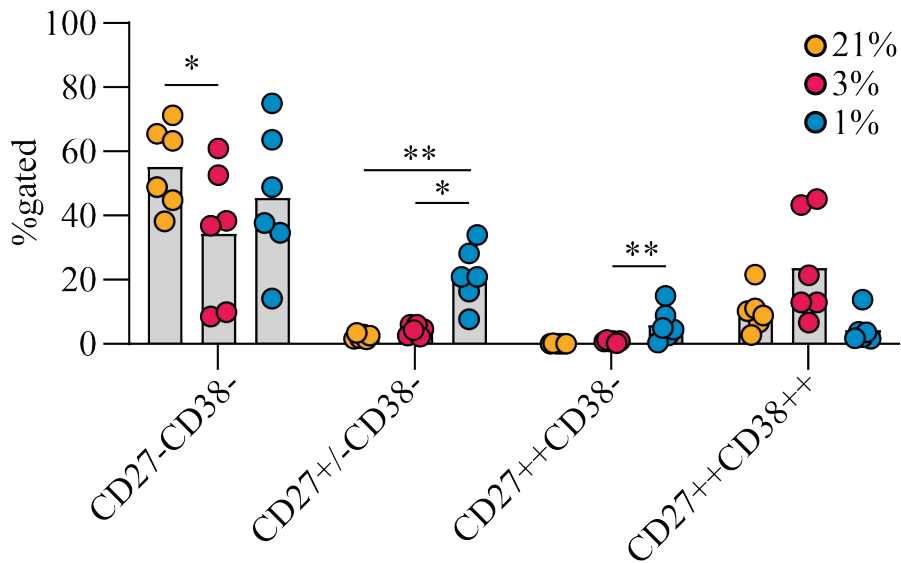


**Figure S5** hypoxic  $pO_2$  leads to generation of pre-ASC CD27<sup>+</sup> B cell subset. **(A)** Quantification of cells in CD27<sup>-</sup>CD38<sup>-</sup>; CD27<sup>+/-</sup>CD38<sup>-</sup>; CD27<sup>++</sup>CD38<sup>-</sup>; CD27<sup>++</sup>CD38<sup>+/-</sup> gates on day 11 of culture ( $n=6$ ) ( $n=5$ ) Bars represent means of biological replicates each composed of two technical replicates of 1 independent experiment. Statistical differences were determined using mixed effects analysis using Tukey's test for multiple comparisons \*  $p < 0.05$ , \*\*  $p < 0.01$ , \*\*\*  $p < 0.001$ , \*\*\*\*  $p < 0.0001$



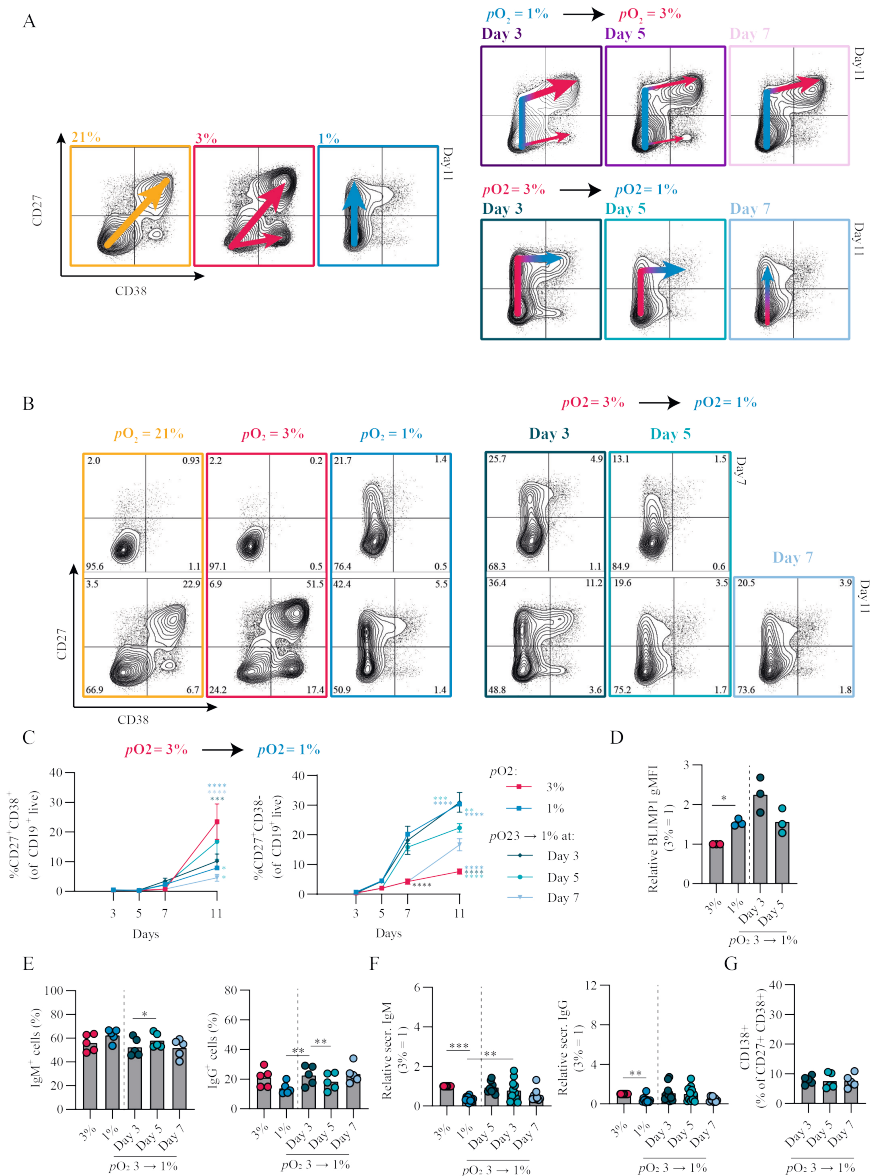


**Figure S6.** Time-dependent  $pO_2$  transitions alter B cell differentiation dynamics and promote CSR to IgG. **(A)** Schematic representation of CD27/CD38 differentiation trajectories of human naive B cells *in vitro*. **(B)** Representative biaxial CD27/CD38 FACS plots of 21, 3 and 1%  $pO_2$  cultures and 3 - 1%  $pO_2$  transition cultures at day 3, 5 and 7 shown for day 7 and 11 of culture. **(C)** Quantification of CD27<sup>+</sup>CD38<sup>+</sup> and CD27<sup>+</sup>CD38<sup>-</sup> B cell formation ( $n = 11$ ) **(D)** gMFI of BLIMP1 at day 7 ( $n = 3$ ) **(E)** Frequency of IgM<sup>+</sup> and IgG<sup>+</sup> cells determined by intracellular flow cytometry ( $n = 5$ ) **(F)** and cumulative IgM and IgG secretion in culture supernatants at day 11 in 3 and 1%  $pO_2$  cultures and 3 - 1%  $pO_2$  transition cultures ( $n = 11$ ). **(G)** CD138 expression within the CD27<sup>+</sup>CD38<sup>+</sup> ASC population ( $n = 5$ ). Bars represent means of biological replicates each composed of two technical replicates of **(C, F)** 3, **(E, G)** 2, or **(D)** 1 independent experiment. Statistical differences were determined using mixed-effects analysis using Tukey's test for multiple comparisons. \*  $p < 0.05$ , \*\*  $p < 0.01$ , \*\*\*  $p < 0.001$ , \*\*\*\*  $p < 0.0001$ .



# **CHAPTER 7**

Summarizing discussion

## SUMMARIZING DISCUSSION

B cell differentiation into memory B cells and antibody-secreting cells (ASCs) is key in generating an effective adaptive immune response. The exact cues that determine whether an activated B cell continues germinal center (GC) cycling or exits the GC to differentiate are unknown and a matter of intense investigation. In order to gain a more in-depth understanding of human B cell differentiation we rely on, and continuously improve, *in vitro* systems to stimulate B cells and analyze the subsequent induction of (phospho) signaling pathways, transcriptional regulation, B cell proliferation, differentiation and efficiency of (class-switched) antibody secretion. In this thesis we sought to further understanding of the regulation of human B cell differentiation into ASCs.

### **Mimicking human B cell responses to study regulation of ASC differentiation**

As dozens of research groups have investigated B cell stimulation and differentiation with their own specific questions in mind it is no surprise a range of different *in vitro* systems have been developed over the years. The heterogeneity of these systems unfortunately makes cross-system data interpretation difficult. This problem was addressed in **chapter 2** with the aim to generate a harmonized, simplistic one-step *in vitro* stimulation assay specifically designed for clinical research studies by optimizing ease of use and, as patient samples are scarce and valuable for multiple other immunological assays, by allowing use of as few cells as possible.

In this chapter we chose to apply the full peripheral blood CD19<sup>+</sup> population as, for a clinical point of view, it is interesting to look at recall responses of memory B cells in, amongst others, patient samples with auto-immunity. For other research purposes it may be more interesting to address the specific contribution of either naïve or memory B cells to the output of the culture but we did not investigate this. Sorting both populations could determine if a certain subpopulation is more or less responsive to a specific T cell dependent (TD) or T cell independent (TI) stimuli as this could differ per (auto-immune) disease setting. For example, it has previously been shown that human memory B cells with mutations in STAT1 or STAT3 alleles are still able to differentiate into ASCs upon IL-21 stimulation whereas naïve B cells with the same mutations are not, showing distinct requirements for ASC differentiation between both B cell subsets<sup>1</sup>. The same manuscript shows that pSTAT1, pSTAT3, pSTAT5 and pSTAT6 are more induced in human naïve B cells compared to memory B cells in healthy individuals, contradiction our data from **chapter 3** where we show that anti-B cell receptor (BCR) antibodies with CD40L (with or without IL-21) stimulation induced higher pSTAT1 and pSTAT3 in memory B cells<sup>2</sup>. These discrepancies could be explained by differences in the *in vitro* stimulation assays or differences in how naïve and memory B cell populations are selected or sorted for, based on the specific selection of membrane markers. This demonstrates both a need to confirm results between different culture systems, which can be expensive and time consuming, and a need to harmonize culture systems with clearly defined sorting or

isolation strategies for naïve, memory and Ig-isotype subsets. With **chapter 2** we hope to provide a base for (clinical) B cell studies and, through optimized assays, be able to better compare and interpret results from future B cell differentiation studies in both healthy and diseased conditions.

For specific studies, isolating either naïve or memory B cell populations is wanted. This still remains challenging on its own and requires proper definitions of B cell subsets and sorting strategies. Classically, memory B cells have been defined as CD27<sup>+</sup> whereas naïve B cells have been defined as CD27<sup>-</sup>IgD<sup>+</sup>. It was only recently shown how to specifically isolate B cells that have not been triggered by antigen and show no BCR mutations, also known as true naïve B cells, and how to isolate antigen-experienced or memory B cells by FACS based cell sorting<sup>3,4</sup>. Now that naïve and memory subsets are clearly defined, the next step would be to standardize isolation of B cell subsets for future B cell clinical studies. For this purpose, multiple options are available with each their own advantages and disadvantages. In **chapter 2** we used CD19<sup>+</sup>-positive selection beads to isolate pan-B cells from PBMC fractions, resulting in a highly purified isolate. Another option is to use negative-selection beads, resulting in a 'untouched' B cell isolate. Currently, naïve and memory B cell magnetic-bead isolation kits are available but they are not up to-do-date with regards to the specific glycosylated isoform of the lymphocyte marker CD45RB, specifically expressed on antigen-experienced B cells<sup>5,6</sup>. Lastly, FACS can be used to sort out specific B cell subsets. As mentioned, all three isolations strategies have their advantages and disadvantages. For example, the effects of positive-bead, negative-bead and FACS sort strategies were investigated with regards to stress induced genes in lymphocytes showing that FACS-based sorting had the lowest immediate effect on gene expression<sup>7</sup>. However, in this study long term effects of the different isolation strategies were not analysed with, for example, stimulation assays. A downside of positive bead-based selection or positive-FACS sorts is that this may trigger signaling cascades when the antibodies or beads crosslinks the targeted marker, possibly triggering signaling cascades and skewing B cell responses upon culturing of the positively selected B cells. In addition, positive-FACS sorts complicate downstream analysis as labeled antibodies can be highly stable and detectable for days after staining. For specific research questions where activation during positive selection may interfere with the subsequent assays, it is recommended to first validate if the positive-selection method in fact does activate the cells of interest. We have checked this for our CD19<sup>+</sup> Dynabead isolations and saw no activation through positive selection. A major advantage of magnetic bead-based isolation kits is that the protocols are easily transferrable to different research centers and there are even options to automate to isolation process<sup>8</sup>. Finally, an advantage of FACS-based sorting is that multiple subsets can be sorted simultaneously. All these pros and cons should be considered carefully when designing future, possibly multicenter, B cell differentiation studies.

For follow-up studies of the data in **chapter 2** is to combine TD and TI stimuli as *in vivo* this may occur and differentially regulate B cell responses. For example, in animal models of autoimmunity such as Systemic lupus erythematosus (SLE), TLR7 triggering by single-stranded RNA (or synthetic oligoribonucleotides in murine SLE models) has been shown to drive generation of spontaneous GCs, exacerbating the disease<sup>9</sup>. In addition, in healthy murine and nonhuman primate B cell responses, TLR7 triggering has been shown to promote somatic hypermutation (SHM), promote memory B cell responses and increase protection by antibodies<sup>10,11</sup>. Altogether this indicates that targeting TLR7, as an TI stimulus, is an interesting option to improve TD B cell responses and to possibly optimize adjuvant design. Interestingly, while we used TLR9 triggering with IL-2 (without CD40 stimulation) to induce ASC differentiation in **chapter 2**, in mice, TLR9 activation during TD B cell responses was shown to inhibit ASC differentiation<sup>12</sup>. Secondly, TLR9 activation during TD B cell responses increased c-MYC expression, promoting GC B cell expansion<sup>13</sup>. Taken together, one explanation may be that when both CD40 stimulation and TLR9 activation occurs, c-MYC and thus the proliferative B cell state is maintained to such an extent that, due to BLIMP1 inhibition by c-MYC<sup>14</sup>, differentiation into ASC is completely inhibited. In mice, a range of TLR triggers together with CD40 stimulation have been tested showing that TLR3, 4 and 9 promote B cell proliferation and activation while TLR1/2, 2/6, 4 and 7 promote differentiation into ASCs<sup>15,16</sup>. Specifically for human B cell responses much less is known about how TLR triggers, or other pathways such as cytosolic pattern recognition receptors, complement receptors and activating cell-surface receptors, can contribute to TD B cell responses<sup>17,18</sup>. More research is required on this and the TD *in vitro* system in **chapter 2** can provide a base for screening compounds that increase efficiency TD B cell responses, possibly allowing discovery or evaluation of new adjuvants.

In **chapter 4** we performed a secretome screen to discover how immune and non-immune related human proteins can modulate human B cell responses. In this chapter it is demonstrated that in a suboptimal TD setting, type I interferons promote differentiation of both naïve and IgG<sup>+</sup> memory B cells into ASCs while also discovering that sFASL is a novel regulator of memory B cell to ASC differentiation. This was relatively surprising as canonically, membrane-bound FASL (mFASL) stimulating the FAS receptor on the cell surface induces a signaling pathway leading to apoptosis<sup>19,20</sup>. Upon cleavage by metalloproteases mFASL turns soluble, losing its ability to induce cell death through classical FASL-FAS interaction. The soluble form of FASL has been proposed as a potential competitor for FASL-FAS interaction, blocking induction of mFASL-mediated apoptosis<sup>20</sup>. However, the function of sFASL has been shown to depend on both concentration and conformation as sFASL, like its membrane-bound form, can in fact induce apoptosis when concentration is optimal, when crosslinking is facilitated by antibodies or when sFASL is multimerized<sup>21,22</sup>. Over the last two decades the non-apoptotic signaling by FASL has been investigated and it is speculated that sFASL induced non-apoptotic signaling can modulate other signaling pathways within cells<sup>23,24</sup>. Even though the exact mechanism

remains elusive, the MAPK and NF- $\kappa$ B pathways have been shown to be involved<sup>25,26</sup>. With regards to B cells and GC responses, it has been shown that stimulation of CD40 on the B cell surface induces FAS expression and subsequent triggering of FAS will induce apoptosis<sup>27</sup>. However, even though apoptosis plays a major role in GC B cell selection, *in vivo* studies have shown that FAS does not contribute to the regulation of GC B cell selection<sup>28,29</sup>. Instead, one explanation is that in B cell responses, sFASL stimulation modulates the NF- $\kappa$ B pathways during CD40L and IL-21 stimulation, allowing for a more efficient induction of the ASC differentiation program while maintaining similar survival and proliferation, as shown in **chapter 4**. Interestingly, sFASL stimulation only increased differentiation of memory B cells and not naïve B cells, further solidifying that these subsets have distinct requirements for differentiation<sup>1</sup>. Additionally, systemic sFASL levels are increased in a number of immune-associated disorders, possibly promoting efficient memory B cell to ASC differentiation, supporting responses against infections or potentially exacerbating disease<sup>30</sup>. To further elucidate the mechanism of sFASL-induced ASC differentiation more in-depth research is required. As we show that sFASL inhibits PAX5 and promotes BLIMP1 other pathways upstream should be analysed. For example, if sFASL is able to modulate CD40L and IL-21 induced signaling the first targets to analyse, using methods described in **chapter 3**, are the NF- $\kappa$ B/C-MYC and pSTAT3/BLIMP1 pathways, as either one or both of these can be affected. Next, a combination of RNA sequencing and (phospho)proteomics can help in an unbiased manner to determine what other signaling pathways and transcription factors are regulated by sFASL stimulation. It would be very insightful to do these analyses on CD40L and IL-21, with or without sFASL, stimulated naïve, antigen-experienced and mature memory B cells<sup>4,31</sup> in order to determine how exactly sFASL can regulate ASC differentiation from CD27<sup>+</sup> memory but not in naïve B cells. Finally, the differences of signal induction by mFASL and sFASL can be determined by adding mFASL-expressing feeder cells to the culture setup used in **chapter 4**. For this to work however, cleavage of mFASL within culture should be blocked and mFASL effects on CD40L-expressing feeder cells should be monitored as this could affect CD40L expression by increasing the rate of irradiation-induced apoptosis.

In the future, when doing high-throughput screening of compounds for B cell differentiation, besides the concerns raised in **chapter 4**, it has to be taken into account and thoroughly determined if the compounds screened directly influence B cells or that they induce secretion of cytokines by the B cells themselves and that this, in an autocrine manner, influences B cell responses<sup>32</sup>. Finally, it should be considered in the screening study-design that some compounds require a pre-incubation before stimulation is applied in order to inhibit specific pathways<sup>33,34</sup>.

### **Spatiotemporal and oxygenic regulation of the germinal center response**

The migration of GC B cells between the light and dark zones of the GC is crucial in generation of effective immunity, as through this cycling SHM and affinity maturation can occur, resulting in high affinity, class-switched antibodies that provide protection

against invading pathogens. This cyclic migration of GC B cells has been described in depth<sup>35</sup>. However, the spatiotemporal regulation of T cell dependent B cell stimulation remains in part unknown, specifically the role of the dynamics of CD40 costimulation in human B cell research. In **chapter 5** we describe how termination of CD40L stimulation regulates B cell responses. In this chapter we investigated transient CD40 stimulation *in vitro*, to assess if B cell differentiation benefits from termination of CD40 stimulation as observed *in vivo* when B cells actively move into GC dark zones after acquiring antigenic and T<sub>FH</sub>-mediated stimulation in GC light zones. Termination of CD40L stimulation *in vitro* resulted in downregulation of NF-κB and pSTAT3/STAT3 signaling and concomitant downregulation of proliferation regulating transcription factor (TF) C-MYC. Subsequently, B cell identity TF PAX5 was downregulated, resulting in BLIMP1<sup>High</sup> cells to efficiently undergo ASC differentiation. Due to technical limitations in the current *in vitro* system, there are differences when comparing this stimulation setup to the *in vivo* situation, although the data corroborate *in vivo* findings. For one, in our system, B cells receive a relatively long stimulation time (48 hours) compared to the *in vivo* situation where multiple, minute-length T<sub>FH</sub>-cell contacts over the course of several hours occur<sup>36,37</sup>. Even though terminating CD40L stimulation earlier than the 48-hour timepoint also resulted in increased ASC differentiation, this timepoint was intentionally chosen to maintain sufficient numbers of CD19<sup>+</sup> cells for analysis. Secondly, we did not re-apply stimulation after termination of CD40L stimulation while *in vivo* this can occur multiple times during cycling between GC light and dark zones. We have shown in the past however, that re-stimulation of stimulated naïve B cells also supports ASC differentiation in a similar manner as shown in **chapter 5**, by inducing downregulation of PAX5 while BLIMP1 expression was already induced<sup>38</sup>. Continuing, by combining both CD40L termination and re-stimulation the significant proportion of non-differentiating cells seen in our cultures may eventually also differentiate into ASCs. It would be interesting to determine, from a naïve B cell, antigen-experienced and memory starting point, how many cycles of *in vitro* stimulation, termination thereof and re-stimulation are required to differentiate all cells into ASCs. In addition to this, different Ig subclasses should be compared in this situation as different B cell subsets and isotypes have been shown to have inherently distinct responses to stimulation<sup>31,39</sup>.

Another less studied layer of regulation in TD B cell responses is the effect of oxygen pressure. Even though the effect of atmospheric oxygen pressure on the adaptive immune system has already been clearly shown more than 15 years ago<sup>40</sup>, the effect of physiological oxygen pressures on B cell responses specifically has only generated some interest in the last few years<sup>41-44</sup>. In **chapter 6**, we addressed how physiologically relevant oxygen pressures regulate naïve B cell class-switch and differentiation by comparing normoxic (3% pO<sub>2</sub>) and hypoxic (1% pO<sub>2</sub>) conditions found in lymph nodes and GCs to atmospheric (21% pO<sub>2</sub>) oxygen pressure generally used in cell culture incubators. We demonstrate that GC dark zone-associated normoxia promotes naïve B cell differentiation into ASCs while GC light zone-associated hypoxic conditions generate a unique CD27<sup>++</sup>



expressing subset with an ASC transcriptional profile. Under hypoxia, both pSTAT3 and pSTAT6 signaling was significantly enhanced with a concomitant increased expression of BLIMP1 and XBP-1s. As GC B cells cycle between hypoxic GC light zones and normoxic GC dark zones, we applied time-dependent transitions between these oxygen pressures, showing that cycling between physiologically relevant oxygen pressures regulates human B cell differentiation trajectories towards CD27<sup>+</sup>CD38<sup>+</sup> ASCs, either directly from CD27<sup>+</sup> cells or through the CD27<sup>+</sup> compartment, and that this oxygenic cycling promotes class-switch to and secretion of IgG. It is clearly described that hypoxia induces Hypoxia-Inducible Factor 1-alpha (HIF1a) and that HIF1a is induced and regulated by NF- $\kappa$ B and pSTAT3 pathways<sup>45</sup>. We indeed see clear differences between 21, 3 and 1% oxygen pressures on these pathways with mainly increased pSTAT signaling when oxygen pressure is lower. However, a clear induction of HIF1a expression was found regardless of oxygen pressure. This indicates that HIF1a may not be the main driver of oxygenic regulation of B cell differentiation, supported by the fact that HIF1a responsive genes were also not found to be upregulated in GC B cells<sup>46</sup>. In our metabolic analysis of the different oxygen pressure cultures, we applied fluorescently labelled glucose and fatty acids to measure uptake of these. However, as our analysis relied on FACS analysis only, we did not study if the fluorescent probes indeed stained intracellularly but rather stuck to the cell surface. This was the case when fluorescently labeled glucose, but not labeled fatty acids, was applied in murine GC B cell metabolic analysis<sup>46</sup>. Sticking of compounds to the cell membrane, instead of uptake, has to be taken into account in future research and can be controlled for by taking microscopy images or doing image-stream FACS analysis. In our hypoxic cultures, mitochondrial mass, potential and reactive-oxygen species (ROS) are elevated while fatty acid uptake is down, indicating that, at least in our cultures, the B cells rely on oxidative phosphorylation (OXPHOS) for energy. Interestingly, it has been recently shown that affinity maturation within GCs relies on OXPHOS, promoting clonal expansion and positive selection of high affinity clones<sup>47</sup>. Hypoxia has been clearly described to inhibit high-fidelity DNA repair machinery in tumors<sup>48</sup> and inhibition of high-fidelity DNA repair leaves more opportunity for error-prone repair to contribute to SHM by leaving in mutations in genes encoding for the BCR<sup>49</sup>. As *in vitro* SHM in primary human B cell cultures has not been shown before, while literature and our data on hypoxic B cell cultures indicate that this might be occurring, BCR sequencing of the hypoxic cultures should be the next step to determine if possibly hypoxia is the missing link in *in vitro* induced SHM.

By combining the most recent literature and data presented in this thesis the following germinal center model is proposed (Figure 1). CD4 T-helper cells are activated after recognizing specific peptide-MHC by their TCRs on the surface of dendritic cells (DCs), subsequently differentiating into T<sub>FH</sub> cells and migrating towards and into the B cell follicle. Next, the amount of antigen acquired by the GC B cell is dependent on the amount of antigen present and the affinity of the BCR towards the antigen<sup>50</sup>. Subsequently, the amount of T<sub>FH</sub> cell help received is dependent on the amount of antigenic peptides

presented. Lower affinity GC B cells will receive less stimulation and have been shown to differentiate into multiple pathways dependent on their affinity, stimulation and the environmental cues they receive<sup>51-53</sup>. First, low affinity activated B cells can undergo differentiation into extrafollicular plasmablasts (EF PBs). These EF PBs arise between 4-6 days after immunization and provide the first layer of protection by secreting antibodies. Secondly, low affinity B cells can differentiate extrafollicularly into early memory B cells. The exact mechanism that determines which B cell goes into EF PB or early memory differentiation is unknown and a matter of intense investigation. B cells that participate in the GC reaction can no longer participate in the extrafollicular differentiation pathway. Thirdly, low affinity cells can acquire T cell help and also differentiate into (late) memory B cells. It has been shown for memory B cell differentiation that this relies on the height of mTORC1 activation, a failure to express MYC, the induction of TF BACH2 and the induction of either TFs BCL2 or Haematopoietically-Expressed Homeobox (HHEX)<sup>53</sup>. Low affinity cells that do upregulate MYC will undergo some divisions in the GC dark zone and may acquire BCR mutations. Some of the lower affinity GC B cells will re-cycle towards the GC light zone while others will also differentiate into (late) memory B cells<sup>53</sup>. High affinity GC B cells will receive more T<sub>FH</sub> cell help, which directly increases the amount of MYC and divisions the cells will undergo in the GC dark zone<sup>54</sup>. Furthermore, high affinity GC B cells will remain longer in the light zone compared to lower affinity siblings<sup>36,55</sup>, meaning they remain longer in the hypoxic area which, as shown in **chapter 6**, promotes pSTAT3 signaling and BLIMP1 expression while preventing actual differentiation into ASCs. Subsequently, as shown in **chapter 5**, release of CD40L stimulation will lower PAX5 expression. As GC B cells undergo divisions, MYC expression goes down. Notably, experimental and modeling data indicate that asymmetric division can contribute to the GC reaction and offers the possibility that mother cells asymmetrically divide the transcriptional profile over their daughter cells<sup>56,57</sup>. Asymmetric cell division is controversial phenomenon in GC B cells but has recently been shown to be important in CD8<sup>+</sup> T cell memory responses showing that, at the very least, asymmetric division can occur in the adaptive immune system<sup>58,59</sup>. The importance and relevance of asymmetric division in GC B cells requires more investigation however. Once the division stage of the dark zone reaction is over, GC B cells can either differentiate or re-cycle to the light zone depending on the transcription factor profile<sup>60</sup>. Both BLIMP1<sup>+</sup> cells and BLIMP1<sup>+</sup>PAX5<sup>+</sup> cells have been shown to be present in the GC dark zone<sup>61-63</sup> and is in accordance with our data in **chapter 5** showing that activated B cells can express both BLIMP1 and PAX5. Indeed, for ASC differentiation to occur, both PAX5 and C-MYC expression must be low while BLIMP1 is highly expressed, altogether indicating that GC B cells can express BLIMP1 without undergoing ASC differentiation and that passing the ASC differentiation threshold requires the concomitant downregulation of both PAX5 and C-MYC. In addition, the normoxic environment of the GC dark zone is most efficient in supporting differentiation into ASCs as shown in **chapter 6**. If the transcription factor profile of GC dark zone cells is not sufficient for ASC differentiation to occur, they will re-cycle back to the GC light zone. However, based on the relative expression of PAX5 and BLIMP1, lower PAX5-expressing cells are more likely to differentiate next cycle as

both re-stimulation<sup>38</sup> and subsequent release of CD40L stimulation will further lower PAX5 expression, eventually allowing BLIMP1 to take over the transcriptional profile. Over time, BCR affinity will increase due to the process of affinity maturation, slowly switching GC output from the low affinity pathways, that preferentially generates EF PBs, memory B cells and GC dark zone cells, to the high affinity pathway generating ASCs<sup>64,65</sup>. If SHM leads to an unfavorable mutation this specific cell will go into apoptosis or remain in the low affinity pathway until such mutations are acquired that the B cell is able to acquire more  $T_{FH}$  cell help, resulting in a longer stay BLIMP1-inducing hypoxic light zone, reducing PAX5 expression through re-stimulation and release from  $T_{FH}$  cells until the GC B cell has completed dividing, finally reaching the ASC differentiation-supporting normoxic area in the GC dark zone. It is important to note that, while it is shown that the GC light zone is hypoxic and the GC dark zone is normoxic, there is most likely one or several oxygen gradients between these zones, providing a layer of transcriptional regulation that remains relatively unexplored. Finally, the induction and phenotype of  $T_{FH}$  cells majorly control GC output through stimulation of B cells. It has been shown that  $T_{FH}$  cells progressively differentiate over the course of the GC response and that different  $T_{FH}$  cell subsets can be found in humans, possibly supporting autoimmune disease progression<sup>66-68</sup>. As  $T_{FH}$  cell differentiation relies on antigen presentation by and interaction with dendritic cells (DCs) it is not unlikely that the type of DC, T cell receptor affinity against the antigen and both cytokine and oxygen environments can affect  $T_{FH}$  cell differentiation and thus their control of GC B cell responses. Indeed, by applying our re-stimulation setup with specific CD40L expression levels and cytokine environments, single-cell RNA sequencing (scRNAseq) showed the generation of GC B, pre-memory B and ASCs from a naïve B cell starting point (Verstegen & Pollastro, *submitted*). This system, possibly combined with other ( $T_{FH}$ -derived) stimulations and spatiotemporal timing thereof, will allow for an in-depth investigation on transcriptional thresholds for differentiation into GC, memory and ASCs.

### Concluding remarks and future prospects

In this thesis we demonstrated that there are multiple ways of inducing ASC differentiation, both in a TD and TI manner (**Chapter 2**). For instance, naïve B cells required the termination of CD40L stimulation before ASC differentiation can occur (**Chapter 5**). In addition, we showed that physiologically relevant oxygen pressure plays a major role in both the regulation of ASC differentiation and in IgG class-switch (**Chapter 6**). In addition, we possibly observed the generation of memory B cells. For example in **chapter 5**, after CD40L is terminated we see an increase of CD27<sup>+</sup> cells that could quite possibly be early memory B cells but, in order to validate this, expression of memory B cell transcription factors should be measured such as BACH2, BCL2 and/or HHEX. Furthermore, in hypoxic cultures we generated CD27<sup>++</sup> cells, indicating at first that memory cells were generated preferentially over ASCs in hypoxic conditions. However, upon further transcriptional analysis we demonstrated that these CD27<sup>++</sup> cells in fact express an ASC phenotype, making them poised to differentiate into ASCs and secrete antibodies. Finally in all

chapters we see the generation of CD27<sup>+</sup>CD38<sup>+</sup> populations, these show a transcriptional heterogeneity (**Chapter 3**) warranting further investigation into these cells. When looking at CD27 and CD38 expression of stimulated B cells, specifically those switched from 1% pO<sub>2</sub> to 3% pO<sub>2</sub> in **chapter 6**, we see that ASCs seem to arise from both CD27<sup>+</sup> single positive cells and CD38<sup>+</sup> single positive cells. This, and the scRNAseq data mentioned above, indicate that ASCs can be generated through multiple different pre-ASC stages. In-depth investigation on these different subsets and the regulation of their differentiation into ASCs will provide much needed insight into the regulation of differentiation pathways. These insights will not only support future research to improve vaccination strategies but also to prevent and treat B cell mediated (auto-immune) diseases.

To continue research on B cell to ASC differentiation new techniques must be applied and innovated on. In this thesis we applied a minimalistic *in vitro* culture system, while proven to be solid in providing answers to how ASC differentiation is regulated it does also have its limitations. For one, as mentioned above, the control of CD40L stimulation is very rigid. We can apply CD40L stimulation, terminate it and possibly re-apply it, in a cytokine environment of choice, but all of this is relatively labor intensive. In the future, solutions for timed control of stimulations must be found. This could be through providing a more *in vivo* like environment with for example, organoid tonsil cultures which are shown to be valid platforms for vaccine testing<sup>69</sup>. Another option is to design 3D lymph node-like structures<sup>70</sup> through which chemokine gradients would allow natural cycling between mimicked light and dark zones. Finally, these 3D lymph node structures can be placed in flow chambers, allowing timed control of ‘cycling’ between stimulatory and non-stimulatory zones through use of physical force. Next to timed control of stimulation other environmental cues should be investigated. Indeed, we set the first steps in this by applying physiologically relevant oxygen pressure to our cultures but other environmental factors, such as cell-cell interactions and nutrient availability, are relevant when aiming to mimic the GC response as closely as possible.

Finally, in 2020 the Nobel prize was awarded to Jennifer Doudna and Emmanuelle Charpentier for their breakthrough research on CRISPR-Cas9 technology as a powerful gene-editing tool. This technology has already been applied to genetically engineer T cells to improve antitumor immunity<sup>71</sup> but has not been applied to the same extent in the study of human B cell responses. Indeed, some groups (including our own) have successfully applied CRISPR-Cas9 in primary human B cells to knockout B cell surface markers, intracellular signaling proteins and transcription factors<sup>72</sup> but major genetic knockout screens have not been done while these could potentially provide the most insight into how specific genes affect human B cell differentiation. Besides fundamental research, CRISPR-Cas9 technology has major therapeutic potential by allowing for the knock-in of gene templates. Indeed, one group has shown to be able to knock-in Factor IX and BAFF into ASCs to secrete these proteins instead of antibodies<sup>73</sup>. Altogether, CRISPR-Cas9 allows for the genetic manipulation of primary human B cells, essentially turning

them into protein factories that could provide life-long secretion of therapeutic proteins when these settle in bone-marrow survival niches, potentially curing protein-deficiency based diseases blood clotting and complement disorders.

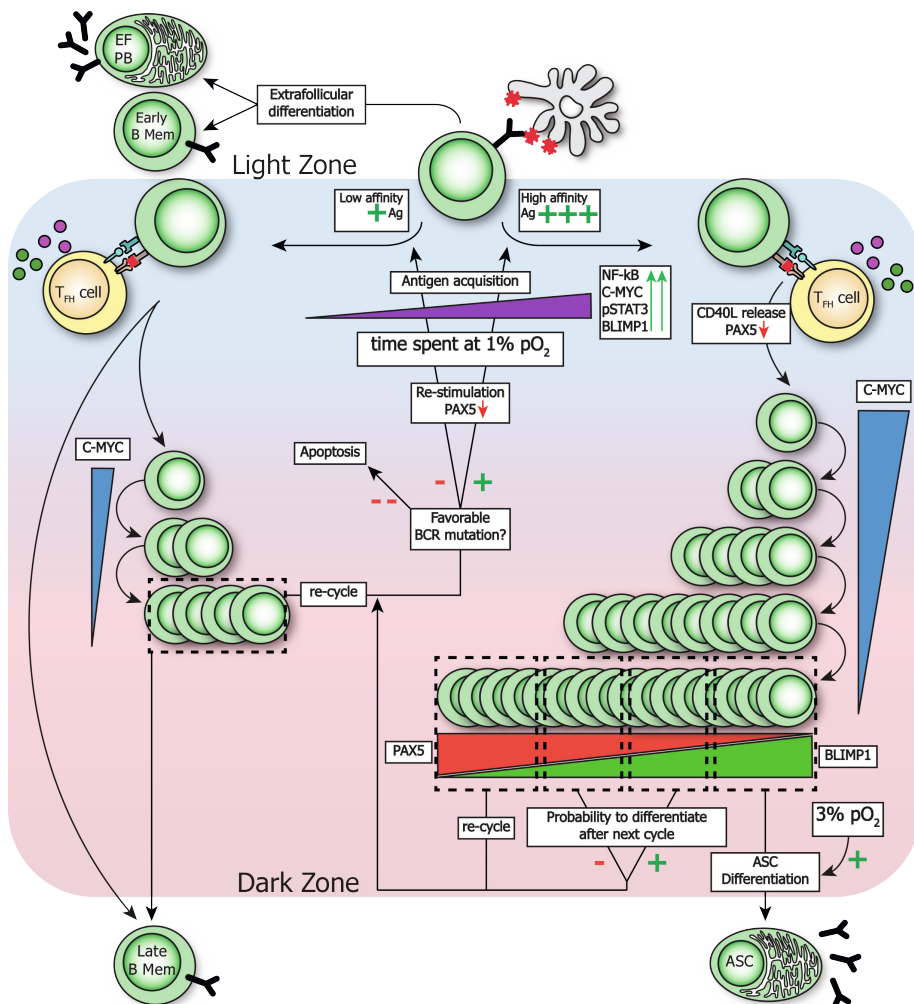


**Figure 1. Spatiotemporal and oxygenic regulation of germinal center output.** Multiple layers control germinal center output. First, BCR affinity towards antigen determines whether the B cell goes into the extrafollicular (EF) differentiation or low affinity or high affinity pathway. During EF differentiation, cells differentiate into EF PBs or early memory B cells but exact cues regulating this are unknown. Low affinity B cells can also acquire T cell help and differentiate into (late) memory B cells. If MYC is induced in low affinity GC B cells these will undergo some proliferation, possibly acquiring mutations in the BCR due to SHM. If mutations are not favorable, GC B cells can either undergo apoptosis or re-enter the low affinity pathway. If a GC B cell has a naturally high affinity or acquired this through SHM these will go into the high affinity pathway. High affinity GC B cells acquire more T cell help which promotes NF- $\kappa$ B and MYC expression while simultaneously prolonging the time spent in the hypoxic light zone, promoting pSTAT3 signaling and induction of BLIMP1. After multiple rounds of proliferation cells expressing low amounts of BLIMP1 will re-cycle. Upon re-entering the high affinity pathway, both T cell re-stimulation and release of CD40L stimulation reduce PAX5 expression and increases the probability of ASC differentiation to occur. The normoxic, 3% pO<sub>2</sub> environment promotes ASC differentiation to occur when BLIMP1 expression is high and both PAX5 and MYC expression is low.

## REFERENCES

1. Deenick EK, Avery DT, Chan A, et al. Naive and memory human B cells have distinct requirements for STAT3 activation to differentiate into antibody-secreting plasma cells. *J Exp Med*. 2013;210(12):2739-2753. doi:10.1084/jem.20130323
2. Marsman C, Jorritsma T, ten Brinke A, van Ham SM. Flow Cytometric Methods for the Detection of Intracellular Signaling Proteins and Transcription Factors Reveal Heterogeneity in Differentiating Human B Cell Subsets. *Cells* 2020, Vol 9, Page 2633. 2020;9(12):2633. doi:10.3390/CELLS9122633
3. Koers J, Pollastro S, Tol S, et al. CD45RB Glycosylation and Ig Isotype Define Maturation of Functionally Distinct B Cell Subsets in Human Peripheral Blood. *Frontiers in Immunology*. 2022;0:1936. doi:10.3389/FIMMU.2022.891316
4. Koers J, Pollastro S, Tol S, et al. Improving naive B cell isolation by absence of CD45RB glycosylation and CD27 expression in combination with BCR isotype. *European Journal of Immunology*. Published online July 21, 2022. doi:10.1002/eji.202250013
5. Naive B Cell Isolation Kit II, human | B cells | MicroBeads and Isolation Kits | Cell separation reagents | MACS Cell Separation | Products | Miltenyi Biotec | Nederland. Accessed August 1, 2022. <https://www.miltenyibiotec.com/NL-en/products/naive-b-cell-isolation-kit-ii-human.html#130-091-150>
6. Memory B Cell Isolation Kit, human | B cells | MicroBeads and Isolation Kits | Cell separation reagents | MACS Cell Separation | Products | Miltenyi Biotec | Nederland. Accessed August 1, 2022. <https://www.miltenyibiotec.com/NL-en/products/memory-b-cell-isolation-kit-human.html#130-093-546>
7. Beliakova-Bethell N, Massanella M, White C, et al. The effect of cell subset isolation method on gene expression in leukocytes. *Cytometry A*. 2014;85(1):94. doi:10.1002/CYTO.A.22352
8. Automated cell isolation | autoMACS® Pro Separator | Miltenyi Biotec | Nederland. Accessed August 1, 2022. <https://www.miltenyibiotec.com/NL-en/products/automacs-pro-separator-starter-kit.html>
9. Fan H, Ren D, Hou Y. TLR7, a third signal for the robust generation of spontaneous germinal center B cells in systemic lupus erythematosus. *Cellular & Molecular Immunology* 2018 15:3. 2017;15(3):286-288. doi:10.1038/cmi.2017.123
10. Castiblanco DP, Maul RW, Knode LMR, Gearhart PJ. Co-stimulation of BCR and toll-like receptor 7 increases somatic hypermutation, Memory B cell formation, and secondary antibody response to protein antigen. *Frontiers in Immunology*. 2017;8(DEC):1833. doi:10.3389/FIMMU.2017.01833/BIBTEX
11. Holbrook BC, D'Agostino RB, Tyler Aycock S, et al. Adjuvanting an inactivated influenza vaccine with conjugated R848 improves the level of antibody present at 6months in a nonhuman primate neonate model. *Vaccine*. 2017;35(45):6137-6142. doi:10.1016/J.VACCINE.2017.09.054
12. Baptista BJA, Granato A, Canto FB, et al. TLR9 Signaling Suppresses the Canonical Plasma Cell Differentiation Program in Follicular B Cells. *Front Immunol*. 2018;9(NOV). doi:10.3389/FIMMU.2018.02281
13. Wigton EJ, DeFranco AL, Ansel KM. Antigen Complexed with a TLR9 Agonist Bolsters c-Myc and mTORC1 Activity in Germinal Center B Lymphocytes. *Immunohorizons*. 2019;3(8):389-401. doi:10.4049/IMMUNOHORIZONS.1900030/-/DCSUPPLEMENTAL

14. Lin KI, Lin Y, Calame K. Repression of c- myc Is Necessary but Not Sufficient for Terminal Differentiation of B Lymphocytes In Vitro . *Molecular and Cellular Biology*. 2000;20(23):8684-8695. doi:10.1128/MCB.20.23.8684-8695.2000/ASSET/827CA3E4-92E2-43A7-8182-6EF72FFD5350/ASSETS/GRAPHIC/MB2300887008.JPEG
15. Boeglin E, Smulski CR, Brun S, Milosevic S, Schneider P, Fournel S. Toll-Like Receptor Agonists Synergize with CD40L to Induce Either Proliferation or Plasma Cell Differentiation of Mouse B Cells. Published online 2011. doi:10.1371/journal.pone.0025542
16. Browne EP. Regulation of B-cell responses by Toll-like receptors. *Immunology*. 2012;136(4):370. doi:10.1111/J.1365-2567.2012.03587.X
17. Pulendran B, S. Arunachalam P, O'Hagan DT. Emerging concepts in the science of vaccine adjuvants. *Nature Reviews Drug Discovery* 2021 20:6. 2021;20(6):454-475. doi:10.1038/s41573-021-00163-y
18. Sicard T, Kassardjian A, Julien JP. B cell targeting by molecular adjuvants for enhanced immunogenicity. <https://doi.org/10.1080/1476058420201857736>. 2020;19(11):1023-1039. doi: 10.1080/14760584.2020.1857736
19. Nagata S. Fas Ligand-Induced Apoptosis. <http://dx.doi.org/101146/annurev.genet33129>. 2003;33:29-55. doi:10.1146/ANNUREV.GENET.33.1.29
20. Brunner T, Wasem C, Torgler R, Cima I, Jakob S, Corazza N. *Fas (CD95/Apo-1) Ligand Regulation in T Cell Homeostasis, Cell-Mediated Cytotoxicity and Immune Pathology*. <http://nbn-resolving.de/urn:nbn:de:bsz:352-143543>
21. Holler N, Tardivel A, Kovacsovics-Bankowski M, et al. Two Adjacent Trimeric Fas Ligands Are Required for Fas Signaling and Formation of a Death-Inducing Signaling Complex. *Molecular and Cellular Biology*. 2003;23(4):1428-1440. doi:10.1128/MCB.23.4.1428-1440.2003/ASSET/414A256F-2F25-4688-9D34-EF0F91C03B79/ASSETS/GRAPHIC/MB0431288007.JPEG
22. Chodorge M, Züger S, Stirnimann C, et al. A series of Fas receptor agonist antibodies that demonstrate an inverse correlation between affinity and potency. *Cell Death & Differentiation* 2012 19:7. 2012;19(7):1187-1195. doi:10.1038/cdd.2011.208
23. Peter ME, Budd RC, Desbarats J, et al. The CD95 Receptor: Apoptosis Revisited. *Cell*. 2007;129(3):447-450. doi:10.1016/J.CELL.2007.04.031
24. Strasser A, Jost PJ, Nagata S. The many roles of FAS receptor signaling in the immune system. *Immunity*. 2009;30(2):180. doi:10.1016/J.IMMUNI.2009.01.001
25. Barnhart BC, Legembre P, Pietras E, Bubici C, Franzoso G, Peter ME. CD95 ligand induces motility and invasiveness of apoptosis-resistant tumor cells. *EMBO J*. 2004;23(15):3175-3185. doi:10.1038/SJ.EMBOJ.7600325
26. Matsumoto N, Imamura R, Suda T. Caspase-8- and JNK-dependent AP-1 activation is required for Fas ligand-induced IL-8 production. *FEBS J*. 2007;274(9):2376-2384. doi:10.1111/J.1742-4658.2007.05772.X
27. Nakanishi K, Matsui K, Kashiwamura SI, et al. IL-4 and anti-CD40 protect against Fasmediated B cell apoptosis and induce B cell growth and differentiation. *International Immunology*. 1996;8(5):791-798. doi:10.1093/INTIMM/8.5.791
28. Smith KGC, Nossal GJV, Tarlinton DM. FAS is highly expressed in the germinal center but is not required for regulation of the B-cell response to antigen. *Proc Natl Acad Sci U S A*. 1995;92(25):11628. doi:10.1073/PNAS.92.25.11628
29. Butt D, Chan TD, Bourne K, et al. FAS Inactivation Releases Unconventional Germinal Center B Cells that Escape Antigen Control and Drive IgE and Autoantibody Production. *Immunity*. 2015;42(5):890-902. doi:10.1016/j.immuni.2015.04.010

30. Wallach-Dayana SB, Petukhov D, Ahdut-Hacohen R, Richter-Dayana M, Breuer R. Sfasl—the key to a riddle: Immune responses in aging lung and disease. *International Journal of Molecular Sciences*. 2021;22(4):1-12. doi:10.3390/ijms22042177
31. Koers J, Pollastro S, Tol S, et al. CD45RB Glycosylation and Ig Isotype Define Maturation of Functionally Distinct B Cell Subsets in Human Peripheral Blood. *Frontiers in Immunology*. 2022;13. doi:10.3389/fimmu.2022.891316
32. Agrawal S, Gupta S. TLR1/2, TLR7, and TLR9 signals directly activate human peripheral blood naive and memory B cell subsets to produce cytokines, chemokines, and hematopoietic growth factors. *J Clin Immunol*. 2011;31(1):89-98. doi:10.1007/S10875-010-9456-8
33. van Asten SD, Raaben M, Nota B, Spaapen RM. Secretome Screening Reveals Fibroblast Growth Factors as Novel Inhibitors of Viral Replication. *Journal of Virology*. 2018;92(16). doi:10.1128/JVI.00260-18/SUPPL\_FILE/ZJV016183782S2.PDF
34. Rip J, de Bruijn MJW, Neys SFH, et al. Bruton's tyrosine kinase inhibition induces rewiring of proximal and distal B-cell receptor signaling in mice. *European Journal of Immunology*. 2021;51(9):2251. doi:10.1002/EJI.202048968
35. Mesin L, Ersching J, Victora GD. Germinal Center B Cell Dynamics. *Immunity*. 2016;45(3):471-482. doi:10.1016/j.immuni.2016.09.001
36. Shulman Z, Gitlin AD, Weinstein JS, et al. Dynamic signaling by T follicular helper cells during germinal center B cell selection. *Science (1979)*. 2014;345(6200):1058-1062. doi:10.1126/science.1257861
37. Victora GD, Schwickert TA, Fooksman DR, et al. Germinal center dynamics revealed by multiphoton microscopy with a photoactivatable fluorescent reporter. *Cell*. 2010;143(4):592-605. doi:10.1016/j.cell.2010.10.032
38. Unger PPA, Verstegen NJM, Marsman C, et al. Minimalistic In Vitro Culture to Drive Human Naive B Cell Differentiation into Antibody-Secreting Cells. *Cells*. 2021;10(5). doi:10.3390/cells10051183
39. Sundling C, Lau AWY, Bourne K, et al. Positive selection of IgG+ over IgM+ B cells in the germinal center reaction. *Immunity*. 2021;54(5):988-1001.e5. doi:10.1016/j.immuni.2021.03.013
40. Atkuri KR, Herzenberg LA, Herzenberg LA. *Culturing at Atmospheric Oxygen Levels Impacts Lymphocyte Function.*; 2005. www.pnas.org/cgi/doi/10.1073/pnas.0409910102
41. Cho SH, Raybuck AL, Blagih J, et al. Hypoxia-inducible factors in CD4+ T cells promote metabolism, switch cytokine secretion, and T cell help in humoral immunity. *Proc Natl Acad Sci U S A*. 2019;116(18):8975-8984. doi:10.1073/PNAS.1811702116/SUPPL\_FILE/PNAS.1811702116.SAPP.PDF
42. Abbott RK, Thayer M, Labuda J, et al. Germinal Center Hypoxia Potentiates Immunoglobulin Class Switch Recombination. *The Journal of Immunology*. 2016;197(10):4014-4020. doi:10.4049/JIMMUNOL.1601401/-/DCSUPPLEMENTAL
43. Cho SH, Raybuck AL, Stengel K, et al. Germinal centre hypoxia and regulation of antibody qualities by a hypoxia response system. *Nature 2016 537:7619*. 2016;537(7619):234-238. doi:10.1038/nature19334
44. Burrows N, Maxwell PH. Hypoxia and B cells. *Experimental Cell Research*. 2017;356(2):197-203. doi:10.1016/J.YEXCR.2017.03.019
45. Castillo-Rodríguez RA, Trejo-Solís C, Cabrera-Cano A, Gómez-Manzo S, Dávila-Borja VM. Hypoxia as a Modulator of Inflammation and Immune Response in Cancer. *Cancers 2022, Vol 14, Page 2291*. 2022;14(9):2291. doi:10.3390/CANCERS14092291



46. Weisel FJ, Mullett SJ, Elsner RA, et al. Germinal center B cells selectively oxidize fatty acids for energy while conducting minimal glycolysis. *Nature Immunology* 2020 21:3. 2020;21(3):331-342. doi:10.1038/s41590-020-0598-4
47. Chen D, Wang Y, Manakkat Vijay GK, et al. Coupled analysis of transcriptome and BCR mutations reveals role of OXPHOS in affinity maturation. *Nat Immunol.* 2021;22(7):904-913. doi:10.1038/S41590-021-00936-Y
48. Kaplan AR, Glazer PM. Impact of hypoxia on DNA repair and genome integrity. *Mutagenesis.* 2020;35(1):61-67. doi:10.1093/MUTAGE/GEZ019
49. Neuberger MS, Rada C. Somatic hypermutation: activation-induced deaminase for C/G followed by polymerase eta for A/T. *J Exp Med.* 2007;204(1):7-10. doi:10.1084/JEM.20062409
50. Gitlin AD, Shulman Z, Nussenzweig MC. Clonal selection in the germinal centre by regulated proliferation and hypermutation. *Nature.* 2014;509(7502):637-640. doi:10.1038/nature13300
51. Victora GD, Nussenzweig MC. Annual Review of Immunology Germinal Centers. Published online 2022. doi:10.1146/annurev-immunol-120419
52. Elsner RA, Shlomchik MJ. Germinal Center and Extrafollicular B Cell Responses in Vaccination, Immunity, and Autoimmunity. *Immunity.* 2020;53(6):1136-1150. doi:10.1016/j.immuni.2020.11.006
53. Laidlaw BJ, Cyster JG. Transcriptional regulation of memory B cell differentiation. doi:10.1038/s41577-020-00446-2
54. Finkin S, Hartweger H, Oliveira TY, Kara EE, Nussenzweig MC. Protein Amounts of the MYC Transcription Factor Determine Germinal Center B Cell Division Capacity. *Immunity.* 2019;51(2):324-336.e5. doi:10.1016/j.immuni.2019.06.013
55. Shulman Z, Gitlin AD, Targ S, et al. T follicular helper cell dynamics in germinal centers. *Science (1979).* 2013;341(6146):673-677. doi:10.1126/science.1241680
56. Barnett BE, Ciocca ML, Goenka R, et al. Asymmetric B cell division in the germinal center reaction. *Science (1979).* 2012;335(6066):342-344. doi:10.1126/SCIENCE.1213495/SUPPL\_FILE/1213495.BARNETT.SOM.PDF
57. Merino Tejero E, Lashgari D, García-Valiente R, et al. Coupled Antigen and BLIMP1 Asymmetric Division With a Large Segregation Between Daughter Cells Recapitulates the Temporal Transition From Memory B Cells to Plasma Cells and a DZ-to-LZ Ratio in the Germinal Center. *Frontiers in Immunology.* 2021;12:3185. doi:10.3389/FIMMU.2021.716240/BIBTEX
58. Borsa M, Barnstorf I, Baumann NS, et al. Modulation of asymmetric cell division as a mechanism to boost CD8+ T cell memory. *Science Immunology.* 2019;4(34). doi:10.1126/SCIIMMUNOL.AAV1730/SUPPL\_FILE/AAV1730\_TABLE\_S1.XLSX
59. Borsa M, Barandun N, Gräbnitz F, et al. Asymmetric cell division shapes naive and virtual memory T-cell immunity during ageing. *Nature Communications* 2021 12:1. 2021;12(1):1-12. doi:10.1038/s41467-021-22954-y
60. Kennedy DE, Okoreeh MK, Maienschein-Cline M, et al. Novel specialized cell state and spatial compartments within the germinal center. *Nature Immunology.* 2020;21(6):660-670. doi:10.1038/s41590-020-0660-2
61. Kräutler NJ, Suan D, Butt D, et al. Differentiation of germinal center B cells into plasma cells is initiated by high-affinity antigen and completed by Tfh cells. *The Journal of Experimental Medicine.* 2017;214(5):1259. doi:10.1084/JEM.20161533
62. Cattoretti G, Shaknovich R, Smith PM, Jäck HM, Murty Vv., Alobeid B. Stages of Germinal Center Transit Are Defined by B Cell Transcription Factor Coexpression and Relative Abundance. *The Journal of Immunology.* 2006;177(10):6930-6939. doi:10.4049/JIMMUNOL.177.10.6930

63. Radtke D, Bannard O. Expression of the plasma cell transcriptional regulator Blimp-1 by dark zone germinal center B cells during periods of proliferation. *Frontiers in Immunology*. 2019;10(JAN). doi:10.3389/fimmu.2018.03106
64. Weisel FJ, Zuccarino-Catania G v., Chikina M, Shlomchik MJ. A Temporal Switch in the Germinal Center Determines Differential Output of Memory B and Plasma Cells. *Immunity*. 2016;44(1):116-130. doi:10.1016/j.immuni.2015.12.004
65. Merino Tejero E, Lashgari D, García-Valiente R, et al. Multiscale Modeling of Germinal Center Recapitulates the Temporal Transition From Memory B Cells to Plasma Cells Differentiation as Regulated by Antigen Affinity-Based Tfh Cell Help. *Frontiers in Immunology*. 2021;11. doi:10.3389/FIMMU.2020.620716/FULL
66. Herman E, Weinstein J, Lainez B, et al. Progressive differentiation of follicular B helper T cells regulates the germinal center response (IRC11P.430). *The Journal of Immunology*. 2015;194(1 Supplement):197.12 LP-197.12. [http://www.jimmunol.org/content/194/1\\_Supplement/197.12.abstract](http://www.jimmunol.org/content/194/1_Supplement/197.12.abstract)
67. Krishnaswamy JK, Alsén S, Yrlid U, Eisenbarth SC, Williams A. Determination of T Follicular Helper Cell Fate by Dendritic Cells. *Frontiers in Immunology*. 2018;9:2169. doi:10.3389/FIMMU.2018.02169/BIBTEX
68. Morita R, Schmitt N, Bentebibel SE, et al. Human Blood CXCR5+CD4+ T Cells Are Counterparts of T Follicular Cells and Contain Specific Subsets that Differentially Support Antibody Secretion. *Immunity*. 2011;34(1):108-121. doi:10.1016/j.immuni.2010.12.012
69. Wagar LE, Salahudeen A, Constantz CM, et al. Modeling human adaptive immune responses with tonsil organoids. doi:10.1038/s41591-020-01145-0
70. Roh KH, Song HW, Pradhan P, et al. A synthetic stroma-free germinal center niche for efficient generation of humoral immunity ex vivo. *Biomaterials*. 2018;164:106-120. doi:10.1016/J.BIOMATERIALS.2018.02.039
71. Stadtmauer EA, Fraietta JA, Davis MM, et al. CRISPR-engineered T cells in patients with refractory cancer. *Science (1979)*. 2020;367(6481). doi:10.1126/SCIENCE.ABA7365/SUPPL\_FILE/ABA7365\_TABLE\_S4.XLSX
72. Wu CAM, Roth TL, Baglaenko Y, et al. Genetic engineering in primary human B cells with CRISPR-Cas9 ribonucleoproteins. *Journal of Immunological Methods*. 2018;457:33-40. doi:10.1016/J.JIM.2018.03.009
73. Hung KL, Meitlis I, Hale M, et al. Engineering Protein-Secreting Plasma Cells by Homology-Directed Repair in Primary Human B Cells. *Molecular Therapy*. 2018;26(2):456-467. doi:10.1016/j.yimthe.2017.11.012





# **APPENDIX**

English Summary  
Nederlandse Samenvatting  
List of publications  
Contributing authors  
PhD portfolio  
Curriculum Vitae  
Acknowledgements

## ENGLISH SUMMARY

As introduced in **Chapter 1** of this thesis, the human immune system consists of two tightly interwoven compartments; the innate and adaptive immune systems. Both layers provide protection against invading pathogens. The innate compartment provides the first, fast-acting layer of defense through the complement protein system and the innate immune cells that recognize pathogen-associated molecular patterns to exert their protective function. Adaptive immunity is provided by B and T cells that recognize antigen through specific B cell and T cell receptors (BCR and TCR respectively). Upon activation of the adaptive immune system both T and B cells can generate immune memory, allowing a faster clearance of pathogens upon reinfection. During the B cell response, the cells can differentiate into either memory B cells, which recognize and quickly react to antigens upon reinfection, and antibody-secreting cells (ASCs), that secrete large quantities of antibodies that specifically bind and neutralize pathogens through cooperation with the innate immune system. During an immune response, B cells can acquire help and stimulation from CD4 T helper ( $T_H$ ) cells, this B cell response is also known as the T cell dependent (TD) response. In order to recruit  $T_H$  cell help, naïve B cells are required to first recognize and internalize antigen and subsequently present antigenic peptides on Major Histocompatibility Complex class II (MHCII). Dendritic Cell-activated  $T_H$  cells that migrate towards activated B cells can specifically recognize the presented antigenic peptides and provide co-stimulation (such as CD40L) and cytokines (such as IL-21 and IL-4) to the B cells. Upon receiving T cell help, activated IgM-expressing B cells can undergo class-switch recombination (CSR), to generate other antibody isotypes such as IgG or IgA, and subsequently form germinal centers (GCs). In these GCs, B cells cycle between GC dark zones, sites of hyperproliferation and somatic hyper mutation (SHM), and GC light zones where GC B cells re-acquire antigen and are selected for and restimulated by T follicular helper ( $T_{FH}$ ) cells based on the BCR affinity against antigen. GC B cells recurrently cycle between GC dark and light zones until eventually they exit and differentiate into memory B cells or ASCs. The exact cues that determine GC exit and induction of differentiation are currently unknown.

B cells can also participate in T cell independent (TI) responses. During these responses, B cells are stimulated by TI antigens through binding and cross-linking of the BCR and by triggering specific Toll-like receptors (TLRs) such as TLR4, TLR7 and TLR9. TI B cell responses are usually marked by short-lived, rapid production of low affinity IgM antibodies. As there is no formation of GCs during TI responses, there is no selection for higher affinity B cells and most TI responses do not result in the formation of long-lived immunological memory.

To study human B cell differentiation, we and others utilize *in vitro* cultures. However, over the years a range of different TD and TI *in vitro* systems have been developed and the heterogeneity of these different systems make the interpretation of results challenging.

In **Chapter 2** we sought to generate minimalistic, one-step B cell differentiation assays requiring low amounts of isolated B cells or PBMCs, making the assays ideally suited for clinical B cell differentiation studies. To mimic TD stimulation of B cells, we started with CD40L-expressing fibroblasts and IL-21 as baseline cultures. By titrating down the amount of starting B cells from 25.000 to 250 cells per well we saw the ratio of secreted IgM antibodies went up at the cost of IgG and IgA. To prevent preferential outgrowth of specific Ig isotypes we opted for 2500 starting B cells as the optimal starting number. To mimic *in vivo* responses more closely, we compared the baseline CD40L/IL-21 cultures to those with added anti-BCR trigger or IL-4. We observed that including anti-BCR triggering slightly increased B cell differentiation into ASCs, but at the same time hampered detection of secreted antibodies. In addition, and in agreement with other B cell differentiation studies, we showed that addition of IL-4 to B cell cultures inhibits secretion of antibodies. To mimic *in vivo* TI B cell stimulation, we started with TLR9-activating CpG and supplemented this with IL-2 as baseline cultures. Within these TI B cell cultures survival was limited and as such, 25.000 starting B cells was chosen as a minimum amount when starting with isolated B cells. Addition of anti-BCR triggering or B cell survival factor BAFF did slightly increase differentiation into ASCs in isolated B cell cultures. In this study we also demonstrate that PBMCs can be used instead of isolated B cells in both TD or TI cultures, omitting the need for B cell isolation. Finally, by comparing fresh and cryopreserved samples we showed that ASC differentiation potential is only slightly decreased in cryopreserved samples, demonstrating that the TD and TI assays are also suitable for longitudinal B cell cohort studies where patient samples are frozen and stored for prolonged periods of time. This study resulted in optimized TD and TI stimulation protocols for analysis of B cell differentiation in isolated B cell and PBMC cultures while requiring low amounts of cells, making these protocols ideally suited for future clinical studies on scarce patient samples.

The regulation of TD human B cell differentiation is a complex and dynamic process involving the induction of multiple (phospho)-signaling pathways and an intricate network of transcription factors (TFs). In **Chapter 3**, we describe a flow cytometric assay allowing detection of B cell differentiation membrane markers CD27 and CD38 together with simultaneous intracellular detection of active NF- $\kappa$ B p65 and phosphorylated STAT1, STAT3, STAT5 and STAT6. These signaling proteins were specifically investigated as they are known regulators of B cell responses and induced by BCR stimulation, CD40L ligation and IL-21 and IL-4 stimulation. In addition, a second flow cytometric assay was designed to allow analysis of the same differentiation membrane markers together with TFs PAX5, BCL6, C-MYC, BLIMP1, XBP-1s and AID. These transcription factors were specifically chosen as they control B cell differentiation into ASCs. By analyzing these transcription factors in combination with CD27 and CD38 we can better discriminate between B cells, B cells undergoing ASC differentiation and fully differentiated ASCs. Both these assays allowed the multiparameter analysis of (phospho)signaling or TFs over time, during

induction of ASC differentiation. In the following chapters these assays were utilized to study regulation of human B cell differentiation in depth.

In **Chapter 4** we utilized a secreted protein library, in combination with a suboptimal CD40L and IL-21 culture, to find unidentified modulators that may aid B cell to ASC differentiation. We found type I interferons, Map19 and soluble FASL (sFASL) conditioned media to promote differentiation of CD27<sup>+</sup>IgG<sup>+</sup> memory B cells into ASCs. As type I interferons were previously described to promote ASC differentiation, we focused on the novel factors Map19 and sFASL. While purified recombinant Map19 did not replicate this effect, purified recombinant sFASL did induce significantly more differentiation into ASCs and concomitant secretion of IgG1 and IgG4 antibodies. While FASL is a known inducer of apoptosis, sFASL did not induce apoptosis in our B cell cultures. Indeed, by adding sFASL to the memory B cell cultures we saw an increased expression of ASC TF BLIMP1, showing that sFASL is a regulator of ASC differentiation. The signaling pathways conveying this regulation remain to be investigated.

It is clear that B cells require CD40L and IL-21 in order to undergo ASC differentiation but this stimulation *in vivo* is highly dynamic; after acquiring stimulation from T<sub>FH</sub> cells B cells actively move away from the site of stimulation and specifically this release of stimulation may contribute to B cell responses. To this end, we investigate in **Chapter 5** that CD40L signaling has to be terminated for efficient ASC differentiation. Termination of CD40L signaling resulted in both a downregulation of the active NF- $\kappa$ B p65 and pSTAT/STAT3 pathways. Downregulation of signaling by termination of CD40L was accompanied by a reduction in both proliferation and C-MYC, the TF that regulates proliferation. Subsequently, the B cell identity TF PAX5 was also downregulated. While BLIMP1<sup>High</sup> expressing cells were generated in both continuous and terminated CD40L cultures, we show that termination of CD40L, with the accompanying downregulation of C-MYC and PAX5 allows the BLIMP1<sup>High</sup> cells to efficiently differentiate into ASCs with high expression of IRF4 and XBP-1s.

An overlooked regulatory layer in B cell differentiation is the effect of oxygen pressure. In **Chapter 6** we addressed how physiological oxygen pressure found in lymphoid organs, 1 – 3% pO<sub>2</sub>, regulate naive B cell class-switch and differentiation compared to atmospheric (21% pO<sub>2</sub>) oxygen pressure generally applied in cell culture incubators. We demonstrated that GC dark zone associated normoxia, 3% pO<sub>2</sub>, promotes differentiation in ASCs while GC light zone associated hypoxia, 1% pO<sub>2</sub>, generated a unique CD27<sup>++</sup> expressing B cell subset with an ASC transcription factor profile. We also showed that normoxic and hypoxic oxygen levels regulate both (phospho)signaling pathways pSTAT3 and pSTAT6, and ASC related transcription factors BLIMP1 and XBP-1s. As GC B cells migrate between hypoxic light and normoxic dark zones during B cell responses we *mimicked* this by applying time-dependent transitions between 1% and 3% pO<sub>2</sub> cultures. This showed



that cycling between physiologically relevant oxygen pressures indeed regulates human B cell differentiation and promotes class switch to and secretion of IgG.

Altogether and as discussed in the **Summarizing discussion**, the results presented in this thesis contribute to the field of human B cell differentiation research by providing optimized TD and TI *in vitro* stimulation protocols that allow in depth analysis of ASC differentiation, specifically for when patient material is limited. Furthermore, this thesis provides multiparameter flow cytometry protocols to analyze B cell differentiation membrane markers over time, together with intracellular (phospho)signaling proteins or transcription factors, allowing in depth investigation into activation and differentiation of B cells. Both the culturing and flow cytometric protocols will support further research into human B cell to ASC differentiation. Indeed, we utilize these techniques to show that naïve B cells efficiently differentiate into ASCs upon termination of CD40L stimulation, by promoting BLIMP1 expression and inhibition of PAX5. Furthermore, this thesis demonstrates how physiologically relevant oxygen pressures found in lymph nodes, 3% and 1% pO<sub>2</sub> compared to 21% pO<sub>2</sub> generally used in cell culture incubators, majorly contribute to ASC differentiation and IgG class-switch recombination. The data in this thesis show that spatiotemporal, environmental and metabolic factors are crucial regulator of human B cell and these should all be considered during *in vitro* and *in vivo* B cell differentiation studies. These insights and techniques will support future B cell related research, both on a fundamental and a clinical level.

## NEDERLANDSE SAMENVATTING

Zoals geïntroduceerd in **Hoofdstuk 1** van dit proefschrift, bestaat het menselijke immuunsysteem uit twee nauw met elkaar verwoven compartimenten; het aangeboren en adaptieve immuunsysteem. Beide lagen bieden bescherming tegen binnendringende ziekteverwekkers zoals bacteriën, virussen en parasieten. Het aangeboren compartiment vormt de eerste, snelwerkende verdedigingslaag via het complement-eiwitsysteem en aangeboren immuun cellen die pathogeen-geassocieerde moleculaire patronen herkennen om hun beschermende functie uit te voeren. Adaptieve immuniteit wordt geleverd door B en T cellen die antigeen herkennen via specifieke B cel en T cel receptoren (respectievelijk BCR en TCR). Na activering van het adaptieve immuunsysteem kunnen zowel T als B cellen immunologische geheugencellen genereren die bij her infectie sneller reageren, zodat pathogenen sneller worden geklaard bij her infectie. Tijdens de B cel respons kunnen de cellen differentiëren in geheugen B cellen, die bij her infectie antigenen herkennen en er snel op reageren door antilichaam-secreterende cellen (ASC) aan te maken. Deze ASC produceren grote hoeveelheden antilichamen die specifiek pathogenen binden en neutraliseren door samenwerking met het aangeboren immuunsysteem. Tijdens een immuunrespons kunnen B cellen hulp en stimulatie krijgen van CD4 T helper ( $T_H$ ) cellen, deze soort B cel respons staat ook bekend als de T cel afhankelijke (TA) respons. Om  $T_H$  cel hulp te werven, moeten naïeve B cellen eerst antigeen herkennen, internaliseren en het antigeen afbreken, om vervolgens antigeen-peptiden te presenteren op het Major Histocompatibility Complex klasse II (MHCII). Dendritische cel-geactiveerde  $T_H$  cellen die migreren naar geactiveerde B-cellen kunnen specifiek de gepresenteerde antigeen-peptiden herkennen en co-stimulatie (zoals CD40L) en cytokines (zoals IL-21 en IL-4) aan de B cellen leveren. Na het ontvangen van T cel hulp kunnen geactiveerde IgM-isotype B cellen klasse-switch recombinatie (KSR) ondergaan, om andere antilichaam isotypen zoals IgG of IgA te genereren, om vervolgens kiemcentra (KC) te vormen. In deze KC bewegen B cellen tussen KC donkere zones, locaties waar hyperproliferatie en somatische hypermutatie (SHM) plaatsvinden, en KC lichte zones waar KC B cellen antigeen opnieuw verkrijgen, worden geselecteerd op basis van de BCR affiniteit tegen het antigeen, en waar ze opnieuw gestimuleerd worden door T folliculaire helper cellen ( $T_{FH}$ ). KC B cellen migreren herhaaldelijk tussen KC donkere en lichte zones totdat ze de KC uiteindelijk verlaten en differentiëren tot geheugen B cellen of ASC. De exacte signalen die het verlaten van de KC en inductie van differentiatie bepalen zijn momenteel onbekend.

B cellen kunnen ook deelnemen aan T cel onafhankelijke (TO) reacties. Tijdens deze reacties worden B cellen gestimuleerd door TO-antigenen door middel van binding aan de BCR, waardoor verschillende BCR samengedreven worden en signalen gaan afgeven, en door het activeren van specifieke Toll-like receptoren (TLR's) zoals TLR4, TLR7 en TLR9. TO B cel reacties worden normaliter gekenmerkt door een kortstondige, snelle productie van IgM antilichamen met lage affiniteit. Aangezien er geen vorming van KC is tijdens TO

responsen is er geen selectie voor B cellen met hogere affiniteit en resulteren de meeste TO responsen niet in de vorming van een langlevend immunologisch geheugen.

Om de differentiatie van menselijke B cellen te bestuderen gebruiken wij en anderen *in vitro* kweken (celkweken in het laboratorium). In de loop der jaren zijn er echter een reeks verschillende TA en TO *in vitro* systemen ontwikkeld en juist de heterogeniteit van deze verschillende systemen maakt de interpretatie van de resultaten moeilijk. In **Hoofdstuk 2** hebben we geprobeerd een minimalistisch, eenstaps B cel differentiatie test te genereren die kleine hoeveelheden geïsoleerde B cellen of PBMC vereisen. Hierdoor zijn de tests bij uitstek geschikt zijn voor klinische B cel differentiatie studies. Om TA stimulatie van B cellen na te bootsen zijn we begonnen met fibroblasten die CD40L tot expressie brengen, met toevoeging van IL-21, als basis kweek. Door het aantal B cellen te verlagen waarmee de kweek wordt gestart van 25.000 naar 250 cellen, zagen we dat de verhouding van uitgescheiden IgM antilichamen steeg ten koste van IgG en IgA. Om preferentiële uitgroei van specifieke Ig isotypes te voorkomen hebben we gekozen voor 2500 B cellen als het optimale aantal om de kweek met de beginnen. Om *in vivo* (in het lichaam) reacties beter na te bootsen hebben we de basis kweek met CD40L en IL-21 vergeleken met die met toegevoegde anti-BCR en/of IL-4 stimulatie. We hebben waargenomen dat het opnemen van anti-BCR een lichte verhoging van B cel differentiatie naar ASC veroorzaakte, maar ook tegelijkertijd de detectie van uitgescheiden antilichamen belemmerde. Bovendien, in overeenstemming met andere B cel differentiatie studies, toonden we aan dat toevoeging van IL-4 aan B cel kweken de uitscheiding van antilichamen remt.

Om *in vivo* TO B cel stimulatie na te bootsen begonnen we met TLR9 activerende CpG met toegevoegde IL-2 als basis kweek. Binnen deze TO B cel kweken was de overleving van de cellen in de kweek beperkt. Daarom werden 25.000 B cellen gekozen als het minimumaantal geïsoleerde B cellen om de kweek mee te beginnen. Toevoeging van anti-BCR stimulans of B cel overlevingsfactor BAFF verhoogde de differentiatie naar ASC in geïsoleerde B cel kweken enigszins. In deze studie laten we ook zien dat perifere bloed mononucleaire cellen (PBMC) kunnen worden gebruikt in plaats van geïsoleerde B cellen in zowel TA als TO culturen. Ten slotte hebben we, door verse en ingevroren monsters te vergelijken, aangetoond dat het ASC differentiatie potentieel slechts licht is afgenomen in ingevroren monsters. Dit toont aan dat de TA en TO testen ook geschikt zijn voor longitudinale B cel cohortstudies waarbij patiëntmonsters worden ingevroren en voor langere tijd worden bewaard. Deze studie resulteerde in geoptimaliseerde TA en TO stimulatie protocollen voor de analyse van B cel differentiatie in geïsoleerde B cel en PBMC kweken, met laag gebruik van cellen, waardoor deze protocollen bij uitstek geschikt zijn voor toekomstige klinische studies schaarse patiënten monsters met vaak weinig cellen.

De regulatie van TA humane B cel differentiatie is een complex en dynamisch proces waarbij meerdere (fosfo)signaleringsroutes en een ingewikkeld netwerk van transcriptie factoren

(TF) worden geïnduceerd. In **hoofdstuk 3**, beschrijven we een flow cytometrische test die detectie van B cel differentiatie membraanmarkers CD27 en CD38 mogelijk maakt, met gelijktijdige intracellulaire detectie van actief NF- $\kappa$ B p65 en gefosforyleerd STAT1, STAT3, STAT5 en STAT6. Deze signaaleiwitten werden specifiek onderzocht omdat ze bekende regulatoren zijn van B cel responsen en worden geïnduceerd door BCR stimulatie, CD40L ligatie en IL-21 en IL-4 stimulatie. Bovendien werd een tweede flow cytometrische test ontworpen om analyse van dezelfde differentiatie membraanmarkers samen met TF PAX5, BCL6, C-MYC, BLIMP1, XBP-1s en AID mogelijk te maken. Deze TF werden specifiek gekozen omdat ze B cel differentiatie tot ASC reguleren. Door deze TF in combinatie met CD27 en CD38 te analyseren kunnen we beter onderscheid maken tussen B cellen, B cellen die ASC differentiatie ondergaan en volledig gedifferentieerde ASC. Beide testen maakten de multiparameter analyse van (fosfo)signalerings of TF in de loop van tijd mogelijk, tijdens inductie van ASC differentiatie. In de volgende hoofdstukken werden deze testen gebruikt om de regulatie van humane B cel differentiatie diepgaand te bestuderen.

In **Hoofdstuk 4** hebben we een bibliotheek van uitgescheiden eiwitten gebruikt, in combinatie met een suboptimale CD40L en IL-21 kweek, om voorheen onbekende regulatoire eiwitten te vinden die B cellen kunnen helpen bij ASC differentiatie. We vonden dat type I interferonen, Map19 en oplosbare FASL (oFASL) geconditioneerd media differentiatie van CD27<sup>+</sup>IgG<sup>+</sup> geheugen B cellen tot ASC bevorderen. Omdat type I interferonen eerder werden beschreven ASC differentiatie te bevorderen, hebben we ons gericht op de nieuwe factoren Map19 en oFASL. Hoewel gezuiverd recombinant Map19 dit effect niet repliceerde, induceerde gezuiverd recombinant oFASL significant meer differentiatie tot ASC en tegelijk meer uitscheiding van IgG1 en IgG4 antilichamen. Hoewel FASL een bekende inductor van apoptose is, induceerde oFASL geen apoptose in onze B cel kweken. Door oFASL aan de geheugen B cel kweken toe te voegen, zagen we een verhoogde expressie van ASC TF BLIMP1, hetgeen aantoont dat oFASL een regulator is van ASC differentiatie. De signaalroutes die deze regulatie overbrengen, moeten nog worden onderzocht.

Het is bekend dat B cellen CD40L en IL-21 nodig hebben om differentiatie tot ASC te kunnen ondergaan. *In vivo* is deze stimulatie erg dynamisch en tijdelijk; doordat de B cellen stimulatie verkrijgen van T<sub>FH</sub> cellen en vervolgens actief weg bewegen van de plaats van stimulatie, om vervolgens verder te differentiëren. Het is mogelijk dat precies deze opheffing van stimulatie zou kunnen bijdragen aan B cel responsen. Daarom onderzoeken we in **Hoofdstuk 5** of beëindiging van CD40L signalering leidt tot meer efficiënte differentiatie van B cellen tot ASC. Beëindiging van CD40L signalering resulteerde in zowel een verlaging van de actieve NF-KB p65 als de pSTAT/STAT3 routes. Verlaging van signalering door beëindiging van CD40L stimulatie ging gepaard met een vermindering van zowel celdeling als C-MYC, de TF die celdeling reguleert. Vervolgens werd de B cel-specifieke TF PAX5 ook minder tot expressie gebracht. Terwijl cellen met veel BLIMP1 expressie werden gegenereerd in zowel de continue gestimuleerde, als beëindigde

CD40L stimulatie kweken, laten we zien dat beëindiging van CD40L met de bijbehorende neerwaartse regulatie van C-MYC en PAX5, de BLIMP1 tot expressie brengende cellen in staat stelt om efficiënt te differentiëren tot ASC met hoge expressie van IRF4 en XBP-1s.

Een over het hoofd geziene laag voor regulatie van B cel differentiatie is mogelijk het effect van de zuurstofdruk. In **Hoofdstuk 6** hebben we onderzocht hoe fysiologische zuurstofdruk normaal gevonden in lymfoïde organen, 1 – 3% pO<sub>2</sub>, naïeve B cel klasse-switch en differentiatie reguleert in vergelijking met de atmosferische (21% pO<sub>2</sub>) zuurstofdruk die in het algemeen wordt toegepast in celkweek incubatoren. We hebben aangetoond dat met KC donkere zone geassocieerde normoxie, 3% pO<sub>2</sub>, differentiatie tot ASC bevordert terwijl met KC lichte zone geassocieerde hypoxie, 1% pO<sub>2</sub>, een unieke CD27<sup>+</sup> B cel subset genereerde met een ASC transcriptiefactorprofiel. We toonden ook aan dat normoxische en hypoxische zuurstofniveaus zowel de (fosfo)signaleringsroutes pSTAT3 en pSTAT6 als ASC gerelateerde transcriptiefactoren BLIMP1 en XBP-1s reguleren. Omdat KC B cellen migreren tussen hypoxische lichte en normoxische donkere zones tijdens B cel responsen, onderzochten we ook of tijdsafhankelijke wisselingen tussen 1% en 3% pO<sub>2</sub> tijdens het kweken B cel differentiatie beïnvloeden. Dit toonde aan dat het wisselen tussen fysiologisch relevante zuurstofdrukken inderdaad de differentiatie van menselijke B cellen reguleert en klasse-switch naar, en secretie van, IgG bevordert.

In het geheel en zoals besproken in de **samenvattende discussie**, dragen de resultaten die in dit proefschrift worden gepresenteerd bij aan het onderzoeksveld naar de differentiatie van menselijke B cellen door geoptimaliseerde TA en TO *in vitro* stimulatie protocollen beschikbaar te stellen die een diepgaande analyse van ASC differentiatie mogelijk maken, specifiek voor wanneer de hoeveelheid patiëntmateriaal beperkt is. Tevens laten de data in dit proefschrift zien dat de dynamische beschikbaarheid van immunologische factoren en metabolische factoren cruciale regulatoren zijn van humane B cel differentiatie en dat ze allemaal in overweging moeten worden genomen tijdens *in vitro* en *in vivo* B cel differentiatie studies. Deze inzichten en technieken zullen toekomstig B cel gerelateerd onderzoek ondersteunen, zowel op fundamenteel als klinisch niveau.

## LIST OF PUBLICATIONS

Bos AV, van Gool MMJ, Breedveld AC, van der Mast R, **Marsman C**, Bouma G, van de Wiel MA, van Ham SM, Mebius RE, van Egmond M.

Fcα Receptor-1-Activated Monocytes Promote B Lymphocyte Migration and IgA Isotype Switching.

*International Journal of Molecular Sciences*. 2022 Sep 22;23(19):11132.

doi: 10.3390/ijms231911132.

**Marsman C**, Verstegen NJ, Streutker M, Jorritsma T, Boon L, Ten Brinke A, van Ham SM. Termination of CD40L co-stimulation promotes human B cell differentiation into antibody-secreting cells.

*European Journal of Immunology*. 2022 Oct;52(10):1662-1675.

doi: 10.1002/eji.202249972.

**Marsman C\***, Verhoeven D\*, Koers J, Rispens T, Ten Brinke A, van Ham SM<sup>‡</sup>, Kuijpers TW<sup>‡</sup>. Optimized Protocols for *In-Vitro* T-Cell-Dependent and T-Cell-Independent Activation for B-Cell Differentiation Studies Using Limited Cells.

*Frontiers in Immunology*. 2022 Jun 29;13:815449.

doi: 10.3389/fimmu.2022.815449

\* shared first authorship, ‡ shared senior authorship

van Asten SD, Unger PP\*, **Marsman C\***, Bliss S, Jorritsma T, Thielens NM, van Ham SM, Spaapen RM.

Soluble FAS Ligand Enhances Suboptimal CD40L/IL-21-Mediated Human Memory B Cell Differentiation into Antibody-Secreting Cells.

*Journal of Immunology*. 2021 Jul 15;207(2):449-458.

doi: 10.4049/jimmunol.2001390.

\* shared second authorship

Unger PA\*, Verstegen NJM\*, **Marsman C**, Jorritsma T, Rispens T, Ten Brinke A, van Ham SM.

Minimalistic In Vitro Culture to Drive Human Naive B Cell Differentiation into Antibody-Secreting Cells.

*Cells*. 2021 May 12;10(5):1183.

doi: 10.3390/cells10051183.

\* shared first authorship

**Marsman C**, Jorritsma T, Ten Brinke A, van Ham SM.

Flow Cytometric Methods for the Detection of Intracellular Signaling Proteins and Transcription Factors Reveal Heterogeneity in Differentiating Human B Cell Subsets.

*Cells*. 2020 Dec 8;9(12):2633.

doi: 10.3390/cells9122633.

**Marsman C**, Lafouresse F, Liao Y, Baldwin TM, Mielke LA, Hu Y, Mack M, Hertzog PJ, de Graaf CA, Shi W, Groom JR.

Plasmacytoid dendritic cell heterogeneity is defined by CXCL10 expression following TLR7 stimulation.

*Immunology & Cell Biology*. 2018 Nov;96(10):1083-1094.

doi: 10.1111/imcb.12173.

van der Mark VA, Ghiboub M, **Marsman C**, Zhao J, van Dijk R, Hiralall JK, Ho-Mok KS, Castricum Z, de Jonge WJ, Oude Elferink RP, Paulusma CC.

Phospholipid flippases attenuate LPS-induced TLR4 signaling by mediating endocytic retrieval of Toll-like receptor 4.

*Cellular and Molecular Life Sciences*. 2017 Feb;74(4):715-730.

doi: 10.1007/s00018-016-2360-5.

## **AUTHOR CONTRIBUTIONS**

### **Chapter 2**

Optimized Protocols for In-Vitro T-Cell-Dependent and T-Cell-Independent Activation for B-Cell Differentiation Studies Using Limited Cells

Casper Marsman<sup>1†</sup>, Dorit Verhoeven<sup>2,3†</sup>, Jana Koers<sup>1</sup>, Theo Rispens<sup>1</sup>, Anja ten Brinke<sup>1</sup>, S. Marieke van Ham<sup>1,4†</sup> and Taco W. Kuijpers<sup>2†</sup> on behalf of the T2B Consortium

<sup>1</sup>Department of Immunopathology, Sanquin Research and Landsteiner Laboratory, University of Amsterdam, Amsterdam, Netherlands,

<sup>2</sup>Department of Pediatric Immunology, Rheumatology and Infectious Diseases, Emma Children's Hospital, Amsterdam University Medical Centers, University of Amsterdam, Amsterdam, Netherlands,

<sup>3</sup>Department of Experimental Immunology, Amsterdam Institute for Infection & Immunity, Amsterdam University Medical Centers (UMC), University of Amsterdam, Amsterdam, Netherlands,

<sup>4</sup>Swammerdam Institute for Life Sciences, University of Amsterdam, Amsterdam, Netherlands

†These authors have contributed equally to this work and share first authorship

‡These authors have contributed equally to this work and share senior authorship

JK, CM, and DV designed the experiments. CM and DV performed the experiments and analyzed the data. TR and AB critically revised the manuscript. SH and TK devised the concept, supervised data interpretation, and critically revised the manuscript. The manuscript was revised and approved by all authors.

### **Chapter 3**

Flow Cytometric Methods for the Detection of Intracellular Signaling Proteins and Transcription Factors Reveal Heterogeneity in Differentiating Human B Cell Subsets

Casper Marsman<sup>1</sup>, Tineke Jorritsma<sup>1</sup>, Anja Ten Brinke<sup>1</sup>, S Marieke van Ham<sup>1,2</sup>

<sup>1</sup>Department of Immunopathology, Sanquin Research and Landsteiner Laboratory, Amsterdam UMC, University of Amsterdam, 1066 CX Amsterdam, The Netherlands.

<sup>2</sup>Swammerdam Institute for Life Sciences, University of Amsterdam, 1098 XH Amsterdam, The Netherlands.

C.M. designed and performed all the laboratory experiments and data analyses and generated all the figures. T.J. performed and analyzed all of the semiquantitative



PCRs. A.t.B. contributed to supervision. S.M.v.H. was the main supervisor. All authors contributed to the writing of the manuscript. All authors have read and agreed to the published version of the manuscript.

## Chapter 4

Soluble FAS ligand enhances suboptimal CD40L/IL-21-mediated human memory B cell differentiation into antibody-secreting cells

Saskia D. van Asten<sup>1,2</sup>, Peter-Paul Unger<sup>1,2,\*</sup>, Casper Marsman<sup>1,2,\*</sup>, Sophie Bliss<sup>1,2</sup>, Tineke Jorritsma<sup>1,2</sup>, Nicole M. Thielens<sup>3</sup>, S. Marieke van Ham<sup>1,2,4</sup>, Robbert M. Spaapen<sup>1,2</sup>

<sup>1</sup>Department of Immunopathology, Sanquin Research, Amsterdam, 1066 CX, The Netherlands

<sup>2</sup>Landsteiner Laboratory, Amsterdam UMC, University of Amsterdam, Amsterdam, 1066 CX, The Netherlands

<sup>3</sup>Univ. Grenoble Alpes, CEA, CNRS, IBS, F-38000, Grenoble, France

<sup>4</sup>Swammerdam Institute for Life Sciences, University of Amsterdam, Amsterdam, the Netherlands.

\*Authors contributed equally

S.A., P.U., C.M., S.H. and R.S designed experiments. S.A., P.U., C.M., S.B., T.J. acquired data. S.A., P.U., C.M., S.B. and R.S performed data analysis. S.A., P.U., C.M., S.B., S.H. and R.S interpreted data. S.A. and R.S wrote the manuscript.

All authors have read and approved the manuscript.

## Chapter 5

Termination of CD40L co-stimulation promotes human B cell differentiation into antibody-secreting cells

Casper Marsman<sup>1,2</sup>, Niels Jm Verstegen<sup>1,2</sup>, Marij Streutker<sup>1,2</sup>, Tineke Jorritsma<sup>1,2</sup>, Louis Boon<sup>3</sup>, Anja Ten Brinke<sup>1,2</sup>, S Marieke van Ham<sup>1,4</sup>

<sup>1</sup>Sanquin Research, Department of Immunopathology, University of Amsterdam, Amsterdam, The Netherlands.

<sup>2</sup>Landsteiner Laboratory, Amsterdam UMC, University of Amsterdam, Amsterdam, The Netherlands.

<sup>3</sup>JJP Biologics, Warsaw, Poland.

<sup>4</sup>Swammerdam Institute for Life Sciences, University of Amsterdam, Amsterdam, The Netherlands.

C.M., NJM.V., A.t.B., and S.M.v.H. designed the research. C.M., M.S., and T.J. performed the research. C.M. analyzed the data. L.B. provided reagents. All authors critically reviewed

the manuscript, gave final approval of the version to be published and agreed to be accountable for all aspects of the work ensuring that questions related to the accuracy or integrity of any part of the work are appropriately investigated and resolved.

## **Chapter 6**

Oxygen level is a critical regulator of human B cell differentiation and IgG class switch recombination

Jana Koers<sup>1\*</sup>, Casper Marsman<sup>1\*</sup>, Juulke Steuten<sup>1\*</sup>, Simon Tol<sup>2</sup>, Ninotska I.L. Derksen<sup>1</sup>, Anja ten Brinke<sup>1</sup>, S. Marieke van Ham<sup>1,3,§</sup>, and Theo Rispens<sup>§</sup>

<sup>1</sup>Sanquin Research, Department of Immunopathology, and Landsteiner Laboratory, Amsterdam University medical centers, University of Amsterdam, Amsterdam, The Netherlands. <sup>2</sup>Sanquin Research, Department of research Facilities, and Landsteiner Laboratory, Amsterdam University medical centers, University of Amsterdam, Amsterdam, The Netherlands. <sup>3</sup>Swammerdam Institute for Life Sciences, University of Amsterdam, Amsterdam, the Netherlands.

\*/§ contributed equally

JK, CM, JS, ST, AB, MH and TR designed research. JK, CM, JS, ST and ND performed research. JK, CM and JS analyzed data. JK, CM, JS, AB, MH and TR wrote the paper. All authors critically reviewed the manuscript, gave final approval of the version to be published, and agreed to be accountable for all aspects of the work ensuring that questions related to the accuracy or integrity of any part of the work are appropriately investigated and resolved.

## PHD PORTFOLIO

Name PhD student: Casper Marsman  
 PhD Period: 01-05-2017 - 01-05-2022  
 Promotor: Prof. dr. S.M. van Ham  
 Copromotor: Dr. A ten Brinke

### PhD training

<b>Courses</b>	<b>Year</b>	<b>ECTS</b>
Postgraduate Course Advanced Immunology	2018	2.9
Project Management	2018	0.5
Advanced Immunology Summer School (ENII)	2018	2
BioBusiness Summer School	2019	2
BCF Grant Application Course	2020	0.5

<b>Seminars &amp; Workshops</b>	<b>Year</b>	<b>ECTS</b>
Weekly Sanquin IP Department meetings	2017-2022	5
Biweekly Journal Club	2017-2022	2.5
Monthly Immunopathology Seminar	2017-2022	2.5
Weekly Sanquin Research Staff meeting	2017-2022	5
Landsteiner lectures & guest speaker seminars	2017-2022	5
Sanquin Science Day	2017-2022	1.5

<b>Masterclasses</b>	<b>Year</b>	<b>ECTS</b>
Prof. dr. Muzlifah Haniffa	2018	0.2

<b>Conferences</b>	<b>Year</b>	<b>ECTS</b>
Nederlandse Vereniging voor Immunologie (NVVI) <i>2x poster presentation, 2x oral presentation</i>	2017-2021	4
Amsterdam Institute for Infection and Immunity PhD Retreat <i>3x oral presentation</i>	2017-2021	3
European Congress of Immunology <i>1x poster presentation, 1x oral presentation</i>	2018 & 2021	2
International Keystone Conference, B-T cells <i>1x poster presentation, 1x oral presentation</i>	2018 & 2021	2

<b>Teaching</b>	<b>Year</b>	<b>ECTS</b>
<b>Lecturing</b>		
Practical course assistant, B.Sc. Immunology course	2019 & 2020	0.5
<b>Supervising</b>		
Msc student, Marij Streutker (8 months)	2019	3
Bsc students, Bilal Bin-Salami & Amber de Groot (4 weeks)	2019	1
<b>Parameters of Esteem</b>	<b>Year</b>	<b>ECTS</b>
<b>Awards</b>		
Poster prize, Sanquin Science Day	2017	
Nominee in-house Sanquin Seminar Award	2018	
Poster prize, Sanquin Science Day	2019	
<b>Grants</b>		
Waived Registration Fee Grant	2021	
Amsterdam Institute for Infection and Immunity Travel Grant	2022	

## CURRICULUM VITAE

Casper Marsman was born on the 19<sup>th</sup> of April 1993, in Hoorn, the Netherlands. He studied Biomedical Sciences at the University of Amsterdam from 2011 until 2017. He finished his bachelor studies with an internship and thesis at the department of Plasma Proteins at Sanquin Research in Amsterdam, under supervision of Dr. Nicoletta Sorvillo and Dr. Robin Hartholt. During his master studies at the University of Amsterdam Casper did two internships. During the first internship at the AMC Tytgat Institute in Amsterdam, under supervision of Dr. Coen Paulusma, Casper studied and characterized P4 ATPase deficient THP-1 Macrophages. During his second internship at the Walter and Eliza Hall Institute in Melbourne, under supervision of Dr. Joanna Groom, Casper investigated IFN induced gene signatures related to SLE. This research led to a scientific publication. Casper finished his master studies in 2017 by writing a thesis on the plasmablast and plasma cell responses, under supervision of Prof. dr. Marieke van Ham. The same year Casper started his PhD studies at the department of Immunopathology at Sanquin Research in Amsterdam, under the supervision of Prof. dr. Marieke van Ham. During his PhD studies Casper investigated the regulation of human B cell differentiation, resulting in this thesis. After his PhD, Casper started working as a Cell Biology Scientist at Kling Biotherapeutics in Amsterdam.



## ACKNOWLEDGEMENTS

To quote almost every scientist at the end of their presentation: I did not do this alone. I would like to thank everyone that directly and indirectly supported me in finishing this thesis.

Beste **Marieke**, lieve mammië-van-Hammie, als promotor wil ik je ontzettend bedanken voor de onmisbare ondersteuning van mijn promotieonderzoek. Sinds de bachelor ben je er eigenlijk al bij geweest, eerst tijdens de immunologie vakken en vervolgens door mij een plekje tegen bij Sanquin voor de bachelor stages. Het was erg fijn om aan het einde van mijn master weer bij je terug te kunnen komen voor die thesis, het begin van een vruchtbaar maar vooral leuk onderzoek naar B cellen. De manier waarop je als opperhoofd altijd tijd maakt voor- en iedereen betreft bij- de Immunopathologie-familie is van onschatbare waarde en mede daardoor zijn we allemaal goed door de lockdowns gekomen. Bedankt voor alles!

**Anja**, als co-promotor was ook jij onmisbaar tijdens dit onderzoekstraject. Je recht-toe-recht-aan instelling bracht een uitstekende balans in de (wetenschappelijke) discussies over de jaren. Soms was het nou eenmaal tijd om te stoppen met dromen en 'gewoon' de experimenten te doen en alles af te maken. Dankjewel!

M'n paranimfen, hoe kon het ook anders. **Niels** en **Jana**, na jaren borrelen, reizen, enthousiast of klagend lullen over wetenschap en (toch) ook onderzoek doen rest er eigenlijk nog maar 1 vraag: wie is nou de echte twerk-koning(in)? Ik denk dat we daar maar op 1 manier achter komen.... Gelukkig komen er een paar mooie promotiefeestjes aan :). Bedankt voor alle gezelligheid en alle ondersteuning met het afronden van dit promotieonderzoek! Ik weet zeker dat we elkaar nog vaak zullen zien.

Lieve **Dorit**, ik weet nog goed hoe je naar me toe stapte na m'n eerste maandag-middag presentatie. Dat moment was het begin van een mooie -maar ook zeker gezellige- samenwerking wat uiteindelijk resulteerde in hoofdstuk 2 van dit boekje. Zonder jou was dit boekje en het T2B consortium een stuk minder geweest, bedankt!

**Tineke**, wat een zootje zou het lab zijn zonder jouw onvermoeibare organisatie. Soms wordt dit voor lief genomen en dat mag best gezegd worden. Je was altijd in voor een praatje en ook al je hulp bij vele experimenten zal ik nooit vergeten. Dankjewel!

**Saskia**, bedankt voor de erg prettige samenwerking dat leidde tot hoofdstuk 4. Het was voor mij de eerste keer om de technieken uit hoofdstuk 3 toe te passen op een leuk biologisch vraagstuk. Je precieze en georganiseerde persoonlijkheid was onmisbaar om alle verschillende personen in dit project in goede banen te blijven leiden.

**Juulke**, zonder jou was het hypoxia project nooit tijdig afgerond. Jouw vrolijkheid en aanstekelijke lach zorgden ervoor dat de uitzonderlijk grote proeven toch eigenlijk niet zo vervelend waren. Ook jij bedankt voor alle gezelligheid en hulp.

**Peter-Paul**, dankzij jou kon ik een mooie vliegende start krijgen in het B cel onderzoek. Je geduld en bekwaamheid waren heel prettig voor een beginnend PhD student. Je stond aan de basis van al het onderzoek dat uiteindelijk in dit boekje is gekomen, dankjewel!

**Taco**, bedankt voor de doeltreffendheid en rust die je bracht in het afronden van hoofdstuk 2. Het was een zeer prettige samenwerking!

**Theo**, jouw kritische blik en sturing hebben het hypoxia project veel goeds gedaan. Bedankt!

**Sophie**, thank you for all the fun times inside the lab and now also outside the labs. It was great having you at IP, I will always remember your jokes and interesting conundrums about what someone might do for a specific amount of money.

**Robbert**, het was leuk om met je samen te werken en hoofdstuk 4 te kunnen afmaken. Ook ben ik je erg dankbaar voor alle gezelligheid, ook buiten Sanquin, en het feit dat ik altijd alle overgebleven taart van jullie meetings mocht opeten. Dankjewel!

**Marij**, je was m'n eerste student en ik heb ontzettend veel van je geleerd. Nogmaals bedankt voor je onfeilbare werk en ook zeker alle gezelligheid buiten het lab!

**Louis Boon**, bedankt voor de schijnbaar oneindige hoeveelheid anti-CD40L en de kritische blik op hoofdstuk 6!

Ciao **Sabrina**! With your great bioinformatic expertise and Italian flair you brought the group to a new level. Thank you for this and all the gezelligheid!

**Amelie**, onze samenwerking was niet heel lang maar wel erg leuk om te doen! Bedankt voor de lesjes in IgA en het is erg leuk om te zien dat je uiteindelijk bij 'ons' terecht bent gekomen.

Alle oud-PhDs: **Anna Kroeze, Anno, Twan, Laura, Sanne, Astrid, Judith, Karin, Willem, Inge, Lea, Richard** en **Anna van Beek**, samen met **Marlieke** stonden jullie allen klaar om mij als nieuwe PhD welkom te heten. Ik voelde me direct thuis en ik heb erg genoten van alle tripjes, borrels en etentjes. Bedankt allemaal!

De huidige PhDs: **Nieke, Esther, Tamara, Yasmin, Nienke, Myrddin, Milou, Lisan, Laura Kummer**, bedankt voor alle interessante discussies en gezelligheid op (en buiten)

de IP-afdeling! Het was wat moeilijker elkaar regelmatig te zien tijdens en na de lockdowns en ieder van jullie is daar op hun eigen manier mee om gegaan. Ik ben zeer benieuwd naar waar jullie allemaal terecht gaan komen na de PhD!

**Annelies** en de **IMS groep**, bedankt voor alle nuttige discussies in de cellulaire meetings!

**Arthur!** Ik ben erg dankbaar voor al het werk dat jij in de borrels hebt gestoken de afgelopen jaren. Wat begon als voorzicht gezellige avondjes met een paar IHEP en IPers liep al snel uit de hand. Het was altijd een groot plezier om jou en **Max** als een soort van broers te horen kibbelen. Ook was het erg leuk om buiten het lab met z'n 3en, op een wetenschappelijk correcte manier, een heerlijk biertje te brouwen! Jullie, samen met de andere vaste borrelaars **Bram, Bogac, Paula, Dorien, Natasja, Giota, Evelien, Rivelino, Felix, Anna Oja, Francesca, Jullien, Carlijn, Roos, Thijs, Florencia**, jullie hebben mijn tijd op Sanquin echt heel mooi gemaakt, ontzettend bedankt!

**Ninotska** bedankt voor alle hulp met het afmaken van het hypoxia project! **Gerard** bedankt alle liedjes in de gangen en je enthousiasme over letterlijk elk onderzoek, **Gijs, Angela, Dorina, Mieke, Miranda, Ingrid, Pleuni** en **Mariel**, bedankt voor alle hulp en discussies!

**Simon**, bedankt voor al het (toch niet zo) oneindige gesort en alle gezellige avonden! **Erik**, bedankt voor alle hulp en de roddels ;). **Mark** en **Tom**, ook jullie bedankt voor al het onderhoud aan de FACS machines!

**Kaoutar** en **Anita**, bedankt voor alle hulp vanuit het secretariaat! **Fatima** ook jij bedankt hiervoor, voor de gezelligheid en natuurlijk voor al het geregel en hulp rond het afwerken van de PhD!

Mijn ouders, Jan en Francine, bedankt voor alle steun en geduld! Mijn broer en zus, **Gerben** en **Judith**, nu is het eindelijk officieel. Op onverklaarbare wijze hebben we alle drie voor een soortgelijke studie gekozen en hebben we nu alle drie een PhD in de biomedische wetenschappen. **Gerben** gooide het balletje een aantal jaar geleden op, misschien echt eens tijd voor een Marsman, Marsman & Marsman stuk?

Beste **Bram, Floris, Jan, Sam, Neil, Laurens, Rosab, Rosak, Myla, Naomi, Lizl** en **Alice**. Ik moet ook jullie bedanken! Ook jullie hebben (onbedoeld?) bijgedragen aan dit boekje doormiddel van alle gezellige avonden en uitstapjes waar ik alles van de PhD lekker kon loslaten.

And finally, **Milena**. My smoll lady. You remind me every day how lucky I am, just by being there. Thank you for all your patience, warmth, love, for always sharing our truths, for all the evaluations and especially for convincing me to adopt not one, but two, beautiful



and funny kitties **Dupe** and **Kate**. You make me a better person and I can't wait for all our upcoming adventures, the next one is going to be a big one, getting married! And then... who knows? But I am convinced it will be one hell of a ride. Обичам те много.